UNIVERSITY OF KENT

State Feedback Sliding Mode Control of Complex Systems with Applications

A Thesis Submitted to the
University of Kent
For the Degree of Doctor of Philosophy in
Electronic Engineering

By

Jianqiu Mu

Jan 2018

Supervisor: Dr. Xinggang Yan

ABSTRACT

This thesis concerns the development of robust nonlinear control design for complex systems including nonholonomic systems and large-scale systems using sliding mode control (SMC) techniques under the assumption that all system state variables are accessible for design. The main developments in this thesis include:

- The concept of generalised regular form and design of a novel sliding function. The mathematical definition of generalised regular form is proposed for the first time. It is an extension of the classical regular form, which makes SMC applicable to a wider class of nonlinear systems. A novel sliding function design, which is based on the global implicit function theorem, is proposed to guarantee unique sliding mode dynamics.
- The development of decentralised SMC for large-scale interconnected systems. For systems with uncertain interconnections which possess the superposition property, a decentralised control scheme is presented to counteract the effect of the uncertainty by using bounds on uncertainties and interconnections. The bounds used in the design are nonlinear functions instead of constant, linear or polynomial functions. The design strategy has also been expanded to a fully nonlinear case for interconnected systems in the generalised regular form.
- Robust decentralised SMC for a class of nonlinear systems with uncertainties in input distribution. A system with uncertainties in input distribution is full of challenges. A novel method is proposed to deal with such uncertainties for a class of nonlinear interconnected systems. The designed decentralised SMC enhances the robustness of the controlled systems.

This thesis also provides case studies of three applications for the proposed approaches. The existence of the generalised regular form is verified in the trajectory tracking control of a wheeled mobile robot (WMR) system. Both simulations and experiments on the WMR are given to demonstrate the validity and effectiveness of the generalised regular form-based SMC design. A continuous stirred tank reactor (CSTR) system and a longitudinal vehicle-following system are used to test the proposed decentralised SMC schemes. An expanded vehicle-following system with both longitudinal and lateral controllers has been developed to demonstrate the robust control design for system with uncertainties in input distribution.

ACKNOWLEDGMENTS

This thesis is the result of a three years' long research activity that I have carried out at the Instrumentation, Control and Embedded Systems Research Group, School of Engineering & Digital Arts of the University of Kent. I would like to thank some people who made a great contribution to this thesis.

First of all, I would like to thank my supervisor Dr Xinggang Yan for his continuous support, professional suggestions and kind guidance during all stages of my work. His patience, motivation, enthusiasm and immense knowledge in this field made my learning process and research experience much more enjoyable and memorable. Thank you very much for your kind help leading me towards the greatness.

Second, I would like to thank Prof. Sarah K. Spurgeon, for the support not only in the research process but also the guidance during my postgraduate study, introduce me the magic of control science. Thank you for your patient guidance.

I would like to thank my college Mokhtar Mohammed and Andrew E Onyeka and visiting experts Wenbo Tian and Xiaolin Gong. I enjoyed our insightful discussions on the research problems and our enjoyable chats outside the university very much. Thank you all for inspiring me with a more delightful future.

I wish to thank all academic staff of my group for providing a stimulating and collaborative working environment, in particular, Prof. Yong Yan, Dr Lu Gang, Dr Peter Lee and Dr Gianluca Marcelli. I am also thankful to the professional support of all the staff in the School.

Last, but certainly not least, I would like to dedicate this thesis to my wife Yuan and my little angel Yinghan, my parents, Wencheng Mu, Mingqiong Yang, and my two little brothers Jiaming and Jianfeng. I could not have done this without them. I would also like to thank all my friends for incredibly loving and supportive for all times. Thank you very much!

CONTENTS

LIST OF FIGURES

LIST OF TABLES

CHAPTER. 1

INTRODUCTION

Automatic control theory can be traced back to the Industrial Revolution with the invention of improved engines and automatic control systems to regulate them. In the mid 18th century, the stability of a feedback control system was then analysed with mathematics for the first time. During the World Wars, the control systems were rapidly developed as the development of control theory has become a matter of survival [3]. Based on a simple input-output description of the plant, the system in classical control theory is usually expressed as a transfer function which simply describes the relationship between the single input and the single output. Without the knowledge of the interior structure of the plant, only limited control behaviour of the closed-loop system can be observed at that time. To solve the control problems of a more complex plant, the study of the modern control theory commenced in the 1960s and turned back to the differential equation techniques of the late 18th century. Based on the relative rich knowledge of the interior structure of the system plant, the modern control theory provides a richer description of the plant dynamics, and the system has become increasingly sophisticated since then. In this thesis, a study focus on the robust control problems for the complex systems has been carried out with a detailed background.

1.1. Background and Motivation

Complex systems appear almost in every field of contemporary science and are inevitably associated with a variety of natural and social phenomena. With our intensive and infinite desire to study and control such systems, complexity has become a crucial issue for the modern control theory and practical engineering, and the system performance is getting higher and higher while the demands of various functions are increasing. As a consequence, the corresponding control schemes of a complex system inevitably tend to be increasingly sophisticated. This issue has motivated an enormous number of advanced control techniques to ensure that the desired performance of the systems meets satisfactory. It is becoming increasingly obvious that "well-organisational complexity" is the way of the future [4].

Although there may be many characteristics in a particular complex system, it has already been stated in [5] that to look for an overarching theory which contains all essential properties of complex systems is rather impractical or at least unlikely to be developed anytime soon. However, it is still valuable and useful to abstract the common features of such systems for the development of modern control theory [5]. Moreover, in fact, numerous theoretical and practical results have been developed over the past few decades. It has been shown that the complexity of a control system is highly dependent on the controlled plant and environment. Higher requirements often result in more complexity of a controlled system [4]. Among all the properties for common complex systems, the following three are studied and focused in this thesis: nonlinearity [6, 7], dimensionality, information structure constraints and uncertainty [5, 4].

- **Nonlinearity.** It has been found that linear dynamical systems are limited to describe many commonly observed phenomena accurately. At certain circumstances, nearly all systems more or less exhibit nonlinearity. Although the linear control theory is well developed, the analysis and design of a nonlinear system are very complex. Therefore, more advanced control techniques are required for such systems, such as linearization technique, so that the system can be transferred to a linear system and thus linear control theory can be applied. However, for some complex systems, linearization may not be available due to some phenomena of the systems, e.g. finite time escape, multiple isolated equilibria, limit cycles, harmonic oscillation, chaos or multiple modes of behaviour [8].

Furthermore, systems such as chaotic systems [9], nonholonomic mechanical systems [10] also have inherent constraints or nonlinearity which greatly increase the system complexity. Therefore, nonlinearity inevitably increases the system complexity, especially when the linearization technique is not available.

- **Dimensionality.** Technically, large memory and fast computing unit are inevitably required by a system with high order, i.e. the so-called *large-scale system* (e.g. see [11]). The inherent computational complexity makes a centralised structure very difficult to be applied. Furthermore, some systems may be physically distributed in space, the reliability of the system is inevitably dependent on the communication network. Thus robustness and reliability problems, e.g. network failure, in such systems may seriously affect or even devastate the system stability with centralised structure. To overcome these technical problems, a large-scale system is inevitably partitioned into many simple systems with local decision makers (DMs) to manage them. To guaranteed the overall system performance, a lot of advanced control architecture is developed. However, such techniques inevitably result in the extra complexity of the controlled system. Thus dimensionality is a very challenging problem for control of complex systems.

- **Information structure constraints.** Due to the computational and network problems related to dimensionality, the DMs in a large-scale system is often designed with *information structure constraints* [5]. Technology like distributed parallel computing with highly reliable low-cost multiprocessor architectures can be used for fast control action in response to local inputs and perturbations in such systems [4]. Therefore, the *decentralised information constraints*, in which DMs in each partitioned system can only access local information, have drawn much attention during the past few decades. Due to the lack of information, instability caused by the interaction of the overlapped dynamics become the main problems of such systems.

- **Uncertainty.** Although classical control methods, i.e. frequency domain methods, and state feedback approach in modern control theory have been developed for the fundamental task of stabilising the system maturely, systems may not have the expected performance in most practical implementation. For a practical system, it is usually very difficult or even impossible to build a mathematical model to describe the system accurately. Moreover, some systems may experience unknown disturbances, worsening the performance or

even causing system instability. The incomplete identification of the system and external disturbances leads to one of the crucial topics of modern control theory, i.e. *robust control theory*, which is to ensure that the control performance of the practical system remains satisfactory in the presence of uncertainties. Since these uncertainties frequently exist in real world, robust control synthesis is relatively essential to maintain the desired performance, which inevitably increases the complexity of the analyse and design of a complex system furthermore.

Robust control theory has become an important subject of research during recent decades. Techniques such as adaptive control [12, 13], variable structure control (VSC) [14, 15] etc. have been developed to improve the robustness of dynamical systems in the presence of heavy uncertainties. By classifying the differences in structure, uncertainties that can be included in the input channel is said to be *matched uncertainty* [16, 17], and the rest is referred to *mismatched uncertainty* [18, 2]. Regarding the resources of the uncertainties, they can be separated into *external disturbances*, or *exogenous disturbances*, and *internal uncertainty*, or equivalent *modelling uncertainty*. The difference between the external disturbance and internal uncertainty is that the former perturbation does not vary with the system variables, i.e. states, input signals or output. If external disturbances are the only uncertainties in the system, then a disturbance observer based control, e.g. see [19, 20], can be applied to estimate the disturbance so that a proper feedback control can be designed with the extra information to achieve better performance. However, it has been pointed out in [20] that if the system experience both external and modelling uncertainty, the disturbance observer will be difficult to be applied since an accurate relative model is required in such approaches. Furthermore, due to the non-vanishing properties of the external disturbance, the design with this approach can only achieve ultimate boundedness stability or only part of the system can achieve asymptotical stability in theory [21, 20].

As a typical VSC, SMC has been recognised as a robust approach in dealing with nonlinear systems with matched uncertainties. With discontinuous control law, the SMC drives the system state trajectory onto a predefined surface in the state space and keeps the system state on the manifold. By choosing a suitable surface, the system will eventually converge to the desired equilibrium point as the time tends to infinity. While the system is on the sliding manifold, it behaves as a reduced order system compared with the original plant. Once the system is on

the manifold, the reduced-order system is independent of the control signal. The invariance property has motivated research with an extensive literature for framework establishing robust SMC for various linear and nonlinear control systems [22, 23, 24, 25]. Methods proposed by Niu in [26] and [27] show the strong robustness of SMC for systems with uncertainties in input distribution. Moreover, it has been demonstrated that sliding mode approach can be applied to control systems with mismatched uncertainties, see for example [28, 19, 29, 30]. Although the so-called "chattering" problem may affect the control performance in the practical implementation, techniques like boundary layer [31], fuzzy sliding mode [9] and high order SMC [18] can be applied to relieve the problems.

Motivated by the existing problems in practical systems, this thesis studied the issue of the SMC for complex systems. Specifically, comprehensive analysis of the robustness of SMC is provided for complex nonlinear systems, particularly nonholonomic systems and large-scale interconnected systems. Moreover, some significant control problems for complex nonlinear systems involving both matched and mismatched uncertainties/interconnections are addressed based on the SMC design. Furthermore, large-scale interconnected systems with uncertainties in input distribution are also discussed, and robust decentralised control strategy against such uncertainties along with matched and mismatched interconnections is also developed with applications.

1.2. Contributions and Thesis Organisation

This thesis contributes to the knowledge and research not only for robust decentralised control but also extend the SMC for a wider class of nonlinear systems. The approaches established in this thesis have been applied to several practical systems through case studies which includes tracking control for wheeled mobile robot (WMR) system, automated highway systems etc. The contribution of this thesis can be summarised as follows:

- Mathematical definition of generalised regular form and a novel sliding function design. The concept of generalised regular form is proposed for the first time. It is an extension of the classical regular form, which makes the traditional regular form-based SMC applicable to a wider class of nonlinear systems. A novel nonlinear sliding function design based on

global implicit function theorem is proposed so that the solution to the sliding function, i.e. the governed sliding surface, does uniquely exist.

- The development of decentralised SMC for large-scale interconnected systems. For systems with uncertain interconnections which possess the superposition property, a decentralised control scheme is presented to counteract the effect of the uncertainty by using the bounds of uncertainties and interconnections. The bounds used in the design are nonlinear functions instead of constant, linear or polynomial function. The design strategy has also been expanded to a fully nonlinear case for interconnected system in the generalised regular form.
- Robust decentralised SMC for a class of nonlinear systems with uncertainties in input distribution. A system with uncertainties in input distribution is full of challenges. A novel method is proposed to deal with such uncertainties for a class of nonlinear interconnected systems. The designed decentralised SMC enhances the robustness of the controlled systems.

The rest of this thesis is structured as follows:

Chapter 2 gives some mathematical preliminaries required for the following chapters. Particularly, the necessary definitions and main results of Lyapunov stability theory and Frobenius theorem required for the following chapters are provided in this chapter.

Chapter 3 gives basic concept and fundamental knowledge needed to help readers to understand this thesis. Basic knowledge of state feedback and SMC are discussed. Notably, the existence of regular form for a nonlinear system is discussed based on the Frobenius theorem, which will be further investigated in the next two chapters. Following the mathematical definition of nonholonomic with two examples, a literature survey and fundamental concept related to large-scale systems are discussed in details with three practical examples. Specifically, two common decomposition techniques and two networked-based system structure are briefly introduced. It gives a detailed literature review of robust decentralised control before concluding this chapter.

Chapter 4 studies the trajectory tracking control problem of a WMR system. The review of the trajectory tracking control of WMRs is discussed, and a robust SMC design for trajectory tracking control of a WMR system is given with both simulation and experiments verification. The nonlinear sliding mode controller can track the time-based trajectory within reasonable

time in a local domain. The simulation and experiment results show that the regular form-based SMC design is capable of working properly on systems that do not even have a regular form, which is of interest to be further investigated.

Chapter 5 presents a generalised regular form-based SMC for nonlinear systems. In this chapter, mathematical definition of generalised regular form is proposed for the first time. The proposed form includes the classical regular form as a special case and expands the regular form-based design approach to a wider class of nonlinear systems. The corresponding SMC design with a novel sliding function design based on global implicit function theorem is then developed. The obtained results are verified on the trajectory tracking control of a two-WMR system developed in Chapter 4 with matched and mismatched uncertainties. Both simulation and experiment results show that the proposed approach is effective.

Chapter 6 focuses on the control problems of large-scale interconnected systems in a decentralised manner. A decentralised control strategy based on sliding mode techniques is proposed for a class of interconnected systems. The considered system has both linear and nonlinear parts with both matched uncertainties in the isolated subsystems and mismatched uncertainties associated with the interconnections. Sliding mode controllers for each subsystem are designed in a decentralised manner by only employing local information. Case studies including a CSTR system and an automated highway system (AHS) are carried with simulation to demonstrate the effectiveness of the approach.

Chapter 7 develops a decentralised SMC design for fully nonlinear interconnected systems in the generalised regular form. The considered isolated subsystem and the interconnection are fully nonlinear. The considered system is in the generalised regular form, which makes this approach applicable to a broader class of nonlinear systems. A numerical example is then given to demonstrate the design process.

Chapter 8 investigates the problem of uncertainties in input distribution caused by modelling errors and uncertainties. By addressing the problems, a decentralised SMC for a class of large-scale nonlinear systems with nonlinear uncertainties in input distribution is then presented. By utilising the bounds of the uncertainties, the system is stabilised asymptotically in the presence of both matched uncertainties and mismatched uncertain interconnections under some mild conditions. The developed results are applied to a vehicle-following system in automated

highway systems with both longitudinal and lateral controllers. The simulation results show that the developed results are effective.

Finally, **Chapter 9** presents a summary of the main conclusions in this thesis. Discussion for the potential future work is also provided in this chapter.

CHAPTER. 2

MATHEMATICAL PRELIMINARIES

In this chapter, some fundamental mathematical definitions and lemmas are given to clearly outline the mathematical terms that will be recurringly used in the following chapters. To be specific, definitions and lemmas related to Lyapunov stability theory are given in Section 2.1, and Section 2.2 presents definitions and results related to the Frobenius Theorem. In Section 2.3, some other useful definitions and theorems, such as the mean-value theorem, are introduced.

2.1. Lyapunov Stability

Throughout the development of entire system theory, stability theory plays a significant role in analysis and design of a system. In this thesis, the stability of equilibrium points, which is usually characterised in the sense of Lyapunov named after a Russian mathematician and engineer who laid the foundation of the entire theory [8], is recurringly discussed. Therefore, some main results of stability of equilibrium points are provided in this section.

Consider an autonomous system

$$\dot{x} = f(x) \tag{2.1}$$

where $x \in \mathcal{D} \subset \mathcal{R}^n$, and $f : D \to \mathcal{R}^n$ is a locally Lipschitz map.

Definition 2.1 (**Stability and Asymptotically Stability** [8])**.** A equilibrium point $x = 0$ of system (2.1) is said to be

- *stable* if, for each $\epsilon > 0$, there exits $\delta = \delta(\epsilon, t_0) > 0$ such that

$$\|x(t_0)\| < \delta \Rightarrow \|x(t)\| < \epsilon, \quad \forall t \geq t_0 \geq 0 \tag{2.2}$$

- *unstable* if it is not stable.
- *uniformly stable* if, for each $\epsilon > 0$, there exits $\delta = \delta(\epsilon) > 0$, independent of t_0, such that (2.2) is satisfied.
- *asymptotically stable* if it is stable and there is a positive constant $c = c(t_0)$ such that $x(t) \to 0$ as $t \to \infty$, for all $\|x(t_0)\| < c$.

Then, without loss of generality, consider a linear autonomous system

$$\dot{x} = Ax \tag{2.3}$$

where $x \in \mathcal{R}^n$.

Lemma 2.1 (**Stability of Linear System** [8])**.** *An equilibrium point $x_0 = 0$ of system (2.3) is said to be stable if and only if all eigenvalues λ_i of A satisfy* $\mathrm{Re}\lambda_i \leq 0$ *and for every eigenvalue with* $\mathrm{Re}\lambda_i = 0$ *and algebraic multiplicity $q_i \geq 0$,* $\mathrm{rank}(A - \lambda_i I) = n - q_i$*. The equilibrium point is said to be asymptotically stable if and only if all eigenvalues of A satisfy* $\mathrm{Re}\lambda_i < 0$*.*

Definition 2.2 (**Hurwitz and Lyapunov Equation** [8])**.** A matrix A of system (2.3) is said to be *Hurwitz* if and only if for any given positive definite symmetric matrix Q there exists a positive definite symmetric matrix P satisfies

$$PA + A^\tau P = -Q \tag{2.4}$$

Moreover, if A is Hurwitz, then P is the unique solution of (2.4), and equation (2.4) is called the *Lyapunov equation*.

For nonlinear systems, the following theorem is usually used to determine the stability of the systems.

Lemma 2.2 (**Lyapunov Stability Theorem** [8]). *Let $x = 0$ be an equilibrium point for system (2.1) and $\mathcal{D} \subset \mathcal{R}^n$ be a domain containing $x = 0$. Let $V : \mathcal{D} \to \mathcal{R}$ be a continuously differentiable function such that*

$$V(0) = 0 \quad \textit{and} \quad V(x) > 0 \quad \textit{in} \quad \mathcal{D} - \{0\} \tag{2.5}$$

$$\dot{V}(x) \leq 0 \quad \textit{in} \quad \mathcal{D} \tag{2.6}$$

Then, $x = 0$ is stable. Moreover, if

$$\dot{V}(x) < 0 \quad \textit{in} \quad \mathcal{D} - \{0\} \tag{2.7}$$

then $x = 0$ is asymptotically stable.

For a non-autonomous system

$$\dot{x} = f(t, x) \tag{2.8}$$

where $x \in \mathcal{D} \subset \mathcal{R}^n$ where $\mathcal{D}$ contains the origin $x = 0$ and $f : \mathcal{R}^+ \times \mathcal{D} \to \mathcal{R}^n$ is piecewise continuous in t and locally Lipschitsz in x on $\mathcal{R}^+ \times \mathcal{D}$.

Definition 2.3 (**Class $\mathcal{K}$ functions** [8]). A continuous function $\alpha : [0, a) \to [0, \infty)$ is said to belong to class $\mathcal{K}$ if it is strictly increasing and $\alpha(0) = 0$. It is said to belong to class $\mathcal{K}_\infty$ if $a = \infty$ and $\alpha(r) \to$ as $r \to \infty$

Definition 2.4 (**Class $\mathcal{KL}$ functions** [8]). A continuous function $\beta : [0, a) \times [0, \infty) \to [0, \infty)$ is said to belong to class $\mathcal{KL}$ if, for each fixed s, the mapping $\beta(r, s)$ belongs to class $\mathcal{K}$ with respect to r and, for each fixed r, the mapping $\beta(r, s)$ is increasing with respective to s and $\beta(t, s) \to \infty$ as $s \to \infty$.

Lemma 2.3 (**Expanded Lyapunov Asymptotically Stability Theorem** [8]). *Let $x = 0$ be an equilibrium point of system (2.8) and $\mathcal{D} \subset \mathcal{R}^n$ be a domain containing $x = 0$. Let $V : [0, \infty) \times \mathcal{D} \to \mathcal{R}$ be a continuously differentiable function such that*

$$W_1(x) \leq V(t, x) \leq W_2(x) \tag{2.9}$$

$$\frac{\partial V}{\partial t} + \frac{\partial V}{\partial x} f(t, x) \leq -W_3(x) \tag{2.10}$$

$\forall t \geq 0$ and $\forall x \in \mathcal{D}$, where $W_i(x)$ for $i = 1, 2, 3$ are continuous positive definite functions on $\mathcal{D}$. Then, $x = 0$ is uniformly asymptotically stable. Moreover, if r and c are chosen such

that $B_r = \{\|x\| \leq r\} \subset D$ *and* $c < \min_{\|x\|=r} W_1(x)$*, then every trajectory starting in* $\{x \in B_r | W_2(x) \leq c\}$ *satisfies*

$$\|x(t)\| \leq \beta(\|x(t_0)\|, t - t_0), \quad \forall t \geq t_0 \geq 0$$

for some class $\mathcal{KL}$ *function* β*. Finally, if* $D = \mathcal{R}^n$ *and* $W_1(x)$ *is radially unbounded, then* $x = 0$ *is globally uniformly asymptotically stable.*

It is straightforward to see that Lemma 2.3 expands the original Lyapunov stability theory to time-varying cases.

Lemma 2.4 (**Converse Lyapunov Function** [8])**.** *Let* $x = 0$ *be an equilibrium point for the nonlinear system*

$$\dot{x} = f(t, x)$$

where $f : [0, \infty) \times \mathcal{D} \to \mathcal{R}^n$ *is continuously differentiable,* $\mathcal{D} = \{x \in \mathcal{R}^n | \|x\| < r\}$*, and the Jacobian matrix* $[\partial f / \partial x]$ *is bounded on* $\mathcal{D}$*, uniformly in* t*. Let* k*,* λ *and* r_0 *be positive constants with* $r_0 < r/k$*. Let* $D_0 = \{x \in \mathcal{R}^n | \|x\| < r_0\}$*. Assume that the trajectories of the system satisfy*

$$\|x(t)\| \leq k\|x(t_0)\|e^{-\lambda(t-t_0)}, \quad \forall x(t_0) \in \mathcal{D}_0, \quad \forall t \geq t_0 \geq 0$$

Then, there exits a function $V : [0, \infty) \times \mathcal{D}_0 \to \mathcal{R}$ *such that*

$$\begin{aligned} \alpha_1(\|x\|) \leq V(t, x) &\leq \alpha_2(\|x\|) \\ \frac{\partial V}{\partial t} + \frac{\partial V}{\partial x} f(t, x) &\leq -\alpha_3(\|x\|) \\ \left\| \frac{\partial V}{\partial x} \right\| &\leq \alpha_4(\|x\|) \end{aligned} \tag{2.11}$$

where $\alpha_i(\cdot)$ *for* $i = 1, 2, 3, 4$ *are class* $\mathcal{K}$ *functions defined on* $[0, r_0]$*. If the system is autonomous,* V *can be chosen independent of* t*.*

From Lemma 2.4, it can be seen that if a system is controllable, then a Lyapunov function always exits.

2.2. Frobenius Theorem

The Frobenius theorem is used for the discussion of existence of regular form for nonlinear systems. The necessary definitions that required for the theorem is provided as follows.

Definition 2.5 (**Nonsingular and Singular Distribution** [32])**.** A distribution Δ on a manifold $\mathcal{N}$ is said to be *nonsingular* if there exits an integer d such that

$$\dim \Delta(p) = d \tag{2.12}$$

for all $p \in \mathcal{N}$, or *singular* otherwise.

Definition 2.6 (**Complete Integrable** [32])**.** A non-singular d-dimensional distribution Δ, defined on an open set U of $\mathcal{R}^n$, is said to be *complete integrable* if, for each point $x^\circ \in U$ there exists a neighborhood U° of x°, and $n-d$ real-valued smooth functions $\lambda_1, \ldots, \lambda_{n-d}$, all defined on U°, such that

$$\text{span}\{\frac{\partial \lambda_1}{\partial x}, \ldots, \frac{\partial \lambda_{n-d}}{\partial x}\} = \Delta^\perp(x) \tag{2.13}$$

on U°, where $\Delta^\perp(x)$ is an annihilator of $\Delta(x)$ that is a set of convectors which annihilates all vectors in $\Delta(x)$.

Definition 2.7 (**Lie Brocket** [32])**.** Let f, g be two smooth vector fields on $U \subset \mathcal{R}^n$, define a product $[f, g]$ with the rule

$$[f, g](x) = \frac{\partial g}{\partial x} f(x) - \frac{\partial f}{\partial x} g(x)$$

$\forall x \in U$. The product $[f, g]$ is said to be the *Lie Bracket* of the two vector fields f and g.

Definition 2.8 (**Involutive** [32])**.** A distribution Δ is said to be *involutive* if the Lie bracket $[\tau_1, \tau_2]$ of any pair of vector fields τ_1 and τ_2 belonging to Δ is a vector field which belongs to Δ, i.e. if

$$\tau_1 \in \Delta, \tau_2 \in \Delta \Rightarrow [\tau_1, \tau_2] \in \Delta$$

Then the Frobenius theorem is ready to be presented.

Lemma 2.5 (**Frobenius Theorem** [32])**.** *A nonsingular distribution is completely integrable if and only if it is involutive.*

2.3. Others

For mapping $f : A \to B$ and $g : C \to D$, define the composition $g \circ f$ with the map

$$g \circ f : f^{-1}(B \cap C) \to D$$

defined by $g \circ f(\xi) = g(f(\xi))$ for every $\xi \in f^{-1}(B \cap C)$. Define function $r_i : \mathcal{R}^d \to \mathcal{R}$ by

$$r_i(x) = x_i$$

where $x = \text{col}(x_1, x_2, \ldots, x_d) \in \mathcal{R}^d$. Let $\alpha = (\alpha_1, \ldots, \alpha_d)$ be a d-tuple of non-negative integers, then define

$$[\alpha] = \sum \alpha_i$$

and

$$\frac{\partial^\alpha}{\partial r^\alpha} = \frac{\partial^{[\alpha]}}{\partial r_1^{\alpha_1} \cdots \partial r_d^{\alpha_d}}$$

If $\alpha = (0, \ldots, 0)$, then let

$$\frac{\partial^\alpha}{\partial r^\alpha}(f) = f$$

Definition 2.9 (**Class $\mathcal{C}^k$ function**[33])**.** Let $\mathcal{D} \subset \mathcal{R}^d$ be open, and let $f : \mathcal{D} \to \mathcal{R}$. for k a non negative integer, if the partial derivatives $\partial^\alpha f / \partial r^\alpha$ exist and are continuous on $\mathcal{D}$ for $[\alpha] \leq k$. f is said to be *differentiable of class* $\mathcal{C}^k$ on $\mathcal{D}$ (or simply that f is $\mathcal{C}^k$), In particular, f is $\mathcal{C}^0$ if f is continuous. If $f : \mathcal{D} \to \mathcal{R}^n$, then f is said to be *differentiable of class* $\mathcal{C}^k$ if each of the component function $f_i = r_i \circ f$ is $\mathcal{C}^k$. f is said to be $\mathcal{C}^\infty$ if it is $\mathcal{C}^k$ for all $k \geq 0$.

Consider a system

$$\dot{x} = f(x, u) \qquad x \in \mathcal{R}^n, \quad u \in \mathcal{R}^m \tag{2.14}$$

where the vector field $f : \mathcal{R}^n \to \mathcal{R}^n$ is $\mathcal{C}^1$. Given a point $x_0 \in \mathcal{R}^n$, and a $\mathcal{C}^1$ feedback control law

$$u = u(x) \tag{2.15}$$

so that the system is locally asymptotically stable at the equilibrium point x_0. Without loss of generality, assume that $x_0 = 0$.

Lemma 2.6 (**Brockett's necessary condition** [34])**.** *A necessary condition for the existence of a class $\mathcal{C}^1$ feedback law (2.15) rendering $x_0 \in \mathcal{R}^n$ locally asymptotically stability for the closed-loop system (2.14) is that for all $\|y\|$ is sufficiently small, the vector field $\tilde{f} : \mathcal{R}^n \to \mathcal{R}^n$ defined by*

$$\tilde{f}(x) = f(x, u) - y,$$

where f is defined in (2.14), has an equilibrium point.

Lemma 2.7. *Assume that $X = X(t) \in \mathcal{R}^n$ and $Z = Z(t) \in \mathcal{R}^n$ are continuous in $t \in \mathcal{R}^+$, and $T(X) \in \mathcal{R}^{n\times n}$ is a functional matrix with*

$$Z = T(X)X \tag{2.16}$$

in $X \in \mathcal{R}^n$. Then $\lim_{t\to\infty} X(t) \to 0$ if $\lim_{t\to\infty} Z(t) \to 0$ when $T(X)$ is nonsingular and bounded in $X \in \mathcal{R}^n$.

Proof. since $T(X)$ is nonsingular, it is straightforward to see that

$$\|X\| = \|T^{-1}(X)Z\| \leq \|T^{-1}(X)\|\|Z\| \tag{2.17}$$

Since $T(X)$ is bounded, there exists a positive constant M such that

$$\|T^{-1}(X)\| \leq M \tag{2.18}$$

Then

$$\|X\| \leq \|T^{-1}(X)\|\|Z\| \leq M\|Z\| \tag{2.19}$$

Hence the conclusion follows. ■

Lemma 2.8 (**Global Implicit Function Theorem** [35]). *Assume that $f : \mathcal{R}^p \times \mathcal{R}^m \longmapsto \mathcal{R}^m$ is a continuous mapping and it is continuously differentiable with respect to the variable $\xi \in \mathcal{R}^m$. If there exists a constant $d > 0$ such that*

$$\Big|[\frac{\partial f}{\partial \xi}]_{ii}\Big| - \sum_{j\neq i}\Big|[\frac{\partial f}{\partial \xi}]_{ij}\Big| \geq d, \quad i = 1, \ldots, m. \tag{2.20}$$

for any $(z, \xi) \in \mathcal{R}^p \times \mathcal{R}^n$ where $\left[\frac{\partial f}{\partial \xi}\right]_{ij}$ denotes the ij th entry of the Jacobian matrix $[\partial f/\partial \xi]$ and $p = n - m$, then there exists an unique mapping $g : \mathcal{R}^p \longmapsto \mathcal{R}^m$ such that $f(z, g(z))$=0. Moreover, this mapping $g(\cdot)$ is continuous. Furthermore, if $f(\cdot)$ is a class $\mathcal{C}^1$ function, then $g(\cdot)$ is a class $\mathcal{C}^1$ function.

If x and y are distinct points in $\mathcal{R}^n$, then the *line segment* $L(x, y)$ joining x and y is

$$L(x, y) = \{z|z = \theta x + (1 - \theta)y, \quad 0 < \theta < 1\}$$

Lemma 2.9 (**Mean-value Theorem** [8]). *Assume that $f : \mathcal{R}^n \to \mathcal{R}$ is continuously differentiable at each point x of an open set $\mathcal{D} \subset \mathcal{R}^n$. Let x and y be two points of $\mathcal{D}$ such that the line segment $L(x, y) \subset \mathcal{D}$. Then there exists a point z of $L(x, y)$ such that*

$$f(y) - f(x) = \frac{\partial f}{\partial x}|_{x=z}(y - z)$$

CHAPTER. 3

FUNDAMENTAL KNOWLEDGE AND BASIC CONCEPT

Chapter 1 has briefly introduced the background and motivation of this research, which includes the challenges of designing control for complex systems. To establish a basic understanding of this work, necessary background knowledge and basic concepts related to this thesis are to be discussed in detail in this chapter. To be specific, basic knowledge of state feedback and related basic definitions are given in Section 3.1. The literature in the area of SMC is then reviewed in Section 3.2. Notably, the regular form-based SMC is introduced in Section 3.2.3, and the existence of such form for a nonlinear system is discussed based on the Frobenius theorem in Section 3.2.4. Section 3.3 presents mathematical definitions of nonholonomic systems in details. In Section 3.4, a literature survey and basic knowledge related to large-scale systems are given in details. Notably, the typical system structures used for large-scale systems are investigated and commented in 3.4.2. Before concluding this chapter in Section 3.6, examples of complex systems with modelling of two nonholonomic systems and three large-scale systems are given in Section 3.5.

3.1. State Space and Feedback Control

Feedback control is one of the most rigorously studied topics during the last few decades, and it has become the basic mechanism for regulation of equilibrium or homeostasis for systems such as mechanical, electrical systems etc. By utilizing mathematical insight, the appropriate feedback control law is designed to use the difference between the actual values of system variables and their desired values to determine the control signals. Thus the system is always making a certain correction to the desired equilibrium with the closed-loop controllers. Meanwhile, it is a common problem that the practical systems may not remain satisfactory due to the incomplete identification and external disturbances. Therefore, the effect of these uncertainties should be carefully taken into account in the control design process to guarantee that the system can still be adequately controlled in the worst scenario.

As the main concept of modern control theory, *state-space* refers to a set of coupled first-order differential equations with a set of internal variables. A minimum set of variables which can fully describe the system and its response to any given set of *inputs* are called *state variables*. Then the set of *outputs* can be represented by a set of algebraic equations which describes the relationship between the state variables and the physical output variables. The diagram of an n-the order system with m inputs and p outputs is shown in Fig.3.1.

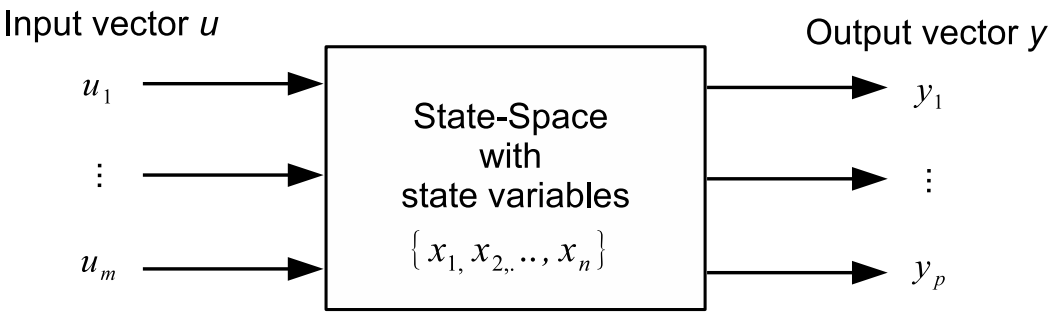

Figure 3.1: Over view of system plant in modern control theory

To be specific, a dynamical control system shown in Fig.3.1 usually can be described by a

set of differential equations:

$$\begin{aligned}\dot{x}_1 =& f_1(t, x, u)\\ \dot{x}_2 =& f_2(t, x, u)\\ \vdots =& \quad \vdots\\ \dot{x}_n =& f_n(t, x, u)\end{aligned} \tag{3.1}$$

where $\dot{\xi} := d\xi/dt$, and $x(t) \in \mathcal{R}^n$ denotes the state vector as a set of state variables with $x(t) := \text{col}(x_1(t), x_2(t), \ldots, x_n(t))$. $u \in \mathcal{R}^m$ and $t \in \mathcal{R}^+$ denote input/control vector and time respectively. Function $f_i(t, x, u)$ describe the dynamics of the state variable x_i for $i = 1, 2, \ldots, n$. With the time-varying n-dimensional vector $x(t)$, an n-dimensional *state-space* is thus described by the set of differential equations (3.1).

The relationship between the outputs and the states can be described by an algebraic equation as

$$\begin{aligned}y_1 =& h_1(t, x)\\ y_2 =& h_2(t, x)\\ \vdots =& \quad \vdots\\ y_p =& h_p(t, x)\end{aligned} \tag{3.2}$$

where $y_1(t), y_2(t), \ldots, y_p(t)$ are the system outputs. Define the output vector

$$y(t) := \text{col}(y_1(t), y_2(t), \ldots, y_p(t)) \in \mathcal{R}^p$$

and function vectors

$$f(\cdot) := \text{col}(f_1(\cdot), f_2(\cdot), \ldots, f_n(\cdot))$$
$$h(\cdot) := \text{col}(h_1(\cdot), h_2(\cdot), \ldots, h_p(\cdot))$$

then equation (3.1)-(3.2) can be rewritten in vector form as:

$$\dot{x} = f(t, x, u) \tag{3.3}$$

$$y = h(t, x) \tag{3.4}$$

A system in the form of (3.3) with $m, p = 1$ is called *single-input single-output* (SISO) system and system with $m, p > 1$ are called *multi-input and multi-output* (MIMO) system.

For the illustrating purposes, consider the following linear system:

$$\dot{x} = Ax + Bu \tag{3.5}$$

$$y = Cx \tag{3.6}$$

where $A \in \mathcal{R}^{n\times n}$, $B \in \mathcal{R}^{n\times m}$ and $C \in \mathcal{R}^{p\times n}$ are constant matrix, (A, B) is controllable and (A, C) is observable. Additionally, since a time delay for an input u will result in the same time delay on the output y in system (3.5), system (3.5) is called a *time-invariant* system [8]. A *time-variant* system is a system that is not time invariant. The vector block diagram for the linear system (3.5) is shown in Fig.3.2.

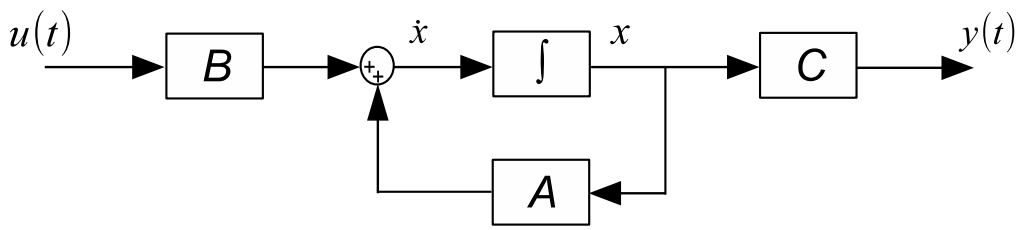

Figure 3.2: Diagram block of system (3.5)-(3.6)

The *state feedback control* refers to the control design that utilize all the state information for the controller $u = u(x)$. For instance, for system (3.5), by using the control law $u = -Kx$, the corresponding closed-loop system is

$$\dot{x} = (A - BK)x \tag{3.7}$$

where K is a constant matrix. Then the problem of the state feedback control is to find a suitable constant feedback gain matrix K such that $(A - BK)$ is Hurwitz. The block diagram of a state feedback controller can be seen in Fig.3.3.

Sometime, the state information may not be accessible by the sensors. In this case, the controller can only access a subset of the state information, i.e. the output y. Controller in the form of $u = u(y)$ that only uses output information is known as *static output feedback control*. For instance, by using output feedback control law in the form $u = -K_c y$ for system (3.3)-(3.4), the corresponding closed-loop system is

$$\dot{x} = (A - BK_cC)x \tag{3.8}$$

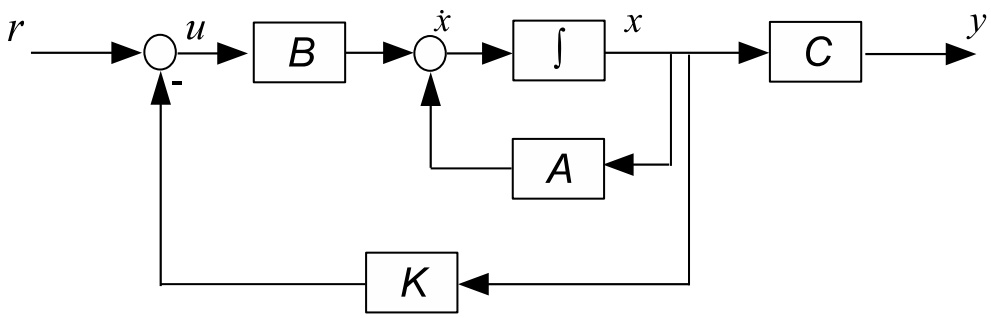

Figure 3.3: Diagram block of state feedback control for system (3.5)

where K_c is a constant matrix. Then the problem of output feedback is to find a constant feedback gain matrix K_c such that $(A - BK_cC)$ is Hurwitz.

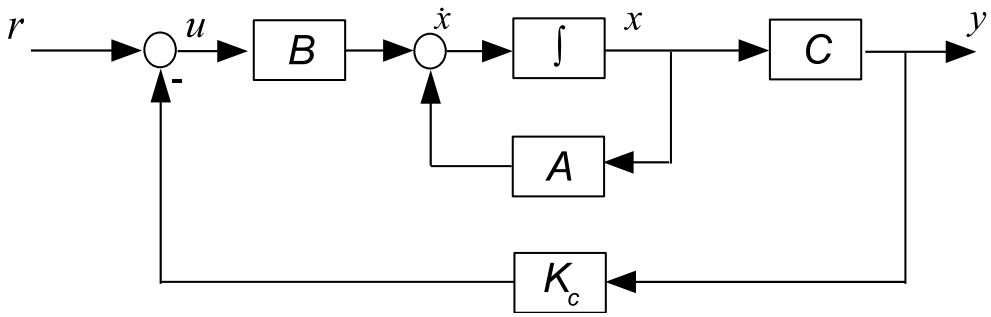

Figure 3.4: Diagram block of static output feedback control for system (3.5)-(3.6)

As mentioned in a survey paper published by V. L. Syrmos et al. in 1997 [36], various methods have been proposed to find a feedback gain K_c stabilising the single-input-single-output systems by using output feedback, such as the Youla parameterization method, inverse linear-quadratic approach, covariance assignability by output feedback, output structural constraint approach and coupled linear matrix inequality formulation, more detail information can be found in [36]. However, it is pointed out in [36] that all the proposed methods cannot be easily expanded to a multi-input-multi-output case. In terms of the pole placement problem, it is shown that if B and C have full rank and the system is minimal, max(m,p) poles can be assignable with output feedback gain K_c in Davison [37, 38, 39]. The necessary and sufficient conditions of existence of gain K_c is

$$m + p \leq n + 1$$

which was obtained by Davison et al. in [39], and Kimura in 1975 and 1978 [40, 41]. More

interesting results can also be found in [36]. However, due to the inefficiently testable necessary and sufficient conditions for the existence of a static output feedback, the static output feedback problems still remain as an open problem as they are just transformed into another unsolved problem or numerical searching problems without strictly proved guarantee of convergence [36].

An alternative method for the limited information problem is to use a dynamical system to estimate the state and then design a feedback controller with the estimated state $\hat{x}$. Such a dynamical system is called *observer*, and the feedback controller with the designed dynamics is called *observer-based control*, which is also known as *dynamic output feedback control*. For instance, for the linear system (3.3)-(3.4), define an observer in the form

$$\dot{\hat{x}} = (A + LC)\hat{x} + Bu - Ly \tag{3.9}$$

where L is a designed constant matrix such that the eigenvalues of $A + LC$ have negative real parts. Then by defining the error between the state and the estimated system with $e = x - \hat{x}$, the dynamic equation of the error system is

$$\dot{e} = (A + LC)e \tag{3.10}$$

With the Judicious choice for the poles of $(A + LC)$, the error $e(t)$ will converge to zero as t tends to infinity from any initial condition and thus $\hat{x}(t)$ will converge to $x(t)$ [16]. Then a feedback controller can be designed with the estimated state $\hat{x}(t)$.

Apparently, either static output feedback control or dynamic output feedback control will increase the system complexity due to the limited system information. It may even be much more challenging to guarantee the performance of the practical implementation due to the presence of uncertainties. Without loss of generality, consider the linear system (3.5) in the presence of uncertainties as

$$\dot{x} = Ax + B(u + \phi(t, x)) + \psi(t, x) \tag{3.11}$$

where $\phi(\cdot) \in \mathcal{R}^m$ and $\psi(\cdot) \in \mathcal{R}^n$ are unknown function vectors which represent the uncertainties. Uncertainties in the input channel, e.g. $\phi(\cdot)$, are often referred as *matched uncertainty*, and the rest, e.g. $\psi(\cdot)$, is called *mismatched uncertainties*. It is clear to see that both closed-loop system (3.7) and (3.8) will be significantly affected by the uncertainties. The convergence of observer (3.9) may not be guaranteed in this case as well. Therefore, it is of great importance to

design a robust feedback control. Among all these feedback methods mentioned above, state feedback control is mainly considered in this thesis.

3.2. Sliding Mode Control

SMC is a particular type of VSC which was firstly developed by Russian researchers Emelyanov and Barbashin in the early 1960s. After the book by Itkis [42] and the survey paper by Utkin in [1] were published, the design ideas were spread outside the Russia. With the development of modern control theory, the study of the nonlinear system in state space commenced in 1970 and MIMO systems are widely considered for more complex tasks since then [2]. This trend has dramatically promoted the development of sliding mode controllers, motivating the application of SMC in many practical systems [17]. In such systems, rules are determined so that the variety of structures can be switched in real time to perform specific system objectives, whereas applying a single structure for the system might be unstable. Based on the introduction of a "custom-designed" function, SMC has become one of the most significant control strategies because of its reduced-order dynamics and strong robustness [43, 16, 17].

Consider a simple double integrator

$$\ddot{\xi} = u \tag{3.12}$$

Then by choosing $x_1 = \xi$ and $x_2 = \dot{\xi}$ with $x = \text{col}(x_1, x_2)$, a simple linear system can be written as

$$\dot{x} = \begin{bmatrix} 0 & 1 \\ 0 & 0 \end{bmatrix} x + \begin{bmatrix} 0 \\ 1 \end{bmatrix} u \tag{3.13}$$

Select a *switching function*, which refers to a custom designed function that describe the dividing of the system plant in VSC theory, with $\sigma(x) = cx_1 + x_2$, and apply a discontinuous feedback control law with

$$u = \begin{cases} -cx_2 - \rho, & \sigma > 0; \\ -cx_2 + \rho, & \sigma < 0, \end{cases} \tag{3.14}$$

for all $\rho > 0$. The time response and the response of the phase-plane of the closed-loop system are shown in Fig.3.5 and Fig.3.6 respectively. From the response in phase portrait, it is clear

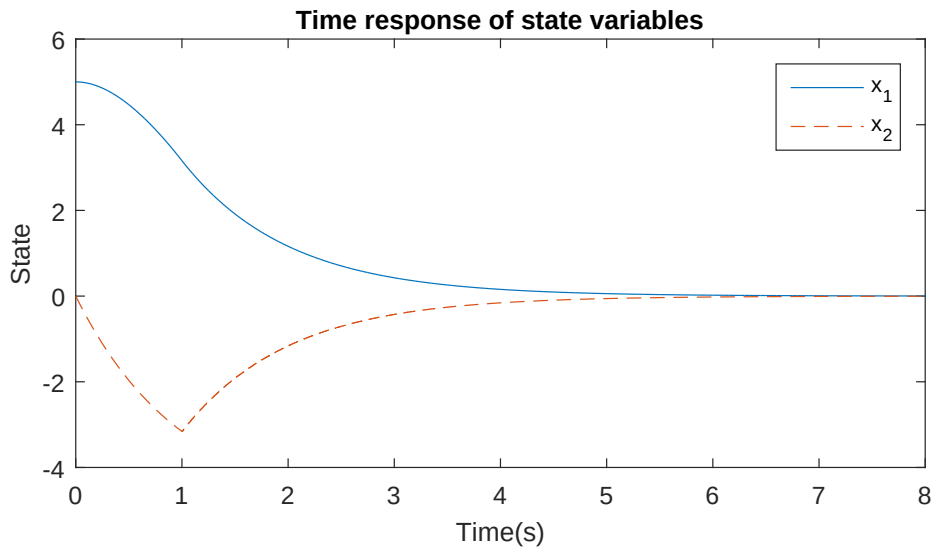

Figure 3.5: Time response of the state variables of system (3.13) with control (3.14)

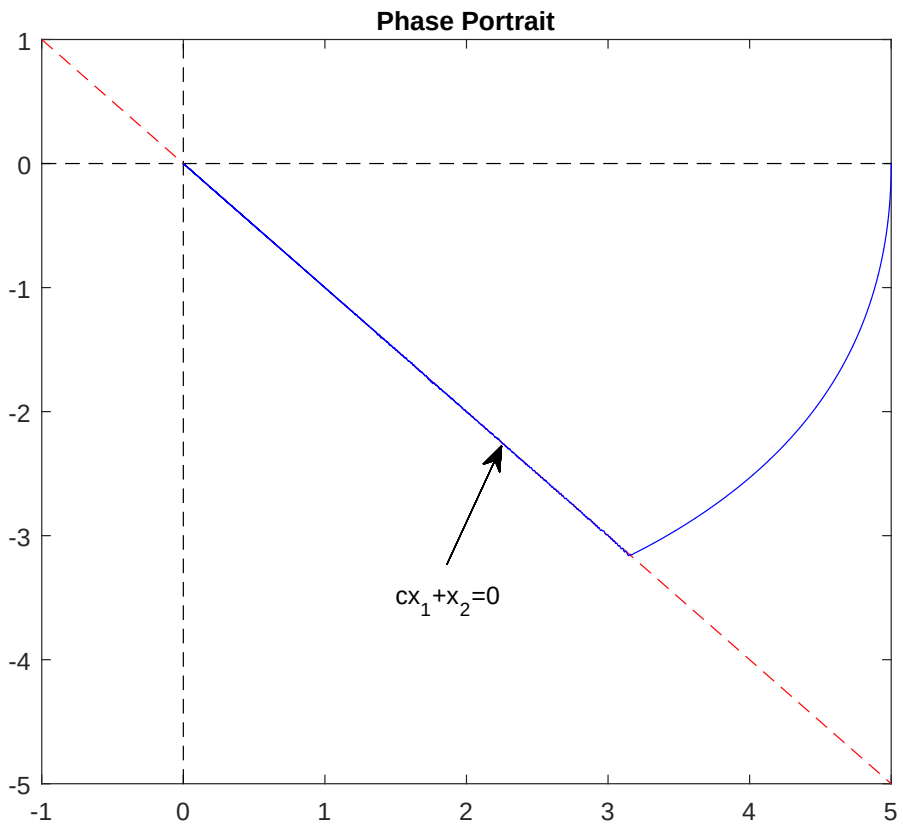

Figure 3.6: Phase portrait of system (3.13) with control (3.14)

that the system (3.13) with control law (3.14) exhibits an ideal sliding motion. From (3.13), it is straightforward to verify that when the sliding motion takes place, the system performance only depends on the constant parameter c in the switching function $\sigma(x) = cx_1 + x_2$.

From the phase portrait in Fig.3.6, it is clear that the system has two phase exhibiting differences response, which can be defined as the *sliding mode* and the *reaching phase* [17].

- **Sliding Mode** refers to the motion when the system trajectory moves along the *sliding surface* which is often defined by designing a switching function. When the system is restricted to the predefined surface, the order of the system is reduced. The reduced-order dynamics are called *sliding mode dynamics*.
- **Reaching Phase** refers to the motion before sliding motion occurs, starting from the initial point. To ensure the reachability, a VSC, which drives the system trajectory to the sliding surface and maintain the sliding motion, should be designed.

3.2.1. Existence of Sliding Mode

The existence of a sliding mode can be seen as a generalised stability problem which requires stability of the state trajectory to the sliding surface governed by the pre-defined switching function at least in a neighbourhood of $\{x|s = 0\}$. Therefore, the system state is required to approach the region of attraction of the sliding surface at least asymptotically [42, 1].

Without loss of generality, consider the following system

$$\dot{x} = f(t, x) + g(t, x)u \tag{3.15}$$

where $x \in \mathcal{R}^n$, $u \in \mathcal{R}^m$, $f(t, x) \in \mathcal{R}^n$ and $g(t, x) \in \mathcal{R}^{n\times m}$. Define the discontinuous feedback control is given by

$$u = \begin{cases} u^+(t, x), & \sigma(x) > 0 \\ u^-(t, x), & \sigma(x) < 0 \end{cases} \tag{3.16}$$

and the sliding surface

$$\sigma(x) = \text{col}(\sigma_1(x), \sigma_2(x), \ldots, \sigma_m(x)) = 0 \tag{3.17}$$

which is a $(n - m)$-dimensional manifold.

Definition 3.1 (**Sliding mode domain** [1]). A domain $\mathcal{S}$ in the manifold $\sigma(x) = 0$ is said to be a *sliding mode domain* if for each $\epsilon > 0$, a $\delta > 0$ exists such that any motion starting in the n-dimensional ϵ-vicinity of $\mathcal{S}$ may leave the n-dimensional ϵ-vicinity of $\mathcal{S}$ only through the n-dimensional ϵ-vicinity of the boundaries of S (Fig. 3.7)

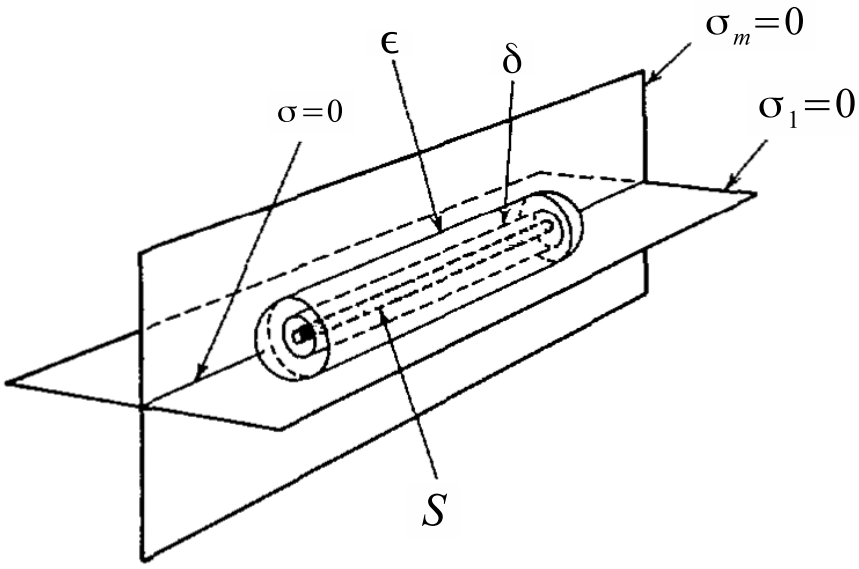

Figure 3.7: Sliding mode domain adapted from [1]

Lemma 3.1 (**Existence of a sliding mode** [1]). *For the $(n-m)$-dimensional domain $\mathcal{S}$ to be the sliding mode domain, it is sufficient that in some n-dimensional domain Ω, $\mathcal{S} \subset \Omega$, there exits a continuously differential function $V(t, x, \sigma)$, satisfying the following condition:*

1). V is positive definite with respect to σ and for any $x \in \mathcal{S}$ and t

$$\inf_{\|\sigma\|=\rho} V = h_\rho, \quad \sup_{\|\sigma\|=\rho} V = H_\rho \tag{3.18}$$

where $h_\rho \neq 0$ if $\rho > 0$, and h_ρ and H_ρ depend only on ρ.

2). Time derivative of V for (3.15) has negative supremum on small enough spheres $\|\sigma\| = \rho$ with removed points on the discontinuity surfaces where this derivative does not exist.

The domain $\mathcal{S}$ is the set of x for which the origin in subspace $(\sigma_1, \sigma_2, \ldots, \sigma_m)$, i.e. $\sigma(x) = 0$, is an asymptotically stable equilibrium point for the dynamic system

$$\dot{\sigma} = \frac{\partial \sigma}{\partial x} f(t, x) + \frac{\partial \sigma}{\partial x} g(t, x) u \tag{3.19}$$

where $\sigma(x)$ is defined in (3.17) and $f(\cdot)$, $g(\cdot)$ and u are defined in (3.15) and (3.16). Since there is no method to generate Lyapunov function for arbitrary nonlinear system, there is no standard method to find the Lyapunov function V for system (3.19).

For the system (3.13) as an example, since it is a single input time-invariant system, a Lyapunov function can be chosen as

$$V(t, x, \sigma) = \frac{1}{2}\sigma^2(x) \tag{3.20}$$

which is globally positive definite with respect to σ. Therefore, by choosing a suitable control such that

$$\dot{V}(t, x, \sigma) = \sigma\dot{\sigma} < 0 \tag{3.21}$$

in the considered domain, the state trajectory of system (3.13) can reach the pre-defined sliding surface and maintain a sliding motion for all subsequent time. By expanding the inequality to system (3.15) on sliding surface $\sigma(x) = 0$, an inequality for the n-dimensional case is obtained as

$$\dot{V}(t, x, \sigma) = \sigma^\tau(x)\dot{\sigma}(x) < 0 \tag{3.22}$$

The inequality (3.22) is known as the *reachability condition* which ensures that the sliding manifold is reached asymptotically [16].

However, condition (3.22) can only guarantee that the system is driven to the sliding surface asymptotically. Therefore, condition (3.22) is often replaced by another reachability condition in the form

$$\dot{V}(t, x, \sigma) = \sigma^\tau(x)\dot{\sigma}(x) \leq -\eta\|\sigma(x)\| \tag{3.23}$$

which is known as η-reachability condition [1, 16]. In this case, it is guaranteed that the system will reach the sliding surface in finite time so that system (3.3) is asymptotically stable. The reaching gain η is then computed with feedback in the SMC design in many application [1].

3.2.2. Existence of Unique Solution and Equivalent Control

It is straightforward to see that the control defined in (3.16) is discontinuous, which results in a discontinuous righthand side of equation (3.15). Therefore, classical solution to the discontinuous system (3.15) may not exist. In this case, as pointed out in [44, 16], one of the conceptually straightforward solutions is the method of Filippov in [45, 46], which is the "average" of the solutions obtained from the approaching the point of discontinuity from different directions. Written for convenience as

$$\dot{x} = F(t, x) \tag{3.24}$$

where $F : \mathcal{R}^+ \times \mathcal{R}^n \to \mathcal{R}^n$ is discontinuous with respect to the state vector $x \in \mathcal{R}^n$. Let x_0 be a point of discontinuity on the surface $\mathcal{S}$, and $F_-(t, x_0)$ and $F_+(t, x_0)$ represents the limits of $F(t, x)$ as the point x_0 is approached from the opposite sides of the tangent plane to $\mathcal{S}$ at x_0, it has been shown in [45, 46] that the state trajectories of (3.24) are the solutions of the equation

$$\dot{x} = (1 - \alpha)F^- + \alpha F^+ = F_\alpha, \quad 0 < \alpha < 1 \tag{3.25}$$

where F_α is the obtained velocity vector of the state trajectory when the system is on the sliding surface. The concept can be conceptually illustrated in Fig. 3.8.

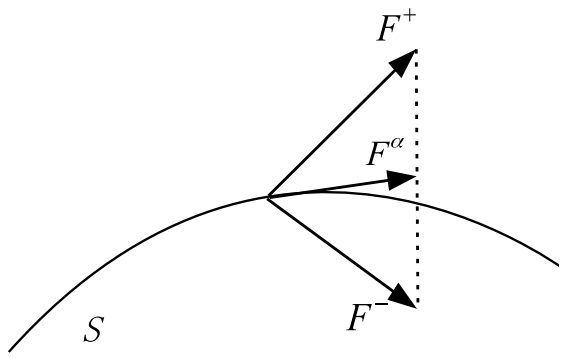

Figure 3.8: Illustration of the Filippov method

Based on that, the so-called *equivalent control* is proposed in [1], which is the solution to

$$\sigma(x) = 0, \quad \dot{\sigma}(x) = 0 \tag{3.26}$$

By differentiating $\sigma(x)$ with respect to t along the trajectory of (3.15), it yields

$$\dot{\sigma}(x) = \frac{\partial \sigma}{\partial x}\dot{x} = \frac{\partial \sigma}{\partial x}(f(t,x) + g(t,x)u) = 0 \tag{3.27}$$

Suppose there exists a solution u to the equation (3.27) with

$$u = u_{eq}(t,x) \tag{3.28}$$

which is the equivalent control of system (3.15) on sliding surface $(\sigma(x) = 0)$ [2]. Then the sliding mode dynamics governing the sliding motion can be obtained by

$$\begin{cases} \dot{x} = & f(t,x) + g(t,x)u_{eq}(t,x)) \\ s(x) = & 0 \end{cases} \tag{3.29}$$

For illustrate purpose, for a linear system described by

$$\dot{x} = Ax + Bu \tag{3.30}$$

when the sliding motion takes place with a predefined sliding function $s(x) = Sx$, it follows from $\dot{s}(x) = 0$ that the corresponding equivalent control is given by (see [16, 2])

$$u_{eq} = -(SB)^{-1}SAx \tag{3.31}$$

where the matrix S is chosen so that SB has full rank, which implies the equivalent control is unique. Then, the corresponding sliding motion can be described by

$$\begin{cases} \dot{x} = & Ax - B(SB)^{-1}SAx \\ s(x) = & 0 \end{cases} \tag{3.32}$$

Since the equivalent control (3.28) is derived from the case that ideal sliding motion occurs, it is not the actual control signals that applied to the system but the action necessary to maintain an ideal sliding motion on $\mathcal{S}$ [16]. The actual control signal often contains compensator that drives the system towards the sliding surface.

3.2.3. regular form-based Approach

Regular form is another method to analyze the sliding mode dynamics. For illustrating purpose, reconsider the linear system (3.5)

$$\dot{x} = Ax + Bu$$

Since the dimension of the input m is often less than the dimension of the system n, i.e. $m < n$, and by assumption rank$(B) = m$, there always exists an invertible matrix $T_r \in \mathcal{R}^{n\times n}$ such that

$$T_r B = \tilde{B} = \begin{bmatrix} 0 \\ \tilde{B}_2 \end{bmatrix} \tag{3.33}$$

where $B_2 \in \mathcal{R}^{m\times m}$. Then a transformation $z = T_r x$ can be constructed that can transfer the system (3.5) into two parts with the form

$$\dot{z}_1 = \tilde{A}_{11} z_1 + \tilde{A}_{12} z_2 \tag{3.34}$$

$$\dot{z}_2 = \tilde{A}_{21} z_1 + \tilde{A}_{22} z_2 + \tilde{B}_2 u \tag{3.35}$$

where $z_1 \in \mathcal{R}^{n-m}$ and $z_2 \in \mathcal{R}^m$, and

$$\tilde{A} = T_r A T_r^{-1} \begin{bmatrix} \tilde{A}_{11} & \tilde{A}_{12} \\ \tilde{A}_{21} & \tilde{A}_{22} \end{bmatrix}$$

It is clear that system (3.34) is independent to the control input. System (3.34)-(3.35) is referred as the *regular form*, equation (3.34) describes the *null space dynamics* and equation (3.35) describes the *range space dynamics* [16].

Lemma 3.2 (see [16])**.** *The matrix pair* $(\tilde{A}_{11}, \tilde{A}_{12})$ *is controllable if and only if the pair* (A, B) *is controllable.*

Define a linear sliding function as

$$\sigma(z) = Sz = Cz_1 + z_2 \tag{3.36}$$

where the design parameter $C \in \mathcal{R}^{m\times(n-m)}$ is a constant matrix.

When the sliding motion takes place

$$z_2 = -Cz_1 \tag{3.37}$$

The sliding mode of system (3.34)-(3.35) is then derived as

$$\dot{z}_1 = (\tilde{A}_{11} - \tilde{A}_{12} C) z_1 \tag{3.38}$$

which is a reduced-order system when compared with the original system (3.5). From Lemma 3.2, it can be seen that C can be chosen such that $(\tilde{A}_{11} - \tilde{A}_{12} C)$ is Hurwitz if (A, B) is controllable. Thus the sliding mode is asymptotically stable.

Invariant Properties

Suppose the system (3.34)-(3.35) are experiencing uncertainties. Then rewrite the system (3.34)-(3.35) as

$$\dot{z}_1 = \tilde{A}_{11}z_1 + \tilde{A}_{12}z_2 + \psi_1(t, z_1, z_2) \tag{3.39}$$

$$\dot{z}_2 = \tilde{A}_{21}z_1 + \tilde{A}_{22}z_2 + B_2u + \psi_2(t, z_1, z_2) \tag{3.40}$$

where $\psi_1(\cdot) \in \mathcal{R}^{(n-m)}$ and $\psi_2(\cdot) \in \mathcal{R}^m$. Then the corresponding sliding mode of system (3.39)-(3.40) with sliding function (3.36) can be described by

$$\dot{z}_1 = \tilde{A}_{eq}z_1 + \psi_1(t, z_1, -Cz_2) \tag{3.41}$$

where $\tilde{A}_{eq} = \tilde{A}_{11} - \tilde{A}_{12}C$. From (3.41), it is straightforward to see that during sliding phase, the dynamics of the sliding mode (3.41) is independent to the disturbance $\psi_2(\cdot)$ in system (3.40), which is the so-called *insensitivity property*. In this case, the system completely insensitive to matched uncertainties/external disturbances [16, 17, 18]. For the mismatched uncertainties $\psi_1(\cdot)$, it has been demonstrated that the sliding mode approach can be applied to control systems with mismatched uncertainties under some proper conditions , see for example [47, 28, 19, 29, 30].

Control Design

After designing a suitable sliding surface, it is naturally important to ensure that the system can reach the designed sliding surface and maintain on it thereafter. Several methods for the reachability problem are available in [1, 16]. Among them, a common structure of control is applied with

$$u = u_{eq} + u_n \tag{3.42}$$

where

$$u_{eq} = -(S\tilde{B})^{-1}S\tilde{A}z$$

is the equivalent control to maintain an ideal sliding motion, and u_n is a discontinuous term so that

$$\begin{aligned}\dot{\sigma}(z) =& S\dot{z} = S\tilde{A}z + S\tilde{B}(u_{eq} + u_n)\\ =& S\tilde{B}u_n = \tilde{B}_2u_n\end{aligned} \tag{3.43}$$

By choosing

$$u_n(z) = -\eta \tilde{B}_2^{-1} \frac{\sigma(z)}{\|\sigma(z)\|}, \quad \eta > 0$$

implies that

$$\sigma^\tau(z)\dot{\sigma}(z) = -\eta\|\sigma(z)\|$$

for $\sigma(z) \neq 0$, thus the η-reachability condition is satisfied which guarantee the finite-time reachability. The controller (3.42) is called unit vector controller.

Define

$$\text{sign}(\xi) = \begin{cases} 1 & \xi > 0 \\ 0 & \xi = 0 \\ -1 & \xi < 0 \end{cases} \tag{3.44}$$

replacing the term $\frac{\sigma(z)}{\|\sigma(z)\|}$, it is clear that sign$(x)$ is discontinuous, resulting in infinite number of switches in finite time when the system is around the designed sliding surfaces/manifolds [17]. To get an ideal sliding mode, it is assumed that the switch of the term sign(x) can be infinitely fast, which is obviously impossible in the practical system due to the delay caused by the physical limitation or any un-modelled dynamics. This phenomenon is known as *the chattering* problem in practical implementation as shown in Fig. 3.9.

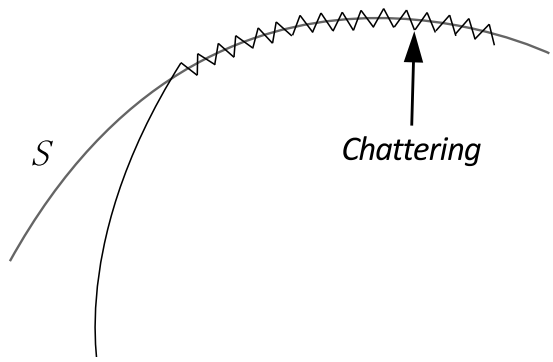

Figure 3.9: Chattering effect

Unexpected dynamics caused by the non-ideal switch may produce chattering which greatly affects the performance for many practical systems. For this reason, many efforts have been used to address the chattering problem. For example, define

$$\text{sgn}(\xi) = \frac{\xi}{\|\xi\| + \epsilon} \tag{3.45}$$

where $\epsilon \in \mathcal{R}^+$ is a small constant. Equation (3.45) is then a *boundary layer* which approximates the discontinuities of equation (3.44) and can be applied to reduce the chattering [31, 48] although the robustness of the systems is mildly reduced due to the approximation. High-order sliding mode techniques recently have been recognised as an effective approach regarding the chattering attenuation if the time derivative of the plant control is considered as the actual control variable [49, 50]. The continuous approximation appears to be much simpler, but the robustness of the systems are degraded at the mean time.

3.2.4. Existence of Regular Form for a Nonlinear Systems

It has been shown in Sec. 3.2.3 that the regular form for a controllable linear system (3.5) always exists if B has full rank. However, it may become a bit difficult when considering the nonlinear system.

Consider the nonlinear time-invariant system

$$\dot{x} = f(x) + g(x)u \tag{3.46}$$

where $x \in \mathcal{D} \subset \mathcal{R}^n$ and $u \in \mathcal{R}^m$. $f(\cdot) \in \mathcal{R}^n$ and $g(x) \in \mathcal{R}^{n\times m}$. Then suppose a transformation $z = T(x)$ with diffeomorphism $T : \mathcal{R}^n \to \mathcal{R}^n$ exists, define

$$T(x) = \text{col}(T_1(x), T_2(x)) \tag{3.47}$$

where $T_1(x) \in \mathcal{R}^{n-m}$ and $T_2(x) \in \mathcal{R}^m$ such that

$$\frac{\partial T}{\partial x} g(x) = \begin{bmatrix} 0 \\ G_2(z) \end{bmatrix} \tag{3.48}$$

Then the nonlinear system (3.46) will be transferred into the regular form

$$\dot{z}_1 = F_1(z) \tag{3.49}$$

$$\dot{z}_2 = F_2(z) + G_2(z)u \tag{3.50}$$

where $z = \text{col}(z_1, z_2)$. Then it is straightforward to see that the existence of the regular form for nonlinear system (3.46) is equivalent to the existence of the solution to the partial differential equation

$$\frac{\partial T_1}{\partial x} g(x) = 0 \tag{3.51}$$

where $T_1(x)$ is defined in (3.47). Let $g(x) = (g_1(x), g_2(x), \ldots, g_m(x))$ where $g_i(x) \in \mathcal{R}^n$ is vector field, and define

$$\mathcal{G} = \text{span}\{g_1, (x), g_2(x), \ldots, g_m(x)\} \tag{3.52}$$

which is a distribution spanned by $g_1(x), g_2(x), \ldots, g_m(x)$. It can be concluded from Definition 2.6 that the existence of solution to the partial differential equation (3.51) relies on the completely integrability of the distribution $\mathcal{G}$. Then from Lemma 2.5, it can be verified that the regular form for nonlinear system (3.46) exists if the distribution $\mathcal{G}$ defined in (3.52) is nonsingular and involutive.

3.3. Nonholonomic Systems

Suppose a mechanical or electrical system described by

$$\dot{q} = f(t, q, u) \tag{3.53}$$

where $q \in Q \in \mathcal{R}^n$ is an n-dimensional vector of generalised coordinates with

$$q = \text{col}(q_1, q_2, \ldots, q_n)$$

Generally, the considered space Q is in an n-dimensional smooth manifold, locally diffeomorphic to the Euclidean space $\mathcal{R}^n$. The generalised velocity at a generic point of a trajectory $q(t) \subset Q$ is described by its tangent vector $\dot{q}$ with

$$\dot{q} = \text{col}(\dot{q}_1, \dot{q}_2, \ldots, \dot{q}_n)$$

The geometric constraints may exist to be imposed on the mechanical system (3.53) with

$$h_i(q) = 0 \qquad i = 1, 2, \ldots, k \tag{3.54}$$

which restrict the possible motions of system (3.53) to an $(n-k)$-dimensional submanifold. For the velocity-dependent constraints which involve generalised coordinates q and their derivatives, e.g. first-order kinematic constraints with the form

$$a_i(q, \dot{q}) = 0 \qquad i = 1, 2, \ldots, k \tag{3.55}$$

In most cases, the kinematic constraints (3.55) are *Praffian constraints* [51], which can be described by

$$a_i^\tau(q)\dot{q} = 0 \qquad i = 1, 2, \ldots, k \tag{3.56}$$

If the kinematic constraints are integrable, there may exist k functions h_i such that

$$\frac{\partial h_i(q)}{\partial q} = a_i^\tau(q) \qquad i = 1, 2, \ldots, k \tag{3.57}$$

Substitute (3.57) into (3.56) yields

$$\frac{\partial h_i(q)}{\partial q}\dot{q} = 0 \qquad i = 1, 2, \ldots, k$$

which implies

$$h_i(q) = c_i \qquad i = 1, 2, \ldots, k$$

where c_i for $i = 1, 2, \ldots, k$ are some constants. In this case, the kinematic constraints are also geometric constraints.

Definition 3.2 (**Nonholonomic Constraints and Nonholonomic Systems** [51])**.** A set of constraints in the form (3.54) or a set of Pfaffian constants (3.56) that is integrable is called *holonomic constraints*. Otherwise, it is called *nonholonomic constraints*. Systems with nonholonomic constraints are said to be *nonholonomic systems*.

Although a nonholonomic system has also been proved to be controllable, the regulation of a nonholonomic system is full of challenges. Specifically, for a drift-less nonholonomic system in the form

$$\dot{q} = \sum_{i=1}^{m} g'(t, x)u \tag{3.58}$$

where $g'(\cdot) \in \mathcal{R}^n$ is smooth enough, then from the Brockett's necessary condition (**??**) in Lemma 2.6, it is straightforward to see that the existence of a continuous time-invariant feedback control law for system (3.58) can be guaranteed if and only if the numbers of inputs m equal to the number of states n. Since the dimension of the inputs is usually less than the dimension of states, it is straightforward that continuous time-invariant feedback control laws cannot achieve regulation control for a drift-less nonholonomic system, which makes the regulation tasks very challenging. To overcome that, the earlier efforts were mostly made on discontinuous time-invariant control law design and time-varying control design [52].

In [53], it is possible to stabilise the nonholonomic systems by designing an appropriate time-varying control law. Based on that, various expansion work for time-varying control laws arise[52]. The fundamental idea of the time-varying control law is to transfer the nonholonomic system into linear time-varying via time-varying coordinate transformation. Another kind of time-varying control laws for the nonholonomic systems is based on the use of homogeneous system coordinates [54]. Although the system in this method has a reasonable convergence rate, it cannot achieve global point stabilisation of nonholonomic systems.

To apply discontinues feedback control law is another alternative to avoid Brockett's necessary conditions. Therefore, various discontinues feedback control law has been developed for the nonholonomic systems, e.g. see σ process based approach [55], feedback linearization [56], invariant manifold technique [57]. As a typical form of discontinuous nonlinear control, VSC systems has its advantage when dealing with discontinuous systems. In [58], a VSC system was applied on a nonholonomic system with feedback linearization techniques for the regulation tasks, and the proposed method has effective simulation results. As the flexible configuration may result in various systems behaviour, the VSC control for regulation of nonholonomic systems is still an active area.

3.4. Large-Scale System

As discussed in Chapter 1, large-scale system is often known as a class of system with plenty of states. The main difficulties have been reported in several works in [59, 5, 4, 7, 2], i.e. dimensionality, information structure constraints, uncertainty and delays. These difficulties motivate the development of the theory of large-scale systems. Several general methodologies have been and are being elaborated, which can usually be concluded into the following three groups: decomposition [4], architectures [60], robustness and model simplification [59].

- *Decomposition* concerns the dimensionality problems of the large-scale systems. By decomposing the system into a collection of subsystems, the analysis and synthesis tasks of a large-scale system are greatly simplified. It has been demonstrated in [4] that decomposition may not only reduce computational complexity but also weaken the interaction effects. Subsystems obtained from the overlapping decomposition may not

even have the problems of interconnections.

- *Architectures* concerns the information structure inherent to the given problem. Because of the wide range of the problems considered and the desired goals to be achieved in a large-scale system, the control structures are various with different focuses, and thus resulting in different merits and limitations. In this thesis, a completely decentralised structure is considered since the reliability of such structure does not depend on the network performance. Besides, the developed decentralised control can be expanded to a quasi-decentralised scheme (e.g. see [61]) to improve the stability and robustness.

- *Robustness* concerns the ability to maintain desired performance in the presence of uncertainties including modelling error or interaction between subsystems, the so-called *interconnection*, on the bases of the stability analysis. It is essential for systems with disjoint decomposition as the interconnection may substantially affect the system stability in such systems. *Model simplification* mainly focuses on model reduction methods and approximations to reduce the complexity of the large-scale system [5].

3.4.1. Decomposition Techniques

Apparently, it is less complicated to analyse the robustness and stability of subsystems rather than the overall system when the dimension of the systems is intensively large, e.g. aircraft and satellite formations [62, 63], or the system is physically composed of several subsystems distributed in space, e.g. multi-machine power system [11]. Meanwhile, with the development of technology such as embedded computing, parallel processing, communication network, it has become increasingly economical and reliable to decompose a system into many simples systems with overlapping dynamics [4]. Therefore, decomposition plays a significant role in the control design phase for large-scale systems. In fact, some large-scale systems, e.g. multi-machine power systems [64, 65, 66], automated highway systems [67], already have natural spatial decompositions, i.e. the subsystems are physically defined according to their different locations/distributions, and thus the interconnections between each subsystem may have their physical significance. However, there are still many systems in reality where it is hard to find appropriate weak couplings [68]. For the system without natural spatial decompositions, the decomposition technique may be a suitable solution. Moreover, a proper decomposition may not only simplify the system but also weaken the interaction effects to improve the system

performance furthermore [4]. There are several decomposition techniques available, and the two typical type of decomposition techniques will be briefly introduced in the following subsection, i.e. disjoint decomposition and overlapping decomposition.

Disjoint decomposition

As been pointed out in [59], a system is often decomposed from conceptual or numerical reasons. The conceptual reason is mainly due to the physical separation of the subsystems. For instance, in automated highway systems [67], each vehicle can be a separate subsystem. On the other hand, a universal control technique for large-scale systems is required for the numerical reasons [59]. A typical disjoint decomposition is the so-called *nested epsilon decomposition* [5, 4]. Except for the system, the disjoint decomposition techniques can also be used to decompose the interconnection [4].

For illustrate purposes, rewrite the linear system (3.5) as

$$\dot{x} = Ax + Bu$$

Definition 3.3 (Epsilon decomposition [5])**.** Matrix A of system (3.5) is said to have an *epsilon decomposition* if there exits a permutation matrix P such that

$$P^{\tau} AP = A_D + \epsilon A_C \tag{3.59}$$

where $A_D = \text{diag} A_1, A_2, \ldots, A_N$ is a block-diagonal, ϵ is a small positive number and all the elements of A_C are smaller than one in magnitude.

Moreover, by increasing the threshold of ϵ, the system can be furthered decomposed, which is also known as the *nested epsilon decomposition*.

Definition 3.4 (**Nested epsilon decomposition** [4])**.** A matrix A is said to have a K*-fold epsilon decomposition* of there are $K > 0$ positive numbers $\epsilon_1 > \epsilon_2 >, \ldots, > \epsilon_K$ such that, by permutations of rows and columns, the matrix A can be represented as

$$\hat{A} = \hat{A}_0 + \epsilon_1 \hat{A}_1 + \cdots + \epsilon_K \hat{A}_K \tag{3.60}$$

where $\hat{A}_0$ is a block diagonal matrix and $\hat{A}_1, \hat{A}_2, \ldots, \hat{A}_K$ are all partitioned matrices with compatible blocks, such that each nonzero block appears in one and only one matrix $\hat{A}_i$ for $i = 1, 2, \ldots, K$, and none of the elements of any $\hat{A}_i$ is larger than one in magnitude.

The choice threshold, i.e. ϵ or $\epsilon_1 > \epsilon_2 >, \ldots, > \epsilon_K$ in nested epsilon decomposition, will significantly affect the strength of interconnections. Appropriate choice of the thresholds in the algorithm may preserve the weak coupling properties of the system, thus maintaining the stability of the overall system. Therefore, the control design for disjoint systems decomposed by nested epsilon decomposition mainly focus on the attenuation of interactions and uncertainties [69, 70, 71, 72, 73, 74]. The advantage of using ϵ decomposition is that it can represent not only the linear interactions but also nonlinear interactions and the uncertainty of the subsystem itself [4].

Overlapping decomposition

In some practical systems, the subsystems often share a common part. For the sake of conceptual or computational reasons, an alternative approach arises by using overlapping information sets [4], i.e. overlapping decomposition. It has been demonstrated in [4] that the interconnection after the decomposed will be a part of the subsystem and some subsystems may not even have an interconnection at all. The fundamental idea of the overlapping decomposition is to numerically expand the original system into a larger dimensional system which has weaker interconnection among subsystems, and then find the solution of the expanded system that can also stabilized the original system. This method has been rigorously developed into a general mathematical framework, i.e. the so-called *inclusion principle* [59, 4]. To rigorously formulate the inclusion principle, consider two dynamic system **S** and $\tilde{\mathbf{S}}$

$$\mathbf{S}: \quad \dot{x} = Ax + Bu \tag{3.61}$$

$$\tilde{\mathbf{S}}: \quad \dot{\tilde{x}} = \tilde{A}\tilde{x} + \tilde{B}u \tag{3.62}$$

where $x \in \mathcal{D} \subset \mathcal{R}^n$ and $\tilde{x} \in \tilde{\mathcal{D}} \subset \mathcal{R}^{\tilde{n}}$ are state of system **S** and $\tilde{\mathbf{S}}$ respectively. $u \in \mathcal{R}^m$ is the input of both systems.

Definition 3.5. System $\tilde{\mathbf{S}}$ is said to *includes* system **S**, or equivalently, a system **S** is said to *be included* by system $\tilde{\mathbf{S}}$ if there exists an ordered pair of matrix (U, V) with $U \in \mathcal{R}^{n\times\tilde{n}}$ and $V \in \mathcal{R}^{\tilde{n}\times n}$ such that $UV = I_n$, and for any initial state $x_0 \in \mathcal{D}$ of **S** and any fixed input $u(t)$, we have

$$x(t; x_0, u) = U\tilde{x}(t; Vx_0, u), \quad \forall t \geq 0 \tag{3.63}$$

After expanding the system into a larger dimensional system without interconnections that includes the original system, a local feedback controller can be designed for each subsystem on the expanded system plant. Although the inclusion principle is expandable to nonlinear systems, constraints may be too strict for practical systems [4]. Since the expansion and contraction operation must be performed with a non-square transformation function, the existence of such transformation function, which is an essential part of the decomposition, may be too difficult to be found for the nonlinear systems. Moreover, since the expanded system has to include the original system, the system complexity is inevitably increased due to the expansion and contraction. Therefore, due to the strict constraints required for the nonlinear system and the increased complexity during the decomposition, the overlapping method is not considered in this thesis.

3.4.2. Architecture

In order to simplify the analysis, consider a large-scale system

$$\dot{x} = F(t, x, u) \tag{3.64}$$

where $x \in \mathcal{R}^N$, $u \in \mathcal{R}^m$ and $F(\cdot) \in \mathcal{R}^N$ are the state, input and vector function respectively. Suppose a proper decomposition process exists, (e.g. see Section 3.4.1), thereby the overall system can be separated into a set of subsystems connected through interconnection, which is described by

$$\dot{x}_i = f_i(t, x_i, u_i) + H_i(t, x), \quad i = 1, 2, \ldots, N \tag{3.65}$$

where $x_i \in \mathcal{R}^{n_i}$ and $u_i \in \mathcal{R}^{m_i}$ denote the state and input signal of ith subsystem. $H_i(\cdot)$ denote the interconnection coming from the other subsystems. System

$$\dot{x}_i = f_i(t, x_i, u_i) \tag{3.66}$$

is called the ith *isolated subsystem* of system (3.65). In such systems, although each isolated subsystem may exhibit desired performance, the unexpected dynamics caused by the interconnection may greatly affect or even devastate the stability of the whole system plant. Consider the form of system (3.65) in

$$\dot{x}_i = f_i(t, x_i) + g_i(t, x_i)(u_i + \phi_i(t, x_i)) + H_i(t, x), \quad i = 1, 2, \ldots, N \tag{3.67}$$

where $\phi_i(\cdot)$ denote the matched uncertainties. Then system

$$\dot{x}_i = f_i(t, x_i) + g_i(t, x_i)u_i \tag{3.68}$$

is called the ith *nominal isolated subsystem* of system (3.67)

As part of the overall system, each subsystem is controlled by its local actuator u_i. In the following subsections, four typical architecture, i.e. centralised structure, hierarchical structure, distributed structure and decentralised structure, will be briefly introduced.

Centralised Structure

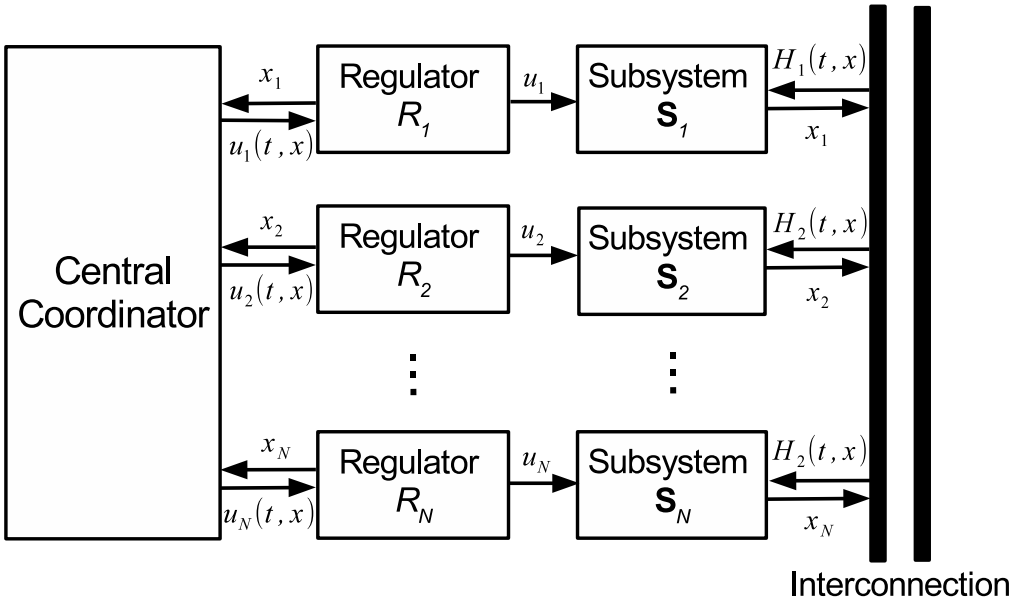

Figure 3.10: Centralised system structure

For a relative small-scale system, a system structure shown in Fig. 3.10, in which the control u_i utilises all the state information to stabilise the overall system, is the so-called *centralised structure*. The local controller with centralised structure is often in the form

$$u_i = u_i(t, x) \tag{3.69}$$

With a complete graph of the system plant, a centralised strategy might provide better control performance than a complete decentralised control strategy since the central coordinator has much more information than a local DM to deal with the interactions. Therefore, centralised

system structure is ubiquitous in most small-scale systems. However, as the system nowadays has become increasingly complicated, the system inevitably requires computing units with much larger memory and much faster computation capability. The extensive amount of information fed into the coordinator and the massive computing tasks may make the centralised scheme difficult or even impossible to be implemented [59]. Furthermore, the scale of the system, such as intelligent transportation infrastructures [67, 75, 76], may keep increasing with extra functionality required or new subsystems joining in, which will eventually become a problem.

Hierarchical Structure

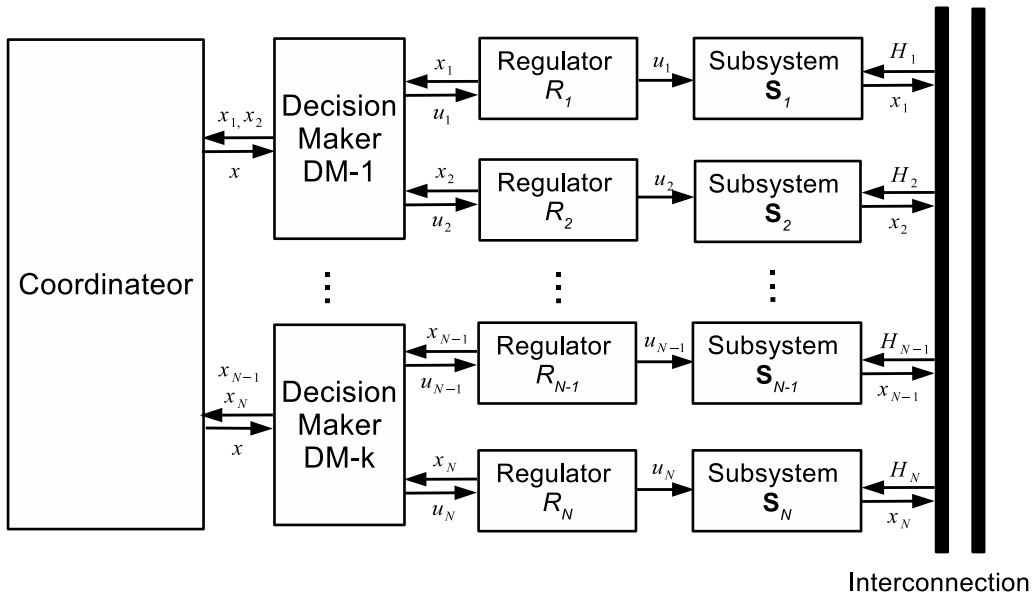

Figure 3.11: Two level hierarchical structure

Many industrial, economic or sociological systems possess a hierarchical structure [60]. The research about hierarchical structure started in the 1960s and attracted increasing attention since then [77, 78, 79]. More work can be found in various application, such as augmenting bulk system [80], power system [81, 82, 83, 84], energy management system [85]. The highest layer of the hierarchy corresponds to a system with slow dynamics, The system then can be controlled by looking at its long-term behaviour, and its calculated control inputs must be efficiently provided by subsystems located at the lower level of the hierarchy, characterised by

faster dynamic. An example of a three-layer structure is shown in Fig. 3.11. As we can see in the Fig. 3.11, the increasing levels that the system structure has inevitably result in increasing complexity of the overall system. The increasing complexity of the structure, as a consequence, limits the implementation of this kind of system structure. Nowadays, hierarchical structures are developed with optimisation techniques for applications to improve the performance as a compromise [77]. Similar optimisation design based on decentralised control in hierarchical structures can also be found in [86, 87, 60].

Distributed Structure

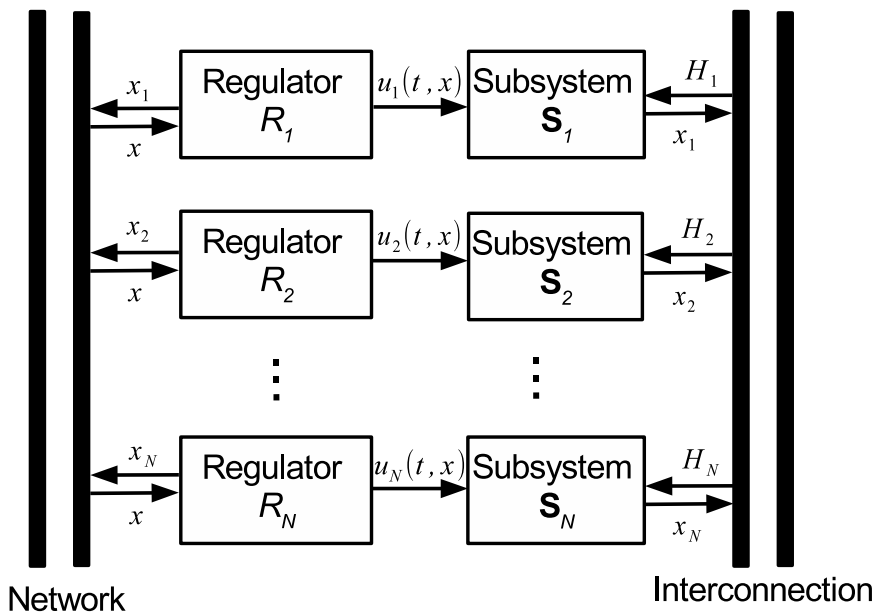

Figure 3.12: Distributed structure

In distributed control structure, it is assumed that some information can be transmitted among those local regulators through a network so that regulators in each subsystem can have some knowledge on the behaviour of the others [88, 60]. This system structure is widely used in power grid regulation [89], intelligent transportation system [76]. Since a subsystem may not need all the information of the system plant, Therefore, the information that is transmitted from the local regulators is usually feed in a given subset of the others, which is also known as *partially connected* [60]. However, the delay of the network is still an essential problem for the distributed control system. Furthermore, the network failure may greatly degrade the control

performance of a local regulator or even devastate the stability of the subsystem.

Decentralized Structure

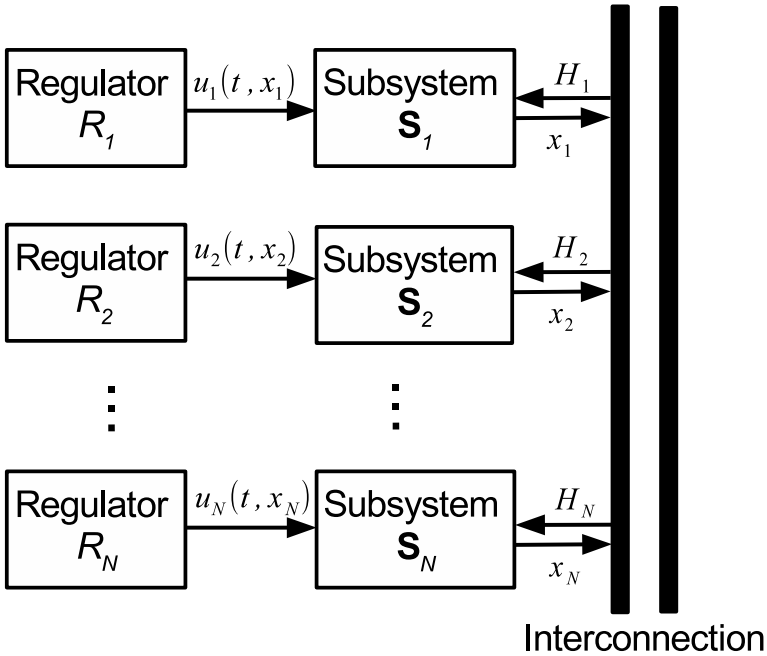

Figure 3.13: Decentralised system structure

In a decentralised control system shown in Fig. 3.13, the local controllers of each subsystem for system (3.64) are often in the form

$$u_i = u_i(t, x_i) \tag{3.70}$$

in which only local state information x_i is used for the local controller in ith subsystem. Since the controller is based only on local information, the reliability of system performance only depends on the control performance of the local controllers. This system structure is also economical since the network for information transmitting is not required and thus the cost of the implementation and complexity of the overall system is reduced. However, due to the lack of information from the other subsystems, maintaining desired control performance in the presence of unknown interconnection usually is full of challenges. Furthermore, disturbances, modelling errors and parameter variation also widely exist in most practical systems. Specifically, uncertainties experienced by one subsystem not only affect its performance but usually affect

the other subsystems' performance as well due to the interactions among subsystems. As a consequence, the uncertainties existing in each subsystem may greatly affect the overall system performance or even completely devastate the stability of entire systems. To overcome such a problem, a bordered block-diagonal form for the gain matrix is proposed in [90] and extended in [91]. As been pointed out in [91], such structure can significantly improve the decentralised stabilisation of large-scale system at the expense of only minimal communication overhead. Following this, a homotopic method based decentralised dynamic control with interconnected descriptor system is proposed in [92]. Adaptive control technique is a powerful tool to estimate the bounds of the uncertainties, which make it very useful for the decentralised control design. As discussed in [93], the adaptive technique based decentralised control strategy was first proposed in [94]. Later in [95], an adaptive algorithm is developed for SISO system with strong nonlinear interactions. Adaptive strategies for uncertain interconnections was further developed in [96, 97]. With the knowledge of the bounds on uncertainties, many robust control designs have been carried out to improve the robustness of the decentralised control systems. In [22, 23, 24, 25], only matched uncertainties are considered, and bounds on the matched uncertainties are assumed to be linear or polynomial. In terms of mismatched uncertainties, in order to achieve asymptotic stability, some limitations on the uncertainties are unavoidable. Mismatched uncertainties have been considered in [28, 98] where centralised dynamical feedback controllers are designed which need more resources to exchange information between subsystems. A class of constraints called integral quadratic constraints is imposed on the considered systems to limit the structure of the original systems [98]. In some cases, adaptive techniques are applied to estimate an upper bound on the mismatched uncertainty to counteract its effect [99]. This approach may be powerful when the uncertainty satisfies a linear growth condition. In [100], although the uncertainties are assumed to be functions, the system needs to be transformed into a special triangular structure. All the literature which considers mismatched uncertainties mentioned above inevitably requires extra resources and increases the system complexity. This problem may make such approaches unattractive from the viewpoint of implementation.

As a typical form of discontinuous nonlinear control, VSC has its advantage when dealing with nonlinear uncertain systems. In [101], a decentralised VSC, which is one of the earliest work applying VSC on decentralised structure, is proposed for interconnected systems. Following that, many researchers worked on the decentralised control based on one particular VSC,

i.e. SMC as mentioned in Section 3.2, owing to its strong robustness and order reduction [16, 44, 102, 17, 103]. For this reason, the problem of robust decentralised SMC design has received much attention, and many results have been obtained during the past 2 decades owing to its strong robustness against matched uncertainties [104, 17] and order reduction for nonlinear systems, e.g. see [105, 47, 11, 71, 99, 106, 107], and the trend is still growing.

It appears that the state variables of each subsystem are also not fully available in some practical applications. An observer-based controller is an option if the subsystem is observable, but the established observers for each subsystem will also increase the complexity of overall systems and needs more computational resources. To avoid the unnecessary cost while keeping strong robustness, robust decentralised control using only output information has been developed rapidly during the past decades [108, 109, 110, 69]. Besides, some SMC schemes by using output feedback have been proposed for large-scale systems [111], and the reachability condition for large-scale systems are well studied [112] and expanded by Hsu, K. C. in [113]. After that, Yan et al. in [105] proposed a decentralised sliding control for a class of nonlinear large-scale interconnected systems with both mismatched uncertainties and mismatched interconnections. The bounds of uncertainties are more general for comparing with the earlier work in [111]. Later, the conservatism is reduced in [47], where the assumptions on the uncertainties are inevitably strong due to the lack of the state information.

Nevertheless, in contrast to the case of networked control, decentralised control can only use local information, and thus the uncertainties within the interconnections may not be well rejected, even if they are matched. Designing a decentralised control scheme to reject the effect of uncertainties in the interconnection terms is still challenging. To overcome the disadvantages of the decentralised control, and to avoid the complexity and lack of flexibility when compared with traditional centralised control and hierarchical control, quasi-decentralised control strategies with cross communication capability between subsystems are provided with an appropriate compromise. Similar to the distributed control, quasi-decentralised also utilise the network for the data transmission between subsystems. However, the central part of the system structure is decentralised, i.e. most signals used for the local regulators are collected and processed locally, which can be expanded from a developed decentralised control strategy. Regarding the interconnections, minimum signals from other subsystems through the network are collected to adequately account for the interactions between subsystems and minimise propagation of

disturbances and process influence from one unit to another [61, 114]. Therefore, decentralised SMC is mainly considered in this thesis since it can be easily expanded to a quasi-decentralised strategy without scarifying the reliability of the decentralised control if extra information is available.

3.5. Practical Examples of Complex Systems

3.5.1. Nonholonomic Systems

To illustrate the nonholonomic systems and nonholonomic constraints, two examples of nonholonomic systems, i.e. unicycle and bicycle (see [115]), are given as follows.

Unicycle

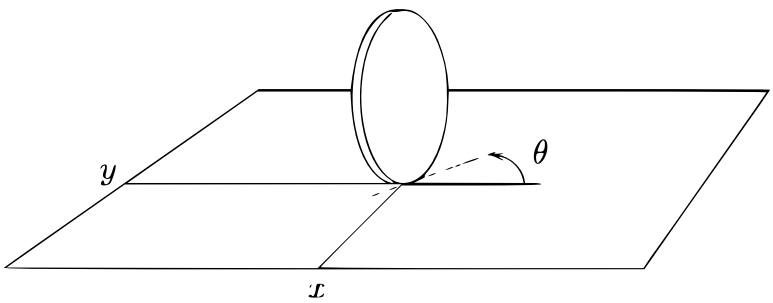

Figure 3.14: Model of a Unicycle

Suppose a unicycle shown in Fig.3.14 with coordinates $q = (x, y, \theta)$, assume that the wheel cannot slip laterally, which result in nonholonomic constraint

$$\dot{x}\sin\theta - \dot{y}\cos\theta = 0 \tag{3.71}$$

Rewrite the constraints in the form of Pfaffian

$$A(q)\dot{q} = 0 \tag{3.72}$$

where

$$A(q) = \begin{bmatrix} \sin\theta & -\cos\theta & 0 \end{bmatrix} \tag{3.73}$$

By expressing all the feasible motion of unicycle as a linear combination of vector fields $S(q)$

$$S(q) = \begin{bmatrix} \cos\theta & 0 \\ \sin\theta & 0 \\ 0 & 1 \end{bmatrix}$$

which spans the null space of matrix $A(q)$, the so-called kinematic model can be obtained as

$$\dot{q} = S(q)u \tag{3.74}$$

where $u = \text{col}(v, \omega)$, and v and ω are the linear velocity and the steering velocity of the unicycle respectively.

Bicycle

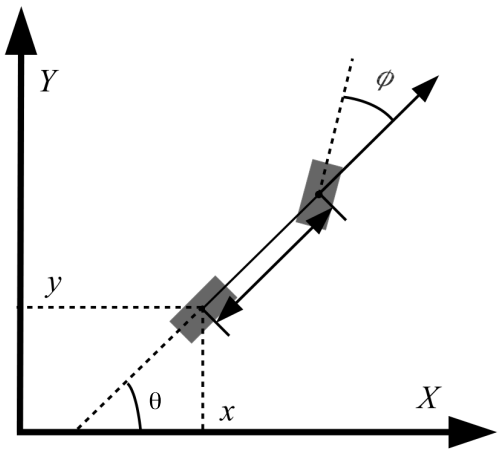

Figure 3.15: Model of Bicycle

For a bicycle shown in Fig.3.15 with coordinates $q = \cos(x, y, \theta, \phi)$, assume that the wheel cannot slip laterally, which result in Pfaffian nonholonomic constraints

$$A(q)\dot{q} = 0 \tag{3.75}$$

where

$$A(q) = \begin{bmatrix} \sin\theta & -\cos\theta & 0 & 0 \\ \sin(\theta+\phi) & -\cos(\theta+\phi) & -l\cos\phi & 0 \end{bmatrix} \tag{3.76}$$

By expressing all the feasible motion of bicycle as a linear combination of vector fields $S(q)$

$$S(q) = \begin{bmatrix} \cos\theta & 0 \\ \sin\theta & 0 \\ \frac{1}{l}\tan\phi & 0 \\ 0 & 1 \end{bmatrix}$$

which spans the null space of matrix $A(q)$, the so-called kinematic model can be obtained as

$$\dot{q} = S(q)u \tag{3.77}$$

where $u = \text{col}(v, \omega)$, and v and ω are the linear velocity of the bicycle and the steering rate of the front wheel respectively.

3.5.2. Large-Scale Systems

Large-scale systems widely exist in the real world, in this section, the model of large-scale system, such as power systems [11], continuously stirred tank reactor system [114] and automated highway system [116], are to be provided.

Power Systems

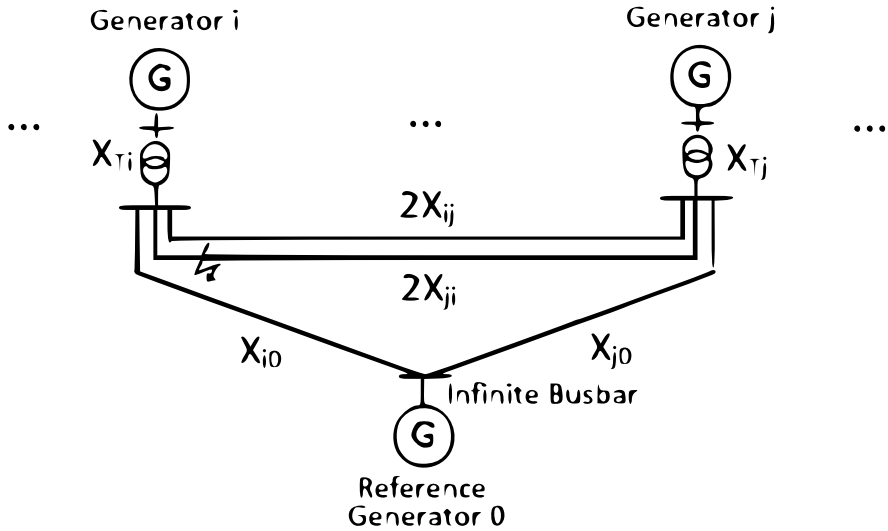

Figure 3.16: Over view of multi-machine power systems with an infinite busbar [2]

Nowadays, electricity plays a crucial role in our daily lives. Apparently, with the increasing complexity of power distribution systems and demands of users, it has become increasingly

important to develop the automation of some tasks such as generation, transmission, distribution etc. Among these tasks, a multi-machine power system with $\mathcal{N}$ synchronous generators as shown in Fig.3.16 is a typical large-scale interconnected system. The interconnection between each local generators through a transmission network greatly increases the system complexity [59].

The mechanical equation of the generator is described by

$$\dot{\delta}_i = \omega_i \tag{3.78}$$

$$\dot{\omega}_i = -\frac{D_i}{2H_i}\omega_i + \frac{\omega_0}{2H_i}(P_{mi0} - P_{ei}) \tag{3.79}$$

where δ_i represent the power angle of the i-th generator and ω_i denote the relative speed with respect to the synchronous machine speed ω_0. D_i, H_i, P_{mi0} and P_{ei} denote the damping constant, inertia constant, mechanical input power and electrical power respectively.

The electrical dynamics of the generator are described by

$$\dot{E}'_{qi} = \frac{1}{T'_{doi}}(E_{f_i} - E_{q_i}) \tag{3.80}$$

with the electrical equations

$$E_{fi} = K_{ci}u_{fi} \tag{3.81}$$

$$E_{qi} = E'_{qi} - (x_{di} - x'_{di})I_{di} \tag{3.82}$$

$$P_{ei} = \sum_{j=1}^{N} E'_{qi}E'_{qj}B_{ij}\sin(\delta_i - \delta_j) \tag{3.83}$$

$$Q_{ei} = -\sum_{j=1}^{N} E'_{qi}E'_{qj}B_{ij}\cos(\delta_i - \delta_j) \tag{3.84}$$

$$I_{qi} = \sum_{j=1}^{N} E'_{qj}B_{ij}\sin(\delta_i - \delta_j) \tag{3.85}$$

$$I_{di} = \sum_{j=1}^{N} E'_{qj}B_{ij}\cos(\delta_i - \delta_j) \tag{3.86}$$

$$E_{qi} = x_{di}I_{fi} \tag{3.87}$$

$$V_{ti} = \sqrt{(E'_{qi} - x'_{di}I_{di})^2 + (x'_{di}I_{qi})^2} \tag{3.88}$$

where Q_{ei}, E'_{qi} and T'_{doi} denote the reactive power, the transient EMF in the quadrature axis and direct axis transient short circuit time constant respectively. x_{di} and x'_{di} represent the reactance

and transient reactance in direct axis respectively, and I_{di} and I_{qi} represent current in direct axis and quadrature axis respectively. K_{ci} and B_{ij} denote the gain of the excitation amplifier and the i-th row and j-th column element of nodal susceptance matrix at internal nodes respectively. u_{fi} is the input signal of the i-th generator. This model has been widely used for the research of multi-machine power system, e.g. see [117, 118, 119].

Continuously Stirred Tank Reactor

For illustrating purposes, a continuously stirred tank reactor system with three reactors is shown in Fig.3.17. The output of local subsystem CSTR 3 is passed through a separator that

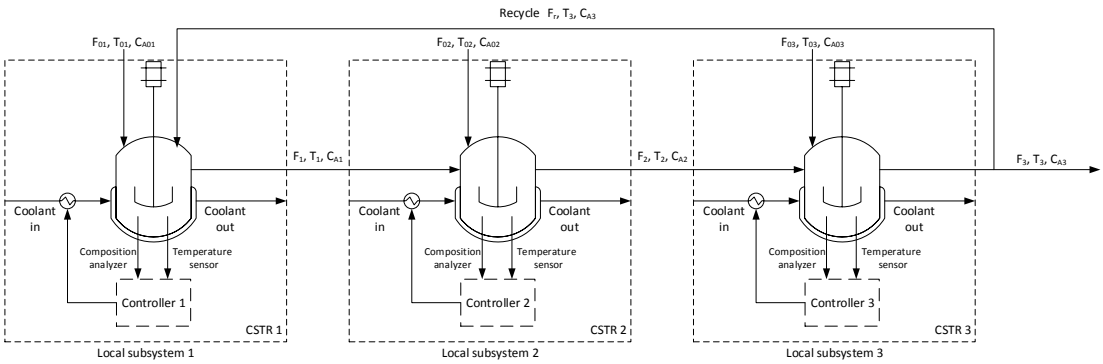

Figure 3.17: Schematic diagram of the CSTR system

recycles unreacted products back to the subsystem CSTR 1. The reactant species are consumed in each reactor by three parallel, irreversible exothermic reactions. Due to the non-isothermal nature of the reactions, a jacket is used to remove/provide heat to each reactor. A plant model based on material and energy balance is described as follows (see [114] for full details):

$$\begin{aligned}\frac{dT_1}{dt} =& \frac{F_1^0}{V_1}(T_1^0 - T_1) + \frac{F_r}{V_1}(T_r - T_1) + \sum_{i=1}^{3} \frac{-\Delta H_i}{\rho c_p} R_i(C_{A1}, T_1) \\ &+ \frac{Q_1}{\rho c_p V_1} \end{aligned} \tag{3.89}$$

$$\frac{dC_{A1}}{dt} = \frac{F_1^0}{V_1}(C_{A1}^0 - C_{A1}) + \frac{F_r}{V_1}(C_{Ar} - C_{A1}) - \sum_{i=1}^{3} R_i(C_{A1}, T_1) \tag{3.90}$$

$$\frac{dT_2}{dt} = \frac{F_2^0}{V_2}(T_2^0 - T_2) + \frac{F_1}{V_2}(T_1 - T_2)$$

$$+\sum_{i=1}^{3}\frac{-\Delta H_i}{\rho c_p}R_i(C_{A2},T_2)+\frac{Q_2}{\rho c_p V_2} \tag{3.91}$$

$$\frac{dC_{A2}}{dt}=\frac{F_2^0}{V_2}(C_{A2}^0-C_{A2})+\frac{F_1}{V_2}(C_{A1}-C_{A2})-\sum_{i=1}^{3}R_i(C_{A2},T_2) \tag{3.92}$$

$$\frac{dT_3}{dt}=\frac{F_3^0}{V_3}(T_3^0-T_3)+\frac{F_2}{V_3}(T_2-T_3)$$

$$+\sum_{i=1}^{3}\frac{-\Delta H_i}{\rho c_p}R_i(C_{A3},T_3)+\frac{Q_3}{\rho c_p V_3} \tag{3.93}$$

$$\frac{dC_{A3}}{dt}=\frac{F_3^0}{V_3}(C_{A3}^0-C_{A3})+\frac{F_2}{V_3}(C_{A2}-C_{A3})-\sum_{i=1}^{3}R_i(C_{A3},T_3) \tag{3.94}$$

where T_i, C_{Ai}, Q_j and V_j denote the temperature, the reactant concentration, the rate of heat, and the volume of the ith reactor, respectively. The terms

$$R_i(C_{Aj},T_j)=k_{i0}e^{\frac{-E_i}{RT_j}}C_{Aj}, \qquad i=1,2,3$$

represent the reaction rate of the ith reaction. F_i^0 denotes the flow rate of a fresh feed stream associated with the ith reactor. F_r represents the flow rate of the recycle stream. It should be noted that the temperature and the reactant concentration of the recycle stream are assumed to be equal to the temperature and the concentration of the CSTR 3 subsystem as the recycled product is directly separated from CSTR 3. ΔH_i, k_i and E_i for $i=1,2,3$ denote the enthalpy, pre-exponential constants and activation energies of the three reactions respectively. The symbols c_p and ρ denote the heat capacity and density of fluid in the reactor.

Automated Highway Systems

In order to achieve high traffic flow rates and reduce congestion, an automated highway systems has been developed [116]. During the automated driving process, cars are driven automatically with both on-board lateral and longitudinal controllers. The lateral controller is used to steer the vehicle and the longitudinal controller is used to follow a lead vehicle at a safe distance. The corresponding overview of this vehicle-following system is shown in Fig.3.18 and the dynamics of the system is described by [67]

$$\dot{\xi}_i=v_i-v_{(i-1)} \tag{3.95}$$

$$\dot{v}_i=\frac{1}{m_i}\left(-A_{ip}v_i^2-d_i+f_i\right) \tag{3.96}$$

$$\dot{f}_i = \frac{1}{\kappa_i}\left(-f_i + u_i\right) \tag{3.97}$$

where ξ_i represents the distance between the ith and the $(i-1)$th vehicle, v_i is the velocity of the ith vehicle and f_i is the force applied to the longitudinal dynamics of the ith vehicle, where if $f_i > 0$ a forward driving force occurs and if $f_i < 0$, then a braking force takes place. m_i is the mass of the ith vehicle, d_i and κ_i are the constant frictional force and the engine brake time constant. The signal u_i is the control variable, where if $u_i > 0$, a throttle input results, and if $u_i < 0$ then a braking input occurs.

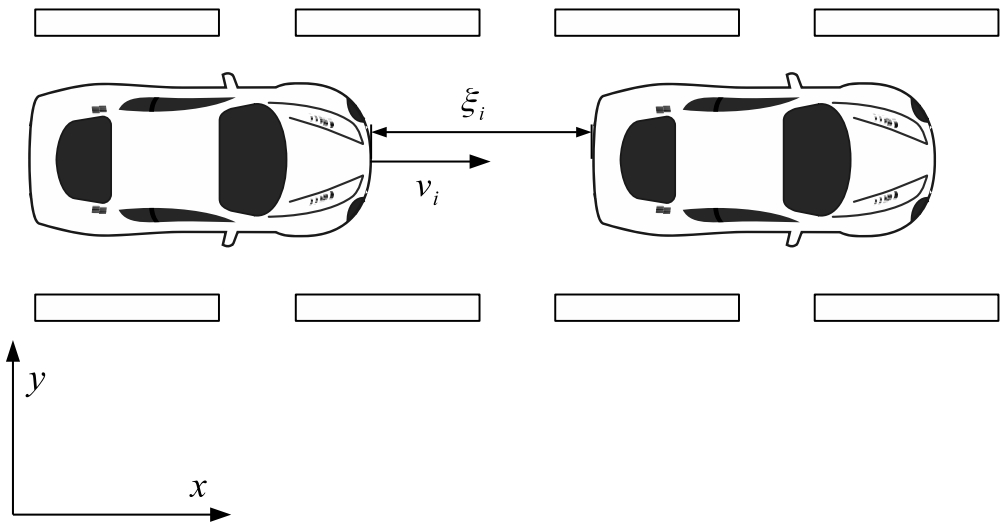

Figure 3.18: Overview of vehicle-following system

3.6. Conclusion

In this chapter, the basic knowledge of state feedback has been provided. The fundamental properties and interests of SMC have been discussed. Owning to the strong robustness and reduced-order properties, SMC is an effective approach for regulation of complex systems. Regarding the difficulties arising in the control of complex systems, nonholonomic systems and large-scale systems are considered in this thesis. The definition of nonholonomic constraints and nonholonomic systems are provided in details with two practical examples. Due to the well

known Brockett's necessary condition, it is proved that a continuous feedback controller for drift-less nonholonomic systems does not exist. To overcome such problems, discontinuous controller, such as VSC, is usually introduced. With the natural decompositions or decomposition techniques, large-scale system is usually partitioned to a collection of subsystem with overlapping dynamics. The computational difficulties motivate the develop of various system structures. Among all the structures, decentralised structure is one of the most reliable and flexible structures regarding the problems arising in network transmission. Moreover, it has been reviewed that decentralised control strategy can be used as a foundation of some hierarchical structures or quasi-decentralised structure to further improve the system performance with network while keeping the advantage of reliability and flexibility when the network is not available. As a result, SMC and decentralised SMC is considered as the main methodology for the works of large-scale systems in the following chapters.

CHAPTER. 4

TRAJECTORY TRACKING CONTROL FOR WMR SYSTEMS

WMRs are increasingly used for both industrial and service purposes owing to its flexible mobility. Several moving mechanisms can be found in applications in [120]. As one of the most common driving methods for single-body WMR, differential driving based WMR is widely used because of the relatively simple configuration and implementation. As a typical nonholonomic system, WMR is a complex nonlinear system with multiple inputs and outputs. A model of the WMR is developed in Section 4.2. The SMC design is presented and analysed in Section 4.3, and the WMR hardware layout is described in Section 4.4. Section 4.5 contains simulation and experimental results before Section 4.6 concludes the chapter.

4.1. Background

Trajectory tracking control refers to find a feedback control laws to track or "move along" a pre-given time-varying trajectory with arbitrary initial conditions in the considered domain. Path following control for WMR systems is similar to trajectory tracking control but without

consideration of speed and temporal position requirements when the robot moves along the defined path [121]. In other words, the tracking tasks are to track a time-varying trajectory in trajectory tracking control while moving along a designed geometric path in path-following control. It should be noted that only trajectory tracking control is discussed in this chapter.

Although it is not necessary to satisfy Brockett's well known necessary condition (**??**) provided in Section 2.3 if the reference trajectory does not involve stabilisation to a rest configuration [122], it is challenging to use conventional control methods to obtain desired tracking performance for WMR systems because of the inherent nonlinearity caused by the nonholonomic constraints. For the WMRs, kinematic models strictly relate to the nonholonomic constraints. Thus many researchers focus on the kinematic models for trajectory tracking control in the early work [123, 124, 125, 126, 127]. To name a few, a local trajectory tracking controller is designed in [123] by locally linearising the system, which can only guarantee the tracking performance locally. Then, Samson and Ait-Abderrahim firstly designed a global trajectory tracking controller based on Lyapunov stability theory in [124]. Since there is no standard method to obtain a nonlinear Lyapunov function, the nonlinear feedback control law may be complicated to be obtained. Thus the design procedure may be relatively complicated. In [126], the WMR system is approximately linearised in the neighbourhood of the equilibrium point, and a relatively simple feedback control law is then applied to the linearised system to track the model-based trajectory. However, due to the approximation of the dynamics, the tracking performance is not as expected. A significant improvement of the controller based on the backstepping method is proposed in [125]. This method has been widely used in many WMR tracking control design [128, 129]. In the recent work in [10], the kinetic controller based on back-stepping techniques is further simplified.

In kinematic control design, the control inputs are chosen with linear velocity and steering velocity. However, the actual inputs of a practical WMR system are usually the torques of two motors [130] or the voltages of the driving circuit [10]. To generate the required input signals in the kinematic layer, it is necessary to design dynamic feedback controller to ensure that the velocities are well-tracked [125]. Thus, dynamic controller design can be found in most literature, e.g. see [128, 129, 131, 10]. In a driftless nonholonomic system, the disturbances mainly come from the input channel. Meanwhile, SMC has been recognised as a robust control method owing to its complete robustness against matched uncertainties when the system is in the

sliding motion as discussed in Chapter 3. Therefore, this approach has been widely employed to the nonholonomic system (see, e.g. [132]). Moreover, the sliding mode approach can also be used to deal with systems in the presence of mismatched uncertainty under suitable conditions even for time-delay systems (see, e.g. [133] and [134]). Therefore, SMC techniques can be a compelling solution to the problem of trajectory tracking control in practical systems. A SMC scheme for trajectory tracking with polar coordinates has been previously proposed by Yang and Kim [127]. However, due to hardware limitation, the designed controller does not exhibit the expected tracking performance in practice. In [135], sliding mode techniques were applied to a WMR system using feedback linearization techniques, and the results have been obtained not only for the tracking control problem but also for regulation task. However, this approach requires that measurement of the propulsive force of the WMR to satisfy strict conditions of the feedback linearization. Consequently, this approach is relatively complicated to implement from the practical point of view. A coordinated control scheme based on a leader-follower approach is developed for the control of cooperative autonomous mobile robots in [136] which enables formation stabilisation and ensures the collision avoidance. An integral SMC strategy is applied to the Heisenberg system, and the developed results have been successfully applied to mobile robot control in [137]. In both [129] and [10], a SMC strategy was used in the dynamic layer. Although simulation results in both cases show robustness against matched uncertainties, the SMC was only applied to the dynamic model, which only ensures that the reference velocities is well tracked. In [138], SMC was applied to the kinematic model of a WMR. However, the designed controller is expressed in implicit form.

Although SMC has strong robustness when in the sliding mode, the system is sensitive to uncertainties in the reaching phase. Thus many techniques have been applied for minimising the reaching time (see, e.g. [139]), such as reaching gain adaptation in [140], time-varying sliding surfaces in [141] or fuzzy moving sliding surfaces in [142]. However, the required extra computation for the adaptation algorithm or time-dependent functions inevitably increases system complexity as mentioned in [139] while the dynamics of the sliding functions are required to satisfy appropriate fuzzy rules for the case of fuzzy moving sliding surfaces. On the other hand, the dynamics of linear sliding surfaces may not align with global dynamic properties required for the system (see, e.g. [143]). To overcome the disadvantages, nonlinear sliding surfaces can be designed for the WMR system to get better performance.

In this chapter, a sliding mode controller is proposed for a two-WMR system. Asymptotic tracking of trajectories based on the kinematic model of the system is considered. A new sliding surface is designed to guarantee the stability of the proposed sliding motion. Then a SMC law is proposed to guarantee the reachability condition is satisfied so that the system attains and maintains the required sliding motion. The implementation of the control in a two-WMR using DC motors as actuators is carried out, and implementation of the proposed scheme is straightforward. The experimental results achieved are consistent with the simulation results which shows that the proposed approach is effective to the control of the two-WMR system.

4.2. Modelling of the two-WMR

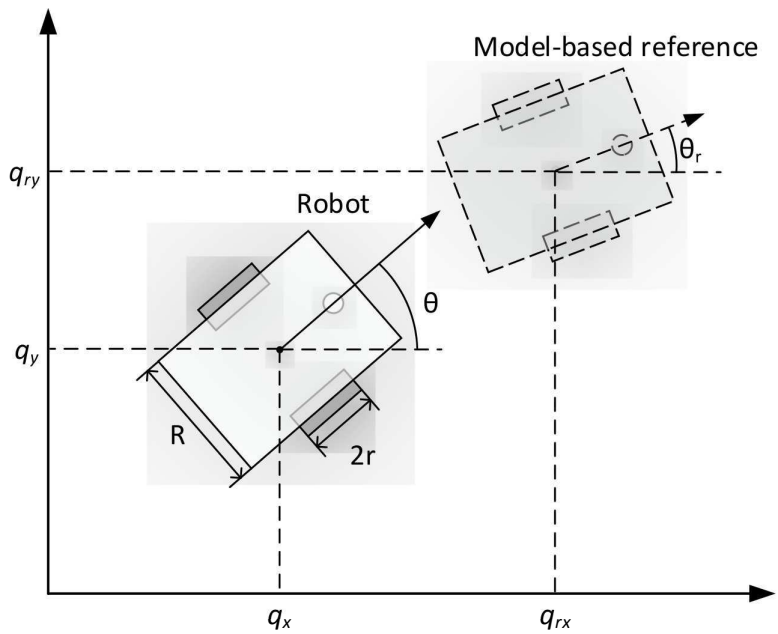

Figure 4.1: Configuration of the robot

The kinematic of the nonholonomic system and the examples of modelling were discussed in Chapter 3. Similar to a unicycle model given in Section 3.5, consider a two-WMR with the generalised n-vector coordinates $q = \text{col}(q_x, q_y, \theta) \in \mathcal{R}^n$ as shown in Fig.4.1. The Pfaffian nonholonomic constraint that the WMR cannot shift laterally is

$$A(q)\dot{q} = 0 \tag{4.1}$$

where

$$A(q) = \begin{bmatrix} \sin\theta & -\cos\theta & 0 \end{bmatrix}$$

by expressing all the feasible motion of WMR as a linear combination of vector field $S(q)$

$$S(q) = \begin{bmatrix} \cos\theta & 0 \\ \sin\theta & 0 \\ 0 & 1 \end{bmatrix}$$

which spans the null space of matrix $A(q)$, the so-called kinematic model can be obtained as (see e.g. [130])

$$\dot{q} = S(q)u \tag{4.2}$$

where $u = \text{col}(v, \omega)$, and v and ω are the linear velocity and the steering velocity of the WMR respectively.

For the differential-driving mechanism, v and ω can be derived from the rotational velocity of two wheels as follows (see e.g. [130])

$$\begin{bmatrix} v \\ \omega \end{bmatrix} = \begin{bmatrix} \frac{r}{2} & \frac{r}{2} \\ \frac{r}{R} & -\frac{r}{R} \end{bmatrix} \begin{bmatrix} \omega_R \\ \omega_L \end{bmatrix} \tag{4.3}$$

where ω_R and ω_L denote the rotational velocity of the wheels on the right side and left side respectively. r and R represent the radius of the wheel and the width of the robot respectively as shown in Fig.4.1.

Remark 4.1. *In this chapter, the actual commands for the WMR in Fig.4.1 are the angular velocities* (ω_R, ω_L) *defined in (4.3) (e.g. see [130]), which is implemented by motors with voltage as input signals. This is also known as the dynamical model, e.g. see [144], [129] and [10]. Since the mapping between these velocities is one-to-one, the pair of velocities for the robot* (v, ω) *with* $u = \text{col}(v, \omega)$ *are implemented by two DC motors generating angular velocities* (ω_R, ω_L) *defined in (4.3).*

Assume the reference trajectory is model based. Then the differential equations of the reference trajectory with reference coordinates $q_r = \text{col}(q_{xr}, q_{yr}, \theta_r)$ and reference velocities $u_r = \text{col}(v_r(t), \omega_r(t))$ are given by the following dynamics

$$\begin{bmatrix} \dot{q}_{xr} \\ \dot{q}_{yr} \\ \dot{\theta}_r \end{bmatrix} = \begin{bmatrix} \cos\theta_r & 0 \\ \sin\theta_r & 0 \\ 0 & 1 \end{bmatrix} \begin{bmatrix} v_r(t) \\ \omega_r(t) \end{bmatrix} \tag{4.4}$$

where $v_r(t) \neq 0$, which implies that the reference trajectory does not have rest configuration (see, e.g. [122]).

Then the objective of the model-based tracking control is to design a controller u for system (4.2) such that

$$\lim_{t\to\infty} \|q_r - q\| = 0$$

where $q_r = \text{col}(q_{xr}, q_{yr}, \theta_r)$ is the reference trajectory created by (4.4).

Introduce a diffeomorphism $T : \mathcal{R}^3 \longrightarrow \mathcal{R}^3$ with $q_e = T(q)$ as (see e.g. [138])

$$q_e := \begin{bmatrix} x_e \\ y_e \\ \theta_e \end{bmatrix} = \tilde{T}(q)(q_r - q) \tag{4.5}$$

where $q = \text{col}(x_c, y_c, \theta)$, $q_r = \text{col}(x_r, y_r, \theta_r)$ and

$$\tilde{T}(q) = \begin{bmatrix} \cos\theta & \sin\theta & 0 \\ -\sin\theta & \cos\theta & 0 \\ 0 & 0 & 1 \end{bmatrix}$$

It is straightforward to verify that the inverse $\tilde{T}^{-1}(q)$ with

$$\tilde{T}^{-1}(q) = \begin{bmatrix} \cos\theta & -\sin\theta & 0 \\ \sin\theta & \cos\theta & 0 \\ 0 & 0 & 1 \end{bmatrix} \tag{4.6}$$

is bounded with $\|\tilde{T}^{-1}(q)\| \leq 1$. Then, from Lemma 2.7, when $\lim_{t\to\infty} \|q_e\| = 0$,

$$\lim_{t\to\infty} \|q_r - q\| = 0$$

Since θ_e represents the angular error between the robot and the reference, without loss of generality, let $|\theta_e| \leq \pi$.

By direct computation, it follows from (4.2) and (4.4) that the differential equation of the new error system can be described by

$$\begin{bmatrix} \dot{x_e} \\ \dot{y_e} \\ \dot{\theta_e} \end{bmatrix} = \begin{bmatrix} v_r \cos\theta_e \\ v_r \sin\theta_e \\ \omega_r \end{bmatrix} + \begin{bmatrix} -1 & y_e \\ 0 & -x_e \\ 0 & -1 \end{bmatrix} \begin{bmatrix} v \\ \omega \end{bmatrix} \tag{4.7}$$

Therefore, the model-based reference tracking control problem based on the kinematic model (4.2) is equivalent to determining a feedback control law to stabilise the new error system (4.7) to the origin.

4.3. Control Design for the WMR

As discussed in Section 3.2, the analysis of SMC is generally separated into two phase, i.e. sliding mode and reaching phase. To be specific, consider the error system (4.7), a sliding function is firstly designed so that the sliding mode of the system (4.7) is asymptotically stable. Then control to guarantee the reachability is designed based on the sliding function. In the following subsections, the tracking control is based on the SMC with limitation on the reference trajectory, which is separated into $v_r > 0$ and $v_r < 0$. The case $v_r > 0$ is mainly considered, and the other case $v_r < 0$ can be obtained directly by slightly modifying sliding function and control design from the case with $v_r > 0$.

4.3.1. Stability of the Sliding Mode

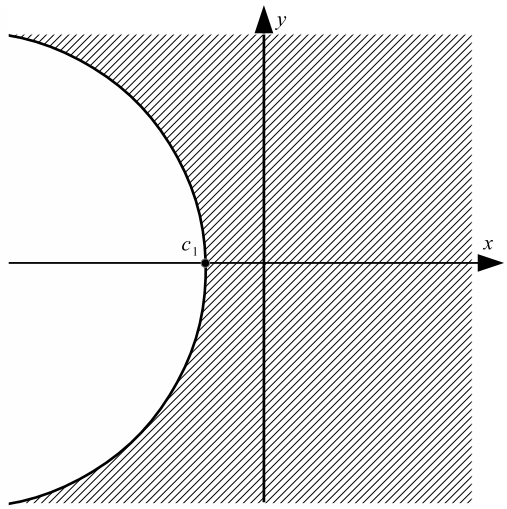

Figure 4.2: Domain Ω in x-y plane.

If $v_r > 0$, consider the system (4.7) in the domain

$$\Omega = \{(x_e, y_e, \theta_e)^\tau | x_e > -c_1(1 + y_e^2), y_e \in \mathcal{R}, |\theta_e| \leq \pi\} \tag{4.8}$$

where c_1 is a designed positive parameter and $c_1 > 0.5$. The domain in x-y plane can be found in Fig. 4.2.

Choose the sliding function $\sigma = \text{col}(\sigma_1^l, \sigma_2^l)$ as follows

$$\sigma = \begin{bmatrix} \sigma_1 \\ \sigma_2 \end{bmatrix} = \begin{bmatrix} c_1\theta_e + \tan^{-1}(y_e) \\ x_e \end{bmatrix} \tag{4.9}$$

When the sliding motion takes place, it is straightforward to verify from $\sigma = 0$ that

$$\begin{cases} x_e &= 0 \\ \theta_e &= -\frac{\tan^{-1}(y_e)}{c_1} \end{cases} \tag{4.10}$$

It is clear that $|\frac{\tan^{-1}(y_e)}{c_1}| < \pi$

Substituting (4.10) into (4.7), the unforced system can be obtained as

$$\dot{y}_e = v_r \sin(-\frac{\tan^{-1}(y_e)}{c_1}) \tag{4.11}$$

It is straightforward to see that although the system (4.7) is not in the regular form, the unforced system can still be expressed when the system is on the sliding surface. Choose the Lyapunov function

$$V = \frac{1}{2}y_e^2 \tag{4.12}$$

Then the derivative of (4.12) is given by

$$\dot{V} = y_e\dot{y}_e = -v_r \sin(-\frac{\tan^{-1}(y_e)}{c_1})y_e \tag{4.13}$$

It is straightforward from (4.13) to verify that the derivative of the selected Lyapunov function is negative definite. Therefore, from Lemma 2.2, the sliding motion of system (4.7) with the sliding surface $\sigma = 0$ is asymptotically stable.

4.3.2. Reachability of the Sliding Mode

Define the input u as

$$u = -\Lambda^{-1}\left\{ J_n \begin{bmatrix} v_r\cos\theta_e \\ v_r\sin\theta_e \\ \omega_r \end{bmatrix} + \begin{bmatrix} \eta_1 \text{sgn}(\sigma_1) \\ \eta_2 \text{sgn}(\sigma_2) \end{bmatrix} \right\} \tag{4.14}$$

where $\sigma_1(y_e, \theta_e)$ and $\sigma_2(x_e)$ defined in (4.9), η_1,η_2 are positive reaching gains, J_n is the Jacobian Matrix of the sliding functions defined by

$$J_n = \begin{bmatrix} 0 & \frac{1}{1+y_e^2} & c_1 \\ 1 & 0 & 0 \end{bmatrix}$$

and the matrix E is defined by

$$\Lambda = \begin{bmatrix} 0 & -(c_1 + \frac{x_e}{1+y_e^2}) \\ -1 & y_e \end{bmatrix}$$

It should be noticed that Λ is invertible for $q_e \in \Omega$ where Ω is defined in (4.8).

Remark 4.2. *The limitation of x_e in the domain Ω is to ensure that the invertible matrix Λ always exists. Since θ_e is periodic in the coordinates, an appropriate equivalent θ_e can always be found in the defined domain Ω.*

Theorem 4.1. *Consider the WMR system (4.7) in the domain Ω. The controller (4.14) drives the system (4.7) to the sliding surface $\sigma = 0$ where $\sigma(\cdot)$ is defined in (4.9) and maintains a sliding motion on it.*

Proof. Rewrite the derivatives of the sliding surface in the following form:

$$\begin{bmatrix} \dot{\sigma}_1 \\ \dot{\sigma}_2 \end{bmatrix} = J_n \begin{bmatrix} v_r \cos\theta_e \\ v_r \sin\theta_e \\ \omega_r \end{bmatrix} + \Lambda u \tag{4.15}$$

Then substituting (4.14) into (4.15), it follows that

$$\begin{bmatrix} \dot{\sigma}_1 \\ \dot{\sigma}_2 \end{bmatrix} = \begin{bmatrix} -\eta_1 \text{sgn}(\sigma_1) \\ -\eta_2 \text{sgn}(\sigma_2) \end{bmatrix} \tag{4.16}$$

It is clear that

$$\sigma^\tau \dot{\sigma} = -\eta_1 \sigma_1 \text{sgn}(\sigma_1) - \eta_2 \sigma_2 \text{sgn}(\sigma_2) \leq \eta \|\sigma\| \tag{4.17}$$

where $\eta > 0$. Then the condition

Thus the results follow. ■

If $v_r < 0$, then choose a sliding surface $\sigma = \text{col}(\sigma_1^l, \sigma_2^l)$ as follows

$$\sigma = \begin{bmatrix} c_1\theta_e - \tan^{-1}(y_e) \\ x_e \end{bmatrix} \tag{4.18}$$

Then following the analysis above, it is straightforward to obtain the required result for tracking in reverse by slightly modifying the case $v_r > 0$.

Remark 4.3. *From sliding mode theory, the controller developed from the proposed nonlinear sliding surface can stabilise the system only locally because the matrix Λ is singular when $x_e = -c_1(1 + y_e^2)$.*

4.4. Hardware description

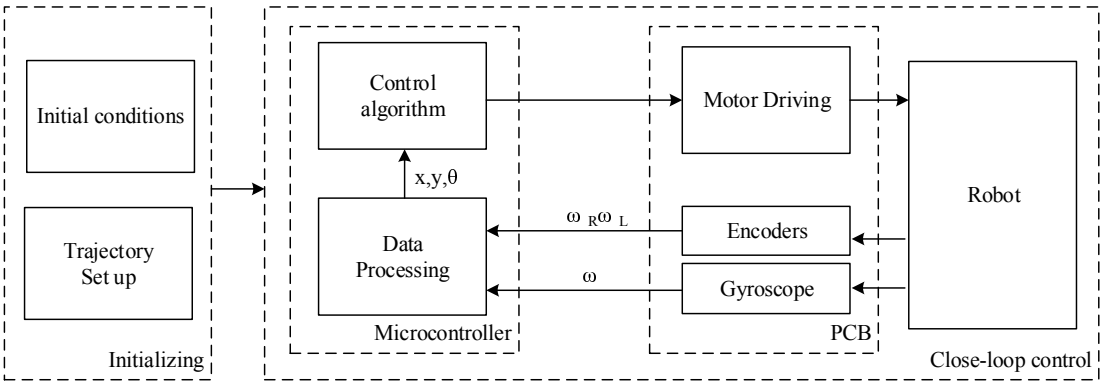

Figure 4.3: System overview for the two-WMR

The overview of the two-WMR built at the University of Kent is shown in Fig.4.3. In order to obtain accurate motion to estimate the coordinates, a rate gyro (LPY503AL) capable of measuring up $\pm 250°/s$ is used. The configuration of the sensor is shown in Fig.4.4. As the gyro produces analog output signals between 0 and 3.3 V, the analog input is processed by the analog-to-digital conversion unit equipped on the micro-controller with up to 12 bits of resolution.

Two DC motors (Pololu 12v 50:1 Gear Motor w/Encoder shown in Fig.4.5) are used as the actuator in the right and left side of the robot body for differential driving, to which gearbox with reduction ratio of 50:1 is mounted. The encoder assembled on the shaft of the motor can create up to 32 pulses per revolution as shown in Fig.4.6. With the gear ratio (50:1), it can create up to 3200 counts per revolution of a wheel by detecting the edge of the pulses. Thus the two encoders and the rate gyro together offer a relative accurate estimation of the position of the robot and feedback of the rotational velocities of each motor.

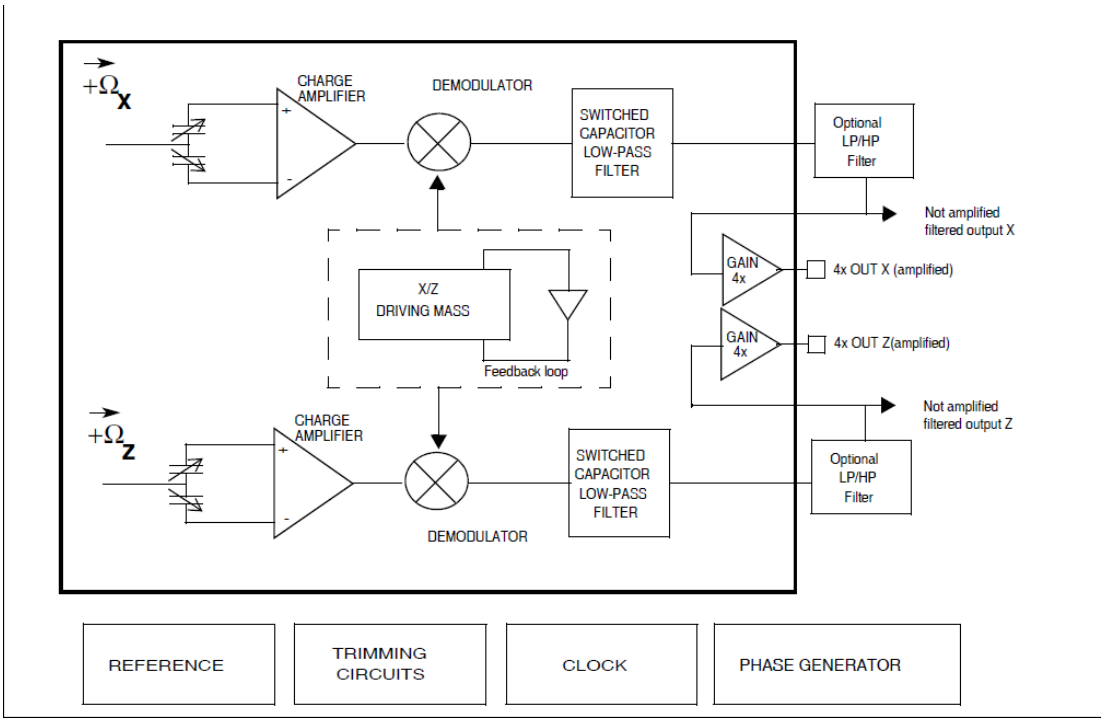

Figure 4.4: Configuration of gyroscope LPY503AL

Figure 4.5: Pololu 12v 50:1 Gear Motor w/Encoder

It should be noticed that the motors are independently drive by two H-bridge MOSFET-based motor drivers (BD6222 HPR7) with 8.7V power supply, which are controlled by the micro-controller with two separate pulse-width-modulation signals shown in Fig.4.7. The micro-controller applied on the robot is a 32-b micro-controller board (Arduino Due) which is based on the Atmel SAM3X8E ARM Cortex-M3 CPU. It has a 84 MHZ clock, 512 kB of

Figure 4.6: Output signals of the encoder assembled on the motor shaft

embedded Flash, 96 kB of SRAM with dual banks and other useful external peripherals. The developed printed circuit board (PCB) is shown in Fig.4.8.

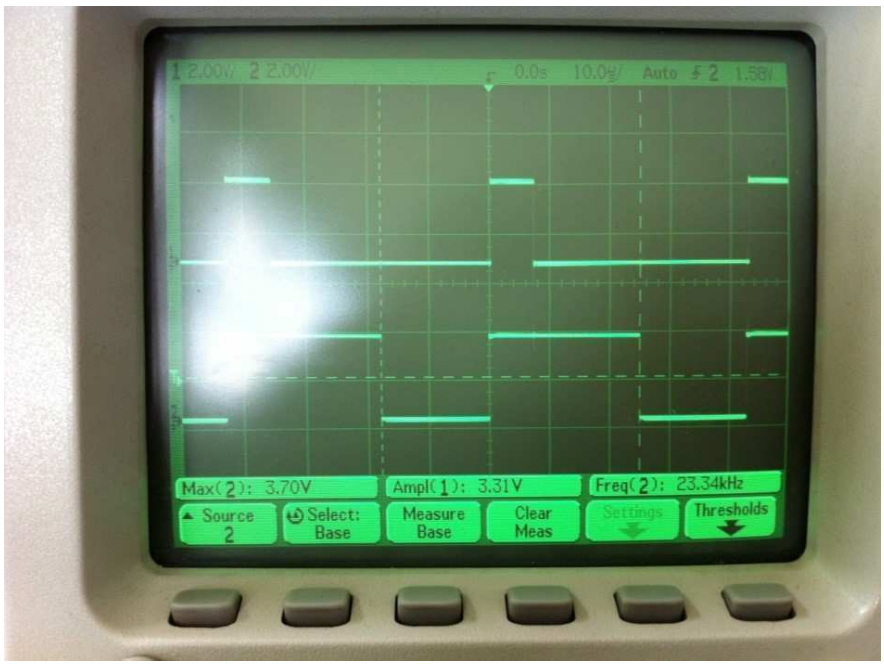

Figure 4.7: Synchronised PWM signals for H-bridge motor drivers

The programming of the micro-controller is user-friendly with C and C++ languages, and the sampling frequency for the main control unit is 100 Hz in the implementation which is sufficient for this application. The phototype of the two-WMR can be described in Fig. 4.9.

4.4.1. Implementation of the Control with DC Motors

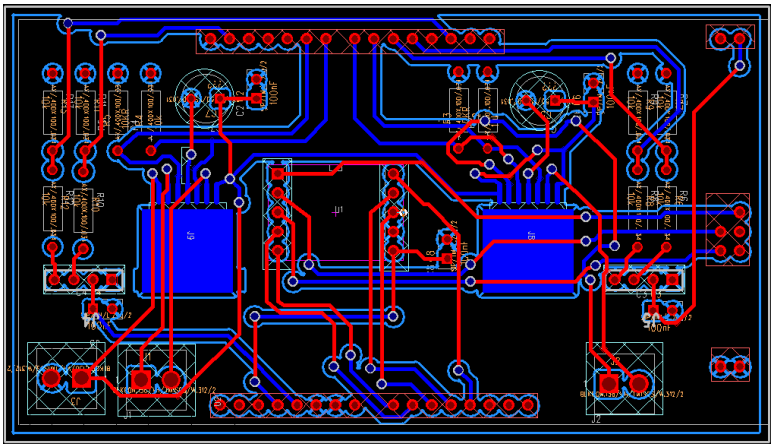

Figure 4.8: Developed PCB for WMR

In order to implement the control algorithm within the robot, two DC motors are used as actuators. The wheels on each side of the robot are driven independently, since the linear velocity and steering velocity correspond to differential driving. The relationship between the velocities of the robot and the rotational velocities of the wheels is given in (4.3).

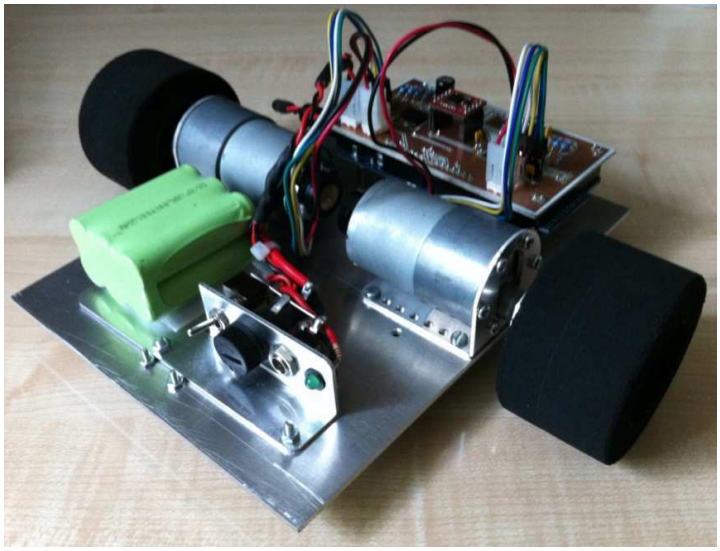

Figure 4.9: Phototype of the WMR

Pulse-width-modulation techniques are used to adjust the supply voltage so that the micro-controller can control the rotational velocities of each wheel independently. The rotational velocity of a motor with no load according to the input voltage adjusted by a PWM signal with 100 Hz sampling rate is shown in Table 4.1.

Table 4.1: Rotational velocities with no load according to the duty cycle of the PWM signals.

	Voltage	Counts	ω(rad/s)
(1)	1.088	2	0.062
(2)	2.175	10	0.31
(3)	3.263	21	0.66
(4)	4.35	31	0.97
(5)	5.438	41	1.28
(6)	6.525	51	1.59
(7)	7.613	61	1.91
(8)	8.697	71	2.22

To avoid unnecessary complexity of the control algorithm, two PI controllers are applied to the two motors to produce the desired inputs $u = \text{col}(v, \omega)$ in the system (4.7) as designed in (4.14). The dynamical parameters of the motors are estimated by experiments based on their specification. With the same strategies proposed by [145], and assuming the two motors have the same parameters, the approximated dynamic model of the DC motor can be described by

$$\dot{\omega}_m = -15.385\omega_m + 3.846u_m \tag{4.19}$$

where ω_m is the rotational velocity of the motor and u_m is the adjusted voltage.

Define the PI controller for the motor as

$$u_m(t) = K_p e_m(t) + K_i \int_0^t e_m(t)dt \tag{4.20}$$

where $e_m(t)$ is the error between the expected and actual rotational velocities of motor. K_p is the proportional gain, and K_i is the integral gain for the motors on the right and left side. It should be noticed that the differences between the dynamics of the two motors are ignored and the PI controllers are simply implemented with identical controller gains.

With 100 Hz sampling rate, the parameter $K_p = 6.96$ and $K_i = 17.94$ are obtained by test. The sine wave tracking response shown in Figure 4.10 shows that the tracking performance is as expected.

Despite the dynamic variability and parameter variations in the motors, for example the slight differences in manufacturing between the two motors, the effect of the inductance, load changes and external forces, these may be ignored in the model as these uncertainties largely occur in the input channel of the kinematic model. The designed SMC system can be made completely insensitive to such matched uncertainty as described in section 3.2.

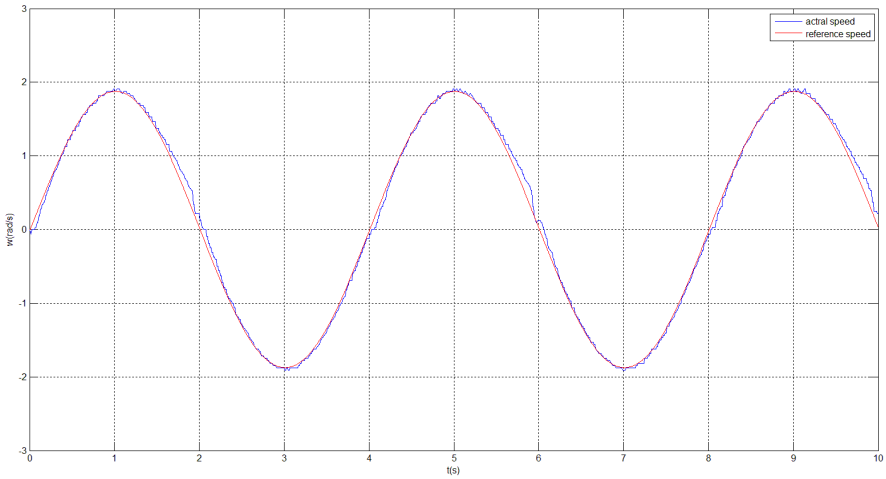

Figure 4.10: Sinewave response of the motor

4.5. Simulation and Experimental Results

In this section, both closed-loop simulation and experimental results are presented to test the behaviour of the SMC proposed in Section 4.3. The simulations are implemented in MATLAB, and the real-time experiments are based on the Arduino Due board with the software configured according to the control design. The measured and estimated parameters are shown in Table 4.2

Remark 4.4. *As in our design the two DC motors are identical, all the parameters of both motors, r, K_p and K_i, are the same.*

Table 4.2: The choice of options.

	Parameters	value
(1)	radium of wheels r(m)	0.0315
(2)	Width between two wheels R(m)	0.09
(3)	Sliding surface parameter c_1	0.6
(4)	Reaching gain η_1	1.2
(5)	Reaching gain η_2	0.1
(6)	Boundary layer parameter δ_1	0.05
(7)	Boundary layer parameter δ_2	0.01

Simulation Results

The simulation is carried out by using MATLAB, and the model for the reference and actual robot used in the simulation is the kinematic model of them defined in (4.4) and (4.2) respectively.

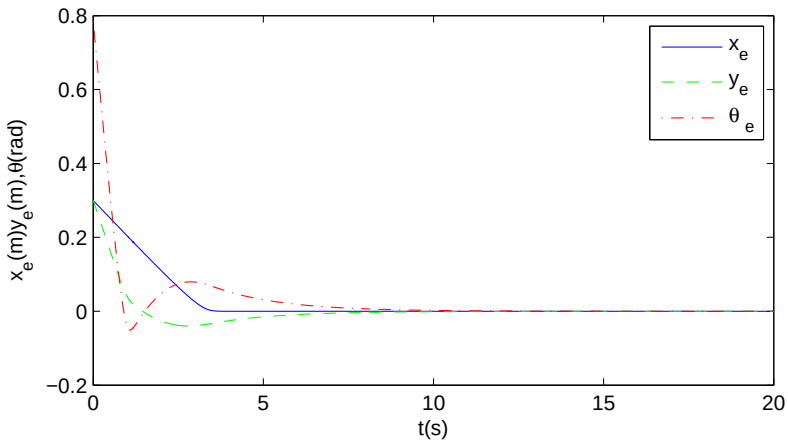

Figure 4.11: Time response of the error states

The main simulation results with a circle reference trajectory with initial condition $q_r(0, 0, \frac{\pi}{4})$, reference control pair $v_r = 0.25, \omega_r = 0.5$ and initial posture of the actual robot $q(-0.2, -0.3, 0)$ are shown in Figures 4.12 to 4.13

Remark 4.5. *The simulation environment is configured to represent the hardware. All the*

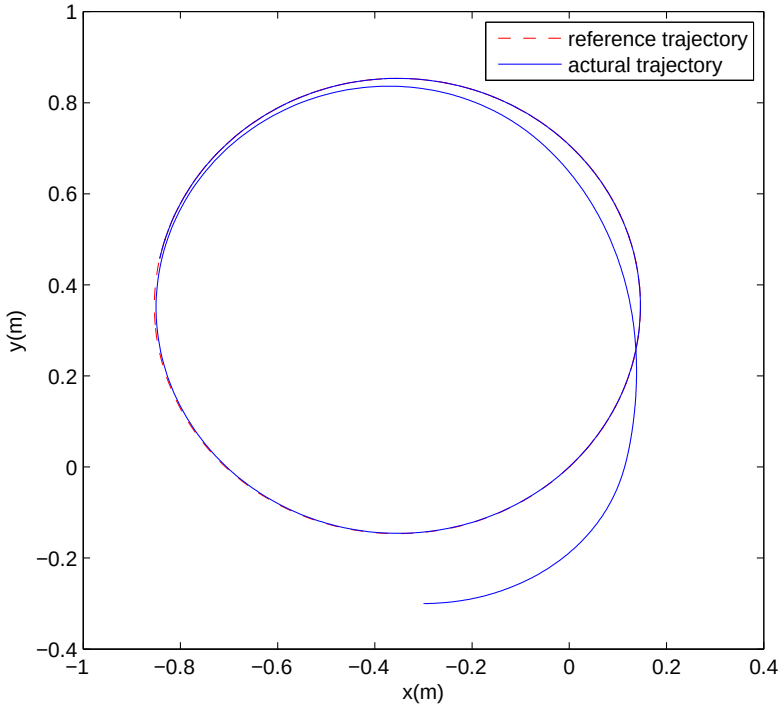

Figure 4.12: Simulated motion shown in the x-y phase plane

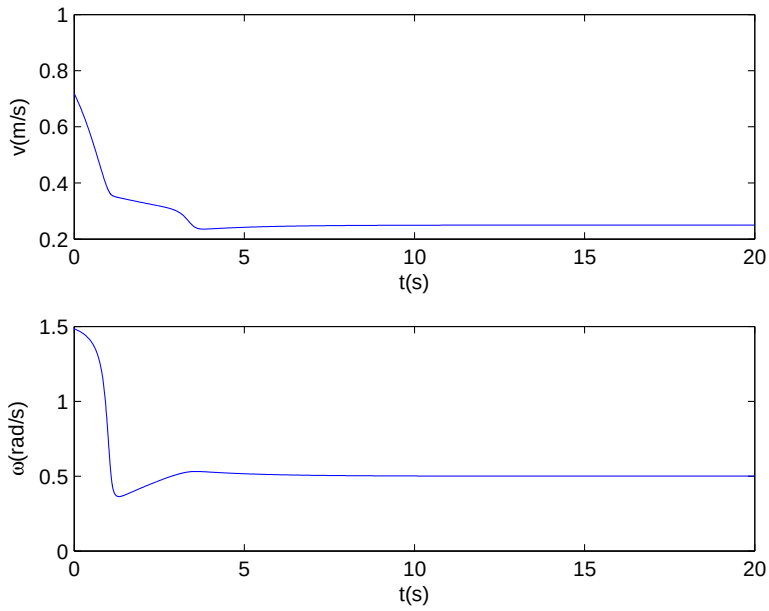

Figure 4.13: Time response of the velocities

parameters are selected corresponding to the hardware constraints. The dynamics of the actuators, in this case the motors, are also incorporated in the simulation.

Experimental results

An image of the WMR during the circle tracking task is shown in Figure 4.14 and the actual motion is compared with simulation results in Figure 4.15.

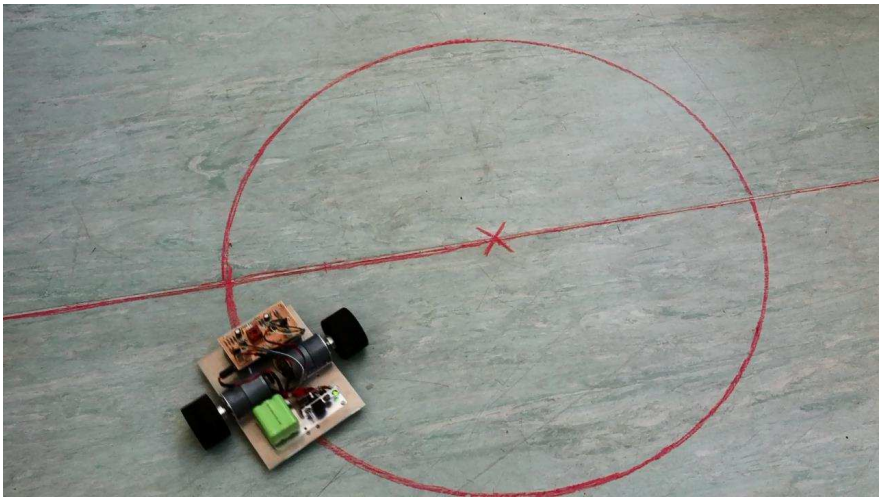

Figure 4.14: Tracking task experiments

From the experimental results, it is evident that although the regular form is not available, the regular form-based SMC can still be used for the control design. Both simulation and experiment results verify the effectiveness of this approach and it has also been demonstrated that although uncertainties may exist, the robustness properties of the SMC ensure that the system exhibits the expected tracking performance. A small tracking error is achieved in the implementation.

4.6. Conclusion

In this chapter, the trajectory tracking control design problem for a differential driving two-WMR has been considered. The proposed regular form-based SMC has been successfully implemented on a real-time WMR platform although the system is not in the regular form. Both simulation results and experimental tests show that the proposed controller is effective,

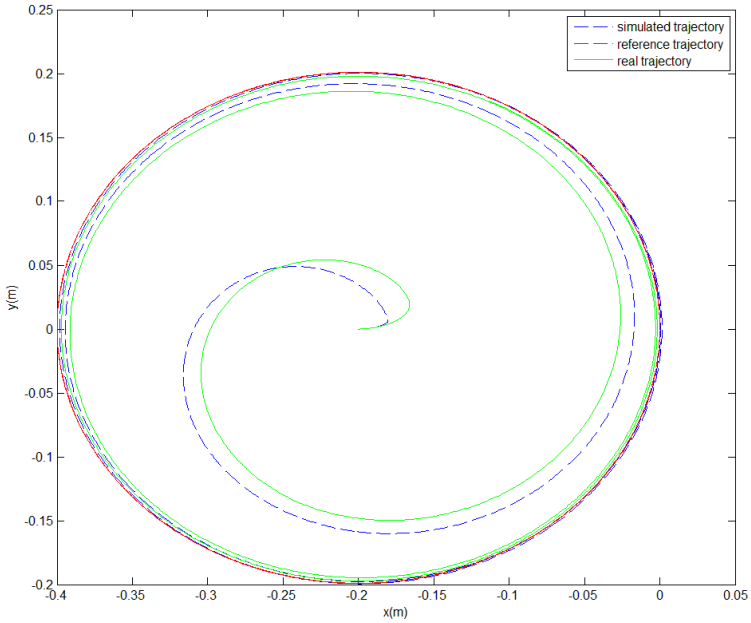

Figure 4.15: Comparison between experiments and simulations

straightforward to implement and exhibiting good tracking performance.

CHAPTER. 5

GENERALISED REGULAR FORM BASED CONTROL

From the previous chapter, a SMC design is established for the tracking control of a WMR with both simulation and experimental verifications. Notably, system (4.7), in which the regular form-based SMC is designed, is not in the exact regular form. By further analysis, a global diffeomorphism which can transfer system (4.7) into the regular form does not even exist according to the Frobenius Theorem discussed in Section 3.2.4. From the simulation and experiment results of control for system (4.7), it indicates that the regular form-based SMC may also be developed on the system in which the classical regular form is not available. Therefore, in this chapter, a generalised regular form is proposed with further analysis and SMC is designed for nonlinear systems in the generalised regular form with both simulation and experiment. Starting with the brief review of related works in Section 5.1, the target system is then introduced in Section 5.2. The corresponding stability analysis and control design are carried out in Section 5.3 and Section 5.4 respectively. Section 5.5 applies the developed results to the trajectory control of WMR in the presence of both matched and mismatched uncertainties with both simulation and experimental verifications. Finally, the conclusion of this chapter is given in Section 5.6.

5.1. Introduction

As mentioned in section 3.2, SMC is a powerful technique because of its fast convergence and strong robustness [17, 18]. The invariance property of systems in the sliding mode to matched uncertainties and parameter variations [16] has motivated numerous applications of sliding mode techniques to nonlinear systems, e.g. multi-machine power systems [11], direct-drive robot system [146], induction motor [147], power converters [148] and WMR systems [10]. The concept of the SMC is also used in observer design and fault detection [149]. To name a few, it has been demonstrated that sliding mode approach can be applied to control systems with mismatched uncertainties, see for example [28, 19, 29, 30]. In [67], the bounds on the uncertainties are estimated using adaptive techniques. However, the uncertainties are inevitably assumed to satisfy a linear growth condition in order to adaptively compensate the parameter uncertainty. In [19], by using an extended disturbance observer with a modified time-varying sliding surface, a novel SMC is applied to stabilise a SISO system with continuous external disturbance which does not vanish at the origin. Ultimate boundedness of the system is guaranteed and the obtained ultimate bound can be further reduced by choosing appropriate design parameters. However, the structure of the system is restricted, which makes the method difficult to extend to the MIMO case. In [20] a sliding mode scheme is proposed for a linear MIMO system which is applied with disturbance observer techniques to reduce the effect caused by mismatched uncertainties with known structure and upper bounds. The external disturbance is attenuated in sliding motion with a H_∞ control-based approach to guarantee ultimate boundedness stability or can be completely eliminated from the output channel at the steady state with steady-state output-based approach such that the output of the system is asymptotically stable. The method proposed by [27] also shows the strong robustness of SMC for systems with an uncertain input distribution where the considered systems are linear with nonlinear disturbances. In [150], SMC for general nonlinear stochastic systems has been investigated. It is shown that for some special nonlinear stochastic systems, LMIs can be used for controller design. Furthermore, this method can also be applied for nonlinear uncertain stochastic systems with state-delay based on a T-S fuzzy modeling and control approach [151]. With the SMC above, the system is usually required to be in regular form or to be transferred into such a form for analysis. It should be noted that the transformation matrix for linear systems

can be easily obtained by basic matrix theory. However, for nonlinear systems, it is usually very difficult to find a diffeomorphism to transfer a nonlinear system into the traditional regular form. Moreover, the associated conditions may be too strong to be applied for most general nonlinear systems even if the traditional regular form exists (see, for example [134] and reference therein).

In this chapter, a generalised regular form is proposed for a class of nonlinear control systems, which is an extension of the traditional/classical regular form for SMC design for the first time. This is an extension of the traditional/classical regular form for sliding mode design. Then, a novel nonlinear sliding surface is designed associated with the generalised regular form such that the corresponding sliding mode dynamics are globally asymptotically stable using implicit function theory. Robust sliding mode controllers are designed to guarantee that the considered system is driven to the sliding surface in finite time and remains on it thereafter even in the presence of matched and mismatched uncertainties. All the uncertainties are assumed to be bounded by known functions and the bounds on the uncertainties are fully used to reduce the effects of the uncertainties. The developed results are tested by model-based tracking control of a WMR with a differential driving mechanism through simulation and experiment. The tracking error dynamics are derived initially, and then the developed results are applied to the error system to demonstrate the developed strategies. Experimental and simulation results on the WMR show that the proposed controller is insensitive to matched uncertainties, and can tolerate a certain level of mismatched uncertainties in both theory and application.

5.2. System Description

Consider a class of nonlinear systems with matched and mismatched uncertainties described by

$$\dot{x} = \mathcal{F}(t,x) + \mathcal{G}(t,x)(u + \Phi(t,x)) + \Psi(t,x) \tag{5.1}$$

where $x \in \mathcal{R}^n$ and $u \in \mathcal{R}^m$ are the state variables and control inputs respectively. The nonlinear vector $\mathcal{F}(\cdot) \in \mathcal{R}^n$ and the input matrix function $\mathcal{G}(\cdot) \in \mathcal{R}^{n\times m}$ are known with full rank for $x \in \mathcal{R}^n$ and $t \in \mathcal{R}^+$. The terms $\Phi(\cdot)$ and $\Psi(\cdot)$ denote the matched and mismatched uncertainties respectively. It is assumed that all the nonlinear functions are smooth enough so that the existence of the solution of system (5.1) is guaranteed.

Assumption 5.1. There exist known continuous nonnegative functions $\delta(t,x)$ and $\mu(t,x)$ such that the mismatched uncertainty $\Psi(t,x)$ and the matched uncertainty $\Phi(\cdot)$ in system (5.1) satisfy

$$\|\Psi(t,x)\| \leq \delta(t,x) \tag{5.2}$$

$$\|\Phi(t,x)\| \leq \mu(t,x) \tag{5.3}$$

Remark 5.1. *Assumption 5.1 requires that the bounds on the uncertainties are known. These will be employed in the control design to reject/reduce the effects of the uncertainties.*

For further analysis, partition $\mathcal{F}(\cdot)$, $\mathcal{G}(\cdot)$ and $\Psi(\cdot)$

$$\mathcal{F}(t,x) := \begin{bmatrix} \mathcal{F}_1(t,x) \\ \mathcal{F}_2(t,x) \end{bmatrix} \tag{5.4}$$

$$\mathcal{G}(t,x) := \begin{bmatrix} \mathcal{G}_1(t,x) \\ \mathcal{G}_2(t,x) \end{bmatrix} \tag{5.5}$$

$$\Psi(t,x) := \begin{bmatrix} \Psi_1(t,x) \\ \Psi_2(t,x) \end{bmatrix} \tag{5.6}$$

where $\mathcal{F}_1(\cdot) \in \mathcal{R}^{n-m}$, $\mathcal{F}_2(\cdot) \in \mathcal{R}^{m}$, $\mathcal{G}_1(\cdot) \in \mathcal{R}^{(n-m)\times m}$, $\mathcal{G}_2(\cdot) \in \mathcal{R}^{m\times m}$, $\Psi_1(\cdot) \in \mathcal{R}^{n-m}$ and $\Psi_2(\cdot) \in \mathcal{R}^{m}$. Then from the partitions (5.4)-(5.6), the system (5.1) can be rewritten as

$$\dot{x}_1 = \mathcal{F}_1(t,x) + \mathcal{G}_1(t,x)\big(u + \Phi(t,x)\big) + \Psi_1(t,x) \tag{5.7}$$

$$\dot{x}_2 = \mathcal{F}_2(t,x) + \mathcal{G}_2(t,x)\big(u + \Phi(t,x)\big) + \Psi_2(t,x) \tag{5.8}$$

where $x_1 \in \mathcal{R}^{n-m}$, $x_2 \in \mathcal{R}^{m}$ and $x = \text{col}(x_1, x_2)$. Since $\mathcal{G}(\cdot) \in \mathcal{R}^{n\times m}$ is full rank for $x \in \mathcal{R}^n$ and $t \in \mathcal{R}^+$. Assume that $\mathcal{G}_2(t,x)$ is nonsingular in $(t,x) \in \mathcal{R}^+ \times \mathcal{R}^n$ or there exists a diffeomorphism such that system (5.1) can be transferred into the form of (5.7)-(5.8) with $\mathcal{G}_2(t,x)$ is nonsingular in $(t,x) \in \mathcal{R}^+ \times \mathcal{R}^n$, then choose the sliding function $\sigma(x)$ as follows:

$$\sigma(x) = Kx_2 + \varphi(x_1, x_2) \tag{5.9}$$

where $K = \text{diag}\{k_1, k_2, \ldots, k_m\}$ with $k_i > 0$ for $i = 1, 2, \ldots, m$, $\varphi(\cdot)$ is a known class $\mathcal{C}^1$ function and each entry of the Jacobian matrix $[\frac{\partial \varphi}{\partial x_2}]_{ij}$ for $i, j = 1, 2, \ldots, m$ is bounded.

Remark 5.2. *There is no general way to design the function $\varphi(x_1, x_2)$ for a general nonlinear system since the function is dependent on the system dynamics. However, for a specific system, system knowledge can be used in conjunction with the assumptions to establish a design. It*

should be noted that the sliding function (5.9) proposed in this chapter includes both the linear sliding function $\sigma(x) = Cx$ where $C \in \mathcal{R}^{m\times n}$ is a constant matrix, and the nonlinear sliding function in the form of $\sigma(x) = x_2 + \vartheta(x_1)$ where $\vartheta(\cdot) \in \mathcal{R}^m$ as special cases.

For the sliding function in (5.9), the sliding surface is described by

$$\mathcal{S} = \{x \in \mathcal{R}^n | \quad \sigma(x) = 0\} \tag{5.10}$$

Definition 5.1. System (5.7)-(5.8) with the sliding function defined in (5.9) is called the generalised regular form of system (5.1) if the function $\mathcal{G}_1(\cdot)$ defined in (5.5) satisfies

$$\mathcal{G}_1(t, x)|_{x\in\mathcal{S}} = 0 \tag{5.11}$$

Remark 5.3. *It should be emphasised that the classical regular form requires that $\mathcal{G}_1(t, x) = 0$ for all $t \geq 0$ and $x \in \mathcal{R}^n$ (see, e.g. [17], [134]) while the generalised regular form defined above requires that $\mathcal{G}_1(t, x) = 0$ only for all $t \geq 0$ and $x \in \mathcal{S}$. It is clear to see that the classical regular form is a special case of the generalised regular form defined above as $\mathcal{S}$ is just a surface in $\mathcal{R}^n$. From the Frobenius Theorem, the distribution spanned by the column vectors of the input matrix $\mathcal{G}(\cdot)$ is completely integrable if and only if the distribution is involutive (detailed discussion can be found in Section 3.2.4). This implies that the classical regular form may not exist for a nonlinear system. In contrast, the generalised regular form may exist and thus to develop a sliding mode theory associated with the proposed generalised regular form is valuable since the proposed method can be applied in cases where the classical regular form is not available.*

Define function matrices $\Gamma_{\mathcal{G}}(t, x)$ and $\Gamma_{\mathcal{F}}(t, x)$ as

$$\Gamma_{\mathcal{G}}(t, x) := \frac{\partial\sigma}{\partial x}\mathcal{G}(t, x) = K\mathcal{G}_2(t, x) + \frac{\partial\varphi}{\partial x}\mathcal{G}(t, x) \tag{5.12}$$

$$\Gamma_{\mathcal{F}}(t, x) := \frac{\partial\sigma}{\partial x}\mathcal{F}(t, x) = K\mathcal{F}_2(t, x) + \frac{\partial\varphi}{\partial x}\mathcal{F}(t, x) \tag{5.13}$$

where $\mathcal{F}_1(\cdot)$, $\mathcal{F}_2(\cdot)$, $\mathcal{G}_1(\cdot)$ and $\mathcal{G}_2(\cdot)$ are defined in (5.4)-(5.5) and $\sigma(\cdot)$ is defined in (5.9). The following assumption is imposed on system (5.7)-(5.8).

Assumption 5.2. The function matrix $\Gamma_{\mathcal{G}}(t, x)$ defined in (5.12) is nonsingular for $x \in \mathcal{R}^n$ and $t \in \mathcal{R}^+$

Remark 5.4. *Assumption 5.2 is a limitation on the input distribution matrix $\mathcal{G}(t,x)$ and the designed sliding surface $\sigma(x)$ in (5.9). It is required to guarantee that the system can be driven to the sliding surface (5.10). Since $\mathcal{G}_2(\cdot)$ is nonsingular, it is straight forward to see from (5.13) that Assumption 5.2 usually can be satisfied by choosing an appropriate parameter K, and thus this condition is not strict.*

It should be noted that under condition (5.11), when the system (5.1) is limited to the sliding surfaces (5.10), the system (5.7) has the following form

$$\dot{x}_1 = \mathcal{F}_1(t,x)|_{x\in\mathcal{S}} + \Psi_1(t,x)|_{x\in\mathcal{S}} \tag{5.14}$$

The objective now is to study under what conditions system (5.14) is the sliding mode dynamics of system (5.1) with respect to the sliding surface (5.10). Therefore it is necessary to guarantee that there exists a unique solution of the functional equation $\sigma(x) = 0$ for x_2 in terms of x_1. The following lemma is introduced to facilitate further analysis.

Lemma 5.1. *Under condition (5.11), there exists a function $g : \mathcal{R}^{n-m} \to \mathcal{R}^m$ such that when system (5.7) is constrained to the sliding surface (5.10), the dynamical system (5.7) can be described by*

$$\dot{x}_1 = \mathcal{F}_1^s(t,x_1) + \Psi_1^s(t,x_1) \tag{5.15}$$

where

$$\mathcal{F}_1^s(t,x_1) = \mathcal{F}_1(t,x)|_{x_2=g(x_1)} \tag{5.16}$$

$$\Psi_1^s(t,x_1) = \Psi_1(t,x)|_{x_2=g(x_1)} \tag{5.17}$$

if $K = \mathrm{diag}\{k_1, k_2, \ldots, k_m\}$ in (5.9) satisfies

$$k_i \geq \varepsilon + \sum_{j=1}^{m} \sup \Big| \Big[\frac{\partial \varphi}{\partial x}\Big]_{ij} \Big|, \quad i = 1, 2, \ldots, m \tag{5.18}$$

where ε is a positive constant.

Proof. When system (5.7) is limited to the sliding surfaces (5.10), it follows from condition (5.11) that the system (5.7) can be described by (5.14). From (5.9) and (5.18),

$$\Big|[\frac{\partial \sigma}{\partial x_2}]_{ii}\Big| = \Big|k_i + [\frac{\partial \varphi}{\partial x_2}]_{ii}\Big| \geq k_i - \Big|[\frac{\partial \varphi}{\partial x_2}]_{ii}\Big|$$

$$
\begin{aligned}
&\geq \varepsilon + \sum_{j=1}^{m} \sup \left| \left[\frac{\partial \varphi}{\partial x} \right]_{ij} \right| - \left| [\frac{\partial \varphi}{\partial x_2}]_{ii} \right| \\
&= \varepsilon + \sum_{\substack{j=1 \\ j \neq i}}^{m} \sup \left| \left[\frac{\partial \varphi}{\partial x} \right]_{ij} \right| \qquad (5.19)
\end{aligned}
$$

for $i = 1, 2, \ldots, m$. This implies that

$$
\left| [\frac{\partial \sigma}{\partial x_2}]_{ii} \right| - \sum_{\substack{j=1 \\ j \neq i}}^{m} \left| [\frac{\partial \sigma}{\partial x_2}]_{ij} \right| \geq \varepsilon, \quad i = 1, 2, \ldots, m \qquad (5.20)
$$

Then from Lemma 2.8, there exists a unique class $\mathcal{C}^1$ function $x_2 = g(x_1)$ satisfying $\sigma(x_1, g(x_1)) = 0$.

The analysis above shows that $x_2 = g(x_1)$ when $x \in \mathcal{S}$. Hence the result follows by substituting $x_2 = g(x_1)$ into the right-hand side of the equation (5.14). ■

5.3. Stability Analysis of the Sliding Mode

It is clear that the corresponding sliding motion of system (5.1) associated with the sliding surface (5.9) is given by (5.15). The stability of system (5.15) will be studied in this section.

Assumption 5.3. There exists a continuously differentiable Lyapunov function $V(t, x_1) : \mathcal{R}^+ \times \mathcal{R}^{n-m} \longmapsto \mathcal{R}$ satisfying the inequalities

$$
\varsigma_1(\|x_1\|) \leq V(t, x_1) \leq \varsigma_2(\|x_1\|) \qquad (5.21)
$$

$$
\frac{\partial V}{\partial t} + \frac{\partial V}{\partial x_1} \mathcal{F}_1^s(t, x_1) \leq -\varsigma_3(\|x_1\|) \qquad (5.22)
$$

$$
\left\| \frac{\partial V}{\partial x_1} \right\| \leq \varsigma_4(\|x_1\|) \qquad (5.23)
$$

where the functions $\varsigma_i(\cdot)$ for $i = 1, 2, 3, 4$ are continuous class $\mathcal{K}$ functions, and $\mathcal{F}_1^s(\cdot)$ is given in (5.15).

Remark 5.5. *Assumption 5.3 implies that the nominal system of the sliding mode dynamics (5.15) is asymptotically stable. The conditions (5.21)-(5.23) are developed from the well known converse Lyapunov Theorem (see Lemma 2.4 in Chatper 2).*

From Assumption 5.1, it is straightforward to see that the mismatched uncertainty $\Psi_1^s(t, x_1)$ in (5.15) satisfies

$$\|\Psi_1^s(t, x_1)\| \leq \gamma(t, x_1) \tag{5.24}$$

where $\gamma(\cdot)$ is a known positive continuous function, which is assumed to satisfy $\gamma(t, 0) = 0$ such that the origin is the invariant equilibrium point of the sliding mode dynamics (14).

Theorem 5.1. *Under condition (5.11) in Definition 5.1 and Assumptions 5.1 and 5.3, the sliding mode (5.15) is globally uniformly asymptotically stable if there exists a continuous nondecreasing function $w : \mathcal{R}^+ \longmapsto \mathcal{R}^+$ satisfying $w(r) > 0$ for $r > 0$ and $w(r) \to \infty$ when $r \to \infty$ such that for any $x_1 \in \mathcal{R}^{n-m}$*

$$w(\|x_1\|) \leq \varsigma_3(\|x_1\|) - \varsigma_4(\|x_1\|)\gamma(t, x_1) \tag{5.25}$$

Proof. Consider the Lyapunov candidate function $V(\cdot)$ satisfying Assumption 5.3 for system (5.15). The time derivative of $V(\cdot)$ along the trajectory of system (5.15) is given by

$$\begin{aligned}
\dot{V} =& \frac{\partial V}{\partial t} + (\frac{\partial V}{\partial x_1})^\tau (\mathcal{F}_1^s(t, x_1) + \Psi_1^s(t, x_1)) \\
\leq& \frac{\partial V}{\partial t} + (\frac{\partial V}{\partial x_1})^\tau \mathcal{F}_1^s(t, x_1) + \left\| (\frac{\partial V}{\partial x_1})^\tau \right\| \|\Psi_1^s(t, x_1)\| \\
\leq& - \varsigma_3(\|x_1\|) + \varsigma_4(\|x_1\|)\gamma(t, x_1) \\
\leq& - w(\|x_1\|)
\end{aligned} \tag{5.26}$$

where the conditions (5.21)-(5.23) are used above. Hence, the conclusion follows. ■

Remark 5.6. *It should be pointed out that condition (5.25) shows the limitation on the mismatched uncertainty $\Psi(t, x)$ in system (5.1) through the bounds $\gamma(t, x_1)$ in (5.24). It should be noted that: i) $\gamma(t, x_1)$ is the bound on $\Psi_1^s(t, x_1)$ (see (5.24), ii) $\Psi_1^s(t, x_1)$ is the contribution from the function $\Psi_1(t, x)$ when the system is on the sliding surface (see (5.17)), and iii) $\Psi_1(t, x)$ is a sub-component of $\Psi(t, x)$ (see (5.6)). Therefore, inequality (5.25) represents the limitation on the bounds of the sub-component $\Psi_1(\cdot)$ of $\Psi(\cdot)$ when $\Psi_1(\cdot)$ is on the sliding surface instead of the uncertainty $\Psi(\cdot)$ in the whole space $x \in \mathcal{R}^n$.*

Remark 5.7. *For systems with mismatched disturbances which do not vanish at the origin or in the presence of mismatched external disturbances $d(t)$ which do not vanish when time t goes to infinity, the problem is particularly challenging. In this case, usually only ultimate*

bounded results can be obtained under appropriate conditions unless other techniques such as adaptive control are used to identify the disturbance [103]. In this chapter, global asymptotic stabilization is considered where it is required that the mismatched disturbances vanish at the origin, which is reflected in (5.24) where $\gamma(t,0)=0$*. For the system with external disturbance* $d(t)$ *which cannot vanish at origin as* $t\to\infty$*, the system can only be proved to be ultimate boundedness stable without extra information of the disturbance since the ebullient point of the system with unvanishing disturbance may not be origin. Since we consider uniform asymptotical stability, part of the mismatched uncertainty* $\psi_1(\cdot)$ *in this chapter is required to vanish at origin.*

Since (5.15) is the associated sliding mode dynamics. Theorem 5.1 shows that the sliding motion is asymptotically stable.

5.4. Reachability

From Assumption 5.2, $\Gamma_{\mathcal{G}}(t,x)$ is nonsingular. Consider the control law

$$\begin{aligned} u(t,x) =& -\Gamma_{\mathcal{G}}^{-1}(t,x)\Gamma_{\mathcal{F}}(t,x)-\Gamma_{\mathcal{G}}^{-1}(t,x)\mathrm{sgn}\big(\sigma(x)\big) \\ & \cdot\Big\{\Big\|\frac{\partial\sigma}{\partial x}\Big\|\delta(t,x)+\|\Gamma_{\mathcal{G}}(t,x)\|\mu(t,x)+\eta\Big\} \end{aligned} \tag{5.27}$$

where $\Gamma_{\mathcal{G}}(\cdot)$ and $\Gamma_{\mathcal{F}}(\cdot)$ are defined in (5.12) and (5.13) respectively, $\delta(\cdot)$ and $\mu(\cdot)$ satisfy (5.2) and (5.3) respectively, and $\eta>0$ is a constant parameter selected to define the reaching behaviour.

Theorem 5.2. *Consider the nonlinear system (5.7)–(5.8). Under Assumptions 5.1 and 5.2, the control (5.27) is able to drive system (5.1) to the sliding surface (5.10) in finite time and maintain a sliding motion on it thereafter.*

Proof. From (5.9)

$$\begin{aligned} \dot\sigma(x) =& \frac{\partial\sigma}{\partial x}\Big(\mathcal{F}(t,x)+\Psi(t,x)\Big)+\frac{\partial\sigma}{\partial x}\mathcal{G}(t,x)(u+\Phi(t,x)) \\ =& \Gamma_{\mathcal{F}}(t,x)+\Gamma_{\mathcal{G}}(t,x)\Big(u+\Phi(t,x)\Big)+\frac{\partial\sigma}{\partial x}\Psi(t,x) \end{aligned} \tag{5.28}$$

Substituting the control in (5.27) into (5.28),

$$\sigma^{\tau}(x)\dot\sigma(x) = \sigma^{\tau}(x)\Big\{\frac{\partial\sigma}{\partial x}\Psi(t,x)+\Gamma_{\mathcal{G}}(t,x)\Phi(t,x)\Big\}-$$

$$
\begin{aligned}
&\sigma^{\tau}(x)\mathrm{sgn}(\sigma(x))\Big\{\left\|\frac{\partial\sigma}{\partial x}\right\|\delta(t,x)+\|\Gamma(t,x)\|\mu(t,x)+\eta\Big\}\\
\leq&\|\sigma(x)\|\Big\{\left\|\frac{\partial\sigma}{\partial x}\Psi(t,x)\right\|+\|\Gamma(t,x)\Phi(t,x)\|\\
&-\left\|\frac{\partial\sigma}{\partial x}\right\|\delta(t,x)-\|\Gamma(t,x)\|\mu(t,x)-\eta\Big\}
\end{aligned}
\tag{5.29}
$$

From Assumption 5.1.

$$
\begin{aligned}
\left\|\frac{\partial\sigma}{\partial x}\Psi(t,x)\right\| &\leq \left\|\frac{\partial\sigma}{\partial x}\right\|\|\Psi(t,x)\|\\
&\leq \left\|\frac{\partial\sigma}{\partial x}\right\|\delta(t,x)
\end{aligned}
\tag{5.30}
$$

$$
\begin{aligned}
\|\Gamma(t,x)\Phi(t,x)\| &\leq \|\Gamma(t,x)\|\|\Phi(t,x)\|\\
&\leq \|\Gamma(t,x)\|\mu(t,x)
\end{aligned}
\tag{5.31}
$$

Substituting inequalities (5.30) and (5.31) into (5.29) yields

$$
\begin{aligned}
\sigma^{\tau}(x)\dot{\sigma}(x) \leq&\|\sigma(x)\|\Big\{\left\|\frac{\partial\sigma}{\partial x}\Psi(t,x)\right\|-\left\|\frac{\partial\sigma}{\partial x}\right\|\delta(t,x)\\
&+\|\Gamma(t,x)\Phi(t,x)\|-\|\Gamma(t,x)\|\mu(t,x)-\eta\Big\}\\
\leq&-\eta\|\sigma(x)\|
\end{aligned}
\tag{5.32}
$$

Hence the conclusion follows. ■

5.5. Case Study: Two-WMR Systems

In this section, the results developed in Section 5.2 - Section 5.4 will be applied to the tracking control of a two-WMR where the reference trajectory is model based. The drift-less model of the WMR has been developed in Section 4.2. However, it is common to have uncertain movement in practical implementation cased by non-ideal environment. For instance, in both [129] and [10], SMC strategies were used in the dynamic layer. Although the simulation results in [129, 10] show robustness against matched uncertainties, the SMC was only applied to the dynamic model, which only ensures that the reference velocities can be tracked. In the following sections, a robust SMC for the WMR system is developed in the presence of mismatched uncertainties.

5.5.1. Problem formulation

Consider a WMR with differential driving mechanism. As the wheels of the robot may drift, which may result in mismatched uncertainty, it is necessary to consider mismatched disturbances. From [130], the kinematic model of the WMR can be described by

$$\dot{q} = \begin{bmatrix} \cos\theta_c & 0 \\ \sin\theta_c & 0 \\ 0 & 1 \end{bmatrix} \Big(u + \phi(t,q)\Big) + \psi(t,q) \tag{5.33}$$

where $q = \text{col}(q_x, q_y, \theta_c) \in \mathcal{R}^3$ is the state with coordinates (q_x, q_y) on the $x - y$ plane and the heading angle θ_c, $u = \text{col}(v, \omega)$ is the control input where v is the linear velocity and ω is the steering velocity, $\phi(\cdot) \in \mathcal{R}^2$ includes all uncertainties in the input channel (i.e. the matched uncertainty) and the term $\psi(\cdot) \in \mathcal{R}^3$ denotes the mismatched uncertainty.

Without loss of generality, it is assumed that $\psi(\cdot)$ has the form

$$\psi(t,q) := \text{col}(\psi_1(t,q), \psi_2(t,q), 0)$$

where $\psi_1(\cdot) \in \mathcal{R}$ and $\psi_2(\cdot) \in \mathcal{R}$. Note that the third component of $\psi(\cdot)$ is assumed to be zero. If it is not zero, then it can be included in the matched uncertainty $\phi(\cdot)$ in (5.33).

Assume that the reference trajectory is model based, and it is given by the following dynamic system

$$\begin{bmatrix} \dot{q}_{xr} \\ \dot{q}_{yr} \\ \dot{\theta}_r \end{bmatrix} = \begin{bmatrix} \cos\theta_r & 0 \\ \sin\theta_r & 0 \\ 0 & 1 \end{bmatrix} \begin{bmatrix} v_r(t) \\ \omega_r(t) \end{bmatrix} \tag{5.34}$$

where $q_r = \text{col}(q_{xr}, q_{yr}, \theta_r)$ is the reference trajectory and $u_r = \text{col}(v_r(t), \omega_r(t))$ is the reference control with $v_r \neq 0$. Then the objective of the model-based tracking control is to design a controller u for the system (5.33) such that $\lim_{t\to\infty} \|q_r - q\| = 0$ where $q = \text{col}(q_x, q_y, \theta_c) \in \mathcal{R}^3$ is the state of the system (5.33) and $q_r = \text{col}(q_{xr}, q_{yr}, \theta_r)$ is the reference trajectory created by (5.34).

Remark 5.8. *Due to the complex nonlinearity in the nonholonomic WMR system, it is straightforward to see that not all trajectories can be tracked. Therefore, the trajectory in this chapter is assumed to be model based. It should be noted that the initial misalignment of the WMR*

may result in different initial misalignment of the tracking error system. Such an effect can be included in the system uncertainty which can be overcome by redesign of the SMC if necessary.

Introduce a diffeomorphism $T : \mathcal{R}^3 \longrightarrow \mathcal{R}^3$ with $x = T(q)$ as (see e.g. [138])

$$x := \begin{bmatrix} x_1 \\ x_2 \end{bmatrix} = \begin{bmatrix} x_1 \\ \hdashline x_{21} \\ x_{22} \end{bmatrix} = \tilde{T}(q)(q_r - q) := T(q) \tag{5.35}$$

where $x_1 \in \mathcal{R}$, $x_2 = \text{col}(x_{21}, x_{22}) \in \mathcal{R}^2$ and

$$\tilde{T}(q) = \begin{bmatrix} -\sin\theta_c & \cos\theta_c & 0 \\ \cos\theta_c & \sin\theta_c & 0 \\ 0 & 0 & 1 \end{bmatrix}$$

From (5.33), (5.34) and (5.35), the dynamics of the new error system in x coordinates is given by

$$\begin{aligned} \dot{x} = & \begin{bmatrix} 0 & -\cos\theta_c(q_{rx} - q_x) - \sin\theta_c(q_{ry} - q_y) \\ -1 & -\sin\theta_c(q_{rx} - q_x) + \cos\theta_c(q_{ry} - q_y) \\ 0 & -1 \end{bmatrix} \Big(u + \hat{\phi}(t,x)\Big) + \Psi(t,x) \\ & + \begin{bmatrix} v_r(t)\sin\theta_r\cos\theta_c - v_r(t)\cos\theta_r\sin\theta_c \\ v_r(t)\cos\theta_r\cos\theta_c + v_r(t)\sin\theta_r\sin\theta_c \\ \omega_r(t) \end{bmatrix} \\ = & \underbrace{\begin{bmatrix} v_r(t)\sin x_{22} \\ v_r(t)\cos x_{22} \\ \omega_r(t) \end{bmatrix}}_{\mathcal{F}(t,x)} + \underbrace{\begin{bmatrix} 0 & -x_{21} \\ -1 & x_1 \\ 0 & -1 \end{bmatrix}}_{\mathcal{G}(t,x)} \Big(u + \hat{\phi}(t,x)\Big) + \Psi(t,x) \end{aligned} \tag{5.36}$$

where

$$\begin{aligned} \hat{\phi}(t,x) = & \phi(t,q)|_{q=T^{-1}(x)} \\ \Psi(t,x) := & \begin{bmatrix} \Psi_1(t,x) \\ \Psi_2(t,x) \end{bmatrix} = \frac{\partial T}{\partial q}\psi(t,q)|_{q=T^{-1}(x)} \end{aligned} \tag{5.37}$$

By direct calculation,

$$\frac{\partial T}{\partial q} = \Big(-\tilde{T}(q) + \hat{T}(x)\Big) \tag{5.38}$$

where

$$\hat{T}(x) = \begin{bmatrix} 0 & 0 & -x_{21} \\ 0 & 0 & x_1 \\ 0 & 0 & 0 \end{bmatrix}$$

Substitute (5.38) into (5.37) yields

$$\Psi(t,x) = -\tilde{T}(q)\psi(t,q)|_{q=T^{-1}(x)} \tag{5.39}$$

Then it is straightforward to see that the mismatched uncertainty $\Psi(t,x)$ in the new error system (5.36) has the form

$$\Psi(t,x) = \begin{bmatrix} \Psi_1(t,x) \\ \Psi_2(t,x) \end{bmatrix} = \begin{bmatrix} \Psi_1(t,x) \\ \hdashline \Psi_{21}(t,x) \\ 0 \end{bmatrix}$$

Thus system (5.36) can be described in the form (5.7)-(5.8) as follows

$$\dot{x}_1 = \underbrace{v_r(t)\sin x_{22}}_{\mathcal{F}_1(t,x)} + \underbrace{\begin{bmatrix} 0 & -x_{21} \end{bmatrix}}_{\mathcal{G}_1(t,x)} \Big(u + \Phi(t,x)\Big) + \Psi_1(t,x) \tag{5.40}$$

$$\dot{x}_2 = \underbrace{\begin{bmatrix} v_r(t)\cos x_{22} \\ \omega_r(t) \end{bmatrix}}_{\mathcal{F}_2(t,x)} + \underbrace{\begin{bmatrix} -1 & x_1 \\ 0 & -1 \end{bmatrix}}_{\mathcal{G}_2(t,x)} \Big(u + \Phi(t,x)\Big) \tag{5.41}$$

where $x_2 = \text{col}(x_{21}, x_{22}) \in \mathcal{R}^2$, $x_1 \in \mathcal{R}$ and

$$\Phi(t,x) := \hat{\phi}(t,x) - \Psi_2(t,x) \tag{5.42}$$

It is straightforward to verify that $\tilde{T}(q)$ is nonsingular and $\tilde{T}^{-1}(q)$ is bounded. From (5.35), $\|q_r - q\| \leq \|\tilde{T}^{-1}(q)\| \, \|x\|$ which implies that $\lim_{t\to\infty} \|q_r - q\| = 0$ if $\lim_{t\to\infty} \|x\| = 0$. Therefore, the model-based reference tracking control problem for the kinematic model (5.33) has now been transformed to a stabilisation problem for the error system (5.36). It remains to design a control u to stabilise the system (5.36) globally and asymptotically.

5.5.2. Control design

Assume that the reference trajectory only moves forward with $v_r(t) \geq \mathcal{V}_m$ where $\mathcal{V}_m$ is a positive constant such that a continuously differentiable feedback control law that asymptotically

stabilizes the tracking error system exists [122, 152], and the reference velocities $(v_r(t), \omega_r(t))$ are bounded with $v_r(t) \leq \mathcal{V}_x$ and $|\omega_r(t)| \leq \mathcal{W}_x$ for any $t \in \mathcal{R}^+$. Further, the mismatched and matched uncertainties $\Psi_1(t,x)$ and $\Phi(t,x)$ satisfy

$$\|\Psi_1(t,x)\| \leq \underbrace{\sin^2(x_{22})\sqrt{x_{21}^2+\alpha} + 0.1|x_1 x_{21}|\sqrt{x_{21}^2+\alpha}}_{\delta(t,x)} \tag{5.43}$$

$$\|\Phi(t,x)\| \leq \underbrace{0.5\|x\| + 0.6|v_r\omega_r|}_{\mu(t,x)} \tag{5.44}$$

where α is a positive constant satisfying $\alpha < \mathcal{V}_m^2$. Design the switching functions

$$\sigma(x) = \begin{bmatrix} k_1 x_{21} \\ k_2 x_{22} \end{bmatrix} + \underbrace{\begin{bmatrix} 0 \\ \frac{x_1}{\sqrt{c+x_1^2+x_{21}^2}} \end{bmatrix}}_{\varphi(x_1,x_2)} \tag{5.45}$$

where $k_1 > 0$ and $k_2 > 1$ are design parameters and $c > 0$ is a constant. The sliding surface is described by

$$\mathcal{S} = \{x \in \mathcal{R}^3 |\ \sigma(x) = 0\} \tag{5.46}$$

where $\sigma(x)$ is defined in (5.45). Then on the sliding surface (5.46), $x_{21} = 0$ and thus from (5.40), $\mathcal{G}_1(t,x) = 0$. Therefore, system (5.40)-(5.41) has the generalised regular form. From $\mathcal{F}(\cdot)$ and $\mathcal{G}(\cdot)$ in (5.36) and by direct calculation,

$$\Gamma_{\mathcal{F}}(t,x) := \frac{\partial\sigma}{\partial x}\mathcal{F}(t,x) = \begin{bmatrix} k_1 v_r \cos x_{22} \\ \frac{(c+x_{21}^2)v_r \sin x_{22} - x_1 x_{21} v_r \cos x_{22}}{\sqrt{c+x_1^2+x_{21}^2}} + k_2\omega_r \end{bmatrix} \tag{5.47}$$

$$\Gamma_{\mathcal{G}}(t,x) := \frac{\partial\sigma}{\partial x}\mathcal{G}(t,x) = \begin{bmatrix} -k_1 & k_1 x_1 \\ \frac{x_1 x_{21}}{(c+x_1^2+x_{21}^2)^{\frac{3}{2}}} & -\frac{x_{21}}{(c+x_1^2+x_{21}^2)^{\frac{1}{2}}} - k_2 \end{bmatrix} \tag{5.48}$$

which is nonsingular when $k_2 \geq 1$. When system (5.40) is limited to the sliding surface (5.46), it can be described by

$$\dot{x}_1 = \underbrace{v_r(t)\sin\Big(-\frac{x_1}{k_2\sqrt{c+x_1^2}}\Big)}_{\mathcal{F}_1^s(t,x_1)} + \Psi_1^s(t,x_1) \tag{5.49}$$

where

$$\|\Psi_1^s(t,x_1)\| \leq \underbrace{\sqrt{\alpha}\sin^2\Big(\frac{x_1}{k_2\sqrt{c+x_1^2}}\Big)}_{\gamma(t,x_1)} \tag{5.50}$$

Therefore system (5.49) with $\Psi_1^s(\cdot)$ satisfying (5.50) is the sliding mode dynamics associated with the sliding surface (5.46). For system (5.49), define the candidate Lyapunov function as $V(t, x_1) = \frac{1}{2}x_1^2$, then it is clear to see that

$$\underbrace{0.4x_1^2}_{\varsigma_1(t,x_1)} \leq V(t, x_1) \leq \underbrace{0.6x_1^2}_{\varsigma_2(t,x_1)}$$

The time derivative of V along the trajectories of system (5.49) is given by

$$\begin{aligned}\frac{\partial V}{\partial t} + \frac{\partial V}{\partial x_1}\mathcal{F}_1^s(t, x_1) =& v_r(t)\sin\Big(-\frac{x_1}{k_2\sqrt{c+x_1^2}}\Big)x_1 \\ \leq& -\underbrace{\mathcal{V}_m \sin(\frac{|x_1|}{k_2\sqrt{c+x_1^2}})|x_1|}_{\varsigma_3(|x_1|)} \end{aligned} \tag{5.51}$$

$$\left\|\frac{\partial V}{\partial x_1}\right\| = \underbrace{|x_1|}_{\varsigma_4(|x_1|)} \tag{5.52}$$

From $k_2 \geq 1 > \frac{2}{\pi}$, which implies

$$\frac{\tau}{k_2\sqrt{c+\tau^2}} < \frac{\pi}{2} \tag{5.53}$$

it is straightforward to see that $\varsigma_3(\tau)$ is a class $\mathcal{K}$ function. Thus

$$\begin{aligned}&\varsigma_3(|x_1|) - \varsigma_4(|x_1|)\gamma(t, x_1) \\ &=\mathcal{V}_m \sin(\frac{x_1}{k_2\sqrt{1+x_1^2}})|x_1| - \big(\sqrt{\alpha}\sin^2(\frac{x_1}{k_2\sqrt{c+x_1^2}})\big)|x_1| \\ &\leq\big(\mathcal{V}_m \sin(\frac{x_1}{k_2\sqrt{1+x_1^2}}) - \sqrt{\alpha}\sin^2(\frac{x_1}{k_2\sqrt{c+x_1^2}})\big)|x_1| \\ &=w(|x_1|)\end{aligned} \tag{5.54}$$

where

$$w(\tau) = \big(\mathcal{V}_m \sin(\frac{\tau}{k_2\sqrt{c+\tau^2}}) - \sqrt{\alpha}\sin^2(\frac{\tau}{k_2\sqrt{c+\tau^2}})\big)\tau \tag{5.55}$$

where $\tau \in \mathcal{R}^+$. Since $\mathcal{V}_m \geq \sqrt{\alpha} \geq \sqrt{\alpha}\sin(\frac{\tau}{k_2\sqrt{c+x_1^2}})$, it is clear that $w(\tau)$ is positive definite. Therefore, the conditions of Theorem 5.1 hold. By limiting the minimum reference velocity $\mathcal{V}_m = 0.01$, the kinematic controller $u = \text{col}(v, \omega)$ is described by

$$\begin{aligned}u(t, x) =& -\Gamma_{\mathcal{G}}^{-1}(t, x)\Gamma_{\mathcal{F}}(t, x) - \Gamma_{\mathcal{G}}^{-1}(t, x)\text{sgn}\big(\sigma(x)\big)\cdot \\ &\Big\{\Big\|\frac{\partial\sigma}{\partial x}\Big\|\delta(t, x) + \|\Gamma_{\mathcal{G}}(t, x)\|\mu(t, x) + 5\Big\}\end{aligned} \tag{5.56}$$

where the uncertainties $\delta(\cdot)$ and $\mu(\cdot)$ for the WMR are defined in (5.43) and (5.44) respectively. $\sigma(x)$ for the WMR is defined in (5.45) with $k_1 = k_2 = 1$ and $c = 0.01$, and the corresponding $\Gamma_{\mathcal{G}}(\cdot)$ and $\Gamma_{\mathcal{F}}(\cdot)$ are defined in (5.47) and (5.48) respectively. Then, from Theorems 5.1 and 5.2, it is straightforward to see that systems (5.40)-(5.41) are globally asymptotically stable.

The performance of the proposed controller is tested in MATLAB using the Lemniscate curve [153] and a sharp corner as a reference trajectory. The model for the reference and actual robot used in the simulation is the kinematic model of them defined in (5.34) and (5.33) respectively.

1). Lemniscate Curve

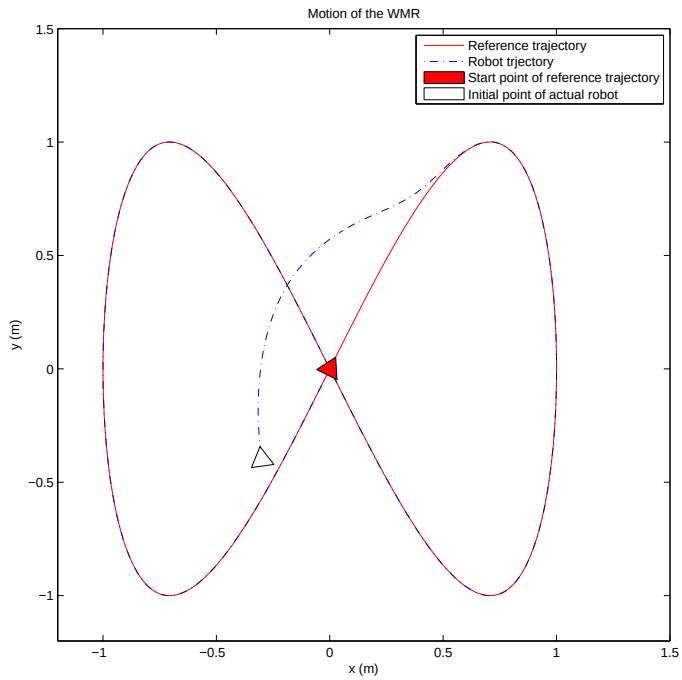

Figure 5.1: The reference trajectory of the Lemniscate curve and the trajectory of the robot in the $x - y$ plane

The Lemniscate curve can be described by the following equations:

$$q_{rx}(t) = \sin(\tfrac{2\pi t}{6}) \tag{5.57}$$

$$q_{ry}(t) = \sin(\tfrac{2\pi t}{3}) \tag{5.58}$$

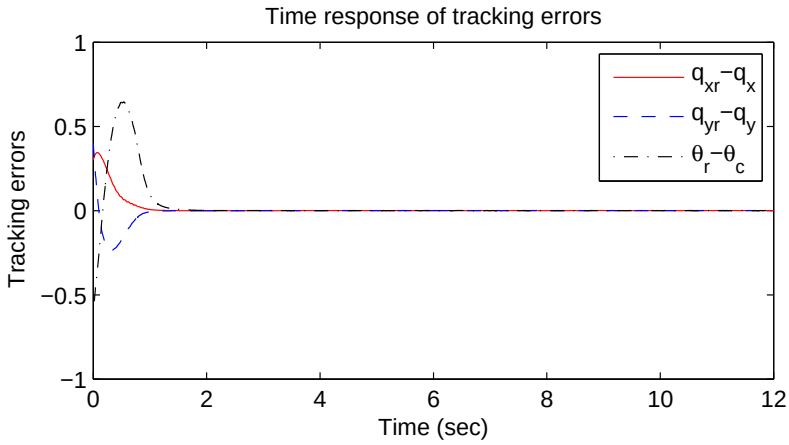

Figure 5.2: Time response of the tracking errors

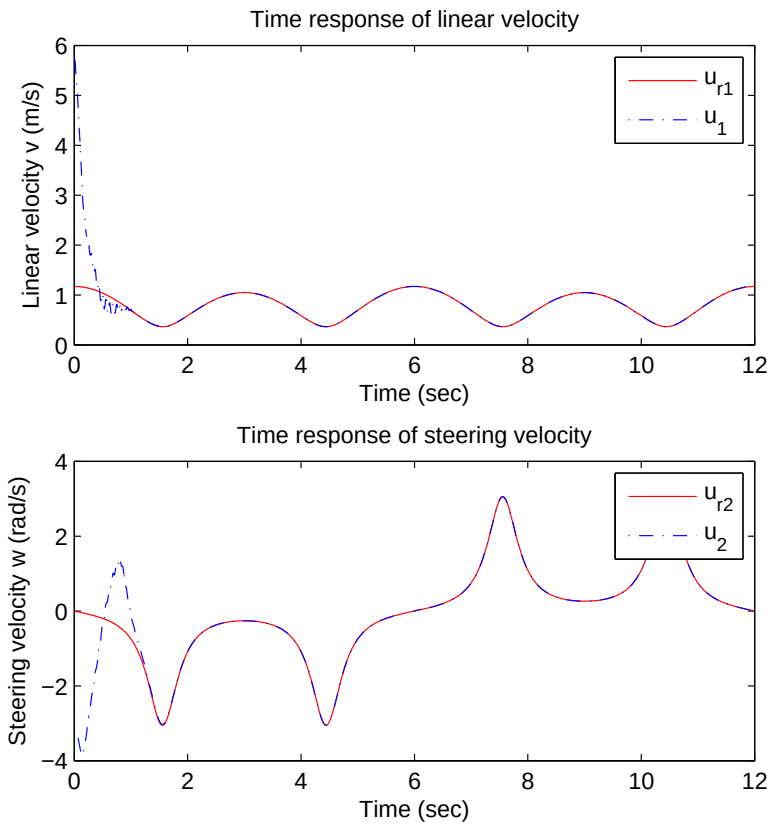

Figure 5.3: Time response of the control pair (v, ω)

The initial point of the reference is $(0, 0, 1.107)$ and the initial point of the robot is chosen as $(-0.3, -0.4, 1.707)$. The motion of the robot and the reference trajectory given by (5.57)-(5.58) are shown in Fig.5.1. The time response of the tracking errors and the control signal

(v, ω) shown in Fig.5.2 and Fig.5.3 respectively.

2). Sharp Corner

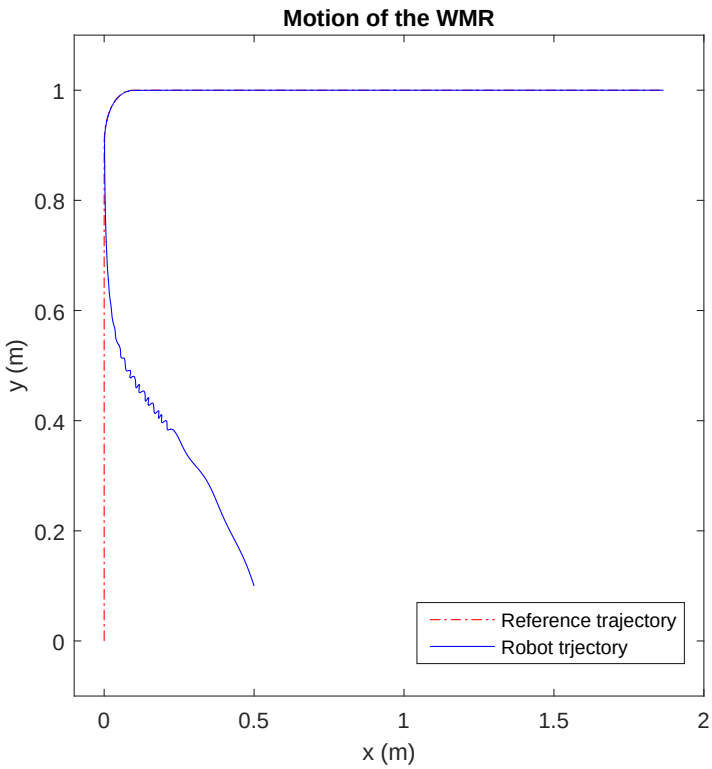

Figure 5.4: The reference trajectory of the Lemniscate curve and the trajectory of the robot in the $x - y$ plane

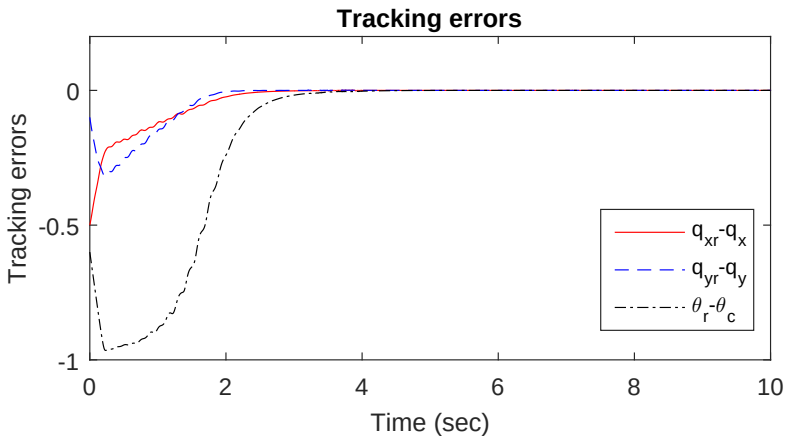

Figure 5.5: Time response of the tracking errors

The sharp corner that will be tested can be described by the following equations:

$$q_{rx}(t) = \begin{cases} 0 & t < 4-\beta \\ \frac{\sqrt{(t+\beta-4)^2+\beta}-\sqrt{\beta}}{\sqrt{16+\beta}} & t \geq 4-\beta \end{cases} \tag{5.59}$$

$$q_{ry}(t) = \begin{cases} 1-\frac{\sqrt{(t-4)^2+\beta}}{\sqrt{16+\beta}} & t < 4 \\ 1 & t \geq 4 \end{cases} \tag{5.60}$$

where $\beta = 0.81$ is a positive parameter that smoothes the corner. The initial point of the

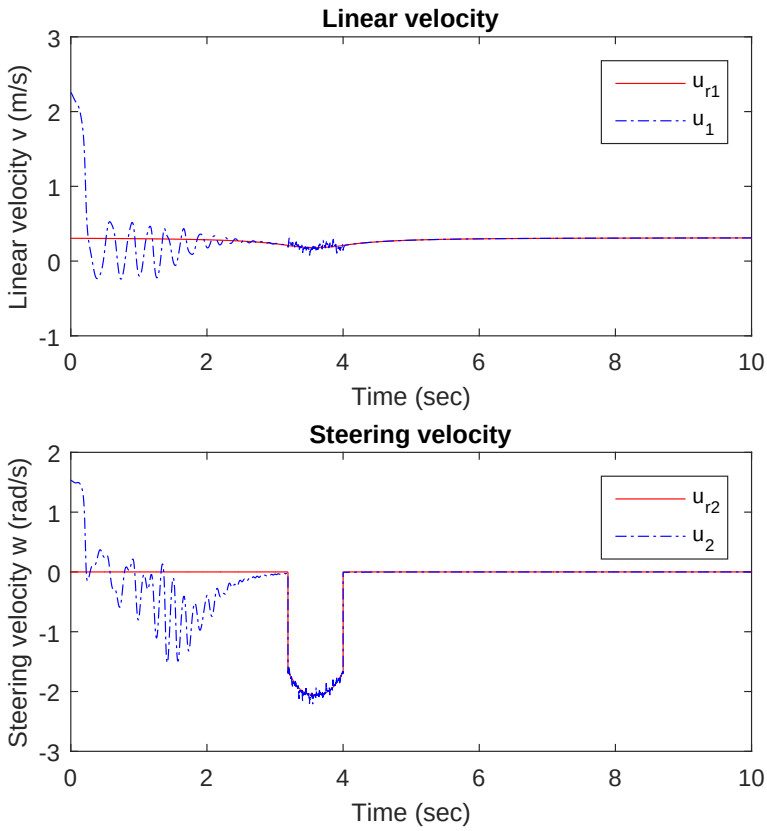

Figure 5.6: Time response of the control pair (v, ω)

reference is $(0, 0, \frac{\pi}{2})$ and the initial point of the robot is chosen as $(0.5, 0.1, 2.17)$. The motion of the robot and the reference trajectory given by (5.59)-(5.60) are shown in Fig.5.4. The time response of the tracking errors and the control signal (v, ω) shown in Fig.5.5 and Fig.5.6 respectively. From Fig.5.3 and Fig.5.6, it can be seen that the system is affected by the matched uncertainties. Particularly, the unvarnished disturbances can be clearly observed in Fig.5.6 at the corner. Due to the complete robustness of SMC to matched uncertainties, the performance

of the system is not affected. From Fig.5.1-Fig.5.6, it is straightforward to see that the proposed approach is effective. It should be noted that due to the discontinuity of the sign function, the control in reality may experience chattering [154] as discussed in Section 3.2. To avoid such problems, the boundary-layer technique proposed in [31], e.g. equation (3.45), has been introduced to reduce the chattering in the simulation and experiments presented in this chapter.

Remark 5.9. *Uncertainties are added in the WMR simulation and bounds on the uncertainties are given to show the robustness of the proposed methodology. In the real system, the uncertainties will vary on a case-by-case basis and can be obtained by statistical data analysis or engineering experience.*

5.5.3. Experimental Test

The low-cost WMR used in this chapter is an updated version of the WMR introduced in Section 4.4 of Chapter 4. The battery of the WMR is replaced with a 12V battery so that the 12V DC motors can run at their maximum speed. The gyroscope is replaced by a 9 degree of freedom motion tracking micro-electro-mechanical System (MEMS) device, i.e. MPU9150, which has 3 axis digital gyroscope, accelerator and compass which enable relatively accurate position estimation. In order to obtain data through wireless communication, a bluetooth module is applied for the serial communication with cycle time of 10ms. The fusion algorithm used in this WMR is based on the combination of the open-source inertial measurement unit (IMU) algorithm proposed in [155] and Kalman filtering techniques. By applying the IMU algorithm to the WMR combing with the encoder, the accuracy of the estimation of the position is increased for the WMR system.

5.5.4. Implementation of the control with DC motors

It should be noted that the control inputs of system (5.40) and (5.41) are the linear velocity v and the steering velocity ω. As assumed by other authors (e.g see [130]), such a controller can be implemented directly using the differential driving mechanism to produce the desired inputs (v, ω) required by the controller (5.27). Two DC motors are used as actuators driving the wheels on each side of the robot independently. The relationship between the velocities of the robot (v, ω) and the rotational velocities of the wheels (ω_R, ω_L) can be described as follows (e.g. see

[130]):

$$\begin{bmatrix} v \\ \omega \end{bmatrix} = \frac{1}{2} \begin{bmatrix} r & r \\ \frac{r}{b} & -\frac{r}{b} \end{bmatrix} \begin{bmatrix} \omega_R \\ \omega_L \end{bmatrix} \tag{5.61}$$

where (ω_R, ω_L) denote the rotational velocities of the wheels on the right and left sides, respectively. r and b denote the radius of the wheel and width of the robot respectively. The dynamics of the motor are also investigated to achieve the input (v, ω) required by controller (5.27). The model of the motor system can be described by (e.g. see [16])

$$\begin{aligned} \begin{bmatrix} \dot{\omega}_m \\ \dot{i}_m \end{bmatrix} = & \begin{bmatrix} 0 & \frac{K_t}{J_m} \\ -\frac{K_e}{L_m} & -\frac{R_m}{L_m} \end{bmatrix} \begin{bmatrix} \omega_m \\ i_m \end{bmatrix} + \begin{bmatrix} 0 \\ \frac{1}{L_m} \end{bmatrix} u_v \\ & + \begin{bmatrix} -T_L \\ 0 \end{bmatrix} \end{aligned} \tag{5.62}$$

$$y = \omega_m \tag{5.63}$$

where ω_m and i_m are the angular velocity and motor current, and y is the measured output. u_v denotes the input voltage adjusted by the microcomputer with Pulse-width modulation techniques. Parameters J_m, L_m, K_t, K_e and R_m denote the motor inertia, inductance, torque constant, back-emf constant and resistance respectively. T_L is the external disturbance representing the effects of friction and the motor load. Parameters identified through experiments with no-load are $J_m = 0.0012Kg \cdot m^2$, $L_m = 0.0054F$, $K_t = 0.034N \cdot m/A$, $K_e = 1.04V \cdot s/rad$ and $R_m = 2.4\Omega$. The comparison between the model response (5.62) and the response of the actual motor is shown in Fig.5.7. The experimental results when tracking a constant reference and sine wave reference signals are shown in Fig.5.8. From the test results, it can be seen that although the system is affected by the limitation of the hardware, the tracking performance is as expected. Although the control performance of the motors may also be affected by parameter variations, the uncertainties caused by friction between the wheels and ground in the motor system will not affect the performance of the WMR system since the SMC is robust to uncertainties implicit in the input channel.

5.5.5. Experimental results

The experimental results for the WMR are presented in this section. The control of the robot is designed with the same process described in Section IV-B. The control performance of

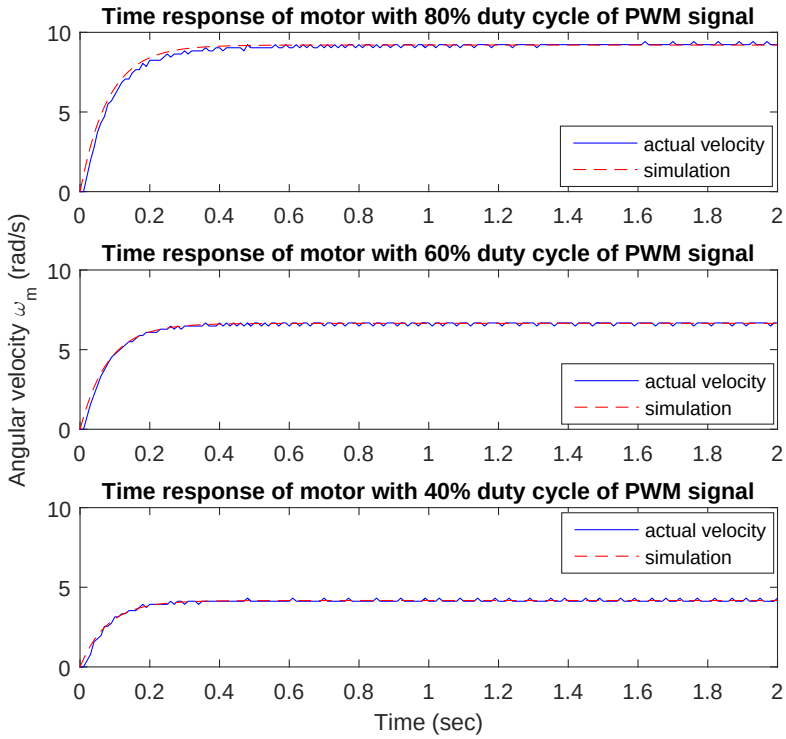

Figure 5.7: Comparison between the actual velocity and the simulation of the motor

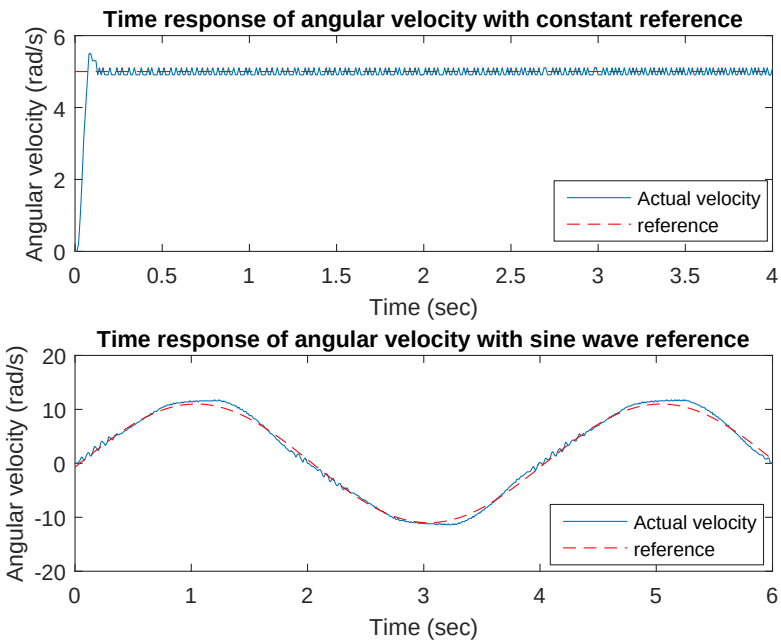

Figure 5.8: Tracking performance of the motor control

the robot is tested with a reference curve described by

$$q_{rx}(t) = 0.05t \tag{5.64}$$

$$q_{ry}(t) = \frac{0.16}{(0.05t - 0.5)^2 + 0.16} - 0.3902 \tag{5.65}$$

and the reference curve described in (5.59)-(5.60) which denotes a smoothed right-angled curve.

For the curve (5.64)-(5.65), the actual motion of the robot and the reference trajectory are shown in Fig.5.9.

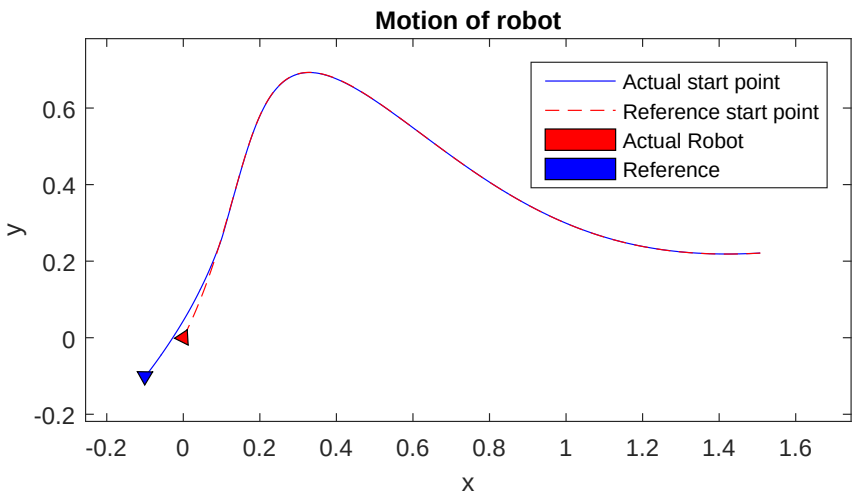

Figure 5.9: Motion of robot in x-y plane in tracking task experiment

The time response of the tracking errors is shown in Fig.5.10, and the control signal is shown in Fig.5.11.

For the curve (5.59)-(5.60) which denotes a smoothed right-angled curve, the actual motion of the robot and the reference trajectory are shown in Fig.5.12. The time response of the tracking errors is shown in Fig.5.13, and the control signal is shown in Fig.5.14.

From Fig.5.10 and Fig.5.13, it can be seen that the system experiences uncertainties caused by the hardware. However, the robot exhibits good tracking performance as shown in Fig.5.12 due to the high robustness of the designed SMC.

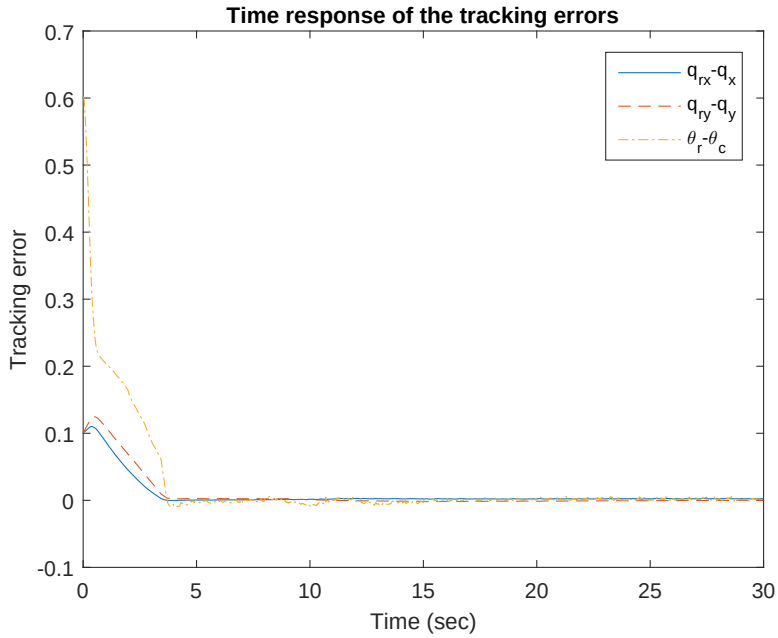

Figure 5.10: Time response of tracking errors in tracking task experiment

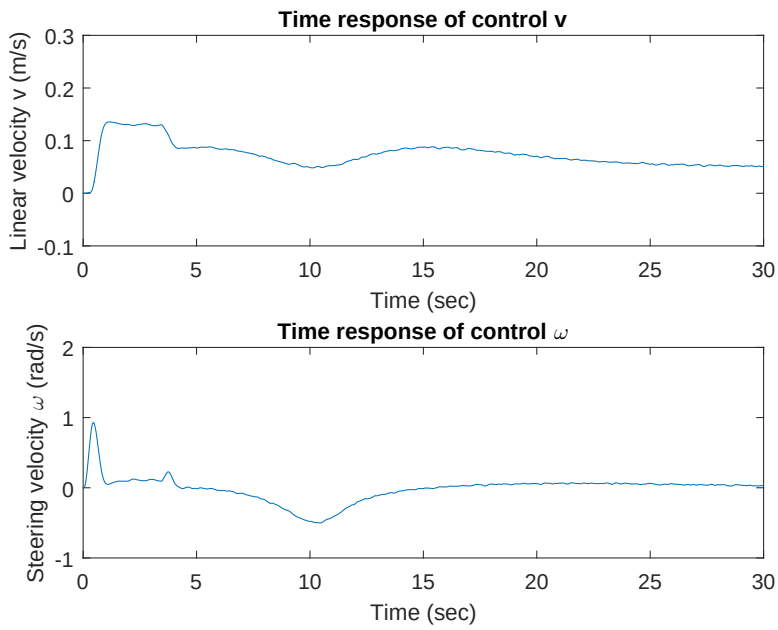

Figure 5.11: Measured control input (v, ω) based on sensors data in tracking task experiment

From the experimental results, it is evident that although modelling error and noise may exist, the robustness properties of the SMC ensure that the system exhibits the expected tracking performance in the presence of uncertainties. It should be noted that the noise usually comes

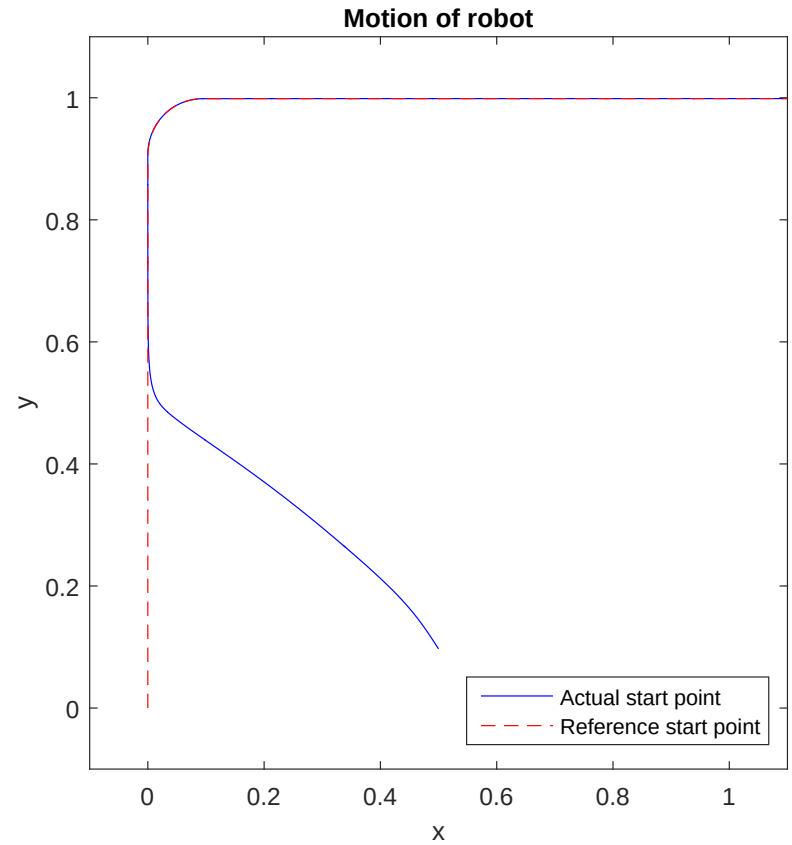

Figure 5.12: Motion of robot in x-y plane in tracking task experiment

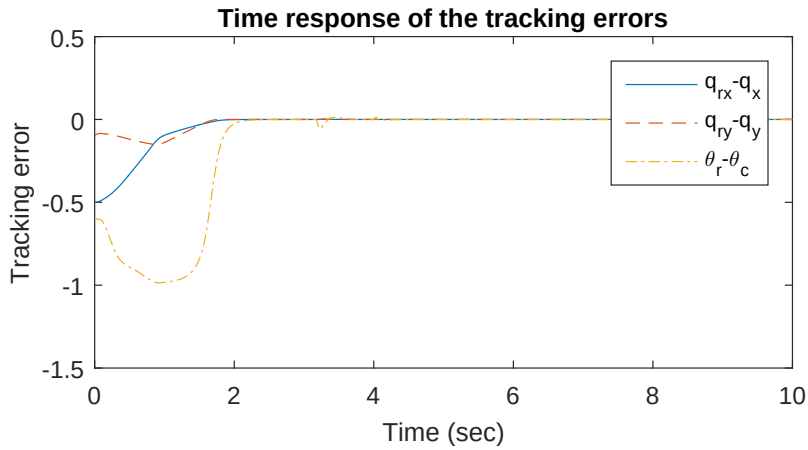

Figure 5.13: Time response of tracking errors in tracking task experiment

from the motors and thus it is matched. Since SMC is completely robust to matched uncertainty, good tracking accuracy is achieved in the experiments.

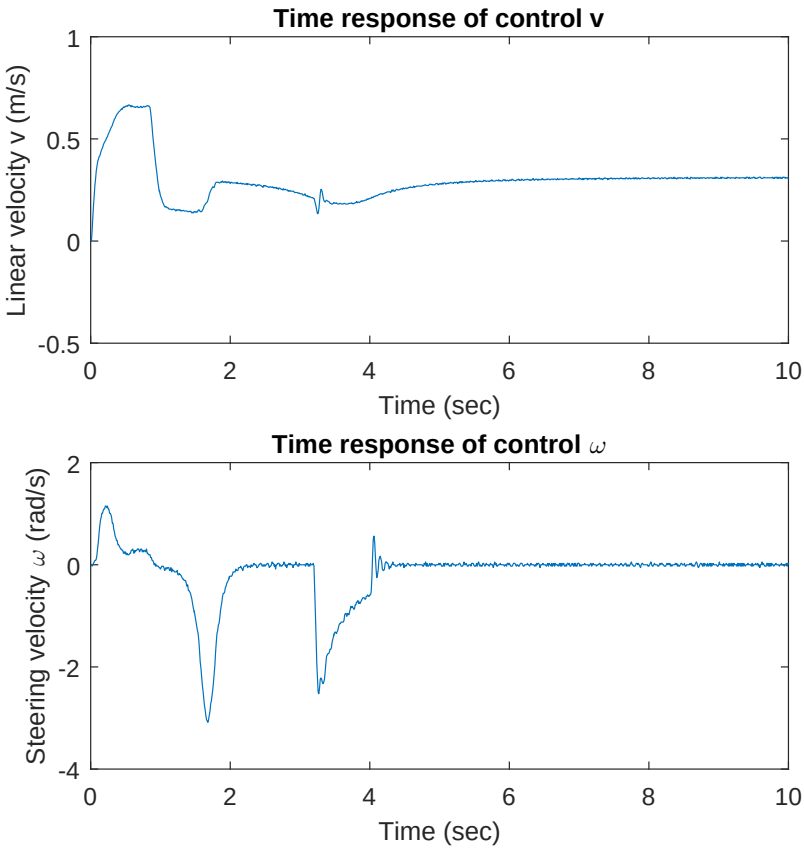

Figure 5.14: Measured control input (v, ω) based on sensors data in tracking task experiment

5.6. Conclusion

In this chapter, a novel generalised regular form for a class of nonlinear systems is proposed for the first time. Based on the generalised regular form, a novel sliding surface has been designed and global asymptotic stability of the corresponding sliding motion has been presented. A SMC scheme is designed to guarantee reachability of the sliding mode. The developed results have been applied to a WMR. Based on the WMR dynamics, a nonlinear sliding surface is formed and global asymptotic stability is exhibited. This application demonstrates that sliding mode techniques can be used to stabilise systems when the normal regular form is not available. Simulation and experimental results show that the proposed results are effective and practicable.

CHAPTER. 6

DECENTRALISED CONTROL FOR LARGE-SCALE SYSTEMS

In this chapter, a decentralised control strategy for a class of nonlinear large-scale interconnected systems is developed in the presence of uncertainties. Since the local controller only utilises the local information, the data transmission is not required in such strategy. To overcome the problem caused by the interconnection, SMC with the following features was applied to improve the robustness. It is shown in this chapter that if the uncertainties/interconnections possess a superposition property, a decentralised control scheme may be designed to counteract the effect of the uncertainty. The study shows that limitations on the bounds assumed on the uncertainties and interconnections can be greatly reduced when compared with the output feedback case. This chapter is organised as follows. Section 6.1 presents a brief review of the existing works. Then, the considered large-scale system is depicted in Section 6.2. The corresponding SMC design is carried out in Section 6.3 and Section 6.4. Two case studies on CSTR system and automated highway system is then provided in Section 6.5.2 before Section 6.6 concludes this chapter.

6.1. Introduction

The problem of robust decentralised controller design has been discussed in Section 3.4. For large scale interconnected systems, uncertainties experienced by one subsystem not only affect its own performance but usually affect the other subsystems' performance as well due to the interactions between the subsystems. SMC has been recognised as a powerful approach in dealing with uncertainties [16, 17] in the presence of unmatched uncertainty [134] although the property of total insensitivity is frequently lost. However, in contrast to the case of centralised control, decentralised scheme can only use local information and thus the uncertainties within the interconnections may not be rejected, even if they are matched. Designing a decentralised control scheme to reject the effect of uncertainties in the interconnection terms is thus challenging. In [22, 23, 24, 25], only matched uncertainties are considered and the bounds on the matched uncertainties are assumed to be linear or polynomial. In terms of mismatched uncertainties, in order to achieve asymptotic stability, some limitations are unavoidable. Mismatched uncertainties have been considered in [134, 98] where centralised dynamical feedback controllers are designed which need more resources to exchange information between subsystems. A class of constraints called integral quadratic constraints is imposed on the considered systems to limit the structure of the original systems [98]. In some cases, adaptive techniques are applied to estimate an upper bound on the mismatched uncertainty which can then be used to counteract its effects [99]. This approach can be powerful when the uncertainty satisfies a linear growth condition. In [69], although the uncertainties are assumed to be nonlinear functions, the system needs to be transformed into a special triangular structure. All the literature which considers mismatched uncertainties mentioned above inevitably requires extra resources and increases system complexity. This may be unattractive from the viewpoint of implementation. Specifically, output feedback control based results impose very strong limitations on the uncertainties and interconnections (see e.g. [22, 156, 47, 11]).

In this chapter, a decentralised control strategy for a class of nonlinear large-scale interconnected systems is proposed based on a SMC paradigm. In terms of the robustness, both matched uncertainties and mismatched unknown interconnections are considered. It is well known that to deal with interconnections is one of the main challenges for large-scale interconnected systems when decentralised control is considered. The main contribution of this section can be

summarized as follows:

i). The uncertain interconnections are separated into two parts to reduce the conservatism.

ii). It is not required that the interconnections vanish at the origin.

iii). The bounds on the uncertainties have a more general form than those imposed in existing work.

Moreover, the uncertainties are assumed to be bounded by known functions which are employed in the control design to counteract the effects of the uncertainties. The bounds on the uncertainties take more general forms when compared with existing work. Based on the approach proposed in [16], a sliding surface for each subsystem is designed. Together these constitute a composite sliding surface for the large-scale system. A set of sufficient conditions is developed such that the corresponding sliding motion is asymptotically stable when the system is restricted to the designed sliding surface. Then, a decentralised SMC is designed to drive the large-scale interconnected system to the sliding surface in finite time. It is shown that if the uncertainties/interconnections possess a superposition property, a decentralised control scheme can be designed to counteract the effect of the uncertainty. Finally, the developed decentralised control scheme is applied to a CSTR system and an automated highway system. Simulation results relating to a high-speed car following system show that the obtained results are effective. The study shows that limitations on the bounds assumed on the uncertainties and interconnections can be greatly reduced when compared with the output feedback case.

6.2. System Description and Preliminaries

Consider a nonlinear large-scale interconnected system composed of N subsystems where the i-th subsystem is described by

$$\dot{x}_i = A_i x_i + B_i \left(u_i + \phi_i(t, x_i)\right) + \sum_{j=1}^{N} \Xi_{ij}(t, x_j) + \psi_i(t, x) \qquad i = 1, 2, \ldots, N \tag{6.1}$$

where $x_i \in \mathcal{D}_i \subset \mathcal{R}^{n_i}$ ($\mathcal{D}_i$ is the neighborhood of the origin $x_i = 0$), $u_i \in \mathcal{R}^{m_i}$ denote the state variables and inputs of the i-th subsystem, respectively. The matrix pairs (A_i, B_i) are constant with appropriate dimensions. The matched uncertainties are denoted by $\phi_i(t, x_i)$.

The terms $\sum_{j=1}^{n} \Xi_{ij}(t, x_j)$ with $\Xi_{ij}(t, 0) = 0$ describe the known interconnection of the i-th subsystem. The nonlinear functions $\psi_i(t, x)$ represent the uncertain interconnections where $x = \text{col}(x_1, x_2, \ldots, x_n)$ is the state of the whole system plant. It is assumed that all the nonlinear functions are sufficiently smooth such that the unforced system has a unique continuous solution.

It should be noted that

$$\sum_{j=1}^{N} \Xi_{ij}(t, x_j) = \Xi_{ii}(t, x_i) + \sum_{\substack{j \neq i \\ j=1}}^{N} \Xi_{ij}(t, x_j) \tag{6.2}$$

In this case, $\Xi_{ii}(t, x_i)$ can be considered as the known nonlinearity in the ith subsystem and the term $\sum_{\substack{j \neq i \\ j=1}}^{N} \Xi_{ij}(t, x_j)$ as the known interconnection within the ith subsystem. It will be shown that such a class of interconnections can be employed in decentralised controller design to reduce conservatism.

The objective of this chapter is to design a decentralised control

$$u_i = u_i(x_i, t), \qquad i = 1, 2, \ldots, N \tag{6.3}$$

for system (6.1) based on sliding mode techniques such that the corresponding closed-loop system formed by applying the controllers (6.3) to the system (6.1) is asymptotically stable.

The following basic assumption is firstly imposed on the system (6.1).

Assumption 6.1. The matrix pairs (A_i, B_i) are controllable and rank$(B_i) = m_i$ for $i = 1, 2, \ldots, N$.

Under the condition that rank$(B_i) = m_i$ in Assumption 1, there exists an invertible matrix $\tilde{T}_i \in \mathcal{R}^{(n_i \times n_i)}$ such that after the coordinate transformation $\tilde{x}_i = \tilde{T}_i x_i$, the matrix pairs (A_i, B_i) with respect to the new coordinates $\tilde{x}_i$ have the following structure

$$\tilde{A}_i = \begin{bmatrix} \tilde{A}_{i1} & \tilde{A}_{i2} \\ \tilde{A}_{i3} & \tilde{A}_{i4} \end{bmatrix} = \tilde{T}_i A_i \tilde{T}_i^{-1} \tag{6.4}$$

$$\tilde{B}_i = \begin{bmatrix} 0 \\ \tilde{B}_{i2} \end{bmatrix} = \tilde{T}_i B_i \tag{6.5}$$

where $\tilde{A}_{i1} \in \mathcal{R}^{(n_i - m_i) \times (n_i - m_i)}$ and the matrix $\tilde{B}_{i2} \in \mathcal{R}^{m_i \times m_i}$ is nonsingular for $i = 1, 2, \ldots, N$. It should be noted that the matrix $\tilde{T}_i$ can be obtained using basic matrix theory.

Assume that (A_i, B_i) is controllable. From [16], it follows that the matrix pair $(\tilde{A}_{i1}, \tilde{A}_{i2})$ in (6.4) is controllable. Then, there exists a matrix $K_i \in \mathcal{R}^{(n_i-m_i)\times m_i}$ such that $\tilde{A}_{i1} - K_i\tilde{A}_{i2}$ is Hurwitz stable. Considering the system (6.1), introduce a new transformation matrix as follows:

$$T_i = \begin{bmatrix} I_{n_i-m_i} & 0 \\ K_i & I_{m_i} \end{bmatrix} \tilde{T}_i \tag{6.6}$$

It is clear that the matrix T_i is nonsingular. Define $z = \text{col}(z_1, z_2, \ldots, z_N)$ where $z_i = T_i x_i$. Then in this new coordinate system, system (6.1) has the following form

$$\dot{z}_i = \begin{bmatrix} A_{i1} & A_{i2} \\ A_{i3} & A_{i4} \end{bmatrix} z_i + \begin{bmatrix} 0 \\ \tilde{B}_{i2} \end{bmatrix} (u_i + g_i(t, z_i)) + \sum_{j=1}^{N} \Gamma_{ij}(t, z_j) + \delta_i(t, z) \tag{6.7}$$

where $z_i \in T_i(D_i) := \Omega_i$, $A_{i1} = \tilde{A}_{i1} - \tilde{A}_{i2}K_i$ is stable,

$$T^{-1} \equiv: \text{diag}\{T_1^{-1}, T_2^{-1}, \ldots, T_N^{-1}\}$$

and

$$g_i(t, z_i) = \phi_i(t, T_i^{-1} z_i) \tag{6.8}$$

$$\Gamma_{ij}(t, z_j) \triangleq \begin{bmatrix} \Gamma_{ij}^a(t, z_j) \\ \Gamma_{ij}^b(t, z_j) \end{bmatrix} = T_i \Xi_{ij}(t, T_j^{-1} z_j) \tag{6.9}$$

$$\delta_i(t, z) \triangleq \begin{bmatrix} \delta_i^a(t, z) \\ \delta_i^b(t, z) \end{bmatrix} = T_i \psi_i(t, T^{-1} z) \tag{6.10}$$

where $\Gamma_{ij}^a(t, z_j) \in \mathcal{R}^{(n_i-m_i)}$, $\delta_i^a(t, z) \in \mathcal{R}^{(n_i-m_i)}$, $\Gamma_{ij}^b(t, z_j) \in \mathcal{R}^{m_i}$, and $\delta_i^b(t, z) \in \mathcal{R}^{m_i}$ for $i, j = 1, 2, \ldots, N$.

For further analysis, now partition $z_i = \text{col}(z_i^a, z_i^b)$ where $z_i^a \in \mathcal{R}^{n_i-m_i}$ and $z_i^b \in \mathcal{R}^{m_i}$. Then the system (6.7) can be rewritten in the following form

$$\dot{z}_i^a = A_{i1} z_i^a + A_{i2} z_i^b + \sum_{j=1}^{N} \Gamma_{ij}^a(t, z_j) + \delta_i^a(t, z) \tag{6.11}$$

$$\dot{z}_i^b = A_{i3} z_i^a + A_{i4} z_i^b + \tilde{B}_{i2}(u_i + g_i(t, z_i)) + \sum_{j=1}^{N} \Gamma_{ij}^b(t, z_j) + \delta_i^b(t, z) \tag{6.12}$$

where the matrix A_{i1} in (6.11) is stable.

The following assumption is imposed on the uncertainty.

Assumption 6.2. There exist known continuous functions $\rho_i(t, z_i)$, $\eta_i^a(t, z)$ and $\eta_i^b(t, z)$ such that for $i = 1, 2, \ldots, N$,

(i) $\|g_i(t, z_i)\| \leq \rho_i(t, z_i)$

(ii) $\|\delta_i^a(t, z)\| \leq \eta_i^a(t, z)\|z\|$

(iii) $\|\delta_i^b(t, z)\| \leq \eta_i^b(t, z)$

Remark 6.1. *Assumption 6.2 is a limitation on all the uncertainties experienced by the interconnected system. It is required that bounds on the uncertainties are known. These bounds will be employed in the control design to reject the effects of the uncertainty. It should be emphasised that the bounds on the uncertainties in Assumption 6.2 have a more general form when compared with existing work [22, 47, 11, 156]. It should be noted that it is only required that $\delta_i^a(\cdot)$ vanish at the origin, and it is not required that $g_i(\cdot)$ and $\delta_i^b(\cdot)$ vanish at the origin.*

6.3. Stability Analysis of the Sliding Motion

In this section, a sliding surface is designed for the system (6.7) and the stability of the corresponding sliding motion is analysed. A set of sufficient conditions is provided such that the sliding motion is asymptotically stable.

It is clear that system (6.11)-(6.12) has regular form. Choose the local sliding surface for the ith subsystem of the large-scale interconnected system (6.7) as follows:

$$\sigma_i(z_i) \equiv: z_i^b = 0, \qquad i = 1, 2, \ldots, N. \tag{6.13}$$

Then, the composite sliding surface for the interconnected system (6.11)-(6.12) is chosen as

$$\sigma(z) = 0 \tag{6.14}$$

where

$$\begin{aligned} \sigma(z) \quad &\equiv: \quad \mathrm{col}\left(\sigma_1(z_1), \sigma_2(z_2), \ldots, \sigma_N(z_N)\right) \\ &= \quad \mathrm{col}\left(z_1^b, z_2^b, \ldots, z_N^b\right) \end{aligned}$$

Since A_{i1} in (6.11) is stable, for any $Q_i > 0$, the following Lyapunov equation has a unique solution $P_i > 0$ such that

$$A_{i1}^\tau P_i + P_i A_{i1} = -Q_i, \qquad i = 1, 2, \ldots, N. \tag{6.15}$$

During sliding motion, $z_i^b = 0$ for $i = 1, 2, \ldots, N$. Then, the sliding mode dynamics for the system (6.11)-(6.12) associated with the designed sliding surface (6.14) can be described by

$$\dot{z}_i^a = A_{i1} z_i^a + \sum_{j=1}^{n} \Gamma_{ij}^s(t, z_j^a) + \delta_i^s(t, z_1^a, z_2^a, \ldots, z_N^a) \tag{6.16}$$

where

$$\Gamma_{ij}^s(t, z_j^a) := \Gamma_{ij}^a(t, z_j)|_{z_j^b=0} \tag{6.17}$$

$$\delta_i^s(t, z_1^a, z_2^a, \ldots, z_N^a) := \delta_i^a(t, z)|_{(z_1^b, z_2^b, \ldots, z_N^b)=0} \tag{6.18}$$

Here $\Gamma_{ij}^a(t, z_j)$ and $\delta_i^a(t, z)$ are defined in (6.9) and (6.10) respectively.

Assumption 6.3. The functions $\Gamma_{ij}^s(\cdot)$ in (6.17) have the following decomposition:

$$\Gamma_{ij}^s(t, z_j^a) = \tilde{\Gamma}_{ij}^s(t, z_j^a) z_j^a \tag{6.19}$$

where $\tilde{\Gamma}_{ij}^s(t, z_j^a)$ is an appropriately-dimensioned matrix function for $i, j = 1, 2, \ldots, N$.

Remark 6.2. *If the term $\Xi_{ij}(t, x_j)$ in system (6.1) is sufficiently smooth with $\Xi_{ij}(t, 0) = 0$, then $\Gamma_{ij}^s(t, z_j^a)$ will be smooth enough with $\Gamma_{ij}^s(t, 0) = 0$. From [47], it is straightforward to see that the decomposition (6.19) holds. It should be noted that in the system (6.11)-(6.12), the interconnection terms are $\Gamma_{ij}^a(t, z_j)$ and $\Gamma_{ij}^b(t, z_j)$. Therefore, it is clear to see from (6.19) and (6.17) that the Assumption 6.3 does not require that the interconnections vanish at the origin. This is in comparison with all of the associated work [22, 98, 100, 47] where it is required that the interconnections vanish at the origin.*

Under Assumptions 6.1-6.3, a reduced order interconnected system composed of $\mathcal{N}$ subsystems with dimension $n_i - m_i$ is obtained as follows:

$$\dot{z}_j^a = A_{i1} z_j^a + \sum_{j=1}^{n} \tilde{\Gamma}_{ij}^s(t, z_j^a) z_j^a + \delta_i^s(t, z_1^a, z_2^a, \ldots, z_N^a) \tag{6.20}$$

which represents the sliding mode dynamics relating to the sliding surface (6.14), where $z_i^a \in \mathcal{R}^{n_i - m_i}$ and $\tilde{\Gamma}_i^s(t, z_j^a)$ is defined in (6.19).

Lemma 6.1. *For the terms $\delta_i^s(t, z_1^a, z_2^a, \ldots, z_N^a)$ in system (6.20), if condition (ii) in Assumption 6.2 holds, then there exist continuous functions $\gamma_{ij}(\cdot)$ such that*

$$\|\delta_i^s(t, z_1^a, z_2^a, \ldots, z_N^a)\| \leq \sum_{j=1}^{N} \gamma_i(t, z^a) \|z_j^a\| \tag{6.21}$$

where

$$\gamma_i(t, z^a) = \eta_i^a(t, z_1^a, 0, z_2^a, 0, \ldots, z_N^a, 0)$$

for $i = 1, 2, \ldots, N$*, and* $z^a = \text{col}(z_1^a, z_2^a, \ldots, z_N^a)$.

Proof. From the definition of $\delta_i^s(\cdot)$ in (6.18), it follows that

$$\delta_i^s(t, z_1^a, z_2^a, \ldots, z_N^a) = \delta_i^a(t, z_1^a, 0, z_2^a, 0, \ldots, z_N^a, 0) \tag{6.22}$$

From condition (ii) in Assumption 6.2,

$$\|\delta_i^a(t, z)\| \leq \eta_i^a(t, z)\|z\| \tag{6.23}$$

From (6.22) and (6.23), it follows that

$$\begin{aligned}
\|\delta_i^s(t, z_1^a, z_2^a, \ldots, z_N^a)\| &= \|\delta_i^a(t, z_1^a, 0, z_2^a, 0, \ldots, z_N^a, 0)\| \\
&\leq \eta_i^a(t, z_1^a, 0, z_2^a, 0, \ldots, z_N^a, 0)\|z^a\| \\
&\leq \sum_{j=1}^{N} \eta_i^a(t, z_1^a, 0, z_2^a, 0, \ldots, z_N^a, 0)\|z_j^a\| \\
&\leq \sum_{j=1}^{N} \gamma_i(t, z^a)\|z_j^a\|
\end{aligned}$$

Hence the result follows. ■

The following result can now be presented.

Theorem 6.1. *Consider the sliding mode dynamics given in equation (6.20). Under Assumptions 6.1-6.3, the sliding motion governed by (6.20) is asymptotically stable if there exists a domain* Ω_{z^a} *of the origin in* $z^a \in \mathcal{R}^{\sum_{i=1}^{N}(n_i - m_i)}$ *such that*

$$M^\tau + M > 0$$

in $\Omega_{z^a} \backslash \{0\}$ *where* $M = (m_{ij})_{N \times N}$*, and*

$$m_{ij} = \begin{cases} \lambda_{min}(Q_i) - 2\|P_i\|\gamma_i(t, z^a) - \varsigma_{ii}(t, z_i^a), & i = j \\ -\varsigma_{ij}(t, z_j^a) - 2\|P_i\|\gamma_i(t, z^a), & i \neq j \end{cases}$$

where P_i *and* Q_i *satisfy (6.15), and the functions* $\varsigma_{ij}(\cdot)$ *are defined by*

$$\varsigma_{ij}(t, z_j^a) :\equiv \|P_i\tilde{\Gamma}_{ij}^s(t, z_j^a) + (\tilde{\Gamma}_{ij}^s)^\tau(t, z_j^a)P_i\|$$

with $\tilde{\Gamma}_{ij}^s(t, z_j^a)$ *given by (6.19), and* $\gamma_i(t, z^a)$ *satisfy (6.21) for* $i, j = 1, 2, \ldots, N$.

Proof. For system (6.20), consider the Lyapunov function candidate

$$V(t, z_1^a, z_2^a, \ldots, z_N^a) = \sum_{i=1}^{N} (z_i^a)^\tau P_i z_i^a \tag{6.24}$$

where P_i satisfies equation (6.15).

Then, from the lyapunov equation (6.15), the time derivative of $V(t, z_1^a, z_2^a, \ldots, z_N^a)$ along the trajectories of system (6.20) is given by

$$\begin{aligned}
\dot{V} =& \sum_{i=1}^{N} \Big\{ (\dot{z}_i^a)^\tau P_i z_i^a + (z_i^a)^\tau P_i \dot{z}_i^a \Big\} \\
\leq& \sum_{i=1}^{N} \Big\{ -\lambda_{min}(Q_i)\|z_i^a\|^2 + 2\|z_i^a\|\|P_i\|\|\delta_i^s(t, z_1^a, z_2^a, \ldots, z_N^a)\| + \\
& \sum_{j=1}^{N} \Big\| P_i \tilde{\Gamma}_{i1}^s(t, z_j^a) + (\tilde{\Gamma}_{ij}^s(t, z_j^a))^\tau z_j^a P_i \Big\| \|z_i^a\|\|z_j^a\| \Big\} \\
\leq& \sum_{i=1}^{N} \Big\{ -\lambda_{min}(Q_i)\|z_i^a\|^2 + \sum_{j=1}^{N} \varsigma_{ij}(t, z_j^a)\|z_i^a\|\|z_j^a\| + 2\|z_i^a\|\|P_i\| \sum_{j=1}^{N} \gamma_i(t, z^a)\|z_j^a\| \Big\} \\
=& -\sum_{i=1}^{N} \Big\{ \lambda_{min}(Q_i) - 2\|P_i\|\gamma_i(t, z^a) - \varsigma_{ii}(t, z_i^a) \Big\} \|z_i^a\|^2 \\
& + \sum_{i=1}^{N} \sum_{\substack{j=1 \\ j \neq i}}^{N} \Big\{ \varsigma_{ij}(t, z_j^a) + 2\|P_i\|\gamma_i(t, z^a) \Big\} \|z_i^a\|\|z_j^a\| \\
=& -\frac{1}{2} Y^\tau (M^\tau + M) Y
\end{aligned} \tag{6.25}$$

where $Y \equiv$: col$(\|z_1^a\|, \ldots, \|z_N^a\|)$.

Thus, the conclusion follows from $M^\tau + M > 0$. ■

Theorem 6.1 shows that the sliding motion corresponding to the designed sliding surface is asymptotically stable. Conditions to ensure this sliding motion is attained and maintained will be developed in the next section.

6.4. Decentralised Sliding Mode Control Design

A SMC is designed to drive the system to the sliding surface. It is well known that an appropriate reachability condition is described by

$$\sigma^\tau(z)\dot{\sigma}(z) < 0$$

for a centralized system with switching surfaces $\sigma(z) = 0$. For the nonlinear interconnected system (6.1), the corresponding reachability condition is described by

$$\sum_{i=1}^{N} \frac{\sigma_i^{\mathcal{T}}(z_i)\dot{\sigma}_i(z_i)}{\|\sigma_i(z_i)\|} < 0 \tag{6.26}$$

where $\sigma_i(z_i)$ is defined by (6.13). It should be noted that the condition (6.26) is proposed in [113] and has been widely used (see, *e.g.* [47]).

Consider system (6.11)-(6.12). In order to reduce the effects of the unknown interconnection $\delta_i^b(\cdot)$, consider the expression

$$\eta_i^b(t, z) = \sum_{j=1}^{N} \mu_{ij}(t, z_j) + \nu_i(t, z) \tag{6.27}$$

where $\nu_i(t, z)$ represents all the coupling terms which cannot be included in the term $\sum_{j=1}^{N} \mu_{ij}(t, z_j)$.

Remark 6.3. *The interconnection decomposition in (6.27) is not unique and is introduced to reduce the conservatism caused by the interconnection terms within the control design. There is no general way to obtain the decomposition. The first interconnection term $\sum_{j=1}^{N} \mu_{ij}(t, z_j)$ has a superposition property. It will be shown that the term $\sum_{j=1}^{N} \mu_{ij}(\cdot)$ in (6.27) can be rejected by selection of an appropriate decentralised control and this will reduce conservatism. The second term, $\nu_i(t, z)$ in (6.27), cannot be rejected by the choice of decentralised control.*

The objective is to design a decentralised sliding mode controller such that the reachability condition (6.26) is satisfied. For $i = 1, 2, \ldots, N$, the following control scheme is proposed:

$$\begin{aligned} u_i = &- \tilde{B}_{i2}^{-1}\Big\{A_{i3}z_i^a + A_{i4}z_i^b + \sum_{j=1}^{N} \Gamma_{ji}^b(t, z_i)\Big\} \\ &- \tilde{B}_{i2}^{-1}\mathrm{sgn}(z_i^b)\Big\{\|\tilde{B}_{i2}\|\rho_i(t, z_i) + \sum_{j=1}^{N} \mu_{ji}(t, z_i) + \zeta_i(t, z_i)\Big\} \end{aligned} \tag{6.28}$$

where $z_i = \mathrm{col}(z_i^a, z_i^b)$, $\rho_i(t, z_i)$ are defined in Assumption 6.2, $\mu_{ji}(t, z_i)$ satisfy (6.27) and $\zeta_i(t, z_i)$ is a reachability function which will be defined later.

Theorem 6.2. *Consider the nonlinear interconnected system (6.7). Under Assumptions 6.1-6.3, the decentralised control (6.28) is able to drive system (6.7) to the composite sliding*

surface (6.14) and maintains a sliding motion on it thereafter if in the considered domain $\Omega = \Omega_1 \times \Omega_2 \cdots \times \Omega_N$*, the functions* $\zeta_i(t, z_i)$ *in (6.28) satisfy*

$$\sum_{i=1}^{N} \zeta_i(t, z_i) > \sum_{i=1}^{N} \nu_i(t, z) \tag{6.29}$$

in $\Omega \backslash \{0\}$ *for all* $t > 0$ *with* $\nu_i(t, z)$ *defined in (6.27).*

Proof. From the analysis above, all that needs to be proved is that the composite reachability condition (6.26) is satisfied. From (6.14), for $i = 1, 2, \ldots, N$,

$$\dot{\sigma}_i(z_i) = \dot{z}_i^b = A_{i3} z_i^a + A_{i4} z_i^b + \tilde{B}_{i2}\big(u_i + \phi_i(t, T_i^{-1} z_i)\big) + \sum_{j=1}^{N} \Gamma_{ij}^b(t, z_j) + \delta_i^b(t, z) \tag{6.30}$$

Substituting (6.28) into (6.30),

$$\begin{aligned}
\sum_{i=1}^{N} \frac{\sigma_i^\tau(z_i)\dot{\sigma}_i(z_i)}{\|\sigma_i(z_i)\|} =& \sum_{i=1}^{N} \Big\{ \frac{(z_i^b)^\tau}{\|z_i^b\|} \big\{ \delta_i^b(t, z) + \tilde{B}_{i2}\phi_i(t, T_i^{-1} z_i) \big\} \\
& - \|\tilde{B}_{i2}\| \rho_i(t, z_i) - \sum_{j=1}^{N} \mu_{ji}(t, z_i) - \zeta_i(t, z_i) \Big\} \\
& + \frac{(z_i^b)^\tau}{\|z_i^b\|} \big\{ \sum_{i=1}^{N} \sum_{j=1}^{N} \Gamma_{ij}^b(t, z_j) - \sum_{i=1}^{N} \sum_{j=1}^{N} \Gamma_{ji}^b(t, z_i) \big\} \\
\leq & \sum_{i=1}^{N} \|\tilde{B}_{i2}\phi_i(t, T_i^{-1} z_i)\| + \sum_{i=1}^{N} \|\delta_i^b(t, z)\| - \sum_{i=1}^{N} \|\tilde{B}_{i2}\| \rho_i(t, z_i) \\
& - \sum_{i=1}^{N} \sum_{j=1}^{N} \mu_{ji}(t, z_i) - \sum_{i=1}^{N} \zeta_i(t, z_i)
\end{aligned} \tag{6.31}$$

From Assumption 6.2,

$$\begin{aligned}
\sum_{i=1}^{N} \|\delta_i^b(t, T^{-1} z)\| \leq & \sum_{i=1}^{N} \sum_{j=1}^{N} \mu_{ij}(t, z_j) + \sum_{i=1}^{N} \nu_i(t, z) \\
= & \sum_{i=1}^{N} \sum_{j=1}^{N} \mu_{ji}(t, z_i) + \sum_{i=1}^{N} \nu_i(t, z)
\end{aligned} \tag{6.32}$$

and

$$\|\tilde{B}_{i2}\phi_i(t, T_i^{-1} z_i)\| \leq \|\tilde{B}_{i2}\| \|\phi_i(t, T_i^{-1} z_i)\| \leq \|\tilde{B}_{i2}\| \rho_i(t, z_i) \tag{6.33}$$

Substituting inequalities (6.32) and (6.33) into (6.31),

$$\sum_{i=1}^{N} \frac{\sigma_i^\tau \dot{\sigma}_i}{\|\sigma_i\|} \leq -\sum_{i=1}^{N} \zeta_i(t, z_i) + \sum_{i=1}^{N} \nu_i(t, z) < 0 \tag{6.34}$$

Then the reachability condition (6.26) is satisfied. Hence, the result follows. ■

Remark 6.4. *It should be noted that the functions $\zeta_i(\cdot)$ in (6.29) are design parameters. Theorem 6.2 shows that if $\zeta_i(\cdot)$ are designed to satisfy condition (6.29), then the well known reachability condition holds and a sliding mode will occur. Moreover, if all the interconnection functions $\nu_i(t, z)$ are bounded for $i = 1, 2, \ldots, N$ in the considered domain Ω, it is straightforward to see that (6.29) always holds by choosing appropriate $\zeta_i(\cdot)$.*

From SMC theory, Theorems 5.1 and 5.2 together guarantee that the closed-loop system formed by applying the decentralised controller (6.28) to the interconnected system (6.7) is asymptotically stable in the domain Ω.

It is clear to see that system (6.7) is an expression of system (6.1) in the new coordinates $z_i(z_i = T_i x_i)$. Partition T_i as follows

$$T_i = \begin{bmatrix} T_i^a \\ T_i^b \end{bmatrix} \tag{6.35}$$

where $T_i^a \in \mathcal{R}^{(n_i - m_i)\times n_i}$ and $T_i^b \in \mathcal{R}^{m_i \times n_i}$.

Then

$$\begin{bmatrix} z_i^a \\ z_i^b \end{bmatrix} := z_i = T_i x_i = \begin{bmatrix} T_i^a x_i \\ T_i^b x_i \end{bmatrix} \tag{6.36}$$

From the relationship between (6.1) and (6.7), it is straightforward to rewrite the control (6.28) in terms of the x coordinates to stabilize the system (6.1) using (6.36).

6.5. Case studies

6.5.1. Control of a CSTR

To illustrate the algorithm, a system composed of three cascaded non-isothermal continuously stirred-tank reactors (CSTRs) with recycling as presented in example 2 of section 3.5.2 is considered. As in [114], it is assumed that the recycle ratio is $r = 0.5$ and the system parameters are given in Table 6.1. The corresponding steady state operating conditions are presented in

Table 6.1: CSTR System Parameters

Parameters	Value	Parameters	Value
F_1^0	4.998 m^3/h	V_1	1.0 m^3
F_2^0	30 m^3/h	V_2	3.0 m^3
F_3^0	60 m^3/h	V_3	9.0 m^3
T_1^0	300.0 K	C_{A1}^0	4.0 kmol/m^3
T_2^0	300.0 K	C_{A2}^0	3.0 kmol/m^3
T_3^0	300.0 K	C_{A3}^0	2.0 kmol/m^3
ΔH_1	-5.0 $\times$ 10^4 KJ/kmol	k_{10}	3.0 $\times$ 10^6 h^{-1}
ΔH_2	-5.2 $\times$ 10^4 KJ/kmol	k_{20}	3.0 $\times$ 10^5 h^{-1}
ΔH_3	-5.4 $\times$ 10^4 KJ/kmol	k_{30}	3.0 $\times$ 10^5 h^{-1}
E_1	5.0 $\times$ 10^4 KJ/kmol	ρ	1000.0 kg/m^3
E_2	7.53 $\times$ 10^4 KJ/kmol	c_p	0.231 KJ/kg K
E_3	7.53 $\times$ 10^4 KJ/kmol	F_r	94.998 m^3/h

Note: $F_r = rF_3$ where r is the recycle ratio.

Table 6.2 (see [114]). The objective is to design a decentralised control strategy to stabilise the

Table 6.2: CSTR System Steady State Operating Conditions

State	Equilibrium Point	State	Equilibrium Point
T_1^s	432.8113 K	C_{A1}^s	1.8864 kmol/m^3
T_2^s	422.1458 K	C_{A2}^s	2.0510 kmol/m^3
T_3^s	427.8888 K	C_{A3}^s	1.8302 kmol/m^3

CSTR system asymptotically. Let $x_{i1} = C_{Ai} - C_{Ai}^s$ and $x_{i2} = T_i - T_i^s$ for $i = 1, 2, 3$. Then, the CSTR system can be described in the form of (6.1) by

$$\dot{x}_1 = \underbrace{\begin{bmatrix} -99.996 & 0 \\ 0 & -99.996 \end{bmatrix}}_{A_1} x_1 + \underbrace{\begin{bmatrix} 0 \\ 0.00433 \end{bmatrix}}_{B_1} (u_1 + \phi_1(t, x_1))$$

$$+\underbrace{\begin{bmatrix} 94.998 & 0 \\ 0 & 94.998 \end{bmatrix}}_{\Xi_{13}} x_3 + \underbrace{\begin{bmatrix} f_{11}(t,x_1) \\ f_{12}(t,x_1) \end{bmatrix}}_{\Xi_{11}} + \psi_1(t,x) \tag{6.37}$$

$$\dot{x}_2 = \underbrace{\begin{bmatrix} -43.332 & 0 \\ 0 & -43.332 \end{bmatrix}}_{A_2} x_2 + \underbrace{\begin{bmatrix} 0 \\ 0.00144 \end{bmatrix}}_{B_2} (u_2 + \phi_2(t,x_2))$$

$$+\underbrace{\begin{bmatrix} 33.332 & 0 \\ 0 & 33.332 \end{bmatrix}}_{\Xi_{21}} x_1 + \underbrace{\begin{bmatrix} f_{21}(t,x_2) \\ f_{22}(t,x_2) \end{bmatrix}}_{\Xi_{22}} + \psi_2(t,x) \tag{6.38}$$

$$\dot{x}_3 = \underbrace{\begin{bmatrix} -21.111 & 0 \\ 0 & -21.111 \end{bmatrix}}_{A_3} x_3 + \underbrace{\begin{bmatrix} 0 \\ 0.000481 \end{bmatrix}}_{B_3} (u_3 + \phi_3(t,x_3))$$

$$+\underbrace{\begin{bmatrix} 14.444 & 0 \\ 0 & 14.444 \end{bmatrix}}_{\Xi_{32}} x_2 + \underbrace{\begin{bmatrix} f_{31}(t,x_3) \\ f_{32}(t,x_3) \end{bmatrix}}_{\Xi_{33}} + \psi_3(t,x) \tag{6.39}$$

where

$$f_{11}(t,x_1) = \Big(-3\times 10^6 \exp(\frac{-6013.952}{x_{12}+432.8113}) - 6\times 10^5 \cdot \exp(\frac{-9057.012}{x_{12}+432.8113})\Big)(x_{11}+1.8864) + 5.2249 \tag{6.40}$$

$$f_{12}(t,x_1) = \Big(6.494\times 10^8 \exp(\frac{-6013.952}{x_{12}+432.8113}) + 1.377\times 10^8 \cdot \exp(\frac{-9057.012}{x_{12}+432.8113})\Big)(x_{11}+1.8864) - 1131.4185 \tag{6.41}$$

$$f_{21}(t,x_2) = \Big(-3\times 10^6 \exp(\frac{-6013.952}{x_{22}+422.1458}) - 6\times 10^5 \cdot \exp(\frac{-9057.012}{x_{22}+422.1458})\Big)(x_{21}+2.051) + 4.0035 \tag{6.42}$$

$$f_{22}(t,x_2) = \Big(6.494\times 10^8 \exp(\frac{-6013.952}{x_{22}+422.1458}) + 1.377\times 10^8 \cdot \exp(\frac{-9057.012}{x_{22}+422.1458})\Big)(x_{21}+2.051) - 865.9556 \tag{6.43}$$

$$f_{31}(t,x_3) = \Big(-3\times 10^6 \exp(\frac{-6013.952}{x_{32}+427.8888}) - 6\times 10^5 \cdot \exp(\frac{-9057.012}{x_{32}+427.8888})\Big)(x_{31}+1.8302) + 4.3212 \tag{6.44}$$

$$f_{32}(t,x_3) = \Big(6.494\times 10^8 \exp(\frac{-6013.952}{x_{32}+427.8888}) + 1.377\times 10^8$$

$$\cdot \exp(\frac{-9057.012}{x_{32}+427.8888})\Big)(x_{31}+1.8302)-935.5439 \tag{6.45}$$

The unknown matched uncertainty $\phi_i(t, x_i, t)$ is assumed to satisfy

$$\|\phi_1(t, x_1)\| \leq 1000|x_{11}| + 800|x_{12}| \tag{6.46}$$

$$\|\phi_2(t, x_2)\| \leq 2000|x_{21}| + 600|x_{22}| \tag{6.47}$$

Consider the system (6.37)-(6.39) in the domain

$$D = \{x_i \in \mathcal{R}^3 | x_{i1} \geq -C^s_{Ai}, |x_{i2}| \leq 100\}$$

It should be noted that since the concentration of each tank cannot be negative and the temperature is upper and lower limited by practical bounds, the domain considered covers a reasonable range from the practical point of view.

By using the algorithm in [16], the coordinate transformation $z_i = T_i x_i$ for $i = 1, 2, 3$ can be obtained with T_i defined by

$$T_i = \begin{bmatrix} 1 & 0 \\ -0.1 & 1 \end{bmatrix}$$

Then the system (6.37)-(6.39) is transformed into the form in (6.11)-(6.12) as

$$\begin{aligned} \dot{z}_1 = & \begin{bmatrix} -99.996 & 0 \\ 0 & -99.996 \end{bmatrix} z_1 + \begin{bmatrix} 0 \\ 0.00433 \end{bmatrix} (u_1 + g_1(t, z_1, t)) \\ & + \underbrace{\begin{bmatrix} 94.998 & 0 \\ 0 & 94.998 \end{bmatrix}}_{\Gamma_{13}(t,z_3)} z_3 + \begin{bmatrix} \Gamma^a_{11}(t, z_1) \\ \Gamma^b_{11}(t, z_1) \end{bmatrix} + \begin{bmatrix} \delta^a_1(t, z) \\ \delta^b_1(t, z) \end{bmatrix} \end{aligned} \tag{6.48}$$

$$\begin{aligned} \dot{z}_2 = & \begin{bmatrix} -43.332 & 0 \\ 0 & -43.332 \end{bmatrix} z_2 + \begin{bmatrix} 0 \\ 0.00144 \end{bmatrix} (u_2 + g_2(t, z_2, t)) \\ & + \underbrace{\begin{bmatrix} 33.332 & 0 \\ 0 & 33.332 \end{bmatrix}}_{\Gamma_{21}(t,z_1)} z_1 + \begin{bmatrix} \Gamma^a_{22}(t, z_2) \\ \Gamma^b_{22}(t, z_2) \end{bmatrix} + \begin{bmatrix} \delta^a_2(t, z) \\ \delta^b_2(t, z) \end{bmatrix} \end{aligned} \tag{6.49}$$

$$\dot{z}_3 = \begin{bmatrix} -21.111 & 0 \\ 0 & -21.111 \end{bmatrix} z_3 + \begin{bmatrix} 0 \\ 0.000481 \end{bmatrix} (u_3 + g_3(t, z_3, t))$$

$$+\underbrace{\begin{bmatrix} 14.444 & 0 \\ 0 & 14.444 \end{bmatrix}}_{\Gamma_{32}(t,z_2)} z_2 + \begin{bmatrix} \Gamma^a_{33}(t,z_3) \\ \Gamma^b_{33}(t,z_3) \end{bmatrix} + \begin{bmatrix} \delta^a_3(t,z) \\ \delta^b_3(t,z) \end{bmatrix} \tag{6.50}$$

where

$$\Gamma^a_{ii}(t,z_i) = f_{i1}(T_i^{-1}z_i)$$
$$\Gamma^b_{ii}(t,z_i) = f_{i2}(T_i^{-1}z_i) - 0.1 f_{i1}(T_i^{-1}z_i)$$

for $i = 1,2,3$ and $j = 1,2$, and the unknown interconnections are assumed to satisfy

$$\delta^a_1(t,z) \leq 5\sin^2(z_{11})\|z\|$$
$$\delta^b_1(t,z) \leq \underbrace{0.5\sin^2(z_{11})\|z_1\|}_{\mu_{11}(t,z_2)} + \underbrace{0.5\sin^2(z_{11})\|z_2\| + 0.5\sin^2(z_{11})\|z_3\|}_{\nu_1(t,z)}$$
$$\delta^b_2(t,z) \leq \underbrace{6|z_{21}| + 5|z_{22}|}_{\mu_{22}(t,z_2)}$$
$$\delta^a_3(t,z) \leq 2\cos^2(z_{31})\|z3\|$$
$$\delta^b_3(t,z) \leq \underbrace{0.2\cos^2(z_{11})\|z_3\|}_{\mu_{31}(t,z_1)} + \underbrace{0.7|z_{22}|}_{\mu_{32}(t,z_2)}$$

During sliding motion, $z_{i2} = 0$ and $\Gamma^s_{ii}(t,z_i)$ is given by

$$\Gamma^s_{11}(t,z_{11}) = \xi_{11}(t,z_{11})z_{11} + 1.8864\xi_{11}(t,z_{11}) + 5.2249 \tag{6.51}$$
$$\Gamma^s_{22}(t,z_{21}) = \xi_{21}(t,z_{21})z_{11} + 2.051\xi_{21}(t,z_{21}) + 4.0035 \tag{6.52}$$
$$\Gamma^s_{33}(t,z_{31}) = \xi_{31}(t,z_{31})z_{11} + 1.8302\xi_{31}(t,z_{31}) + 4.3212 \tag{6.53}$$

where

$$\xi_{11}(t,z_{11}) = -3\times 10^6 \exp(\frac{-6013.952}{0.1z11 + 432.8113}) - 6\times 10^5 \exp(\frac{-9057.012}{0.1z11 + 432.8113})$$
$$\xi_{11}(t,z_{21}) = -3\times 10^6 \exp(\frac{-6013.952}{0.1z21 + 422.1458}) - 6\times 10^5 \exp(\frac{-9057.012}{0.1z21 + 422.1458})$$
$$\xi_{11}(t,z_{31}) = -3\times 10^6 \exp(\frac{-6013.952}{0.1z31 + 427.8888}) - 6\times 10^5 \exp(\frac{-9057.012}{0.1z31 + 427.8888})$$

It is straightforward to verify that the term $1.8864\xi_{11}(t,z_{11}) + 5.2249$ in (6.51) vanishes to 0 when $x_{11} = 0$, which means that the term can be approximated with a Taylor series. By using a Taylor series of order 6, the term can be expressed as follows:

$$1.8864\xi_{11}(t,z_{11}) + 5.2249 = d_1(t,z_{11})z_{11} \tag{6.54}$$

where

$$\begin{aligned} d_1(t, z_{11}) =& 1.43 \times 10^{-15} z_{11}^4 + 7.27 \times 10^{-12} z_{11}^3 \\ &+ 1.73 \times 10^{-8} z_{11}^2 + 2.31 \times 10^{-5} z_{11} + 0.0168 \end{aligned} \tag{6.55}$$

With the same procedure, the Taylor series' expansions for similar terms in $\Gamma_{22}^s(t, z_2)$ and $\Gamma_{33}^s(t, z_3)$ can also be expressed with $d_2(t, z_{21})$ and $d_3(t, z_{31})$

$$\begin{aligned} d_2(t, z_{21}) =& 7.67 \times 10^{-16} x_{22}^4 + 3.45 \times 10^{-12} x_{22}^3 \\ &+ 7.61 \times 10^{-9} x_{22}^2 + 9.55 \times 10^{-6} x_{22} + 0.00658 \end{aligned} \tag{6.56}$$

$$\begin{aligned} d_3(t, z_{31}) =& 7.64 \times 10^{-16} x_{32}^4 + 3.67 \times 10^{-12} x_{32}^3 \\ &+ 8.42 \times 10^{-9} x_{32}^2 + 1.09 \times 10^{-5} x_{32} + 0.00776 \end{aligned} \tag{6.57}$$

Thus the known nonlinearity $\Gamma_{ii}^s(t, z_{i1})$ in (6.48)-(6.50) can be expressed as

$$\Gamma_{ii}^s(t, z_{i1}) = \underbrace{(\xi_{i1}(t, z_{i1}) + d_i(t, z_{i1}))}_{\tilde{\Gamma}_{ii}^s(t, z_{i1})} z_{i1}$$

It is clear that the known nonlinear interconnections $\Gamma^s ij(t, z_{j1})$ can be expressed as

$$\Gamma_{13}^s(t, z_{31}) = 94.998 z_{31} \quad \Gamma_{21}^s(t, z_{11}) = 33.332 z_{31} \quad \Gamma_{32}^s(t, z_{21}) = 14.444 z_{31}$$

From Lemma 1,

$$\begin{aligned} \delta_1^a(t, z_{11}, z_{21}, z_{31}) \leq& \sum_{j=1}^{3} 5 \sin^2(z_{21}) \|z_{11}\| \\ \delta_3^a(t, z_{11}, z_{21}, z_{31}) \leq& 2 \cos^2(z_{31}) \|z_{31}\| \end{aligned}$$

Choosing $Q_i = I_2$ for $i = 1, 2, 3$ and solving the Lyapunov equation (6.15) yields

$$P_1 = -0.005 \quad P_2 = -0.0115 \quad P_3 = -0.0237$$

Then, the matrix function M will be

$$\begin{bmatrix} 1 - \frac{\|\tilde{\Gamma}_{11}^s(t, z_{11})\|}{99.996} - 0.05 \sin^2(z_{11}) & -0.05 \sin^2(z_{11}) & -0.95 - 0.05 \sin^2(z_{11}) \\ -0.7692 & 1 - \frac{\|\tilde{\Gamma}_{22}^s(t, z_{21})\|}{43.332} & 0 \\ 0 & -0.6842 & 1 - \frac{\|\tilde{\Gamma}_{33}^s(t, z_{31})\|}{21.11} - 0.0947 \cos^2(z_{31}) \end{bmatrix}$$

By the help of computing such as LMI toolbox in MATLAB, it is straightforward to verify that in the domain D,

$$M^{\tau} + M > 0$$

It follows from Theorem 6.1 that the designed sliding mode is asymptotically stable. From Theorem 6.2, define the following decentralised control law

$$\begin{aligned} u_1(t, z_1) =& 15395.8441 z_{12} - 230.9469 \Gamma_{11}^{b}(t, z_1) \\ & - \operatorname{sgn}(z_{13}) \Big\{ 1000|z_{11}| + 800|z_{12} - 0.1 z_{11}| \\ & + 115.47 \sin^2(z_{11}) \|z_1\| + 230.9469 \zeta_1(z_1) \Big\} \end{aligned} \tag{6.58}$$

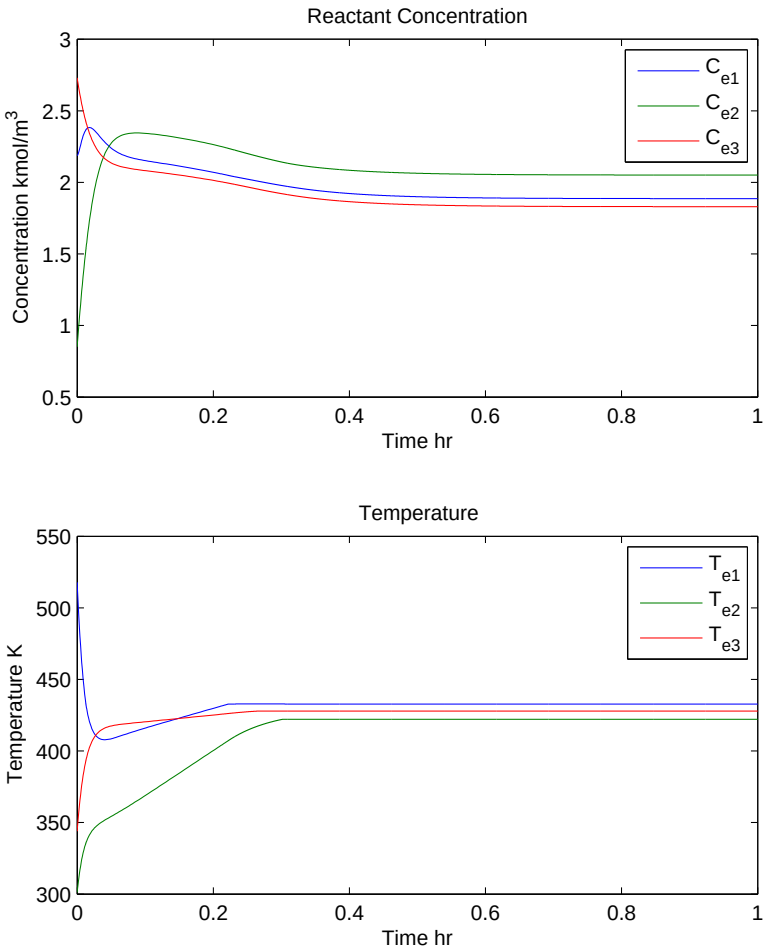

Figure 6.1: Time response of the states of the CSCTR system from (3.89)-(3.94)

$$
\begin{aligned}
u_2(t, z_2) =& 20014.7806 z_{22} - 692.8406 \Gamma_{22}^b(t, z_2) \\
& - \operatorname{sgn}(z_{23}) \Big\{ 2000|z_{21}| + 600|z_{22} - 0.1 z_{21}| \\
& + 692.8406 \zeta_2(z_2) \Big\} \qquad (6.59) \\
u_3(t, z_3) =& - 153575.7506 z_{32} - 2078.5219 \Gamma_{11}^b(t, z_3) \\
& - \operatorname{sgn}(z_{33}) \Big\{ 415.70348 \cos^2(z_{31}) \|z_3\| + 2078.5219 \zeta_3(z_3) \Big\} \qquad (6.60)
\end{aligned}
$$

where $\zeta_1(z_1) = 250 + 0.5\|z_1\|$, $\zeta_2(z_2) = 100$, and $\zeta_3(z_3) = 100$.

By direct computation, it follows that the condition $\sum_{i=1}^N \zeta_i(z_i) \geq \sum_{i=1}^N \nu_i(t, z)$ is satisfied in the domain D, and thus the designed controllers (6.58)–(6.60) stabilise the system (6.37)-(6.39) asymptotically. The time responses of the system states of the CSCTR described in equations (3.89)-(3.94) are given in Figure 6.1 where the upper figure shows the reactant concentration while the lower figure shows the tank temperature. The time response of the control input signals are shown in Figure 6.2. The simulation results show that the proposed approach is effective.

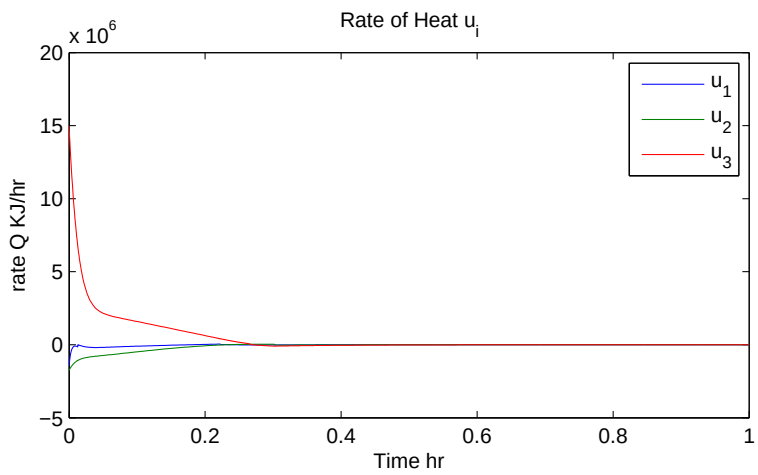

Figure 6.2: Time response of the control input signals

6.5.2. Automated Highway Systems

To illustrate the algorithm, an automated high systems composed of six vehicles as presented in example 3) of section 3.5.2 is considered. The stability and the robustness of the vehicle-following system will be considered as a case study to demonstrate the theoretical results

and the parameters are chosen as in [67]:

$$\begin{aligned} m_i = &\quad 1300\text{kg}, \quad A_{ip} = \quad 0.3\text{Ns}^2/\text{m}^2, \quad d_i = 100\text{N} \\ \kappa_i = &\quad 0.2\text{s}, \qquad v_0 = \quad 20\text{m/s} \end{aligned}$$

As in [157], a safety distance frequently used in automated highway systems based on the Time-Headway policy (CTH) is used in this design. The safety distance defined by the CTH policy is described by (e.g. see [157])

$$\xi_d(v_i) = \xi_{d0} + \beta v_i \tag{6.61}$$

where ξ_{d0} is the distance between stationary vehicles, and β is the so-called headway time. It is well known that the safety distance is closely related to the vehicle's velocity. Therefore, the safety distances in (6.61) are more practicable when compared with the work in [67] and [116] in which the safety distance is chosen as a constant.

Define $\xi_{d0} = 1$, $\beta = 0.5$ and $v_d = v_0$ as an ideal driving velocity, and let

$$x_{i1} = \xi_i - \xi_d(v_i) \tag{6.62}$$

$$x_{i2} = v_i - v_d \tag{6.63}$$

$$x_{i3} = \frac{f_i - A_{ip}v_0^2 - d_i}{1000} \tag{6.64}$$

for $i = 1, 2, \ldots, 6$. Then, a 6-vehicle following system can be described in the form of (6.1) as follows:

$$\begin{aligned} \dot{x}_i = &\underbrace{\begin{bmatrix} 0 & 1.0046 & -0.3846 \\ 0 & -0.0092 & 0.7692 \\ 0 & 0 & -5 \end{bmatrix}}_{A_i} x_i + \underbrace{\begin{bmatrix} 0 \\ 0 \\ 0.005 \end{bmatrix}}_{B} (u_i + 220 + \phi_i(x_i, t)) \\ &+ \underbrace{\begin{bmatrix} -x_{(i-1)2} \\ 0 \\ 0 \end{bmatrix}}_{\Xi_{i(i-1)}} + \underbrace{\begin{bmatrix} 0.00046x_{i2}^2 \\ -0.00023x_{i2}^2 \\ 0 \end{bmatrix}}_{\Xi_{ii}} + \psi_i(t, x), \qquad i = 1, 2, \ldots, 6 \end{aligned} \tag{6.65}$$

where $\Xi_{ij} = 0$ if $i \neq j$ and $j \neq i - 1$, and

$$\Xi_{i0} = \begin{bmatrix} -x_{02} \\ 0 \\ 0 \end{bmatrix} = \begin{bmatrix} -v_0 + v_d \\ 0 \\ 0 \end{bmatrix} = 0$$

The bounds of the unknown matched uncertainty $\phi_i(x_i, t)$ are assumed to satisfy

$$\|\phi_1(x_1, t)\| \leq 20|x_{11} + x_{12}| + 80|x_{13}| \tag{6.66}$$

$$\|\phi_2(x_2, t)\| \leq 25|x_{21} + x_{22}| + 75|x_{23}| \tag{6.67}$$

$$\|\phi_3(x_3, t)\| \leq 30|x_{31} + x_{32}| + 70|x_{33}| \tag{6.68}$$

$$\|\phi_4(x_4, t)\| \leq 35|x_{41} + x_{42}| + 65|x_{43}| \tag{6.69}$$

$$\|\phi_5(x_5, t)\| \leq 40|x_{51} + x_{52}| + 60|x_{53}| \tag{6.70}$$

$$\|\phi_6(x_6, t)\| \leq 45|x_{61} + x_{62}| + 55|x_{63}| \tag{6.71}$$

Remark 6.5. *The high-speed following system is a physical system and the mass of each vehicle is relatively large and thus the corresponding driving/braking forces are large. It should be noted that the uncertainty added to the system in the current study is to illustrate the robustness of the designed control system to verify the results obtained in this chapter. This element is not a feature of the system in [67].*

Consider the system (6.65) in the domain

$$D_i = \{(x_{i1}, x_{i2}, x_{i3}) \quad |x_{i2}| < 20\} \tag{6.72}$$

which, from (6.63), implies that the maximus speed of all the cars is $40m/s$ (144 Km/h).

By using the algorithm in [16], the coordinate transformation $z_i = T_i x_i$ for $i = 1, 2, \ldots, 6$ can be obtained with T_i defined by

$$T_i = \begin{bmatrix} 1 & 0 & 0 \\ 0 & 1 & 0 \\ 13 & 20.79 & 1 \end{bmatrix}$$

then the system (6.65) is transformed into the form (6.11)-(6.12) with

$$\begin{bmatrix} A_{i1} & A_{i2} \\ A_{i3} & A_{i4} \end{bmatrix} = \left[\begin{array}{cc:c} 5 & 9 & -0.3846 \\ -10 & -16 & 0.7692 \\ \hdashline -77.88 & -111.668 & 5.9908 \end{array}\right]$$

$$B_i = \begin{bmatrix} 0 \\ 0 \\ \hdashline 0.005 \end{bmatrix}$$

for $i = 1, 2, \ldots, 6$ and

$$\Gamma_{ii}(t, z_j) = \begin{bmatrix} \Gamma^a_{ii}(t, z_j) \\ \Gamma^b_{ii}(t, z_j) \end{bmatrix} = \begin{bmatrix} 0.000115x_{i2}^2 \\ -0.00023x_{i2}^2 \\ \hdashline -0.0033x_{i2}^2 \end{bmatrix}$$

for $i = 1, 2, \ldots, 6$ and

$$\Gamma_{i(i-1)} = \begin{bmatrix} \Gamma^a_{i(i-1)}(t, z_j) \\ \Gamma^b_{i(i-1)}(t, z_j) \end{bmatrix} = \begin{bmatrix} -x_{(i-1)2} \\ 0 \\ \hdashline -13x_{(i-1)2} \end{bmatrix}, \qquad i = 2, \ldots, 6$$

The bounds on the unknown interconnections satisfy

$$\begin{aligned}
\delta^a_1(t, z) \leq & 0.01\cos^2(z_{12})\|z_1\| + 0.008\sin^2(z_{21})\|z_2\| \\
\delta^a_2(t, z) \leq & 0.009\cos^2(z_{21})\|z_2\| + 0.016\sin^2(z_{13})\|z_1\| + 0.0096\cos^2(z_{33})\|z_3\| \\
\delta^a_3(t, z) \leq & 0.008\sin^2(z_{32})\|z_3\| + 0.007\cos^2(z_{11})\|z_1\| + 0.011\cos^2(z_{22})\|z_2\| \\
& + 0.0095\cos^2(z_{42})\|z_4\| \\
\delta^a_4(t, z) \leq & 0.011\cos^2(z_{41})\|z_4\| + 0.012\cos^2(z_{22})\|z_2\| + 0.01\cos^2(z_{31})\|z_3\| \\
& + 0.0078\cos^2(z_{51})\|z_5\| \\
\delta^a_5(t, z) \leq & 0.012\sin^2(z_{51})\|z_5\| + 0.016\cos^2(z_{23})\|z_2\| + 0.009\sin^2(z_{42})\|z_4\| \\
& + 0.0074\cos^2(z_{63})\|z_6\| \\
\delta^a_6(t, z) \leq & 0.02\sin^2(z_{63})\|z_6\| + 0.0075\sin^2(z_{13})\|z_1\| + 0.012\sin^2(z_{51})\|z_5\|
\end{aligned}$$

and

$$\begin{aligned}
\delta^b_1(t, z) \leq & \underbrace{0.24\cos^2(z_{12})\|z_1\|}_{\mu_{11}(t,z_1)} + \underbrace{0.192|z_{22}|}_{\mu_{12}(t,z_2)} \\
\delta^b_2(t, z) \leq & \underbrace{0.18\cos^2(z_{21})\|z_2\|}_{\mu_{22}(t,z_2)} + \underbrace{0.38\sin^2(z_{13})\|z_1\|}_{\mu_{21}(t,z_1)} \\
& + \underbrace{0.32\sin^2(z_{22})\|z_1\| + 0.192\sin^2(z_{22}z_{33})\|z_3\|}_{\nu_2(t,z)}
\end{aligned}$$

$$\delta_3^b(t,z) \leq \underbrace{0.2|z_{21}+z_{22}|+0.1|z_{23}|}_{\mu_{32}(t,z_2)}$$

$$\delta_4^b(t,z) \leq \underbrace{0.3|z_{11}+z_{13}|+0.2|z_{12}|}_{\mu_{41}(t,z_1)}+\underbrace{0.6|z_{51}+z_{52}|+0.4|z_{53}|}_{\mu_{45}(t,z_5)}$$

$$\delta_6^b(t,z) \leq \underbrace{0.6|z_{21}+z_{22}|+0.4|z_{23}|}_{\mu_{62}(t,z_2)}$$

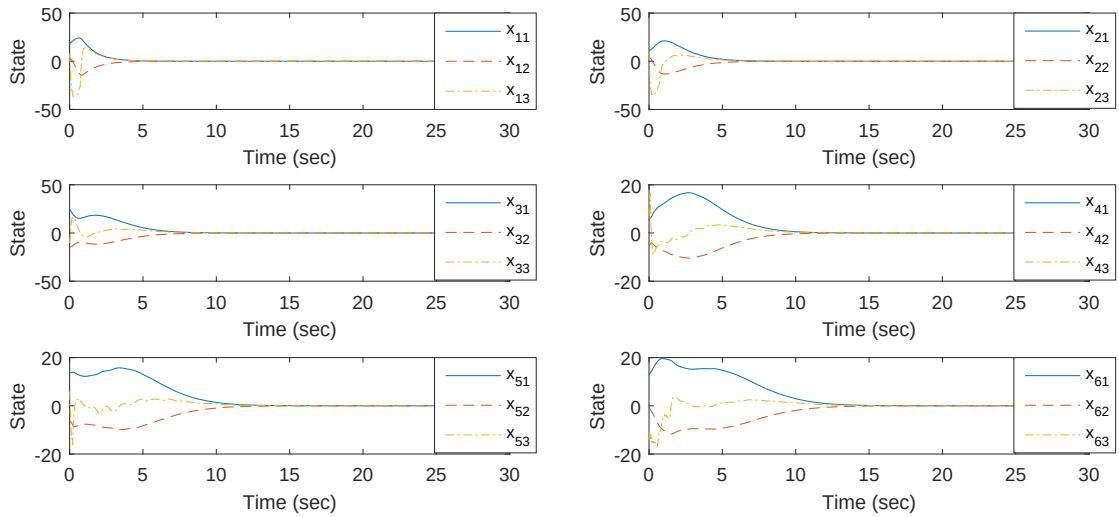

Figure 6.3: Time responses of the state variables of the system (6.65)

It is clear that the known nonlinear interconnections $\Gamma_{ij}(t,z_j)$ in equation (6.19) can be expressed as

$$\Gamma_{ii}^s = \begin{bmatrix} 0 & \frac{0.3}{1300}x_{i2} & 0 \\ 0 & -\frac{0.3}{1300}x_{i2} & 0 \\ 0 & -\frac{4.2864}{1300}x_{i2} & 0 \end{bmatrix}, \qquad i=1,\ldots,6$$

$$\Gamma_{21}^s = \Gamma_{32}^s = \begin{bmatrix} 0 & -1 & 0 \\ 0 & 0 & 0 \\ 0 & -13 & 0 \end{bmatrix}$$

which, by direct verification, satisfy (6.19). Now define the sliding surface as

$$\sigma(z_i) = z_{i3}, \qquad i=1,\ldots,6$$

Then, when the sliding motion takes place, from Lemma 1,

$$\begin{aligned}
\delta_1^a(t, z_1^a, \ldots, z_6^a) \leq & 0.01\cos^2(z_{12})\|z_1^a\| + 0.008\sin^2(z_{21})\|z_2^a\| \\
\delta_2^a(t, z_1^a, \ldots, z_6^a) \leq & 0.009\cos^2(z_{21})\|z_2^a\| + 0.016\sin^2(z_{12})\|z_1^a\| \\
\delta_3^a(t, z_1^a, \ldots, z_6^a) \leq & 0.008\sin^2(z_{32})\|z_3^a\| + 0.007\cos^2(z_{11})\|z_1^a\| \\
& + 0.011\cos^2(z_{22})\|z_2^a\| + 0.0095\cos^2(z_{42})\|z_4^a\| \\
\delta_4^a(t, z_1^a, \ldots, z_6^a) \leq & 0.011\cos^2(z_{41})\|z_4^a\| + 0.012\cos^2(z_{22})\|z_2^a\| \\
& + 0.01\cos^2(z_{31})\|z_3^a\| + 0.0078\cos^2(z_{51})\|z_5^a\| \\
\delta_5^a(t, z_1^a, \ldots, z_6^a) \leq & 0.012\sin^2(z_{51})\|z_5^a\| + 0.009\sin^2(z_{42})\|z_4^a\| \\
\delta_6^a(t, z_1^a, \ldots, z_6^a) \leq & 0.012\sin^2(z_{51})\|z_5^a\|
\end{aligned}$$

Choose $Q_1 = 1000I_2, Q_2 = 234I_2, Q_3 = 23I_2, Q_4 = 1.3I_2, Q_5 = 0.05I_2$ and $Q_6 = 0.01I_2$, by solving the Lyapunov equation, (6.15) yields

$$P_1 = \begin{bmatrix} 1577.27 & -931.82 \\ -931.82 & 613.64 \end{bmatrix} \quad P_2 = \begin{bmatrix} 369.08 & -218.05 \\ -218.05 & 143.59 \end{bmatrix}$$
$$P_3 = \begin{bmatrix} 36.28 & -21.43 \\ -21.43 & 14.11 \end{bmatrix} \quad P_4 = \begin{bmatrix} 2.05 & -1.21 \\ -1.21 & 0.80 \end{bmatrix}$$
$$P_5 = \begin{bmatrix} 0.079 & -0.047 \\ -0.047 & 0.031 \end{bmatrix} \quad P_6 = \begin{bmatrix} 0.016 & -0.0093 \\ -0.0093 & 0.0061 \end{bmatrix}$$

Then, the matrix function M can be obtained. It is straightforward to verify that in the domain $\Omega = T(\mathcal{D}_1 \times \mathcal{D}_2 \times \cdots \times \mathcal{D}_6)$ where $\mathcal{D}_i$ are given in (6.72) for $i = 1, \ldots, 6$,

$$M^\tau + M > 0$$

It follows from Theorem 6.1 that the designed sliding mode is asymptotically stable.

Choose

$$\begin{aligned}
&\zeta_1 = 200 + 0.32\|z_1\| \quad \zeta_2 = 200 \quad \zeta_3 = 200 + 0.192\|z_3\| \\
&\zeta_4 = 200 \qquad\qquad\quad \zeta_5 = 200 \quad \zeta_6 = 200
\end{aligned}$$

From (6.28), the controller u_i for $i = 1, \ldots, 3$ is well defined and the condition (8.35) in Theorem 6.2 is satisfied in the considered domain.

Simulation results are obtained and shown in Fig.6.3-Fig.6.7. The time responses of all the system states are shown in Fig.6.3. From Fig.6.3, it is clear to see that all subsystems are

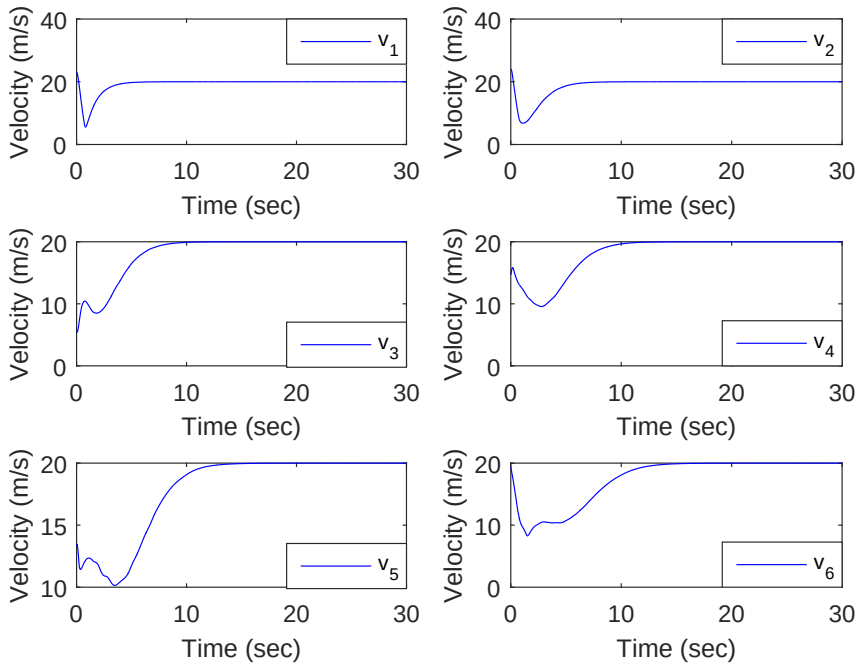

Figure 6.4: Time responses of the velocities of the vehicles

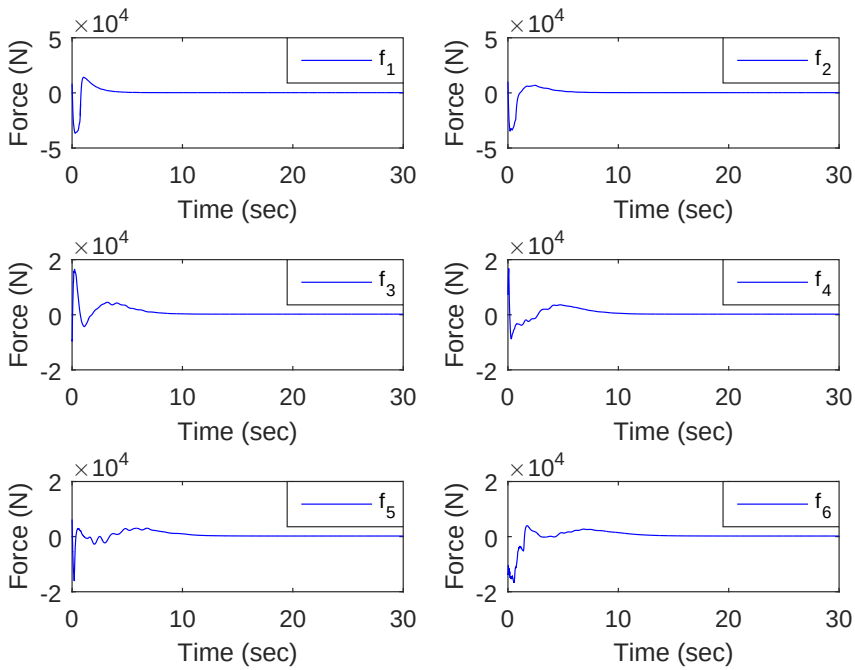

Figure 6.5: Time responses of the driving/braking forces of the vehicles

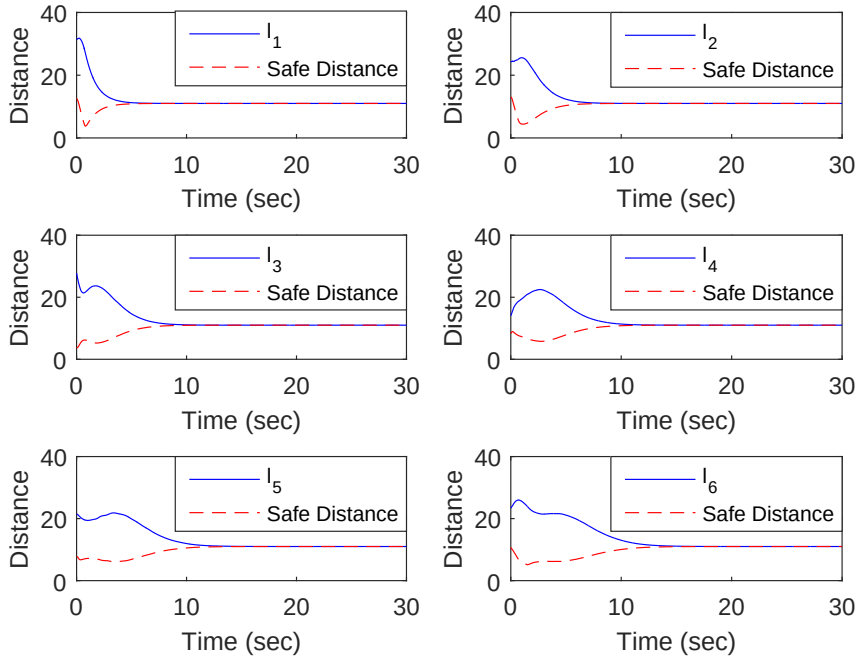

Figure 6.6: Time responses of the actual distances and the safe distance defined in (6.61)

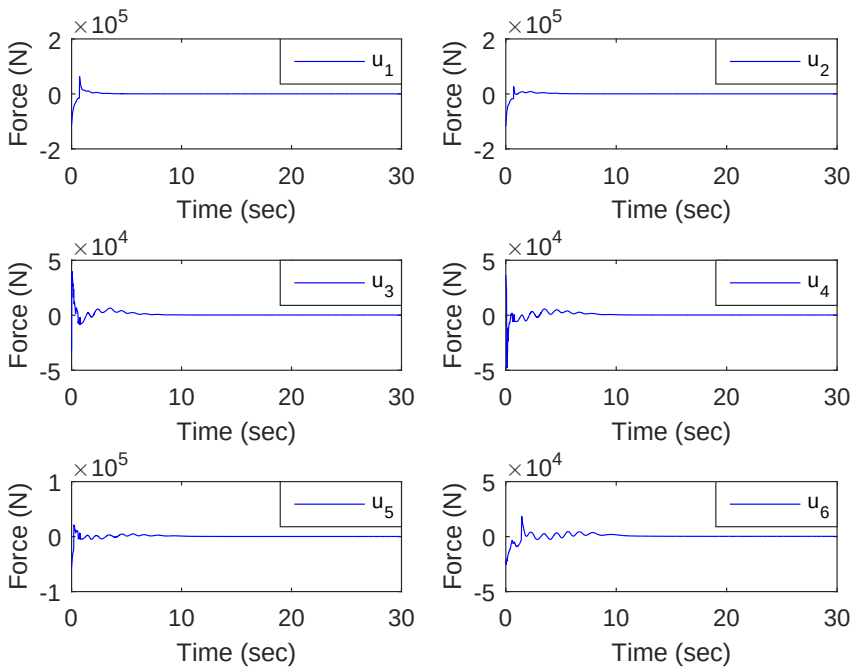

Figure 6.7: Time responses of the system input

stabilized even in the presence of uncertainties. The time response of velocities, driving/braking forces and distances with safe distances defined in (6.61) are shown in Fig.6.4-Fig.6.6 respectively. According to Fig.6.6, all cars are running within the prescribed safe distance to avoid collision. In Fig.6.5, it is clear to see that some subsystems, e.g. the 4th and 5th subsystems, experienced relatively large disturbances. However, owing to the robustness of the controller with respect to matched uncertainties when in the sliding mode, the closed-loop performance is robust. The control input signals applied to the system (6.65) are shown in Fig.6.7. It should be noted that a boundary layer approximation is used in the simulation, and thus there is no chattering. The simulation results show that the proposed approach is effective.

Remark 6.6. *From the simulation example, it is clear to see that the bounds on the uncertainties have a more general form in this chapter when compared with the existing work in [67] and [158]. In fact, in [67], the uncertainties are inevitably assumed to be a linear combination of known nonlinear functions in order to adaptively compensate parameter uncertainty. Furthermore, the bounds on the interconnections are assumed to satisfy a linear growth condition (i.e.* $\|\delta_i\| \leq \sum_{j=0}^{N} c_j \|x_j\|$*). In [158], an adaptive fuzzy control is applied on an automated highway system. In order to counteract the effect of the uncertainties, the bounds on the interconnection terms are assumed to have a special structure [158].*

6.6. Conclusion

In this chapter, a decentralised state feedback SMC law has been proposed to asymptotically stabilise a class of nonlinear interconnected systems with known and unknown interconnections in the considered domain. Both matched and mismatched uncertainties are considered. The bounds on the uncertainties can be nonlinear functions instead of constants or polynomial bounds as in previous work. Both known interconnections and the bounds on the unknown interconnections have been fully considered in the control design to reject their effects on the system to reduce conservatism. The developed results are applicable to a wide class of interconnected systems. Simulations for a CSTR system and a vehicle-following system have been presented to show that the results obtained are effective.

CHAPTER. 7

DECENTRALISED CONTROL FOR LARGE-SCALE SYSTEMS IN GENERALISED REGULAR FORM

For a linear system, the regular form can be obtained through basic matrix calculation. However, for a fully nonlinear MIMO interconnected system, the regular form does not always exist as discussed in Section 3.2.4. For a system that the classical regular form is not available, it is useful to develop control strategy based on the generalised regular form defined in Chapter 5. In this chapter, a nonlinear decentralised control strategy for a class of nonlinear interconnected systems in generalised regular form is proposed based on a SMC paradigm. The considered large-scale systems with fully nonlinear isolated subsystem have more general form than the system with the classical regular form considered in Chapter 6. The uncertainties are assumed to be bounded by known functions which are employed in the control design to counteract the effects of the uncertainties in the controlled interconnected system. It is shown that if the uncertainties/interconnections possess a superposition property, a decentralised control scheme may be designed to counteract the effect of the uncertainty for the nonlinear large-scale systems as well. To be specific, a class of nonlinear interconnected systems with subsystems in the

generalised regular form is studied in Section 7.1. Decentralised structure based on SMC technique for such systems is developed in the presence of both matched and mismatched uncertainties in Sections 7.2 and 7.3 regarding the stability of the sliding mode and reachability of the decentralised controller respectively. A numerical example with simulation results is presented in Section 7.4 to demonstrate the proposed control scheme. Finally, the conclusion of this chapter is presented in Section 7.5.

7.1. System Description

Consider a class of nonlinear large-scale interconnected systems composed of N subsystems where the i-th subsystem can be transformed or described by

$$\dot{X}_i = F_i(t, X_i) + G_i(t, X_i)(U_i + \Phi_i(t, X_i)) + \sum_{j=1}^{N} H_{ij}(t, X_j) \tag{7.1}$$

where $X_i \in \Omega_i \subset \mathcal{R}^{n_i}$ are the state variables of the i-th subsystem. The vector $F_i(\cdot)$ with $F_i(t, 0) = 0$ and the function matrix $G_i(\cdot)$ are continuous with appropriate dimensions. $U_i \in \mathcal{R}^{m_i}$ denote inputs of the i-th subsystem respectively for $i = 1, 2, \ldots, N$. Matched uncertainty is denoted by $\Phi_i(\cdot)$. The nonlinear functions $H_{ij}(\cdot) \in \mathcal{R}^{n_i}$ represent the uncertain interconnections. Specifically, $H_{ii}(\cdot)$ represent the uncertainty in the i-th subsystem. It is assumed that all the nonlinear functions are sufficiently smooth such that the unforced system has a unique continuous solution.

For further discussion and analysis, rewrite system (7.1) as follows

$$\dot{X}_i^a = F_i^a(t, X_i) + G_i^a(t, X_i)(U_i + \Phi_i(t, X_i)) + \sum_{j=1}^{N} H_{ij}^a(t, X_j) \tag{7.2}$$

$$\dot{X}_i^b = F_i^b(t, X_i) + G_i^b(t, X_i)(U_i + +\Phi_i(t, X_i)) + \sum_{j=1}^{N} H_{ij}^b(t, X_j) \tag{7.3}$$

where $X_i^a = \text{col}(X_{i1}^a, X_{i2}^a, \ldots, X_{i(n_i - m_i)}^a) \in \mathcal{R}^{n_i - m_i}$ and $X_i^b \in \mathcal{R}^{m_i}$ are derived from $X_i := \text{col}(X_i^a, X_i^b)$, and

$$F_i(t, X_i) := \begin{bmatrix} F_i^a(t, X_i) \\ F_i^b(t, X_i) \end{bmatrix}, \quad G_i(t, X_i) := \begin{bmatrix} G_i^a(t, X_i) \\ G_i^b(t, X_i) \end{bmatrix} \tag{7.4}$$

$$H_{ij}(t, X_j) := \begin{bmatrix} H_{ij}^a(t, X_j) \\ H_{ij}^b(t, X_j) \end{bmatrix} \tag{7.5}$$

where the function vectors $F_i^a(\cdot) \in \mathcal{R}^{(n_i - m_i)}$ and $F_i^b(\cdot) \in \mathcal{R}^{m_i}$, the function matrices $G_i^a(\cdot) \in \mathcal{R}^{(n_i - m_i)}$ and $G_i^b(\cdot) \in \mathcal{R}^{m_i}$ and the uncertainties $H_{ij}^a(\cdot) \in \mathcal{R}^{n_i - m_i}$ and $H_{ij}^b(\cdot) \in \mathcal{R}^{m_i}$ are continuous with appropriate dimensions.

Choose the sliding function $\sigma_i(X_i)$ as follows:

$$\sigma_i(X_i) = X_i^b + \varphi_i(X_i^a), \quad i = 1, 2, \ldots, N. \tag{7.6}$$

where $\varphi_i(\cdot)$ is a known Frechet-differentiable function with $\varphi_i(0) = 0$ satisfying

$$M_{\varphi_i}(\xi_i)\,(M_{\varphi_i}(\xi_i))^\tau \leq \beta_i I_{m_i} \quad \forall \xi_i \in \mathcal{R}^{n_i - m_i} \tag{7.7}$$

where $M_{\varphi_i}(\cdot) \in \mathcal{R}^{m_i \times (n_i - m_i)}$ represent the Jacobian matrix of the function $\varphi_i(\cdot)$, and β_i is a positive constant.

For the sliding functions in (7.6), the sliding surface is described by

$$\mathcal{S}_i = \{X_i \in \mathcal{R}^{n_i} | \quad \sigma_i(X_i) = 0\}, \quad i = 1, 2, \ldots, N. \tag{7.8}$$

Define function matrix $\Gamma_i(t, X_i)$ as

$$\Gamma_i(t, X_i) := G_i^b(t, X_i) + M_{\varphi_i}(X_i^a) G_i^a(t, X_i) \tag{7.9}$$

where $G_i^a(\cdot)$ and $G_i^b(\cdot)$ are defined in systems (7.2)-(7.3) and $\varphi_i(\cdot)$ are defined in (7.6).

Assumption 7.1. System (7.1) is in the generalised regular from, see Definition 5.1 in Section 5.2 of Chapter 5, described by (7.2)-(7.3), and the function $\Gamma_i(\cdot)$ defined in (7.9) is nonsingular for $X_i \in \Omega_i$ for $i = 1, 2, \ldots, N$.

Remark 7.1. *As discussed in Section 3.2.4 in Chapter 3, the distribution spanned by the column vectors of the input matrix is completely integrable if and only if the distribution is involutive (e.g. see [32]). This implies that the classical regular form does not always exist. As the generalised regular form include the classical regular form as a special case, which further shows that the proposed method has more general form than the existing work.*

Assumption 7.2. There exist known continuous nondecreasing functions $\Xi_{ij}^a(\cdot)$ in $\mathcal{R}^+$ with $\Xi_{ij}^a(0) = 0$, and known continuous functions $\Xi_i^b(\cdot)$ and $\rho_i(\cdot)$ such that

(i) $\left\|H_{ij}^a(t, X_j)\right\| \leq \Xi_{ij}^a(\|X_j\|)$ (7.10)

(ii) $\left\|H_{ij}^b(t, X_j)\right\| \leq \Xi_{ij}^b(\|X_j\|)$ (7.11)

(iii) $\|\Phi_i(t, X_i)\| \leq \rho_i(t, X_i)$ (7.12)

for all $t \in \mathcal{R}^+$, and $X_i \in \Omega_i$ for $i = 1, 2, \ldots, N$.

Remark 7.2. *Assumption 7.2 is a limitation on all the uncertainties experienced by the system. It is required that bounds on the uncertainties are known and the bounds will be employed in the control design to reject or reduce the effect caused by the uncertainties. It should be pointed out that only uncertainties $H_{ij}^a(\cdot)$ are required to vanish at the origin, which are reflected through $\Xi_{ij}^a(0) = 0$ while it is not required that $H_{ij}^b(t, X_j)$ are vanished at the origin in this chapter.*

7.2. Stability Analysis of the Sliding Mode

Choose the composite sliding surface for the interconnected system (7.2)-(7.3) as follows

$$\sigma(X) = 0 \tag{7.13}$$

where $\sigma(X) \equiv: \text{col}\,(\sigma_1(X_1), \sigma_2(X_2), \ldots, \sigma_N(X_N))$ and $X := \text{col}(X_1, X_2, \ldots, X_N)$ with $\sigma_i(\cdot)$ defined in (7.6). During sliding motion, $\sigma_i(X_i) = 0$ for $i = 1, 2, \ldots, N$. Therefore, when sliding motion occurs, from Assumption 7.1,

$$G_i^a(t, X_i) = 0$$

and from (7.6),

$$X_i^b = -\varphi_i(X_i^a)$$

for $i = 1, 2, \ldots, N$. Then, the sliding mode dynamics for the system (7.2)-(7.3) associated with the designed sliding surface (7.13) can be described by

$$\dot{X}_i^a = F_i^s(t, X_i^a) + \sum_{j=1}^{N} H_{ij}^s(t, X_j^a) \tag{7.14}$$

where

$$F_i^s(t, X_i^a) := F_i^a(t, X_i^a, -\varphi_i(X_i^a)) \tag{7.15}$$

and

$$H_{ij}^s(t, X_j^a) := H_{ij}^a(t, X_j^a, -\varphi_j(X_j^a)) \tag{7.16}$$

for $i, j = 1, 2, \ldots, N$ with $H_{ij}^a(t, X_j)$ defined in (7.2).

Lemma 7.1. *For terms $H_{ij}^s(t, X_j^a)$ in system (7.14), if inequality (7.10) in Assumption 7.2 holds, then*

$$\|H_{ij}^s(t, X_j^a)\| \leq \Xi_{ij}^s(\|X_j^a\|) \tag{7.17}$$

where

$$\Xi_{ij}^s(\|X_j^a\|) = \Xi_{ij}^a(\sqrt{1+\beta_i}\|X_j^a\|)$$

where $\Xi_{ij}^a(\cdot)$ are defined in (7.10).

Proof. From the definition of $H_{ij}^s(\cdot)$ in (7.16), it follows that

$$H_{ij}^s(t, X_j^a) = H_{ij}^a(t, X_j^a, -\varphi_i(X_j^a)) \tag{7.18}$$

From (7.7), it is straightforward to see that

$$\|M_{\varphi_i}(\xi)\| \leq \sqrt{\beta_i} \tag{7.19}$$

Then from the mean value theorem,

$$\|\varphi_i(h) - \varphi_i(0)\| = \|\varphi_i(h)\| \leq \sqrt{\beta_i}\|h\| \tag{7.20}$$

When the system is on the sliding surface

$$\begin{aligned}
\|X_i\| =& \sqrt{(X_i^a)^\tau X_i^a + (X_i^b)^\tau X_i^b} \\
=& \sqrt{(X_i^a)^\tau X_i^a + \varphi_i^\tau(X_i^a)\varphi_i(X_i^a)} \\
\leq& \sqrt{\|X_i^a\|^2 + \beta_i\|X_i^a\|^2} \\
=& \sqrt{1+\beta_i}\|X_i^a\|
\end{aligned} \tag{7.21}$$

From (7.18), (7.10) and (7.21), it follows that

$$\|H_{ij}^s(t, X_j^a)\| \leq \Xi_{ij}^a(\|X_j\|) \leq \Xi_{ij}^a(\sqrt{1+\beta_i}\|X_j^a\|) = \Xi_{ij}^s(\|X_j^a\|) \tag{7.22}$$

Hence the result follows. ■

Assumption 7.3. There exist continuous $\mathcal{C}^1$ function $V_i : \mathcal{R}^+ \times \mathcal{R}^{n_i - m_i} \to \mathcal{R}^+$ and functions $\varsigma_{i1}(\cdot)$, $\varsigma_{i2}(\cdot)$, $\varsigma_{i3}(\cdot)$ and $\varsigma_{i4}(\cdot)$ of class $\mathcal{K}$ such that for all $X_i \in \Omega_i$ and $t \in \mathcal{R}^+$

(i) $\varsigma_{i1}(\|X_i^a\|) \leq V_i(t, X_i^a) \leq \varsigma_{i2}(\|X_i^a\|)$

(ii) $\dfrac{\partial V_i(t, X_i^a)}{\partial t} + \dfrac{\partial V_i(t, X_i^a)}{\partial X_i^a} F_i^s(t, X_i^a) \leq -\varsigma_{i3}^2(\|X_i^a\|)$

(iii) $\left\| \dfrac{\partial V_i(t, X_i^a)}{\partial X_i^a} \right\| \leq \varsigma_{i4}(\|X_i^a\|)$

where

$$\frac{\partial V_i(t, X_i^a)}{\partial X_i^a} = \left(\frac{\partial V_i(t, X_i^a)}{\partial X_{i1}^a}, \frac{\partial V_i(t, X_i^a)}{\partial X_{i2}^a} \cdots \frac{\partial V_i(t, X_i^a)}{\partial X_{i(n_i - m_i)}^a} \right)$$

with $X_i^a = \mathrm{col}(X_{i1}^a, X_{i2}^a, \ldots, X_{i(n_i - m_i)}^a)$.

Assumption 7.3 is employed to guarantee that all the isolated nominal subsystems of the interconnected system (7.14) are asymptotically stable. The following result is ready to be presented.

Theorem 7.1. *Under Assumptions 7.1, 7.2 and 7.3, the sliding modes (7.14) of the systems (7.2)-(7.3) for $i = 1, 2, \ldots, N$ associated with the sliding surface (7.13) are asymptotically stable if there exists a domain Ω_{X^a} of the origin in $X^a = \mathrm{col}(X_1^a, X_2^a, \ldots, X_N^a) \in \mathcal{R}^{\sum_{i=1}^N (n_i - m_i)}$ such that*

$$(W(t, X^a))^\tau + W(t, X^a) > 0$$

in domain $\Omega_{X^a} \backslash \{0\}$ with $W(t, X^a) = (w_{ij}(t, X_i^a, X_j^a))_{N \times N}$ and for $i, j = 1, 2, \ldots, N$

$$w_{ij}(t, X_i^a, X_j^a) = \begin{cases} \mu_{i3}(\|X_i^a\|) - \mu_{i4}(\|X_i^a\|)\gamma_{ii}(\|X_i^a\|), & i = j \\ -\mu_{i4}(\|X_i^a\|)\gamma_{ij}(\|X_j^a\|), & i \neq j \end{cases}$$

where $\mu_{i3}(\cdot)$, $\mu_{i4}(\cdot)$ and $\gamma_{ij}(\cdot)$ are defined respectively by

$$\mu_{i3}(\xi) = \int_0^1 \frac{\partial \varsigma_{i3}(\xi h)}{\partial h} \mathrm{d}h \tag{7.23}$$

$$\mu_{i4}(\xi) = \int_0^1 \frac{\partial \varsigma_{i4}(\xi h)}{\partial h} \mathrm{d}h \tag{7.24}$$

$$\gamma_{ij}(\xi) = \int_0^1 \frac{\partial \Xi_{ij}^s(\xi h)}{\partial h} \mathrm{d}h \tag{7.25}$$

with $h \in \mathcal{R}$, and ς_{i3}, ς_{i3} and Ξ_{ij}^s are defined in Assumption 7.3 and (7.17) respectively.

Proof. From (7.23)-(7.25), it can be observed that

$$\varsigma_{i3}(\|X_i^a\|) = \mu_{i3}(\|X_i^a\|)\|X_i^a\| \tag{7.26}$$

$$\varsigma_{i4}(\|X_i^a\|) = \mu_{i4}(\|X_i^a\|)\|X_i^a\| \tag{7.27}$$

$$\Xi_{ij}^s(\|X_j^a\|) = \gamma_{ij}(\|X_j^a\|)\|X_j^a\| \tag{7.28}$$

From the analysis above, it is seen that system (7.14) represents the sliding mode dynamics of the system (7.2)-(7.3) corresponding to the sliding surface (7.13). For system (7.14), consider the candidate Lyapunov function

$$V(t, X^a) = \sum_{i=1}^{N} V_i(t, X_i^a) \tag{7.29}$$

where $V_i(t, X_i^a)$ is given in Assumption 7.3. Then, the time derivative of $V(t, X_i^a)$ along equation (7.14) is given by

$$\begin{aligned}
\dot{V} =& \sum_{i=1}^{N} \Big\{ \frac{\partial V_i(t, X_i^a)}{\partial t} + \frac{\partial V_i(t, X_i^a)}{\partial X_i^a} F_i^s(t, X_i^a) + \frac{\partial V_i(t, X_i^a)}{\partial X_i^a} \sum_{j=1}^{N} H_{ij}^s(t, X_j^a) \Big\} \\
\leq& \sum_{i=1}^{N} \Big\{ -\varsigma_{i3}^2(\|X_i^a\|) + \varsigma_{i4}(\|X_i^a\|) \sum_{j=1}^{N} \Xi_{ij}^s(\|X_j^a\|) \Big\} \\
=& -\sum_{i=1}^{N} \mu_{i3}^2(\|X_i^a\|)\|X_i^a\|^2 + \sum_{i=1}^{N}\sum_{j=1}^{N} \mu_{i4}(\|X_i^a\|)\gamma_{ij}(\|X_j^a\|)\|X_i^a\|\|X_j^a\| \\
=& -\frac{1}{2}(\|X_1^a\|, \|X_2^a\|, \ldots, \|X_N^a\|)\,(W^\tau + W) \begin{pmatrix} \|X_1^a\| \\ \|X_2^a\| \\ \vdots \\ \|X_N^a\| \end{pmatrix}
\end{aligned}$$

Since the matrix function $W^\tau + W$ is positive definite in $\Omega_{X^a} \backslash \{0\}$, it follows that V is negative definite in domain Ω_{X^a}. Hence, the result follows. ■

7.3. Decentralised Control Design

For nonlinear interconnected system (7.2)-(7.3) with sliding surface (7.13), the corresponding reachability condition is described by (e.g. see [113, 47])

$$\sum_{i=1}^{N} \frac{\sigma_i^\tau(X_i)\dot{\sigma}_i(X_i)}{\|\sigma_i(X_i)\|} < 0 \tag{7.30}$$

where $\sigma_i(X_i)$ is defined in (7.6).

Consider the decentralised control

$$\begin{aligned} U_i = &- \Gamma_i^{-1}(t, X_i)\Big\{M_{\varphi_i}(X_i^a)F_i^a(t, X_i) + F_i^b(t, X_i)\Big\} \\ &- \Gamma_i^{-1}(t, X_i)\text{sgn}(\sigma_i(X_i))\Big\{\sum_{j=1}^{N}\varepsilon_j^{-1}\left(\Xi_{ji}^a(\|X_i\|)\right)^2 \\ &+ \sum_{j=1}^{N}\Xi_{ji}^b(t, X_i) + N\varepsilon_i\beta_i + \|\Gamma_i(t, X_i)\|\rho_i(t, X_i) + \zeta_i\Big\} \end{aligned} \tag{7.31}$$

where $\Xi_{ji}^a(\cdot)$, $\Xi_{ji}^b(\cdot)$ and $\rho_i(t, X_i)$ are defined in Assumption 7.2, ζ_i and ε_j are positive constants which can be considered as design parameters.

Theorem 7.2. *Consider the nonlinear interconnected systems (7.2) - (7.3) for $i = 1, 2, \ldots, N$. Under Assumptions 7.1-7.2, the closed-loop systems (7.2)-(7.3) with the decentralised control (7.31) are driven to the composite sliding surface (7.13) and maintain a sliding motion on it thereafter.*

Proof. From the analysis above, all that needs to be proved is that the composite reachability condition (7.30) is satisfied. From (7.6), for $i = 1, 2, \ldots, N$

$$\begin{aligned} \dot{\sigma}_i(X_i) =& M_{\varphi_i}(X_i^a)F_i^a(t, X_i) + F_i^b(t, X_i) + M_{\varphi_i}(X_i^a)\sum_{j=1}^{N}H_{ij}^a(t, X_j) \\ &+ \sum_{j=1}^{N}H_{ij}^b(t, X_j) + \Gamma_i(t, X_i)(U_i + \Phi_i(t, X_i)) \end{aligned} \tag{7.32}$$

Substituting (7.31) into (7.32),

$$\begin{aligned} \sum_{i=1}^{N}\frac{\sigma_i^\tau(X_i)\dot{\sigma}_i(X_i)}{\|\sigma_i(X_i)\|} =& \sum_{i=1}^{N}\Big\{\frac{\sigma_i^\tau(X_i)}{\|\sigma_i(X_i)\|}\Big\{\sum_{j=1}^{N}H_{ij}^b(t, X_j) + M_{\varphi_i}(X_i^a)\sum_{j=1}^{N}H_{ij}^a(t, X_j) \\ &+ \Gamma_i(t, X_i)\Phi_i(t, X_i)\Big\} - \|\Gamma_i(t, X_i)\|\rho_i(t, X_i) \\ &- \sum_{j=1}^{N}\varepsilon_j^{-1}\left(\Xi_{ji}^a(\|X_j\|)\right)^2 - \sum_{j=1}^{N}\Xi_{ji}^b(t, X_i) - N\varepsilon_i\beta_i - \zeta_i\Big\} \\ \leq& \sum_{i=1}^{N}\|\Gamma_i(t, X_i)\Phi_i(t, X_i)\| + \sum_{i=1}^{N}\sum_{j=1}^{N}\|H_{ij}^b(t, X_j)\| \\ &+ \sum_{i=1}^{N}\sum_{j=1}^{N}\frac{\sigma_i^\tau(X_i)}{\|\sigma_i(X_i)\|}M_{\varphi_i}(X_i^a)H_{ij}^a(t, X_j) \end{aligned}$$

$$
\begin{aligned}
&-\sum_{i=1}^{N}\|\Gamma_i(t,X_i)\|\rho_i(t,X_i)-\sum_{i=1}^{N}\sum_{j=1}^{N}\varepsilon_j^{-1}\left(\Xi_{ji}^a(\|X_i\|)\right)^2\\
&-\sum_{i=1}^{N}\sum_{j=1}^{N}\Xi_{ji}^b(t,X_i)-N\sum_{i=1}^{N}\varepsilon_i\beta_i-\sum_{i=1}^{N}\zeta_i
\end{aligned}
\tag{7.33}
$$

From the fact that for any positive constant ε (e.g. see [73]),

$$
2W^\tau Z\le\varepsilon W^\tau W+\varepsilon^{-1}Z^\tau Z,\quad \forall W,Z\in\mathcal{R}^l
\tag{7.34}
$$

Then, from (7.11) and (7.7), it is straightforward to obtain that

$$
\begin{aligned}
&\sum_{i=1}^{N}\sum_{j=1}^{N}\frac{\sigma_i^\tau(X_i)}{\|\sigma_i(X_i)\|}M_{\varphi_i}(X_i^a)H_{ij}^a(t,X_j)\\
&\quad\le N\sum_{i=1}^{N}\varepsilon_i\frac{\sigma_i^\tau(X_i)}{\|\sigma_i(X_i)\|}M_{\varphi_i}(X_i^a)\left(M_{\varphi_i}(X_i^a)\right)^\tau\frac{\sigma_i(X_i)}{\|\sigma_i(X_i)\|}\\
&\qquad+\sum_{i=1}^{N}\sum_{j=1}^{N}\varepsilon_i^{-1}\left(H_{ij}^a(t,X_j)\right)^\tau H_{ij}^a(t,X_j)\\
&\quad\le N\sum_{i=1}^{N}\varepsilon_i\beta_i\frac{\sigma_i^\tau(X_i)\sigma_i(X_i)}{\|\sigma_i(X_i)\|^2}+\sum_{i=1}^{N}\sum_{j=1}^{N}\varepsilon_i^{-1}\left\|H_{ij}^a(t,X_j)\right\|^2\\
&\quad=N\sum_{i=1}^{N}\varepsilon_i\beta_i+\sum_{i=1}^{N}\sum_{j=1}^{N}\varepsilon_i^{-1}\left\|H_{ij}^a(t,X_j)\right\|^2
\end{aligned}
\tag{7.35}
$$

where ε_i is a positive constant.

Then, from Assumption 7.2 and the identity

$$
\sum_{i=1}^{N}\sum_{j=1}^{N}a_{ij}\equiv\sum_{i=1}^{N}\sum_{j=1}^{N}a_{ji}
$$

it is straightforward to see that

$$
\begin{aligned}
\sum_{i=1}^{N}\sum_{j=1}^{N}\varepsilon_i^{-1}\|H_{ij}^a(t,X_j)\|^2&\le\sum_{i=1}^{N}\sum_{j=1}^{N}\varepsilon_i^{-1}\left(\Xi_{ij}^a(\|X_j\|)\right)^2\\
&=\sum_{i=1}^{N}\sum_{j=1}^{N}\varepsilon_j^{-1}\left(\Xi_{ji}^a(\|X_i\|)\right)^2
\end{aligned}
\tag{7.36}
$$

$$
\begin{aligned}
\sum_{i=1}^{N}\sum_{j=1}^{N}\|H_{ij}^b(t,X_j)\|&\le\sum_{i=1}^{N}\sum_{j=1}^{N}\Xi_{ij}^b(t,X_j)\\
&=\sum_{i=1}^{N}\sum_{j=1}^{N}\Xi_{ji}^b(t,X_i)
\end{aligned}
\tag{7.37}
$$

Further from (7.12) in Assumption 7.2,

$$\begin{aligned}\|\Gamma_i(t,X_i)\Phi_i(t,X_i)\| \leq & \|\Gamma_i(t,X_i)\|\|\Phi_i(t,X_i)\| \\ \leq & \|\Gamma_i(t,X_i)\|\rho_i(t,X_i)\end{aligned} \tag{7.38}$$

Then from inequalities (7.35)-(7.38), it is straightforward to verify that

$$\sum_{i=1}^{N}\frac{\sigma_i(X_i)^\tau\dot{\sigma}_i(X_i)}{\|\sigma_i(X_i)\|} \leq -\sum_{i=1}^{N}\zeta_i < 0 \tag{7.39}$$

Hence, the result follows. ■

Remark 7.3. *The result in Theorem 7.2 shows that if the nonlinear function $\varphi_i(\cdot)$ defined in (7.6) satisfies (7.7), then the proposed controller (7.31) can guarantee that all the subsystems will reach the composite sliding surface (7.13).*

From sliding mode control theory, Theorems 1 and 2 together guarantee that the systems (7.2)-(7.3) are stabilized by the designed decentralised control (7.31).

7.4. Numerical Simulation

Consider the following nonlinear interconnected system composed of three subsystems described by

$$\begin{aligned}\dot{X}_1^a = & \underbrace{-0.6X_{11}\cos(X_{12}) + X_{13}}_{F_1^a(t,X_1)} + \sum_{j=1}^{3} H_{1j}^a(t,X_j) \\ & + \underbrace{\begin{bmatrix} 0 & \sin(X_{12}) \end{bmatrix}}_{G_1^a(t,X_1)}(U_1 + \Phi_1(t,X_1))\end{aligned} \tag{7.40}$$

$$\begin{aligned}\dot{X}_1^b = & \underbrace{\begin{bmatrix} 0.2X_{11}X_{13} \\ -X_{11} + 0.8X_{13}\cos(X_{12}) \end{bmatrix}}_{F_1^b(t,X_1)} + \sum_{j=1}^{3} H_{1j}^b(t,X_j) \\ & + \underbrace{\begin{bmatrix} 1 & X_{13} \\ 0 & 1 \end{bmatrix}}_{G_1^b(t,X_1)}(U_1 + \Phi_1(t,X_1))\end{aligned} \tag{7.41}$$

$$\dot{X}_2^a = \underbrace{-0.5X_{21}\cos(X_{22}) + X_{23}}_{F_2^a(t,X_2)} + \sum_{j=1}^{3} H_{2j}^a(t,X_j)$$

$$+\underbrace{\begin{bmatrix} 0 & \sin(X_{22}) \end{bmatrix}}_{G_2^a(t,X_2)}(U_2+\Phi_2(t,X_2)) \tag{7.42}$$

$$\dot{X}_2^b = \underbrace{\begin{bmatrix} 0.4X_{21}X_{23} \\ -0.8X_{21}+0.8X_{23}\cos(X_{22}) \end{bmatrix}}_{F_2^b(t,X_2)} + \sum_{j=1}^{3} H_{2j}^b(t,X_j)$$

$$+\underbrace{\begin{bmatrix} 1 & X_{23} \\ 0 & 1 \end{bmatrix}}_{G_2^b(t,X_2)}(U_2+\Phi_2(t,X_2)) \tag{7.43}$$

$$\dot{X}_3^a = \underbrace{-0.7X_{31}\cos(X_{32})+X_{33}}_{F_3^a(t,X_3)} + \sum_{j=1}^{3} H_{3j}^a(t,X_j)$$

$$+\underbrace{\begin{bmatrix} 0 & \sin(X_{32}) \end{bmatrix}}_{G_3^a(t,X_3)}(U_3+\Phi_3(t,X_3)) \tag{7.44}$$

$$\dot{X}_3^b = \underbrace{\begin{bmatrix} 0.2X_{31}X_{33} \\ -X_{31}+0.9X_{33}\cos(X_{32}) \end{bmatrix}}_{F_3^b(t,X_3)} + \sum_{j=1}^{3} H_{3j}^b(t,X_j)$$

$$+\underbrace{\begin{bmatrix} 1 & X_{33} \\ 0 & 1 \end{bmatrix}}_{G_3^b(t,X_3)}(U_3+\Phi_3(t,X_3)) \tag{7.45}$$

where $X_{i1} := X_i^a$, $\mathrm{col}(X_{i2}, X_{i3}) := X_i^b$ for $i = 1, 2, 3$.

Assume the matched uncertainties satisfy

$$\|\Phi_1(t,X_1)\| \leq \underbrace{0.24\sqrt{X_{13}^2+1}}_{\rho_1(t,X_1)}, \qquad \|\Phi_2(t,X_2)\| \leq \underbrace{0.16\sqrt{X_{23}^2+1}}_{\rho_2(t,X_2)}$$

$$\|\Phi_3(t,X_3)\| \leq \underbrace{0.18\sqrt{X_{33}^2+1}}_{\rho_3(t,X_3)}$$

Assume that the bounds on the uncertain interconnections satisfy

$$\sum_{j=1}^{2} \|H_{1j}^a(t,X_j)\| \leq \underbrace{0.72|\cos(X_{12})|\|X_1\|}_{\Xi_{11}^a(\|X_1\|)} + \underbrace{0.5\|X_2\|}_{\Xi_{12}^a(\|X_2\|)} + \underbrace{0.64\|X_3\|}_{\Xi_{13}^a(\|X_3\|)}$$

$$\sum_{j=1}^{2} \|H_{1j}^b(t,X_j)\| \leq \underbrace{0.83\|X_1\|}_{\Xi_{11}^b(\|X_1\|)} + \underbrace{1.01\|X_2\|}_{\Xi_{12}^b(\|X_2\|)} + \underbrace{0.68\|X_3\|}_{\Xi_{13}^b(\|X_3\|)}$$

$$\sum_{j=1}^{2}\|H_{2j}^{a}(t,X_j)\| \leq \underbrace{0.5\|X_1\|}_{\Xi_{21}^{a}(\|X_1\|)} + \underbrace{0.78|\cos(X_{22})|\|X_2\|}_{\Xi_{22}^{a}(\|X_2\|)} + \underbrace{0.58\|X_3\|}_{\Xi_{23}^{a}(\|X_3\|)}$$

$$\sum_{j=1}^{2}\|H_{2j}^{b}(t,X_j)\| \leq \underbrace{0.63\|X_1\|}_{\Xi_{21}^{b}(\|X_1\|)} + \underbrace{0.63\|X_2\|}_{\Xi_{22}^{b}(\|X_2\|)} + \underbrace{0.42\|X_3\|}_{\Xi_{23}^{b}(\|X_3\|)}$$

$$\sum_{j=1}^{2}\|H_{3j}^{a}(t,X_j)\| \leq \underbrace{0.64\|X_1\|}_{\Xi_{31}^{a}(\|X_1\|)} + \underbrace{0.78\|X_2\|}_{\Xi_{32}^{a}(\|X_2\|)} + \underbrace{0.64|\cos(X_{33})|\|X_3\|}_{\Xi_{33}^{a}(\|X_3\|)}$$

$$\sum_{j=1}^{2}\|H_{3j}^{b}(t,X_j)\| \leq \underbrace{0.64\|X_1\|}_{\Xi_{31}^{b}(\|X_1\|)} + \underbrace{0.65\|X_2\|}_{\Xi_{32}^{b}(\|X_2\|)} + \underbrace{0.73\|X_3\|}_{\Xi_{33}^{b}(\|X_3\|)}$$

Now define the sliding function in the form of (7.6) by

$$\varphi_i(X_i^a) = \begin{bmatrix} 0 \\ \frac{\sqrt{\beta_i c_i}X_{11}}{\sqrt{c_i+X_{11}^2}} \end{bmatrix} \quad i = 1,2,3$$

where the design parameters β_i and c_i are chosen as $\beta_i = 1$ and $c_i = 0.25$. Then it is straightforward to verify that

$$M_{\varphi_i}(X_i^a)M_{\varphi_i}(X_i^a)^{\tau} = \begin{bmatrix} 0 & 0 \\ 0 & \frac{\beta_i c_i^3}{(c_i+X_{11}^2)^3} \end{bmatrix} \leq \beta_i I_2$$

From Lemma 1, when the sliding motion takes place,

$$\sum_{j=1}^{2}\|H_{1j}^{s}(t,X_j^a)\| \leq \underbrace{0.51\|X_1^a\|}_{\Xi_{11}^{s}(\|X_1\|)} + \underbrace{0.35\|X_2^a\|}_{\Xi_{12}^{s}(\|X_2\|)} + \underbrace{0.45\|X_3^a\|}_{\Xi_{13}^{s}(\|X_3\|)}$$

$$\sum_{j=1}^{2}\|H_{2j}^{s}(t,X_j^a)\| \leq \underbrace{0.35\|X_1^a\|}_{\Xi_{21}^{s}(\|X_1\|)} + \underbrace{0.55\|X_2^a\|}_{\Xi_{22}^{s}(\|X_2\|)} + \underbrace{0.41\|X_3^a\|}_{\Xi_{23}^{s}(\|X_3\|)}$$

$$\sum_{j=1}^{2}\|H_{3j}^{s}(t,X_j^a)\| \leq \underbrace{0.45\|X_1^a\|}_{\Xi_{31}^{s}(\|X_1\|)} + \underbrace{0.55\|X_2^a\|}_{\Xi_{32}^{s}(\|X_2\|)} + \underbrace{0.45\|X_3^a\|}_{\Xi_{33}^{s}(\|X_3\|)}$$

Choose the candidate Lyapunov function for system (7.40) - (7.45) as

$$V = \sum_{i=1}^{3} V_i \tag{7.46}$$

where

$$V_i = \frac{1}{2}(X_i^a)^{\tau}X_i^a, \quad i = 1,2,3$$

Then,

$$\underbrace{0.4\|X_i^a\|^2}_{\varsigma_{i1}} \leq V_i(t, X_i^a) \leq 0.6\underbrace{\|X_i^a\|^2}_{\varsigma_{i2}}$$

Define $\varsigma_{i3}(\cdot)$ for $i = 1, 2, 3$ as

$$\varsigma_{13}(r) = \underbrace{0.6}_{\mu_{13}} r, \quad \varsigma_{23}(r) = \underbrace{0.5}_{\mu_{23}} r, \quad \varsigma_{33}(r) = \underbrace{0.7}_{\mu_{33}} r$$

and $\varsigma_{i4}(\cdot)$ as

$$\varsigma_{i4}(r) = \underbrace{1}_{\mu_{i4}} \cdot r, \quad i = 1, 2, 3$$

By direct computation, it is straightforward to verify that

$$W(t, X) + (W(t, X))^\tau > 0$$

with

$$\begin{aligned}
\gamma_{11}(\|X_1\|) &= 0.51, \quad \gamma_{12}(\|X_2\|) = 0.35, \quad \gamma_{13}(\|X_3\|) = 0.45 \\
\gamma_{21}(\|X_1\|) &= 0.35, \quad \gamma_{22}(\|X_2\|) = 0.55, \quad \gamma_{23}(\|X_3\|) = 0.41 \\
\gamma_{31}(\|X_1\|) &= 0.45, \quad \gamma_{32}(\|X_2\|) = 0.55, \quad \gamma_{33}(\|X_3\|) = 0.45
\end{aligned}$$

Thus the designed sliding modes are asymptotically stable.

From (7.31), the controllers U_i are well defined with $\zeta_i = 1$ and $\varepsilon_i = 0.5$ for $i = 1, 2, 3$, which guarantee that the condition (6.26) is satisfied for $X_i \in \mathcal{R}^3$, $i = 1, 2, 3$. Thus systems (7.40)-(7.43) for $i = 1, 2, 3$ can be stabilised by the designed controls U_i proposed in (7.31). The time response of the system states is shown in Fig.7.1, and the time responses of the decentralised controllers are shown in Fig. 7.2. The simulation results show that the proposed approach is effective. It should be noted that in the simulation, a boundary layer is used to remove the chattering.

7.5. Conclusion

This chapter has proposed a robust decentralised sliding mode control design approach for a class of nonlinear large-scale interconnected systems in generalised regular form with uncertain interconnections. The bounds on the uncertainties are assumed to be known functions which have been used to enhance robustness. Decentralized sliding mode controllers are designed to reduce the effects of the interconnections on the entire system. The developed results can be

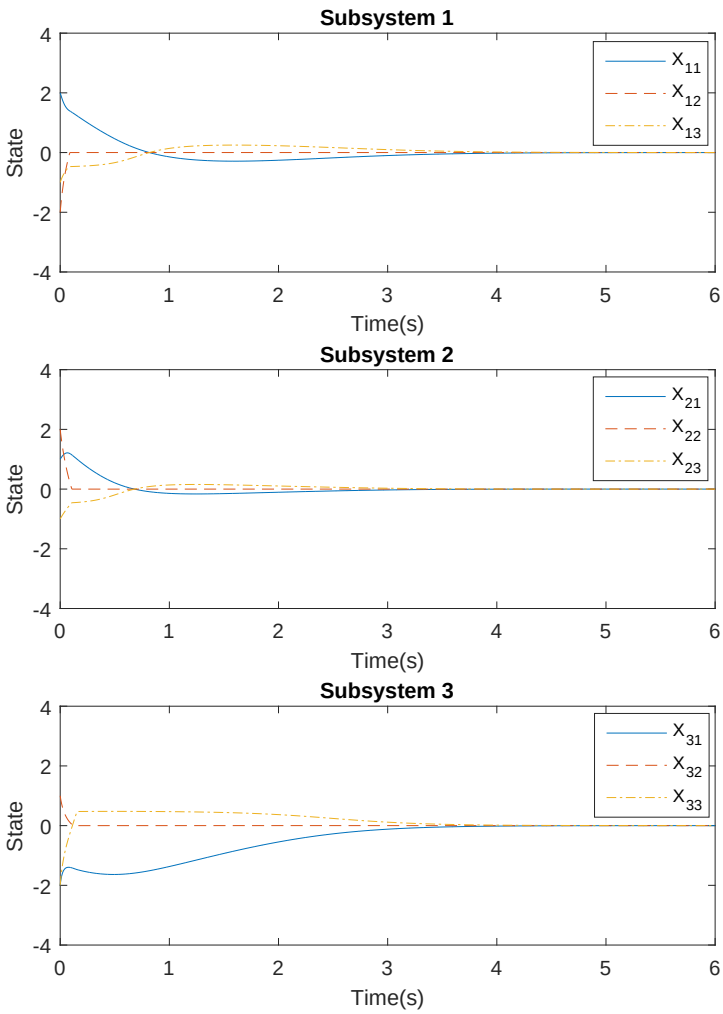

Figure 7.1: Time response of the state variables of system (7.40)-(7.45).

applied to all the interconnected systems which can be transformed to the generalised regular form described in (7.2)-(7.3). A numerical example is given to show how to use the sliding mode technique to stabilise a system with uncertain interconnections. Simulations have been presented to demonstrate the effectiveness of the proposed approach.

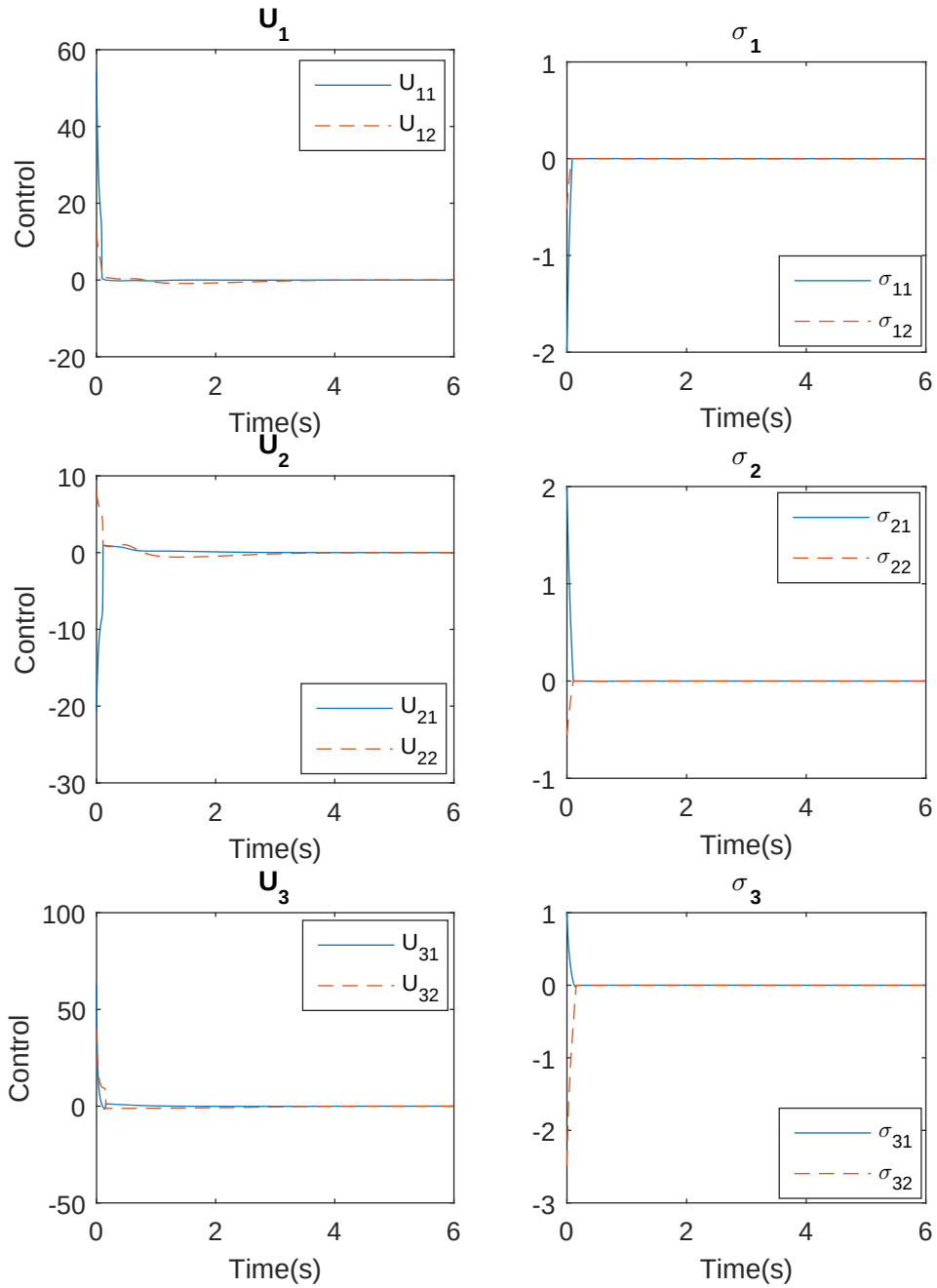

Figure 7.2: Time response of control signals (left) and sliding functions (right).

CHAPTER. 8

DECENTRALISED CONTROL FOR LARGE-SCALE SYSTEMS WITH UNCERTAINTIES IN INPUT DISTRIBUTION

The research on systems with uncertainties in input distribution is limited since such uncertainties often affect the systems through the input signals, which makes the attenuation of such uncertainties very challenging in the large-scale systems. In this chapter, a class of nonlinear system with uncertainties in input distribution is considered, and strategy based on sliding mode techniques is developed in the presence of uncertain interconnections. After a brief review of related work in Section 8.1, the problem is rigorously formulated in Section 8.2. The corresponding control design is separated which is given in Section 8.3 and 8.4 regarding the stability of the sliding mode and reachability of decentralised control respectively. After the case study on a 3D vehicle-following system in Section 8.5, a summary of this chapter is presented in Section 8.6.

8.1. Introduction

For practical systems, it is well known that uncertainties or modelling errors may seriously affect control system performance. In large-scale interconnected systems, the effect of uncertainties on the whole system is even more challenging. To be specific, uncertainties experienced by a subsystem will affect not only its own performance but also the other subsystems through the interactions between subsystems. Thus designing a decentralised control scheme to reject or reduce the effect of uncertainties in the interconnection terms is challenging. As discussed in Section 3.2 in Chapter 3, SMC has been recognised as a robust approach in dealing with nonlinear systems with uncertainties [17] owing to its unique structure and complete robustness against matched uncertainties [16, 17]. In [28], it is shown that the sliding mode approach can be used to deal with the systems in the presence of unmatched uncertainty. Methods proposed by Niu in [26] and [27] also show the strong robustness of SMC for uncertain systems. Therefore, many researchers have tried to develop a decentralised SMC strategy for large-scale interconnected systems in the presence of uncertainties and interconnections. However, as the information available to the controllers of each subsystem is limited in a decentralised strategy, it is difficult to reject the uncertainties within the interconnections even if they are matched [159].

For robust decentralised controller design problems, many results have been obtained using various methods. In [22, 23, 24, 25], robust control strategy is used for interconnected systems. However, only matched uncertainties are considered, and the bounds on the matched uncertainties are assumed to be linear or polynomial. In [28], mismatched uncertainties are considered with centralised dynamical feedback controllers which need more resources to exchange information between subsystems. In [98], a decentralised state feedback controller is proposed for systems with a class of constraints called integral quadratic constraints to limit the structure of the original system. In some cases, adaptive techniques are applied to estimate an upper bound on the mismatched uncertainty, and this is used in control design to counteract the effects of uncertainty [99]. This approach is powerful for the case where the uncertainty satisfies a linear growth condition. Regarding mismatched uncertainties, it is inevitable to impose some limitations to achieve asymptotic stability. After transforming the system into a special triangular structure, the uncertainties of the system in [100] have more general forms when compared with previous work. For uncertainties in input distribution, the existing research

is limited. In [26] and [27], SMC design is proposed for systems with uncertainties in the control matrix. However, the uncertainties in [26, 27] are assumed to have a particular structure, for example, the uncertainty is required to lie in the range of the control input distribution matrix. In most previous work, the nominal part of the system is usually assumed to be linear, which limits the application of the obtained results. In [160], a decentralised quantitative feedback control is proposed for a class of large-scale systems in the presence of uncertainties in the state-space matrices, and the work has also been implemented on a selective compliance assembly robot arm system. However, both the nominal part of the system and the interconnection between subsystem are assumed to be linear. In [161], a robust nonlinear output feedback control is proposed for a class of nonlinear time-delay interconnected systems with complete nonlinear nominal isolated subsystems. With artificial interconnections, the real interconnections are separated into an accessible part and an inaccessible part to reduce conservatism. The conditions for this method are relatively strong which can be relaxed when a state feedback control system is considered.

In this chapter, a nonlinear decentralised control strategy for a class of nonlinear interconnected systems is proposed based on a SMC paradigm. Compared with the results in Chapter 6, the interconnected system is assumed to be fully nonlinear with unknown interconnections and uncertainties in input distribution term. Moreover, the uncertainties are assumed to be bounded by known functions which are employed in the control design to counteract the effects of the uncertainties in the controlled interconnected system. The bounds on the uncertainties take more general forms when compared with existing work. A set of sufficient conditions is developed such that the corresponding sliding motion is asymptotically stable when the system is restricted to the designed sliding surface. Then, a decentralised SMC is designed to drive the interconnected system to the sliding surface in the presence of uncertainties. It is also shown that if the uncertainties/interconnections possess a superposition property, a decentralised control scheme may be designed to counteract the effect of the uncertainty. The developed results are applied to a vehicle-following system in automated highway system with both longitudinal and lateral controllers. Since the proposed controller for each vehicle does not require data transmission from the other vehicles, the proposed method is more reliable than a centralised method or networked control. The simulation results show that the proposed method is effective as expected.

8.2. System Description

Consider a class of nonlinear large-scale interconnected systems composed of $\mathcal{N}$ subsystems where the i-th subsystem can be transformed or described by

$$\dot{x}_i^a = f_i^a(t, x_i) + \psi_i^a(t, x) \tag{8.1}$$

$$\dot{x}_i^b = f_i^b(t, x_i) + (g_i(t, x_i) + \tilde{g}_i(t, x_i))u_i + \psi_i^b(t, x) \tag{8.2}$$

where the state variables of the i-th subsystem are represented by $x_i := \text{col}(x_i^a, x_i^b) \subset \Omega_i \in \mathcal{R}^{n_i}$ where $x_i^a \in \mathcal{R}^{n_i - m_i}$, $x_i^b \in \mathcal{R}^{m_i}$ and $x = \text{col}(x_1, x_2, \ldots, x_N)$. $u_i \in \mathcal{R}^{m_i}$ denote inputs of the i-th subsystem respectively for $i = 1, 2, \ldots, N$. The function $f_i^a(\cdot)$, $f_i^b(\cdot)$ with $f_i^a(t, 0) = 0$ and $f_i^b(t, 0) = 0$ and the function matrix $g_i(\cdot)$ are continuous and nonsingular for all $x_i \in \mathcal{R}^{n_i}$ with appropriate dimensions. Uncertainty in input distribution is denoted by $\tilde{g}_i(t, x_i)$. The nonlinear functions $\psi_i^a(t, x) \in \mathcal{R}^{n_i - m_i}$ and $\psi_i^b(t, x) \in \mathcal{R}^{m_i}$ represents the uncertain interconnection and mismatched uncertainties. It is assumed that all the nonlinear functions are sufficiently smooth such that the unforced system has a unique continuous solution.

The existence of the transformation $T_i(t, x_i)$ to transfer system

$$\dot{x}_i = \hat{f}_i(t, x_i) + \hat{g}_i(t, x_i)u_i$$

into the form of system (8.1)-(8.2), which is equivalent to the existence of the solution of equation

$$w_i(t, x_i)\hat{g}_i(t, x_i) = 0, \quad j = 1, 2, \ldots, n_i - m_i$$

where

$$w_i(t, x_i) = \frac{\partial T_i}{x_i^a}, \quad j = 1, 2, \ldots, n_i - m_i$$

which can be checked by the Frobeninus Theorem [32].

In this chapter, the focus is to design a decentralised control scheme to stabilise system (8.1)-(8.2) under the assumptions that the isolated nominal system has the desired performance. The following basic assumptions are imposed on the uncertainties of the system (8.1)-(8.2).

Assumption 8.1. There exists known continuous nondecreasing function $\delta_{ij}^a(\cdot)$ in $\mathcal{R}^+$ with $\delta_{ij}^a(t, 0) = 0$, and known continuous functions $\delta_i^b(\cdot)$ and $\rho_i(\cdot)$ such that

(i) $\|\psi_i^a(t, x)\| \leq \sum_{j=1}^{n} \delta_{ij}^a(\|x_j\|)$ (8.3)

(ii) $\left\|\psi_i^b(t,x)\right\| \leq \delta_i^b(t,x)$ (8.4)

(iii) $\|\tilde{g}_i(t,x_i)\| \leq \rho_i(t,x_i)$ (8.5)

for all $t \in \mathcal{R}^+$, $x_i \in \Omega_i$.

Remark 8.1. *Assumption 8.1 is a limitation on all the uncertainties experienced by the system. It is required that bounds on the uncertainties are known and the bounds will be employed in the control design to reject or reduce the effects caused by the uncertainties. It should be pointed out that only uncertainties $\psi_i^a(\cdot)$ are required to vanish at the origin. The form of the bounds is more general comparing with existing work (e.g. see [22, 23, 24, 25]).*

Assumption 8.2. There exist a constant α_i with $0 \leq \alpha_i < \frac{2}{\sqrt{n_i}}$ such that the uncertainty $\tilde{g}_i(t,x_i)$ with the input distribution $g_i(t,x_i)$ of system (8.1)-(8.2) satisfies

$$\tilde{g}_i(t,x_i)g_i^{-1}(t,x_i) + \left(g_i^{-1}(t,x_i)\right)^\tau \tilde{g}_i^\tau(t,x_i) + \alpha_i I_m \geq 0 \tag{8.6}$$

for all $t \in \mathcal{R}^+$, $x_i \in \Omega_i$.

Remark 8.2. *Assumption 8.2 is made on the uncertainties in input distribution term. It will be shown that a class of uncertainties in input distribution can be rejected by designing an appropriate control. Comparing with existing work, e.g. see [26, 27, 160], the uncertainties in input distribution are nonlinear instead of linear. It is emphasised that the uncertainties $\tilde{g}_i(\cdot)$ are not required to be matched, and only $g_i^b(\cdot)$ is required to be nonsingular for $t \in \mathcal{R}^+$, $x_i \in \Omega_i$.*

Since $\tilde{g}_i(t,x_i)$ are the uncertainties in input distribution, their effects are closely related to the control signal u_i for $i = 1, 2, \ldots, N$. This can be seen from the terms $\tilde{g}_i(t,x_i)u_i$ in system (8.2). Therefore, the uncertainties existing in input distribution make the control design much more difficult. This chapter will present an approach to deal with nonlinear uncertainties in input distribution when the input distribution is nonlinear.

Lemma 8.1. *For any square matrix $A \in \mathcal{R}^{n\times n}$ and vector $\xi = \mathrm{col}(\xi_1, \xi_2, \ldots, \xi_n) \in \mathcal{R}^n$, if there exists a non-negative scalar h such that*

$$A^\tau + A + hI_n \geq 0 \tag{8.7}$$

then

$$\xi^\tau A\mathrm{sgn}(\xi) \geq -\frac{h\sqrt{n}}{2}\|\xi\| \tag{8.8}$$

Proof. The proof is based on three different cases of the vector ξ.

(i). If $\xi = 0$, then $\text{sgn}(\xi) = 0$. Thus it is straightforward to see that

$$\xi^\tau A\text{sgn}(\xi) = 0 \tag{8.9}$$

Hence (8.8) holds.

(ii). Assume that $\min\{|\xi_1|, |\xi_2|, \ldots, |\xi_3|\} > 0$. Then by definition of the function $\text{sgn}(\xi)$,

$$\text{sgn}(\xi) = \begin{bmatrix} \text{sgn}(\xi_1) \\ \text{sgn}(\xi_2) \\ \vdots \\ \text{sgn}(\xi_n) \end{bmatrix} = \begin{bmatrix} \frac{\xi_1}{|\xi_1|} \\ \frac{\xi_2}{|\xi_2|} \\ \vdots \\ \frac{\xi_n}{|\xi_n|} \end{bmatrix} = R\xi \tag{8.10}$$

where

$$R = \begin{bmatrix} \frac{1}{|\xi_1|} & 0 & \cdots & 0 \\ 0 & \frac{1}{|\xi_2|} & & 0 \\ \vdots & & \ddots & \cdots \\ 0 & \cdots & & \frac{1}{|\xi_n|} \end{bmatrix}$$

If condition (8.7) holds, then from $R \geq \lambda_{\min}(R)I_n$,

$$RA^\tau + AR + hR \geq \lambda_{\min}(R)(A^\tau + A + hI_n) \geq 0 \tag{8.11}$$

which implies

$$RA^\tau + AR \geq -hR \tag{8.12}$$

then from (8.12)

$$\begin{aligned} \xi^\tau A\text{sgn}(\xi) =& \xi^\tau AR\xi = \frac{1}{2}\xi^\tau(RA^\tau + AR)\xi \\ \geq& -\frac{h}{2}\xi^\tau R\xi = -\frac{h}{2}\xi^\tau\text{sgn}(\xi) = -\frac{h}{2}\sum_{i=1}^{n}\xi_i\text{sgn}(\xi_i) \\ =& -\frac{h}{2}\sum_{i=1}^{n}|\xi_i| \geq -\frac{h}{2}\sqrt{n}\sqrt{\sum_{i=1}^{n}\xi_i^2} = -\frac{h\sqrt{n}}{2}\|\xi\| \end{aligned} \tag{8.13}$$

(iii). For the case that some elements of the vector ξ equals to 0, without loss of generality, assume that $\xi_{k+1}, \xi_{k+2}, \ldots, \xi_n = 0$ with $0 < k < n$, then by the definition of the $\text{sgn}(\cdot)$,

$\text{sgn}(\xi_{k+1}), \text{sgn}(\xi_{k+2}), \ldots, \text{sgn}(\xi_n) = 0$. Let a_{ij} denotes the element in i-th row and j-th column of the matrix A, then

$$\begin{aligned}\xi^\tau A\text{sgn}(\xi) &= \sum_{i=1}^{n}\sum_{j=1}^{n} a_{ij}\xi_i\text{sgn}(\xi_j) \\ &= \sum_{i=1}^{k}\sum_{j=1}^{k} a_{ij}\xi_i\text{sgn}(\xi_j) \end{aligned} \tag{8.14}$$

By similar reasoning as in (8.16), it is straightforward to see that

$$\xi^\tau A\text{sgn}(\xi) = \sum_{i=1}^{k}\sum_{j=1}^{k} a_{ij}\xi_i\text{sgn}(\xi_j) \geq -\frac{h\sqrt{k}}{2}\|\tilde{\xi}\| \geq -\frac{h\sqrt{n}}{2}\|\xi\| \tag{8.15}$$

where $\tilde{\xi} \in \mathcal{R}^k$ with $\tilde{\xi} = \text{col}(\xi_1, \xi_2, \ldots, \xi_k)$. Thus from (i)-(iii) above, it follows that for all $\xi \in \mathcal{R}^n$,

$$\xi^\tau A\text{sgn}(\xi) \geq -\frac{h\sqrt{n}}{2}\|\xi\| \tag{8.16}$$

Hence the conclusion follows. ■

8.3. Stability Analysis of the Sliding Mode

Choose the sliding function $\sigma_i(x)$ for the i-th subsystem as follows:

$$\sigma_i(x_i) = x_i^b + \varphi_i(x_i^a), \quad i = 1, 2, \ldots, N. \tag{8.17}$$

where $\varphi_i(\cdot)$ is a known Frechet-differentiable function with $\tilde{g}_i(0) = 0$ satisfy

$$M_{\tilde{g}_i}(\xi)(M_{\tilde{g}_i}(\xi))^\tau \leq \beta_i I_m \quad \forall \xi \in \mathcal{R}^{n_i - m_i} \tag{8.18}$$

where $M_{\tilde{g}_i}(\cdot) \in \mathcal{R}^{m_i \times (n_i - m_i)}$ represent the Jacobian matrix of function $\tilde{g}_i(\cdot)$, and β_i is a positive constant.

Choose the composite sliding surface for the interconnected system as (8.1)-(8.2) is chosen as

$$\sigma(x) = 0 \tag{8.19}$$

where $\sigma(x) \equiv: \text{col}\,(\sigma_1(x_1), \sigma_2(x_2), \ldots, \sigma_N(x_N))$. During sliding motion, $\sigma_i(x_i) = 0$ for $i = 1, 2, \ldots, N$, the sliding mode dynamics for the system (8.1)-(8.2) associated with the designed sliding surface (8.19) can be described by

$$\dot{x}_i^a = f_i^s(t, x_i^a) + \psi_i^s(t, x_1^a, x_2^a, \ldots, x_N^a) \tag{8.20}$$

where

$$f_i^s(t, x_i^a) := f_i^a(t, x_i)|_{x_i^b = -\varphi_i(x_i^a)} \tag{8.21}$$

and

$$\psi_i^s(t, x_1^a, x_2^a, \ldots, x_N^a) := \psi_i^a(t, x)|_{x_j^b = -\varphi_j(x_j^a), j=1,2,\ldots,N} \tag{8.22}$$

for $i = 1, 2, \ldots, N$ with $\psi_i^a(t, x)$ defined in (8.1).

From Lemma 7.1, it is straightforward to be verified that

$$\|\psi_i^s(t, x_1^a, x_2^a, \ldots, x_N^a)\| \leq \sum_{j=1}^{N} \delta_{ij}^s(\|x_j^a\|) \tag{8.23}$$

where

$$\delta_{ij}^s(\|x_j^a\|) = \delta_{ij}^a(\sqrt{1+\beta_i}\|x_j^a\|)$$

where $\delta_{ij}^a(\cdot)$ are defined in (8.3).

Assumption 8.3. There exist continuous $\mathcal{C}^1$ function $V_i : \mathcal{R}^+ \times \mathcal{R}^{n_i - m_i} \to \mathcal{R}^+$ and functions $\varsigma_{i1}(\cdot)$, $\varsigma_{i2}(\cdot)$, $\varsigma_{i3}(\cdot)$ and $\varsigma_{i4}(\cdot)$ of class $\mathcal{K}$ such that for all $x_i \in \Omega_i$ and $t \in \mathcal{R}^+$

(i) $$\varsigma_{i1}(\|x_i^a\|) \leq V_i(t, x_i^a) \leq \varsigma_{i2}(\|x_i^a\|)$$

(ii) $$\frac{\partial V_i(t, x_i^a)}{\partial t} + \frac{\partial V_i(t, x_i^a)}{\partial x_i^a} f_i^s(t, x_i^a) \leq -\varsigma_{i3}^2(\|x_i^a\|)$$

(iii) $$\left\| \frac{\partial V_i(t, x_i^a)}{\partial x_i^a} \right\| \leq \varsigma_{i4}(\|x_i^a\|)$$

where

$$\frac{\partial V_i(t, x_i^a)}{\partial x_i^a} = \left(\frac{\partial V_i(t, x_i^a)}{\partial x_1^a}, \frac{\partial V_i(t, x_i^a)}{\partial x_2^a} \cdots \frac{\partial V_i(t, x_i^a)}{\partial x_n^a} \right)$$

Remark 8.3. *Assumption 8.3 is a limitation on the function $f_i^a(\cdot)$. From Lyapunov function theorem in Section 2.1 in Chapter 2, it implies that the system*

$$\dot{x}_i^a = f_i^s(t, x_i^a)$$

is asymptotically stable with Lyapunov function $V_i(\cdot)$ for $i = 1, 2, \ldots, N$.

Theorem 8.1. *Under Assumptions 8.1 and 8.3, the sliding mode (8.20) of the system (8.1)-(8.2) associated with the sliding surface in (8.19) is asymptotically stable if there exists a domain Ω_{x^a} of the origin in $x^a \in \mathcal{R}^{\sum_i^N (n_i - m_i)}$ such that*

$$M(t, x)^T + M(t, x) > 0$$

in domain $\Omega_{x^a}\backslash\{0\}$ *with* $M(t,x) = (m_{ij}(t,x_i,x_j))_{N\times N}$ *and for* $i,j = 1,2,\ldots,N$

$$m_{ij}(t,x_i,x_j) = \begin{cases} \mu_{i3}(\|x_i^a\|) - \mu_{i4}(\|x_i^a\|)\gamma_{ii}(\|x_i^a\|), & i = j \\ -\mu_{i4}(\|x_i^a\|)\gamma_{ij}(\|x_j^a\|), & i \neq j \end{cases}$$

where $\mu_{i3}(\cdot)$*,* $\mu_{i4}(\cdot)$ *and* $\gamma_{ij}(\cdot)$ *are defined respectively by*

$$\mu_{i3}(x) = \int_0^1 \frac{\partial \varsigma_{i3}(x\tau)}{\partial \tau}\mathrm{d}\tau \tag{8.24}$$

$$\mu_{i4}(x) = \int_0^1 \frac{\partial \varsigma_{i4}(x\tau)}{\partial \tau}\mathrm{d}\tau \tag{8.25}$$

$$\gamma_{ij}(x) = \int_0^1 \frac{\partial \delta_{ij}^s(x\tau)}{\partial \tau}\mathrm{d}\tau \tag{8.26}$$

Proof. From (8.24)-(8.26), it can be observered that

$$\varsigma_{i3}(\|x_i^a\|) = \mu_{i3}(\|x_i^a\|)\|x_i^a\| \tag{8.27}$$

$$\varsigma_{i4}(\|x_i^a\|) = \mu_{i4}(\|x_i^a\|)\|x_i^a\| \tag{8.28}$$

$$\delta_{ij}^s(\|x_i^a\|) = \gamma_{ij}(\|x_i^a\|)\|x_i^a\| \tag{8.29}$$

From the analysis above, it is seen that the system (8.20) represents the sliding mode dynamics of the system (8.1)-(8.2) corresponding to the sliding surface (8.19).

For system (8.20), consider the Lyapunov function candidate

$$V(t,x_i^a) = \sum_{i=1}^N V_i(t,x_i^a) \tag{8.30}$$

where $V_i(t,x_i^a)$ is given by Assumption 8.3. Then, the time derivative of $V(t,x_i^a)$ along equation (8.20) is given by

$$\begin{aligned}
\dot{V} =& \sum_{i=1}^N \Big\{ \frac{\partial V_i(t,x_i^a)}{\partial t} + \frac{\partial V_i(t,x_i^a)}{\partial x_i^a} f_i^s(t,x_i^a) + \frac{\partial V_i(t,x_i^a)}{\partial x_i^a}\psi_i^a(t,x) \Big\} \\
\leq& \sum_{i=1}^N \Big\{ -\varsigma_{i3}^2(\|x_i^a\|) + \varsigma_{i4}(\|x_i^a\|)\sum_{j=1}^N \delta_{ij}^s(\|x_j^a\|) \Big\} \\
=& -\sum_{i=1}^N \mu_{i3}^2(\|x_i^a\|)\|x_i^a\|^2 + \sum_{i=1}^N\sum_{j=1}^N \mu_{i4}(\|x_i^a\|)\gamma_{ij}(\|x_j^a\|)\|x_i^a\|\|x_j^a\| \\
=& -\frac{1}{2}(\|x_1^a\|,\|x_2^a\|,\ldots,\|x_N^a\|)\left(M^T + M\right)\begin{pmatrix} \|x_1^a\| \\ \|x_2^a\| \\ \vdots \\ \|x_N^a\| \end{pmatrix}
\end{aligned}$$

Since the matrix function $M^T + M$ in $\Omega_{x^a}\backslash\{0\}$ is positive definite, therefore, it follows that V is a negative definite function in Domain Ω_{x^a}. Hence, the results follow. ■

8.4. Decentralised Control Design

For the nonlinear interconnected system (8.1)-(8.2), the corresponding reachability condition is described by (e.g. see [113, 47])

$$\sum_{i=1}^{N} \frac{\sigma_i^{\tau}(x_i)\dot{\sigma}_i(x_i)}{\|\sigma_i(x_i)\|} < 0 \tag{8.31}$$

where $\sigma_i(x_i)$ is defined in (8.17). In order to reduce the effects of the unknown interconnection $\psi_i^b(\cdot)$, consider the expression

$$\delta_i^b(t,x) = \sum_{j=1}^{N} \eta_{ij}(t,x_j) + \nu_i(t,x) \tag{8.32}$$

where δ_i^b is defined in (8.4) and $\nu_i(t,x)$ represents all the coupling terms which cannot be included in the term $\sum_{j=1}^{N} \eta_{ij}(t,x_j)$

Remark 8.4. *The decomposition in (8.32) is not unique and is introduced to reduce the conservatism caused by the interconnection terms within the control design. There is no general way to obtain the decomposition. The first interconnection term $\sum_{j=1}^{N} \eta_{ij}(t,x_j)$ has a superposition property. It will be shown that the term $\sum_{j=1}^{N} \eta_{ij}(\cdot)$ in (8.32) can be rejected by selection of an appropriate decentralised control and this will reduce conservatism. The second term, $\nu_i(\cdot)$ in (8.32), cannot be rejected by the choice of decentralised control.*

The objective is to design a decentralised sliding mode controller such that the reachability condition (8.31) is satisfied. Consider the decentralised control

$$u_i = -\, g_i^{-1}(t,x_i)\mathcal{F}_i - g_i^{-1}(t,x_i)\mathrm{sgn}(\sigma_i(x_i))\Big\{\frac{2}{2-\alpha_i\sqrt{n_i}}\mathcal{W}(t,x_i) + \zeta_i(t,x_i)\Big\} \tag{8.33}$$

where

$$\begin{aligned}
\mathcal{F}_i(t,x_i) =& \frac{\partial \varphi_i}{\partial x_i^a} f_i^a(t,x_i) + f_i^b(t,x_i) \\
\mathcal{W}_i(t,x_i) =& \sum_{j=1}^{N} \sqrt{\beta_j}\delta_{ji}^a(\|x_i\|) + \sum_{j=1}^{N} \eta_{ji}(t,x_i) + \|g_i^{-1}(t,x_i)\mathcal{F}_i(t,x_i)\|\rho_i(t,x_i)
\end{aligned} \tag{8.34}$$

and $\rho_i(t, x_i)$ are defined in Assumption 8.1, and $\eta_{ji}(t, x_i)$ satisfy (8.32). The term $\zeta_i(t, x_i)$ is a reachability function which can be considered as a design parameter to be defined.

Theorem 8.2. *Consider the nonlinear interconnected system (8.1) and (8.2). Under Assumptions 1-3, the closed-loop system (8.1)-(8.2) with the decentralised control (8.33) is converged to the composite sliding surface (8.19) and maintain a sliding motion on it thereafter if there exits positive constant ϵ in the considered domain $\Omega = \Omega_1 \times \Omega_2 \cdots \times \Omega_N$ such that the functions $\zeta_i(t, x_i)$ in (8.33) satisfy*

$$\sum_{i=1}^{N}(1 - \frac{\alpha_i\sqrt{n_i}}{2})\zeta_i(t, x_i) > \sum_{i=1}^{N}\nu_i(t, x) \tag{8.35}$$

in Ω for all $t > 0$ with $\nu_i(t, x)$ defined in (8.32).

Proof. From the analysis above, all that needs to be proved is that the composite reachability condition (8.31) is satisfied. From (8.17), for $i = 1, 2, \ldots, N$

$$\begin{aligned}\dot{\sigma}_i(x_i) =& \frac{\partial\varphi_i}{\partial x_i^a} f_i^a(t, x_i) + f_i^b(t, x_i) + \frac{\partial\varphi_i}{\partial x_i^a}\psi_i^a(t, x) + \psi_i^b(t, x) \\ &+ (g_i(t, x_i) + \tilde{g}_i(t, x_i))u_i \end{aligned} \tag{8.36}$$

Substituting (8.33) into (8.36),

$$\begin{aligned}&\sum_{i=1}^{N}\frac{\sigma_i^\tau(x_i)\dot{\sigma}_i(x_i)}{\|\sigma_i(x_i)\|} \\ &= \sum_{i=1}^{N}\Big\{\frac{\sigma_i^\tau(x_i)}{\|\sigma_i(x_i)\|}\{\frac{\partial\varphi_i}{\partial x_i^a}\psi_i^a(t, x) + \psi_i^b(t, x) - \tilde{g}_i(t, x_i)g_i^{-1}(t, x_i)\mathcal{F}_i(t, x_i)\} \\ &\quad - \frac{\sigma_i^\tau(x_i)}{\|\sigma_i(x_i)\|}\tilde{g}_i(t, x_i)g_i^{-1}(t, x_i)\mathrm{sgn}(\sigma_i(x_i))\left(\frac{2}{2 - \alpha_i\sqrt{n_i}}\mathcal{W}_i(t, x_i) + \zeta_i(t, x_i)\right) \\ &\quad - \frac{\alpha_i\sqrt{n_i}}{2 - \alpha_i\sqrt{n_i}}\mathcal{W}_i(t, x_i) - \mathcal{W}_i(t, x_i) - \zeta_i(t, x_i)\Big\} \\ &\le \sum_{i=1}^{N}\|\tilde{g}_i(t, x_i)g_i^{-1}(t, x_i)\mathcal{F}_i(t, x_i)\| + \sum_{i=1}^{N}\|\psi_i^b(t, x)\| + \sum_{i=1}^{N}\left\|\frac{\partial\varphi_i}{\partial x_i^a}\psi_i^a(t, x)\right\| \\ &\quad - \sum_{i=1}^{N}\frac{\sigma_i^\tau(x_i)}{\|\sigma_i(x_i)\|}\tilde{g}_i(t, x_i)g_i^{-1}(t, x_i)\mathrm{sgn}(\sigma_i(x_i))\left(\frac{2}{2 - \alpha_i\sqrt{n_i}}\mathcal{W}_i(t, x_i) + \zeta_i(t, x_i)\right) \\ &\quad - \sum_{i=1}^{N}\sum_{j=1}^{N}\sqrt{\beta_j}\delta_{ji}^a(\|x_i\|) - \sum_{i=1}^{N}\sum_{j=1}^{N}\mu_{ji}(t, x_i) - \sum_{i=1}^{N}\|g_i^{-1}(t, x_i)\mathcal{F}_i(t, x_i)\|\rho_i(t, x_i) \\ &\quad - \sum_{i=1}^{N}\frac{\alpha_i\sqrt{n_i}}{2 - \alpha_i\sqrt{n_i}}\mathcal{W}_i(t, x_i) - \sum_{i=1}^{N}\zeta_i(t, x_i)\end{aligned} \tag{8.37}$$

From Assumption 8.1,

$$\sum_{i=1}^{N} \|\frac{\partial \varphi_i}{\partial x_i^a}\psi_i^a(t,x)\| \leq \sum_{i=1}^{N}\sum_{j=1}^{N} \sqrt{\beta_i}\delta_{ij}^a(\|x_j\|) = \sum_{i=1}^{N}\sum_{j=1}^{N} \sqrt{\beta_j}\delta_{ji}^a(\|x_i\|) \tag{8.38}$$

$$\begin{aligned}\sum_{i=1}^{N} \|\psi_i^b(t,x)\| &\leq \sum_{i=1}^{N}\sum_{j=1}^{N} \mu_{ij}(t,x_j) + \sum_{i=1}^{N} \nu_i(t,x) \\ &= \sum_{i=1}^{N}\sum_{j=1}^{N} \mu_{ji}(t,x_i) + \sum_{i=1}^{N} \nu_i(t,x)\end{aligned} \tag{8.39}$$

$$\begin{aligned}\|\tilde{g}_i(t,x_i)g_i^{-1}(t,x_i)\mathcal{F}_i(t,x_i)\| &\leq \|\tilde{g}_i(t,x_i)\|\|g_i^{-1}(t,x_i)\mathcal{F}_i(t,x_i)\| \\ &\leq \|g_i^{-1}(t,x_i)\mathcal{F}_i(t,x_i)\|\rho_i(t,x_i)\end{aligned} \tag{8.40}$$

and from Assumption 8.2 and Lemma 8.1, for any positive scale h

$$\begin{aligned}\frac{h}{\|\sigma_i(x_i)\|}\sigma_i^{\mathcal{T}}(x_i)\tilde{g}_i(t,x_i)g_i^{-1}(t,x_i)\mathrm{sgn}(\sigma_i(x_i)) &\geq -\frac{h}{\|\sigma_i(x_i)\|}\cdot\frac{\alpha_i\sqrt{n_i}}{2}\|\sigma_i(x_i)\| \\ &= -\frac{\alpha_i\sqrt{n_i}}{2}\cdot h\end{aligned} \tag{8.41}$$

Substituting inequalities (8.38)-(8.41) into (8.37), implies

$$\begin{aligned}\sum_{i=1}^{N}\frac{\sigma_i^{\mathcal{T}}(x_i)\dot{\sigma}_i(x_i)}{\|\sigma_i(x_i)\|} &\leq \sum_{i=1}^{N}\frac{\alpha_i\sqrt{n_i}}{2-\alpha_i\sqrt{n_i}}\mathcal{W}_i(t,x_i) + \sum_{i=1}^{N}\frac{\alpha_i\sqrt{n_i}}{2}\zeta_i(t,x_i) \\ &\quad - \sum_{i=1}^{N}\frac{\alpha_i\sqrt{n_i}}{2-\alpha_i\sqrt{n_i}}\mathcal{W}_i(t,x_i) - \sum_{i=1}^{N}\zeta_i(t,x_i) + \sum_{i=1}^{N}\nu_i(t,x) \\ &= -\sum_{i=1}^{N}(1-\frac{\alpha_i\sqrt{n_i}}{2})\zeta_i(t,x_i) + \sum_{i=1}^{N}\nu_i(t,x) < 0\end{aligned} \tag{8.42}$$

Then the reachability condition (8.31) is satisfied. Hence, the result follows. ■

From SMC theory, Theorems 8.2 and 8.2 together guarantee that the system (8.1)-(8.2) is stabilized by the designed decentralised control (8.33).

Remark 8.5. *It should be pointed out that the developed results are suitable for fully nonlinear interconnected systems specifically with uncertainties in both the input distributions and interconnections. It is not required that the nominal isolated subsystem is either linearizable or partially linearizable.*

8.5. Case Study - Automated Highway Systems

In order to achieve high traffic flow rates and reduce congestion, an automated highway system has been developed [116]. The SMC of the longitudinal vehicle following system has been developed in [74]. In order to improve the feasibility of the system, it is necessary to consider both on-board lateral and longitudinal controllers during the automated driving process. Therefore, the stability and the robustness of the 3D vehicle-following system will be considered as a case study to demonstrate the theoretical results developed above.

Modelling of 3D car-following system

The kinematic model of the i-th vehicle under nonholonomic constraints (i.e. rolling without slipping) can be described by (e.g. see [162])

$$\begin{bmatrix} \dot{q}_{x_i} \\ \dot{q}_{y_i} \\ \dot{q}_{\theta_i} \end{bmatrix} = \begin{bmatrix} \cos(q_{\theta_i}) - \frac{\epsilon_i \tan\phi_i \sin(q_{\theta_i})}{l_i} \\ \sin(q_{\theta_i}) + \frac{\epsilon_i \tan\phi_i \cos(q_{\theta_i})}{l_i} \\ \frac{\tan\tilde{g}_i}{l_i} \end{bmatrix} v_i \tag{8.43}$$

where $(q_{x_i}, q_{y_i}, q_{\theta_i})$ denote the position of a point of the vehicle, and ϵ_i represents the distance between the position and the center of the real wheel center, see [163]. ϕ_i denotes the steering angle of the front inner wheel, which is bounded with $|\phi_i| \leq 0.691$ for $i = 1, 2, 3$ in common car design. l_i is the length between the rear and front shafts. v_i represents the linear velocity of the vehicle toward the heading direction with

$$v_i = r\tilde{\omega}_i$$

for rear wheel driving or

$$v_i = r\hat{\omega}_i \cos\phi_i$$

for front wheel driving where r represents the radius of the wheels, and $\tilde{\omega}_i$ and $\hat{\omega}_i$ denote the angular velocity of the rear shaft and the front inner wheel respectively.

Define $(q^f_{x_i}, q^f_{y_i}, q^f_{\theta_i})$ and $(q^r_{x_i}, q^r_{y_i}, q^r_{\theta_i})$ as the position of the front and rear edge of the vehicle respectively. From Fig.(8.1) , it is straightforward to see that the dynamic of the position $(q^f_{x_i}, q^f_{y_i}, q^f_{\theta_i})$ can be described by (8.43) with $\epsilon_i = b_i$, and the dynamic of the position $(q^r_{x_i}, q^r_{y_i}, q^r_{\theta_i})$ can be described by (8.43) with $\epsilon_i = -a_i$. Then, define the error coordinates

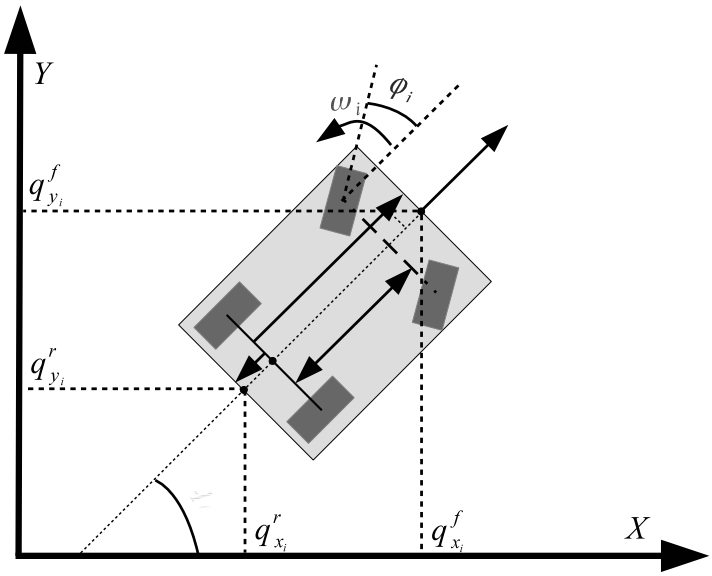

Figure 8.1: Model of the vehicle in Catersian Coordinate System

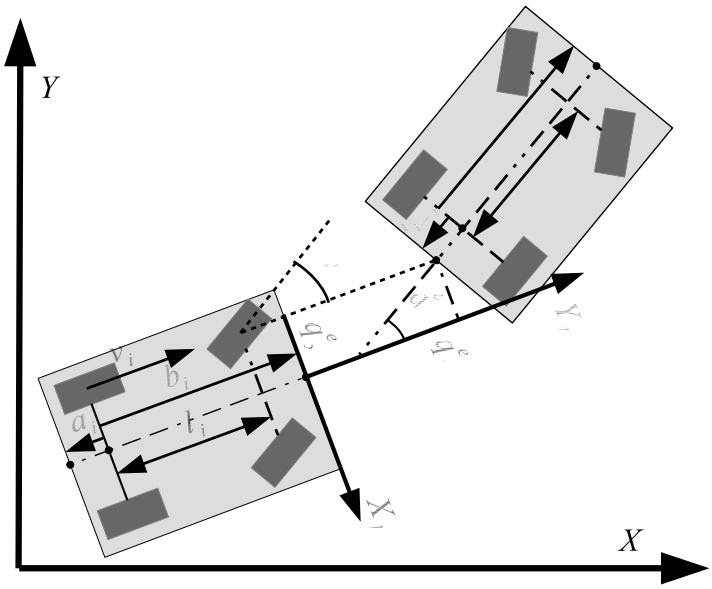

Figure 8.2: Model of error position between the i-th and $i(-1)$-th vehicles

$(q^e_{x_i}, q^e_{y_i}, q^e_{\theta_i})$ shown in Fig.8.2

$$\begin{bmatrix} q^e_{x_i} \\ q^e_{y_i} \\ q^e_{\theta_i} \end{bmatrix} = T_i \begin{bmatrix} q^r_{x_{i-1}} - q^f_{x_i} \\ q^r_{y_{i-1}} - q^f_{y_i} \\ q^r_{\theta_{i-1}} - q^f_{\theta_i} \end{bmatrix} \tag{8.44}$$

with local coordinate transformation matrix (e.g. see [164])

$$T_i = \begin{bmatrix} -\sin(q_{\theta_i}) & \cos(q_{\theta_i}) & 0 \\ \cos(q_{\theta_i}) & \sin(q_{\theta_i}) & 0 \\ 0 & 0 & 1 \end{bmatrix} \tag{8.45}$$

Then the kinematic model of the 3D car-following system can be described by

$$\begin{bmatrix} \dot{q}^e_{x_i} \\ \dot{q}^e_{y_i} \\ \dot{q}^e_{\theta_i} \end{bmatrix} = \begin{bmatrix} v_{(i-1)} \sin x_{i3} - l^{-1}_{i-1} a_{i-1} v_{i-1} \tan\phi_{i-1} \cos q^e_{\theta_{i-1}} \\ v_{(i-1)} \cos x_{i3} + l^{-1}_{i-1} a_{i-1} v_{i-1} \tan\phi_{i-1} \sin q^e_{\theta_{i-1}} \\ l^{-1}_{i-1} v_{i-1} \tan\phi_{i-1} \end{bmatrix}$$

$$+ \begin{bmatrix} -l^{-1}_i (b_i + q^e_{x_i}) v_i \tan\phi_i \\ l^{-1}_i q^e_{x_i} v_i \tan\phi_i - v_i \\ -l^{-1}_i v_i \tan\phi_i \end{bmatrix} \tag{8.46}$$

In the 3D car-following system proposed in this chapter, the main objective is to control each vehicle moving at desired velocity with pre-defined safe distance apart for other vehicles in the system. Assume that the vehicle is driving safely which does not slip laterally, and each tire share the same parameters, then, the dynamic model of the velocity v_i and steering angle ϕ_i can be simplified from [165] and described by

$$\begin{bmatrix} \dot{v}_i \\ \dot{\phi}_i \end{bmatrix} = \begin{bmatrix} \frac{\cos\phi_i F^{fy}_i - \sin\phi_i F^{fx}_i + F^{ry}_i}{m_i} \\ \omega_i \end{bmatrix} \tag{8.47}$$

where m_i and ω_i denotes the mass of the vehicle and steering velocity of the front inner wheel respectively. F^{fy}_i and F^{ry}_i denote the longitudinal driving force from the front wheels and rear wheels respectively and F^{fx}_i denote the lateral force of the front wheels which is unknown and can be calculated by (e.g. see [166])

$$F^{fx}_i = C^f_i (\phi - \frac{\tilde{l}_i \tan\phi}{l_i})$$

where C^f_i denotes the lateral tire stiffness and $\tilde{l}_i$ denote the distance between the front shaft and the central mass of the vehicle.

As in [157], a safety distance frequently used in automated highway systems based on the Time-Headway policy (CTH) is used in this design. The safety distance defined by the CTH policy is described by (e.g. see [157])

$$\xi_{d_i}(v_i) = \xi_{d0} + t_s v_i \tag{8.48}$$

where ξ_{d0} is the distance between stationary vehicles, and t_s is the so-called headway time. Then the objective of the vehicle-following system is equivalent to stabilize the error position $(q^e_{x_i}, q^e_{y_i}, q^e_{\theta_i})$ at the equilibrium point $(0, \xi_{d_i}(v_i), 0)$ with constant velocity v_0 and safety distance $\xi_{d_i}(v_i)$ given by the corresponding highway policy.

Simulation

Let $x_{i1} = q^e_{x_i}$, $x_{i2} = q^e_{y_i} - t_s v_0$, $x_{i3} = q^e_{\theta_i}$, $x_{i4} = v_i - v_0$ and $x_{i5} = \phi_i$, and define

$$Q_i(t, x_i) = l_i^{-1}(x_{i4} + v_0) \tan x_{i5} \tag{8.49}$$

Then the vehicle-following system with three vehicles can be described by

$$\underbrace{\begin{bmatrix} \dot{x}_{i1} \\ \dot{x}_{i2} \\ \dot{x}_{i3} \end{bmatrix}}_{x_i^a} = \underbrace{\begin{bmatrix} (-b_i - t_s v_0 - x_{i2}) Q_i(t, x_i) + v_0 \sin x_{i3} \\ Q_i(t, x_i) x_{i1} + v_0 \cos x_{i3} - x_{i4} - v_0 \\ -Q_i(t, x_i) \end{bmatrix}}_{f_i^a(t, x_i)} + \psi_i^a(t, x) \tag{8.50}$$

$$\underbrace{\begin{bmatrix} \dot{x}_{i4} \\ \dot{x}_{i5} \end{bmatrix}}_{x_i^b} = \left(\underbrace{\begin{bmatrix} m_i^{-1} & 0 \\ 0 & 1 \end{bmatrix}}_{g_i(t, x_i)} + \tilde{g}_i(t, x_i) \right) u_i + \psi_i^b(t, x_i) \tag{8.51}$$

where $u = \mathrm{col}(F_i, \omega_i)$ where $F_i := F_i^{fy} \cos \phi_i + F_i^{ry}$ represent the overall longitudinal driving force and $Q_i(\cdot)$ is defined in (8.49) and the interconnection $\psi_i^a(t, x)$ with $\psi_1^a(t, x) = 0$ can be described by

$$\psi_i^a(t, x) = \begin{bmatrix} x_{(i-1)4} \sin x_{i3} - a_{i-1} Q_{i-1}(t, x_{i-1}) \cos x_{i3} \\ x_{(i-1)4} \cos x_{i3} + a_{i-1} Q_{i-1}(t, x_{i-1}) \sin x_{i3} \\ Q_{i-1}(t, x_{i-1}) \end{bmatrix} \tag{8.52}$$

for $i = 2, 3$. The corresponding parameters are chosen based on real vehicle model as shown in Table.8.1. Assume that the size of one vehicle is not known by the others, but the range of the corresponding parameters, i.e. a_i, b_i and l_i, are known, then it is straightforward to verify that

$$\|\psi_i^a(t, x)\| \leq \sqrt{x^2_{(i-1)4} + (1 + a^2_{i-1}) Q^2_{i-1}(t, x_{i-1})}$$

and assume the uncertain interconnections $\psi_i^b(t, x)$ for $i = 1, 2, 3$ satisfy

$$\|\psi_1^b(t, x)\| \leq \underbrace{0.292|x_{14} + 30.07| + 0.6x_{15}^2}_{\eta_{11}(t, x_1)} + \underbrace{0.2 \cos(x_{13})|x_{24} + v_0|}_{\nu_1(t, x)}$$

Table 8.1: Parameters of the vehicle-tracking system

i	a_i(m)	b_i(m)	l_i(m)	m_i(Kg)
1	0.565	3.149	2.467	1200
2	1.019	3.827	2.895	2160
3	1.016	3.614	2.699	1450

$$\|\psi_2^b(t,x)\| \leq \underbrace{0.12\|x_1^b\|}_{\eta_{21}(t,x_1)} + \underbrace{0.33|x_{24}+30.08| + 0.56x_{25}^2}_{\eta_{22}(t,x_2)}$$
$$+ \underbrace{0.8\cos(x_{23})\|x_1^b\| + 0.1\cos x_{33}|x_{24}+v_0|}_{\nu_2(t,x)}$$
$$\|\psi_3^b(t,x)\| \leq \underbrace{0.12\|x_2^b\|}_{\eta_{32}(t,x_2)} + \underbrace{0.35|x_{34}+30.05| + 0.4x_{35}^2}_{\eta_{33}(t,x_3)}$$

Furthermore, since the weight of the vehicle may be various because of uncertain load, and the steering velocity may also affected by other factors, e.g. the speed of the vehicle, the input distribution has uncertainty that may affect the control performance. Therefore, assume that the actual input distribution $\hat{g}_i(\cdot)$ is

$$\hat{g}_i(t,x_i) = \begin{bmatrix} -\frac{1}{\hat{m}_i} & \frac{\hat{k}_i(x_{i4}+v_0)}{\hat{m}_i} \\ 0 & 1 \end{bmatrix}$$

where $\hat{m}_i$ is the uncertain actual weight of the i-th vehicle with load, and $\hat{k}_i$ denotes the impact factor which reflects how the steering velocity of the front wheels ω_i affecting the driving force F_i. Then assume the uncertainties $\tilde{g}_i(\cdot)$ satisfy

$$\|\tilde{g}_1(t,x_1)\| \leq \underbrace{0.00055}_{\rho_1(t,x_1)}, \qquad \|\tilde{g}_2(t,x_2)\| \leq \underbrace{0.00031}_{\rho_2(t,x_2)}$$
$$\|\tilde{g}_3(t,x_3)\| \leq \underbrace{0.00046}_{\rho_2(t,X_3)}$$

with $\alpha_1 = 0.61$, $\alpha_2 = 0.65$ and $\alpha_3 = 0.63$ satisfy (8.6). It should be noted that due to the large mass of the vehicle, the uncertainty $\tilde{g}_i(\cdot)$ in (8.51) is relatively small, resulting that the bounds of the uncertainty ρ_i is relatively small. Since the high-speed following system is a physical system and the mass of each vehicle is relatively large. Therefore, for the simulation purpose, the maximus speed of all the vehicles in the system is limited within $40m/s$ (144 Km/h) and the

error angle $q^e_{\theta_i}$ is limited with $|q^e_{\theta_i}| \leq \frac{\pi}{4}$. Furthermore, it may not be measurable for too large longitudinal and lateral error distance $q^e_{x_i}$ and $q^e_{x_i}$ in pratical, e.g. the limitation of the stereo vision measurement technique. And assume the desired speed of the vehicles $v_0 = 30$m/s (108 Km/h), then the considered domain of the proposed vehicle-tracking system is

$$\begin{aligned} D_i = \{(x_{i1}, x_{i2}, x_{i3}, x_{i4}, x_{i5}) \quad & |x_{i1}| < 10, |x_{i2}| < 20, \\ & |x_{i3}| \leq \frac{\pi}{4}, -30 < x_{i4} \leq 10, |x_{i1}| \leq 0.691\} \end{aligned} \tag{8.53}$$

Now define the sliding function in the form of (8.17) with

$$\varphi_i(t, x_i) = \begin{bmatrix} -k_{i1}x_{i2} + v_0(1 - \cos x_{i3}) \\ -\tan^{-1} \frac{l_i(k_{i2}x_{i1} + v_0 \sin x_{i3})}{d_i(k_i x_{i2} + v_0 \cos x_{i3})} \end{bmatrix} \tag{8.54}$$

where d_i is a constant with $d_i = t_s v_0 + b_i$, k_{i1} and k_{i2} are design parameters with $k_{i1} = k_{i2} = 1$. Then it is straightforward to verify that

$$M_{\varphi_i}(x^a_i) M_{\varphi_i}(x^a_i)^\tau \leq \beta_i I_2$$

with $\beta_1 = 22.8$, $\beta_2 = 22.84$ and $\beta_3 = 22.82$.

When the system is on the sliding surface,

$$\|\psi^s_1(t, x)\| = 0 \tag{8.55}$$

$$\|\psi^s_2(t, x)\| \leq \underbrace{\underbrace{(13.9\sqrt{0.0001 + x^2_{13}} + 0.7)}_{\gamma_{21}(\|x^a_1\|)} \|x^a_1\|}_{\delta^s_{21}(\|x^a_1\|)} \tag{8.56}$$

$$\|\psi^s_3(t, x)\| \leq \underbrace{\underbrace{(13.6\sqrt{0.001 + x^2_{23}} + 0.84)}_{\gamma_{32}(\|x^a_2\|)} \|x^a_2\|}_{\delta^s_{32}(\|x^a_2\|)} \tag{8.57}$$

Choose the Lyapunov function candidate

$$V = \sum_{i=1}^{3} V_i \tag{8.58}$$

where

$$V_i = \frac{K_i}{2}(x^a_i)^\tau x^a_i, \quad i = 1, 2, 3 \tag{8.59}$$

with $K_1 = 1000$, $K_2 = 20$ and $K_3 = 0.05$. Then,

$$\underbrace{\frac{K_i}{3}\|x_i^a\|^2}_{\varsigma_{i1}} \leq V_i(t, x_i^a) \leq \underbrace{K_i\|x_i^a\|^2}_{\varsigma_{i2}}, \quad i = 1, 2, 3$$

Define $\varsigma_{i3}(\cdot)$ for $i = 1, 2, 3$ as

$$\varsigma_{13}(r) = \underbrace{K_1\sqrt{\frac{0.902\sin x_{13}}{x_{13}}}}_{\mu_{13}} r, \quad \varsigma_{23}(r) = \underbrace{K_2\sqrt{\frac{0.884\sin x_{23}}{x_{23}}}}_{\mu_{23}} r$$

$$\varsigma_{33}(r) = \underbrace{K_3\sqrt{\frac{0.89\sin x_{33}}{x_{33}}}}_{\mu_{33}} r$$

and $\varsigma_{i4}(\cdot)$ as

$$\varsigma_{i4}(r) = \underbrace{K_i}_{\mu_{i4}} r, \quad i = 1, 2, 3$$

By direct computation, it is straightforward to verify that

$$M(t, x) + M(t, x)^\tau > 0$$

in $D_1 \times D_2 \times D_3 \backslash \{0\}$. Thus the designed sliding mode are locally asymptotically stable in the considered domain.

From (8.33), the controller u_i for $i = 1, 2, 3$ are well defined with $\zeta_1 = 1 + 1.44\|x_1\|$, $\zeta_2 = 1 + 1.19\|x_2\|$ and $\zeta_3 = 1$ which guarantee the condition (8.35) in Theorem 8.2 is satisfied for $x \in D_1 \times D_2 \times D_3$. Therefore system (8.1)-(8.2) can be stabilised by the designed control.

The time response of the system states is shown in Fig.8.3, and the time response of the control inputs is shown in Fig.8.4.

From the simulation results, it can be seen that all three vehicles converge to the steady state within a reasonable time. From Fig.8.4, it can be seen that the control signals do not tends to zeros, which indicates that the vehicle systems are experiencing unvarnished uncertainties $\psi_i^b(\cdot)$. However, owing to the strong robustness of the SMC and the extra design for the uncertainties in input distribution, the stability of the overall system is barely affected, showing that the proposed approach is effective for system with uncertainties in input distribution. It should be noted that in the simulation, a boundary layer is used to reduce the chattering.

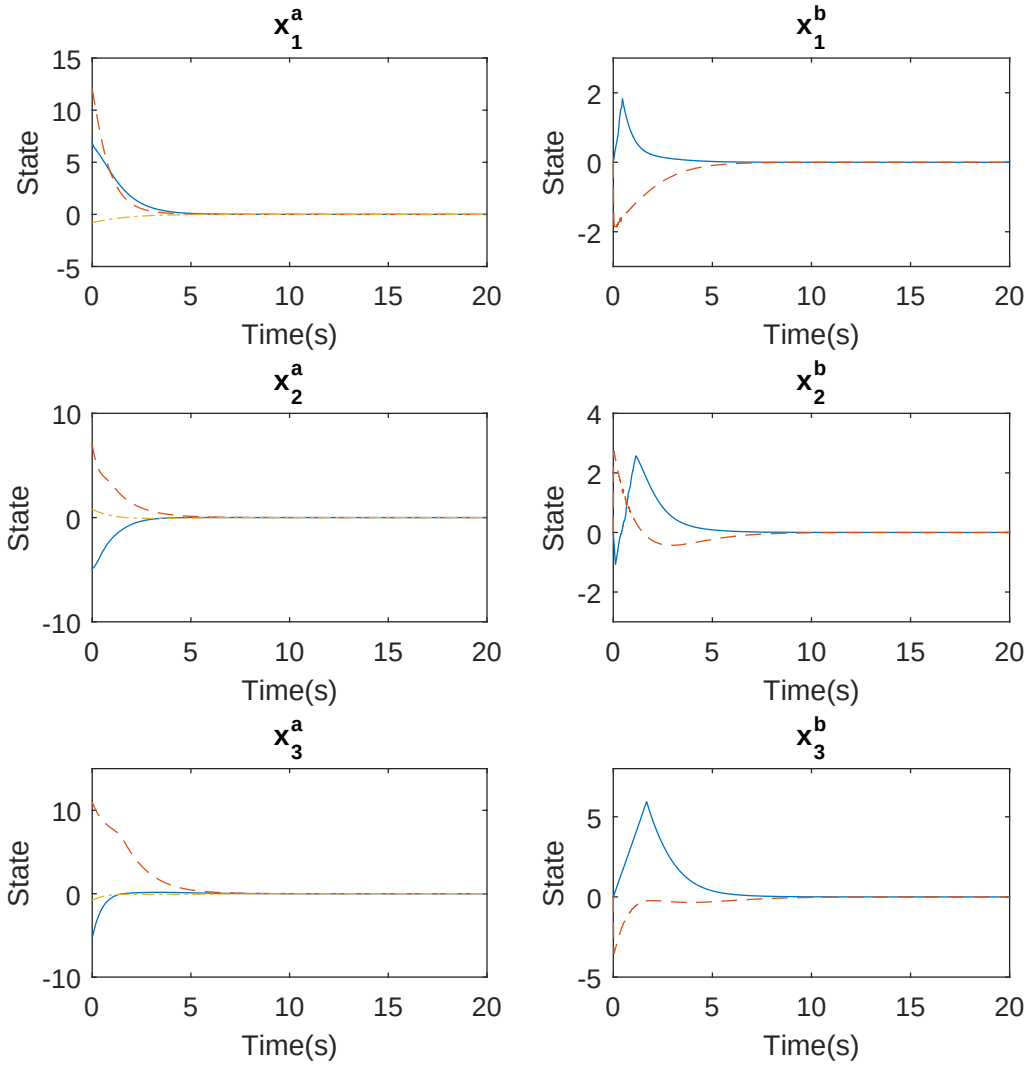

Figure 8.3: Time response of the state variables of system (8.50)-(8.51).

8.6. Conclusion

In this chapter, uncertainties in input distribution are discussed, and a robust decentralised control design approach for a class of nonlinear large-scale interconnected systems with such uncertainties and unknown interconnection is introduced. The bounds on the uncertainties are assumed to be known functions which have been used to enhance robustness against the uncertainties. A SMC is designed to guarantee reachability. The developed results are also

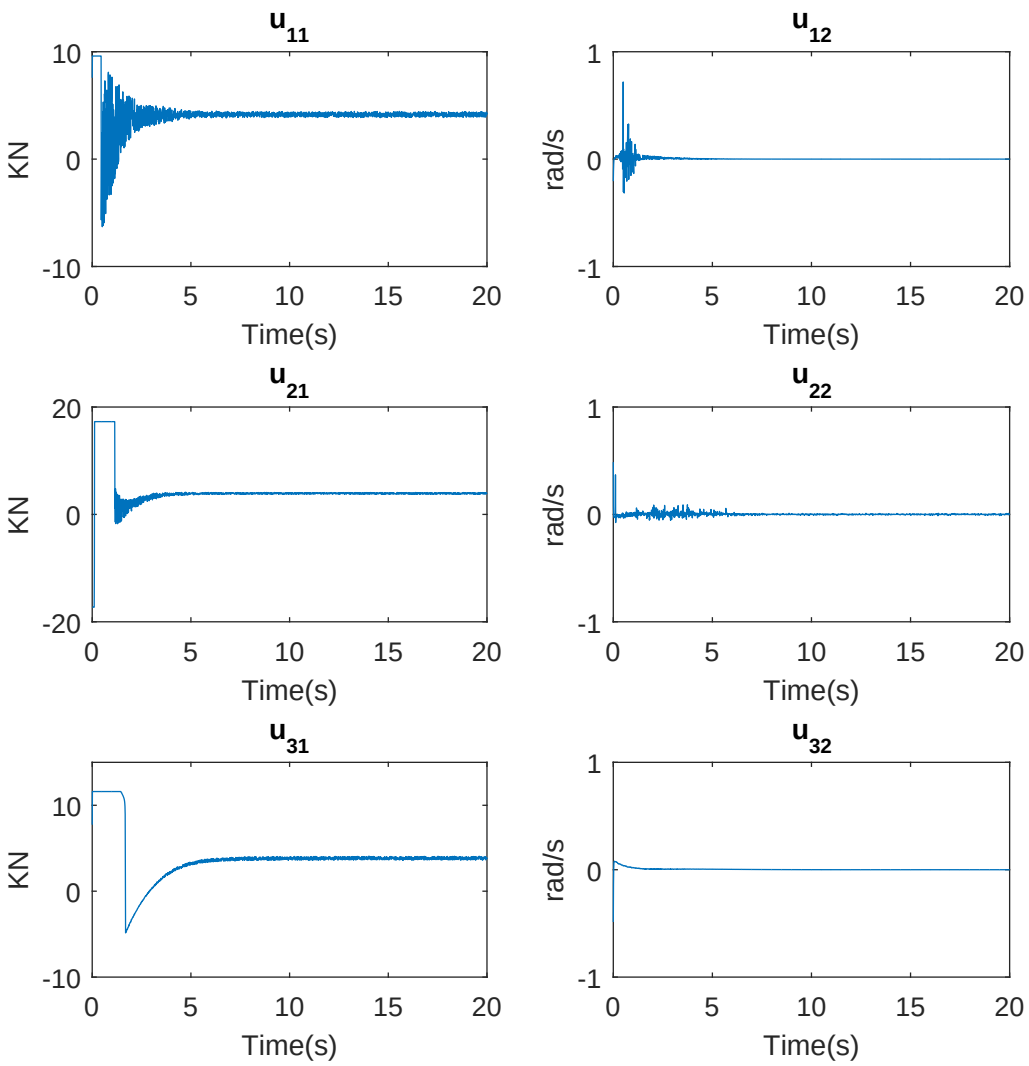

Figure 8.4: Time response of the control inputs of system (8.50)-(8.51).

applied to automated highway system with both onboard longitudinal and lateral controllers. With decentralised control strategy, the proposed controller can be applied to each vehicle for automation or driving assistance without data transmission from the other vehicles in the system. The simulation given for the vehicle-tracking system with interconnection and uncertain input distribution has been presented to demonstrate the effectiveness of this approach.

CHAPTER. 9

CONCLUSIONS AND FUTURE WORK

9.1. Summary and Conclusions

In this thesis, a survey of the background of SMC for complex systems has been presented, in particular for nonholonomic systems and interconnected systems. By introducing the concept of generalised regular form, SMC can be applied to a broader class of nonlinear systems in the presence of uncertainties. It also demonstrated the robust control design for nonlinear interconnected systems in a decentralised manner.

The fundamental knowledge and the basic concept of complex systems and SMC have been given in Chapter 3 after a outline of mathematical preliminaries in Chapter 2. Practical examples of both nonholonomic systems and interconnected systems have been introduced, and a brief review of the SMC has also been provided.

In Chapter 4, trajectory tracking control design for a two-wheeled differential drive WMR has been discussed. A SMC design has been carried out for the trajectory tracking control of the WMR systems in a local domain. The simulation results and experimental test on the developed real-time WMR platform, it has shown that even if the regular form of a system is

not available, a sliding mode controller can still be applied if the sliding mode of the system is independent of the control signal during sliding motion. This class of systems has been studied furthermore in Chapter 5 by proposing the concept of generalised regular form. From the theory point of view, the classical regular form is a particular case of the generalised regular form. By introducing the generalised regular form, the SMC can be applied to a broader class of nonlinear systems. The robustness of the systems in the generalised regular form has also been discussed, and the corresponding nonlinear SMC design has been proposed and implemented on the WMR platform. By introducing a novel nonlinear sliding function design based on global implicit function theorem, a nonlinear sliding surface is formed, and global asymptotic stability is exhibited. Thus the developed controller can drive the robot tracking the time-based trajectory with an arbitrary initial condition. Both simulation and experiment results show that sliding mode techniques can be used to stabilise systems when the classical regular form is not available.

Some robust decentralised control problems have been addressed and solved in Chapter 6-8.

More specifically, in Chapter 6, a decentralised state feedback SMC law has been proposed to asymptotically stabilise a class of nonlinear interconnected systems with known and unknown interconnections in the considered domain. Both matched, and mismatched uncertainties are considered. The bounds on the uncertainties can be functions instead of constants or polynomial as considered in previous work. Both known interconnections and the bounds on the unknown interconnections have been fully considered in the control design to reduce conservatism. The developed results is applicable to a broad class of interconnected systems. Simulations based on a vehicle-following system have been presented to show that if the bounds of the unknown interconnection possess a superposition property, a decentralised control scheme may be designed to counteract the effect of the uncertainty. In Chapter 7, the developed results have been expanded to systems in the generalised regular form with fully nonlinear nominal isolate subsystems. A numerical example has been given to demonstrate the design process.

Uncertainties in input distribution have been discussed in Chapter 8. Robust decentralised control design based on sliding mode techniques has been proposed for fully nonlinear systems with uncertainties in input distribution. Both matched uncertainties in the isolated subsystems and mismatched uncertainties associated with the interconnections are considered. Conditions

are developed for the uncertainties in input distribution so that the bounds information on the uncertainties can be employed within the decentralised controller design to reduce the effect caused by the uncertainties. The developed results are applied to the automated highway systems with both longitudinal and lateral controllers. With decentralised control strategy, the proposed controller can be applied to each vehicle for automation or driving assistance without data transmission from the other vehicles in the system. The simulation given for the vehicle-tracking system with interconnection and uncertain input distribution has been presented to demonstrate the effectiveness of this approach.

9.2. Ideas for Future Research

There are some possible interesting ideas for further research.

Although it has been shown that the SMC can be applied to a broader class of nonlinear systems by introducing generalised regular form, how to find a diffeomorphism that can transfer a nonlinear system into such a form is still challenging. From the fact that the generalised regular form has to be paired with a sliding function, the implicit Lyapunov function theorem may be a possible solution to this problem. Furthermore, for the chattering problems, second-order SMC for systems with the relative degree of 1 in generalised regular form deserves to be considered. Thus the rapidly changing control action can be avoided so that possible damage to the WMR systems caused by the high-frequency switching action can be significantly reduced. For the WMR systems, the robustness can be further improved by introducing the disturbance observer to estimate the mismatched uncertainties caused by the drift of the WMR.

For decentralised control design, the attenuation of unknown interconnection for systems based on SMC with finite-time reachability is a considerable challenging due to the lack of information from other subsystems. Meanwhile, the rapid development of the Internet of Vehicles encourages the communication network between vehicles in automated highway systems. However, as mentioned in Chapter 3, the communication problems such as transmission failure or time delay during the communication process between different vehicles to the cloud server may still affect the control performance if centralised or networked controllers are applied. To overcome these problems, the quasi-decentralised control strategy may be a better solution for overcoming the drawback of both centralised and decentralised strategy for the automated

highway systems. With extra information periodically coming from the other subsystems, the control performance of the developed decentralised controller in Chapters 6-8 may be further improved without scarifying the reliability of the decentralised schemes while the finite-time reachability of the sliding mode may be guaranteed.

APPENDIX. A

LIST OF PUBLICATION

Publication in Journal

[1] J. Mu, X. G. Yan, S. K. Spurgeon, and Z. Mao, "Nonlinear SMC of a two-wheeled mobile robot system," *International Journal of Modelling, Identification and Control*, vol. 27, no. 2, 2017.

[2] J. Mu, X. G. Yan, S. K. Spurgeon, and Z. Mao, "Generalised regular form-based SMC for nonlinear systems with application to a WMR," *IEEE Transactions on Industrial Electronics*, vol. 64, no. 8, pp. 6714–6723, 2017.

[3] J. Mu, X. G. Yan, S. K. Spurgeon, and D. Zhao, "Nonlinear SMC for interconnected systems with application to automated highway systems," *IEEE Transactions on Control of Network Systems*, doi: 10.1109/TCNS.2016.2642589, 2016. (Accepted)

Publication in book chapter

[1] J. Mu, X.-G. Yan, and S. K. Spurgeon, *Decentralised Sliding Mode Control for Nonlinear Interconnected Systems with Application to a Continuously Stirred Tank Reactor*. In

Recent Advances in Sliding Modes: From Control to Intelligent Mechatronics, Springer, 2015.

Publication in conferences

[1] J. Mu, X.-G. Yan, and S. K. Spurgeon, "Decentralised SMC for a class of nonlinear interconnected systems," in *2015 American Control Conference (ACC)*, pp. 5170–5175, 2015.

[2] J. Mu, X.-G. Yan, S. K. Spurgeon, and Z. Mao, "Trajectory tracking control of a two-wheeled mobile robot using sliding mode techniques," in *the 34th Chinese Control Conference (CCC)*, pp. 3307–3312, 2015.

[3] J. Mu, X. G. Yan, B. Jiang, S. K. Spurgeon, and Z. Mao, "Sliding mode control for a class of nonlinear systems with application to a wheeled mobile robot," in *the 54th IEEE Conference on Decision and Control (CDC)*, pp. 4746–4751, Dec. 2015.

[4] J. Mu, X. G. Yan, S. K. Spurgeon, and Z. Mao, "Decentralised sliding mode control for nonlinear interconnected systems in the regular form," in *the 55th IEEE Conference on Decision and Control (CDC)*, pp. 6452–6457, Dec. 2016.

[5] J. Mu, X. G. Yan, Q. Zhang, and Z. Mao, "Decentralised SMC for nonlinear interconnected systems in the generalised regular form," in *the 20th World Congress of the International Federation of Automatic Control (IFAC)*, Toulouse, France, Jul. 9-14, 2017.

BIBLIOGRAPHY

[1] V. Utkin, "Variable structure systems with sliding modes," *IEEE Transactions on Automatic control*, vol. 22, no. 2, pp. 212–222, 1977.

[2] X. Yan, S. K. Spurgeon, and C. Edwards, *Variable-Structure Control of Complex Systems: Analysis and Design*. Springer, 2017.

[3] F. L. Lewis, *Applied optimal control and estimation*. Prentice Hall PTR, 1992.

[4] D. D. Siljak, *Decentralized control of complex systems*. Courier Corporation, 2011.

[5] A. Zecevic and D. D. Siljak, *Control of complex systems: Structural constraints and uncertainty*. Springer Science & Business Media, 2010.

[6] J. D. Sterman, "System dynamics modeling: tools for learning in a complex world," *California management review*, vol. 43, no. 4, pp. 8–25, 2001.

[7] K. Vamvoudakis and S. Jagannathan, *Control of Complex Systems: Theory and Applications*. Butterworth-Heinemann, 2016.

[8] H. K. Khalil and J. Grizzle, *Nonlinear systems*, vol. 3. Prentice hall New Jersey, 1996.

[9] H.-T. Yau and C.-L. Chen, "Chattering-free fuzzy sliding-mode control strategy for uncertain chaotic systems," *Chaos, Solitons & Fractals*, vol. 30, no. 3, pp. 709–718, 2006.

[10] M. Asif, M. J. Khan, and N. Cai, "Adaptive sliding mode dynamic controller with integrator in the loop for nonholonomic wheeled mobile robot trajectory tracking," *International Journal of Control*, vol. 87, no. 5, pp. 964–975, 2014.

[11] X.-G. Yan, C. Edwards, S. K. Spurgeon, and J. Bleijs, "Decentralised sliding-mode control for multimachine power systems using only output information," in *Control Theory and Applications, IEE Proceedings-*, vol. 151, pp. 627–635, IET, 2004.

[12] M. Krstic, I. Kanellakopoulos, and P. V. Kokotovic, *Nonlinear and adaptive control design*. Wiley, 1995.

[13] H. Li, P. Shi, and D. Yao, "Adaptive sliding-mode control of markov jump nonlinear systems with actuator faults," *IEEE Transactions on Automatic Control*, vol. 62, no. 4, pp. 1933–1939, 2017.

[14] S. H. Zak and S. Hui, "On variable structure output feedback controllers for uncertain dynamic systems," *IEEE Transactions on Automatic Control*, vol. 38, no. 10, pp. 1509–1512, 1993.

[15] K.-K. Shyu, Y.-W. Tsai, and C.-K. Lai, "A dynamic output feedback controllers for mismatched uncertain variable structure systems," *Automatica*, vol. 37, no. 5, pp. 775–779, 2001.

[16] C. Edwards and S. K. Spurgeon, *Sliding mode control: Theory and applications*. London: Taylor & Francis, 1998.

[17] V. Utkin, J. Guldner, and J. Shi, *Sliding mode control in electro-mechanical systems*, vol. 34. CRC press, 2009.

[18] Y. Shtessel, C. Edwards, L. Fridman, and A. Levant, *Sliding mode control and observation*. Springer, 2014.

[19] D. Ginoya, P. D. Shendge, and S. B. Phadke, "Sliding mode control for mismatched uncertain systems using an extended disturbance observer," *IEEE Transactions on Industrial Electronics*, vol. 61, pp. 1983–1992, April 2014.

[20] J. Zhang, X. Liu, Y. Xia, Z. Zuo, and Y. Wang, "Disturbance observer-based integral sliding-mode control for systems with mismatched disturbances," *IEEE Transactions on Industrial Electronics*, vol. 63, pp. 7040–7048, Nov 2016.

[21] S. Li, J. Yang, W.-H. Chen, and X. Chen, *Disturbance observer-based control: methods and applications*. CRC press, 2014.

[22] H. Trinh and M. Aldeen, "Decentralised feedback controllers for uncertain interconnected dynamic systems," *IEE Proceedings D (Control Theory and Applications)*, vol. 140, pp. 429–434(5), November 1993.

[23] C.-F. Cheng, "Disturbances attenuation for interconnected systems by decentralized control," *International journal of control*, vol. 66, no. 2, pp. 213–224, 1997.

[24] L. Jiang, Q. Wu, and J. Wen, "Decentralized nonlinear adaptive control for multimachine power systems via high-gain perturbation observer," *Circuits and Systems I: Regular Papers, IEEE Transactions on*, vol. 51, pp. 2052–2059, Oct 2004.

[25] Y. Mi, Y. Fu, C. Wang, and P. Wang, "Decentralized sliding mode load frequency control for multi-area power systems," *Power Systems, IEEE Transactions on*, vol. 28, pp. 4301–4309, Nov 2013.

[26] Y. Niu, J. Lam, and X. Wang, "Sliding-mode control for uncertain neutral delay systems," *Control Theory and Applications, IEE Proceedings-*, vol. 151, no. 1, pp. 38–44, 2004.

[27] Y. Niu, T. Jia, J. Huang, and J. Liu, "Design of sliding mode control for neutral delay systems with perturbation in control channels," *Optimal Control Applications and Methods*, vol. 33, no. 3, pp. 363–374, 2012.

[28] X.-G. Yan, S. K. Spurgeon, and C. Edwards, "Dynamic sliding mode control for a class of systems with mismatched uncertainty," *European Journal of Control*, vol. 11, no. 1, pp. 1–10, 2005.

[29] X.-G. Yan and C. Edwards, "Adaptive sliding-mode-observer-based fault reconstruction for nonlinear systems with parametric uncertainties," *IEEE Transactions on Industrial Electronics*, vol. 55, no. 11, pp. 4029–4036, 2008.

[30] J. Yang, S. Li, J. Su, and X. Yu, "Continuous nonsingular terminal sliding mode control for systems with mismatched disturbances," *Automatica*, vol. 49, no. 7, pp. 2287 – 2291, 2013.

[31] J. Burton and A. S. Zinober, "Continuous approximation of variable structure control," *International journal of systems science*, vol. 17, no. 6, pp. 875–885, 1986.

[32] A. Isidori, *Nonlinear control systems*. Springer Science & Business Media, 2013.

[33] F. W. Warner, *Foundations of differentiable manifolds and Lie groups*, vol. 94. Springer Science & Business Media, 2013.

[34] R. W. Brockett, *Differential Geometric Control Theory*, ch. Asymtotic stability and feedback stabilization, pp. PP. 181–191. Eds. Boston, MA: Birkhauser, 1983.

[35] W. Zhang and S. S. Ge, "A global implicit function theorem without initial point and its applications to control of non-affine systems of high dimensions," *Journal of Mathematical Analysis and Applications*, vol. 313, no. 1, pp. 251–261, 2006.

[36] V. L. Syrmos, C. T. Abdallah, P. Dorato, and K. Grigoriadis, "Static output feedback—a survey," *Automatica*, vol. 33, no. 2, pp. 125–137, 1997.

[37] E. Davison and R. Chatterjee, "A note on pole assignment in linear systems with incomplete state feedback," *IEEE Transactions on Automatic Control*, vol. 16, no. 1, pp. 98–99, 1971.

[38] E. Davison and S. Chow, "An algorithm for the assignment of closed-loop poles using output feedback in large linear multivariable systems," *IEEE Transactions on Automatic Control*, vol. 18, no. 1, pp. 74–75, 1973.

[39] E. Davison and S. Wang, "On pole assignment in linear multivariable systems using output feedback," *IEEE Transactions on Automatic Control*, vol. 20, no. 4, pp. 516–518, 1975.

[40] H. Kimura, "Pole assignment by gain output feedback," *IEEE Transactions on automatic Control*, vol. 20, no. 4, pp. 509–516, 1975.

[41] H. KIMURA, "On pole assignment by output feedback," *International Journal of Control*, vol. 28, no. 1, pp. 11–22, 1978.

[42] U. Itkis, *Control systems of variable structure*. Halsted Press, 1976.

[43] J. Y. Hung, W. Gao, and J. C. Hung, "Variable structure control: A survey," *IEEE transactions on industrial electronics*, vol. 40, no. 1, pp. 2–22, 1993.

[44] V. Utkin, "Sliding modes in optimization and control problems," 1992.

[45] A. F. Filippov, "Differential equations with discontinuous right-hand side," *Amer. Math. Soc. Translations Ser. 2*, vol. 42, pp. 199–231, 1964.

[46] A. F. Filippov, *Differential equations with discontinuous righthand sides: control systems*, vol. 18. Springer Science & Business Media, 2013.

[47] X.-G. Yan, C. Edwards, and S. K. Spurgeon, "Decentralised robust sliding mode control for a class of nonlinear interconnected systems by static output feedback," *Automatica*, vol. 40, no. 4, pp. 613–620, 2004.

[48] S. Spurgeon, "Choice of discontinuous control component for robust sliding mode performance," *International journal of control*, vol. 53, no. 1, pp. 163–179, 1991.

[49] G. Bartolini, A. Ferrara, and E. Usai, "Chattering avoidance by second-order sliding mode control," *IEEE transactions on Automatic Control*, vol. 43, no. 2, pp. 241–246, 1998.

[50] A. Levant, "Higher-order sliding modes, differentiation and output-feedback control," *International journal of Control*, vol. 76, no. 9-10, pp. 924–941, 2003.

[51] J. I. Ne_mark and N. A. Fufaev, *Dynamics of nonholonomic systems*, vol. 33. American Mathematical Soc., 2004.

[52] I. Kolmanovsky and N. H. McClamroch, "Developments in nonholonomic control problems," *IEEE control systems*, vol. 15, no. 6, pp. 20–36, 1995.

[53] L. Praly, B. d'Andréa Novel, and J.-M. Coron, "Lyapunov design of stabilizing controllers," in *Decision and Control, 1989., Proceedings of the 28th IEEE Conference on*, pp. 1047–1052, IEEE, 1989.

[54]

[55] A. Astolfi, "On the stabilization of nonholonomic systems," in *Decision and Control, 1994., Proceedings of the 33rd IEEE Conference on*, vol. 4, pp. 3481–3486, IEEE, 1994.

[56] Z. Sun, S. S. Ge, W. Huo, and T. H. Lee, "Stabilization of nonholonomic chained systems via nonregular feedback linearization," *Systems & Control Letters*, vol. 44, no. 4, pp. 279–289, 2001.

[57] A. Tayebi, M. Tadjine, and A. Rachid, "Invariant manifold approach for the stabilization of nonholonomic chained systems: application to a mobile robot," *Nonlinear Dynamics*, vol. 24, no. 2, pp. 167–181, 2001.

[58] M. Belhocine, M. Hamerlain, and F. Meraoubi, "Variable structure control for a wheeled mobile robot," *Advanced Robotics*, vol. 17, no. 9, pp. 909–924, 2003.

[59] L. Bakule, "Decentralized control: An overview," *Annual reviews in control*, vol. 32, no. 1, pp. 87–98, 2008.

[60] R. Scattolini, "Architectures for distributed and hierarchical model predictive control–a review," *Journal of process control*, vol. 19, no. 5, pp. 723–731, 2009.

[61] Y. Sun and N. H. El-Farra, "Quasi-decentralized model-based networked control of process systems," *Computers & Chemical Engineering*, vol. 32, no. 9, pp. 2016–2029, 2008.

[62] F. Giulietti, L. Pollini, and M. Innocenti, "Autonomous formation flight," *IEEE Control Systems*, vol. 20, no. 6, pp. 34–44, 2000.

[63] S. Tsujii, M. Bando, and H. Yamakawa, "Spacecraft formation flying dynamics and control using the geomagnetic lorentz force," *Journal of Guidance, Control, and Dynamics*, vol. 36, no. 1, pp. 136–148, 2012.

[64] G. Fusco and M. Russo, "Design of decentralized robust controller for voltage regulation and stabilization of multimachine power systems," *International Journal of Control, Automation and Systems*, vol. 11, no. 2, pp. 277–285, 2013.

[65] A. K. Singh and B. C. Pal, "Decentralized control of oscillatory dynamics in power systems using an extended lqr," *IEEE Transactions on Power Systems*, vol. 31, pp. 1715–1728, May 2016.

[66] S. Xie, L. Xie, Y. Wang, and G. Guo, "Decentralised control of multimachine power systems with guaranteed performance," *IEE Proceedings - Control Theory and Applications*, vol. 147, pp. 355–365, May 2000.

[67] J. Spooner and K. Passino, "Adaptive control of a class of decentralized nonlinear systems," *Automatic Control, IEEE Transactions on*, vol. 41, pp. 280–284, Feb 1996.

[68] L. Bakule, "Decentralized control: Status and outlook," *Annual Reviews in Control*, vol. 38, no. 1, pp. 71–80, 2014.

[69] Z.-P. Jiang, "Decentralized and adaptive nonlinear tracking of large-scale systems via output feedback," *IEEE Transactions on Automatic control*, vol. 45, no. 11, pp. 2122–2128, 2000.

[70] D. D. Siljak, D. M. Stipanovic, and A. I. Zecevic, "Robust decentralized turbine/governor control using linear matrix inequalities," *IEEE Transactions on Power Systems*, vol. 17, no. 3, pp. 715–722, 2002.

[71] K.-K. Shyu, W.-J. Liu, and K.-C. Hsu, "Design of large-scale time-delayed systems with dead-zone input via variable structure control," *Automatica*, vol. 41, no. 7, pp. 1239–1246, 2005.

[72] Y. Zhu and P. R. Pagilla, "Decentralized output feedback control of a class of large-scale interconnected systems," *IMA Journal of Mathematical Control and Information*, vol. 24, no. 1, pp. 57–69, 2007.

[73] X.-G. Yan, S. K. Spurgeon, and C. Edwards, "Global decentralised static output feedback slidingmode control for interconnected time-delay systems," *IET control theory & applications*, vol. 6, no. 2, pp. 192–202, 2012.

[74] J. Mu, X. G. Yan, S. K. Spurgeon, and D. Zhao, "Nonlinear sliding mode control for interconnected systems with application to automated highway systems," *IEEE Transactions on Control of Network Systems*, vol. PP, no. 99, pp. 1–1, 2016.

[75] D. Swaroop and J. Hedrick, "Constant spacing strategies for platooning in automated highway systems," *Journal of dynamic systems, measurement, and control*, vol. 121, no. 3, pp. 462–470, 1999.

[76] R. Negenborn and H. Hellendoorn, "Intelligence in transportation infrastructures via model-based predictive control," *Intelligent Infrastructures*, pp. 3–24, 2010.

[77] M. G. Singh, M. F. Hassan, and A. Titli, "Multilevel feedback control for interconnected dynamical systems using the prediction principle," *IEEE Transactions on Systems, Man, and Cybernetics*, no. 4, pp. 233–239, 1976.

[78] M. S. Mahmoud, "Multilevel systems control and applications: A survey," *IEEE transactions on Systems, Man, and Cybernetics*, vol. 7, no. 3, pp. 125–143, 1977.

[79] M. G. Singh and A. Titli, *Systems: decomposition, optimisation, and control*. Pergamon, 1978.

[80] J. Meisel, "Transient stability augmentation using a hierarchical control structure," *IEEE Transactions on Power Apparatus and Systems*, no. 1, pp. 256–267, 1980.

[81] T. Van Cutsem, J.-L. Horward, and M. Ribbens-Pavella, "A two-level static state estimator for electric power systems," *IEEE transactions on power apparatus and systems*, no. 8, pp. 3722–3732, 1981.

[82] A. Rubaai, "Transient stability control: a multi-level hierarchical approach," *IEEE Transactions on Power Systems*, vol. 6, no. 1, pp. 262–268, 1991.

[83] F. Okou, L.-A. Dessaint, and O. Akhrif, "Power systems stability enhancement using a wide-area signals based hierarchical controller," *IEEE Transactions on Power Systems*, vol. 20, no. 3, pp. 1465–1477, 2005.

[84] P.-H. Chen, "Two-level hierarchical approach to unit commitment using expert system and elite pso," *IEEE Transactions on Power Systems*, vol. 27, no. 2, pp. 780–789, 2012.

[85] A. Gomez-Exposito and A. de la Villa Jaen, "Two-level state estimation with local measurement pre-processing," *IEEE Transactions on Power Systems*, vol. 24, no. 2, pp. 676–684, 2009.

[86] T. Backx, O. Bosgra, and W. Marquardt, "Integration of model predictive control and optimization of processes: enabling technology for market driven process operation," *IFAC Proceedings Volumes*, vol. 33, no. 10, pp. 249–260, 2000.

[87] S. J. Qin and T. A. Badgwell, "A survey of industrial model predictive control technology," *Control engineering practice*, vol. 11, no. 7, pp. 733–764, 2003.

[88] F. Goktas, "Distributed control of systems over communication networks," 2000.

[89] P. Kundur, N. J. Balu, and M. G. Lauby, *Power system stability and control*, vol. 7. McGraw-hill New York, 1994.

[90] D. Šiljak, "Decentralized control and computations: status and prospects," *Annual Reviews in Control*, vol. 20, pp. 131–141, 1996.

[91] D. Šiljak and A. Zečević, "Control of large-scale systems: Beyond decentralized feedback," *Annual Reviews in Control*, vol. 29, no. 2, pp. 169–179, 2005.

[92] N. Chen, M. Ikeda, and W. Gui, "Design of robust h_∞ control for interconnected systems: a homotopy method," *International Journal of Control, Automation, and Systems*, vol. 3, no. 2, pp. 143–151, 2005.

[93] K. Perutka, "A survey of decentralized adaptive control," in *New Trends in Technologies: Control, Management, Computational Intelligence and Network Systems*, InTech, 2010.

[94] D. T. Gavel and D. D. Siljak, "Decentralized adaptive control: structural conditions for stability," *IEEE Transactions on Automatic Control*, vol. 34, no. 4, pp. 413–426, 1989.

[95] L. Shi and S. K. Singh, "Decentralized adaptive controller design for large-scale systems with higher order interconnections," *IEEE Transactions on Automatic Control*, vol. 37, no. 8, pp. 1106–1118, 1992.

[96] H. Wu, "Decentralized adaptive robust control for a class of large-scale systems including delayed state perturbations in the interconnections," *IEEE Transactions on Automatic Control*, vol. 47, no. 10, pp. 1745–1751, 2002.

[97] H. Wu, "Decentralized adaptive robust control for a class of large scale systems with uncertainties in the interconnections," *International Journal of Control*, vol. 76, no. 3, pp. 253–265, 2003.

[98] V. A. Ugrinovskii, I. R. Petersen, A. V. Savkin, and E. Y. Ugrinovskaya, "Decentralized state-feedback stabilization and robust control of uncertain large-scale systems with

integrally constrained interconnections," *Systems & Control Letters*, vol. 40, no. 2, pp. 107–119, 2000.

[99] C.-C. Cheng and Y. Chang, "Design of decentralised adaptive sliding mode controllers for large-scale systems with mismatched perturbations," *International Journal of Control*, vol. 81, no. 10, pp. 1507–1518, 2008.

[100] Z.-P. Jiang, "Recent developments in decentralized nonlinear control," in *Control, Automation, Robotics and Vision Conference, 2004. ICARCV 2004 8th*, vol. 1, (Kunming, China), pp. 326–331, IEEE, 2004.

[101] S. Richter, S. Lefebvre, and R. DeCarlo, "Control of a class of nonlinear systems by decentralized control," *IEEE Transactions on Automatic Control*, vol. 27, no. 2, pp. 492–494, 1982.

[102] A. Levant, "Robust exact differentiation via sliding mode technique," *automatica*, vol. 34, no. 3, pp. 379–384, 1998.

[103] L. Fridman, S. Li, A. Levant, X. Chen, and X. Yu, "Editorial: Sliding-mode based disturbance estimation, attenuation and fault detection," *IET Control Theory Applications*, vol. 9, no. 4, pp. 511–514, 2015.

[104] C. Edwards and S. K. Spurgeon, "Sliding mode stabilization of uncertain systems using only output information," *International Journal of Control*, vol. 62, no. 5, pp. 1129–1144, 1995.

[105] X.-G. Yan, S. K. Spurgeon, and C. Edwards, "Decentralised robust sliding mode control for a class of nonlinear interconnected systems by static output feedback," *Journal of Optimization Theory and Application*, vol. 119, no. 3, pp. 597–614, 2003.

[106] X.-G. Yan, S. K. Spurgeon, and C. Edwards, "Global time-delay dependent decentralised sliding mode control using only output information," in *Decision and Control, 2009 held jointly with the 2009 28th Chinese Control Conference. CDC/CCC 2009. Proceedings of the 48th IEEE Conference on*, pp. 6709–6714, IEEE, 2009.

[107] K. Kalsi, J. Lian, and S. H. Zak, "Decentralized dynamic output feedback control of nonlinear interconnected systems," *IEEE Transactions on Automatic Control*, vol. 55, no. 8, pp. 1964–1970, 2010.

[108] X.-G. Yan and G.-Z. Dai, "Decentralized output feedback robust control for nonlinear large-scale systems," *Automatica*, vol. 34, no. 11, pp. 1469–1472, 1998.

[109] X.-G. Yan, J. Lam, H.-S. Li, and I. Chen, "Decentralized control of nonlinear large-scale systems using dynamic output feedback," *Journal of Optimization Theory and Applications*, vol. 104, no. 2, pp. 459–475, 2000.

[110] X.-G. Yan, J.-J. Wang, X.-Y. Lu, and S.-Y. Zhang, "Decentralized output feedback robust stabilization for a class of nonlinear interconnected systems with similarity," *IEEE Transactions on Automatic Control*, vol. 43, no. 2, pp. 294–299, 1998.

[111] J. Lee, "On the decentralized stabilization of interconnected variable structure systems using output feedback," *Journal of the Franklin Institute*, vol. 332, no. 5, pp. 595–605, 1995.

[112] K. SHYU, J. YAN, *et al.*, "Variable-structure model-following adaptive-control for systems with time-varying delay," *Control-Theory and Advanced Technology*, 1994.

[113] K.-C. Hsu, "Decentralized variable-structure control design for uncertain large-scale systems with series nonlinearities," *International Journal of Control*, vol. 68, no. 6, pp. 1231–1240, 1997.

[114] Y. Sun and N. H. El-Farra, "Resource aware quasi-decentralized control of networked process systems over wireless sensor networks," *Chemical engineering science*, vol. 69, no. 1, pp. 93–106, 2012.

[115] A. Bloch, J. Baillieul, P. Crouch, J. E. Marsden, D. Zenkov, P. S. Krishnaprasad, and R. M. Murray, *Nonholonomic mechanics and control*, vol. 24. Springer, 2003.

[116] S. Shladover, C. Desoer, J. Hedrick, M. Tomizuka, J. Walrand, W.-B. Zhang, D. McMahon, H. Peng, S. Sheikholeslam, and N. McKeown, "Automated vehicle control developments in the path program," *Vehicular Technology, IEEE Transactions on*, vol. 40, pp. 114–130, Feb 1991.

[117] Y. Guo, D. J. Hill, and Y. Wang, "Nonlinear decentralized control of large-scale power systems," *Automatica*, vol. 36, no. 9, pp. 1275–1289, 2000.

[118] Q. Lu, S. Mei, W. Hu, F. F. Wu, Y. Ni, and T. Shen, "Nonlinear decentralized disturbance attenuation excitation control via new recursive design for multi-machine power systems," *IEEE Transactions on Power Systems*, vol. 16, no. 4, pp. 729–736, 2001.

[119] Y. Wang, G. Guo, and D. J. Hill, "Robust decentralized nonlinear controller design for multimachine power systems," *Automatica*, vol. 33, no. 9, pp. 1725–1733, 1997.

[120] R. Siegwart, I. R. Nourbakhsh, and D. Scaramuzza, *Introduction to autonomous mobile robots*. MIT press, 2011.

[121] J. Ghommam, H. Mehrjerdi, M. Saad, and F. Mnif, "Adaptive coordinated path following control of non-holonomic mobile robots with quantised communication," *IET control theory & applications*, vol. 5, no. 17, pp. 1990–2004, 2011.

[122] B. Thuilot, B. d'Andrea Novel, and A. Micaelli, "Modeling and feedback control of mobile robots equipped with several steering wheels," *Robotics and Automation, IEEE Transactions on*, vol. 12, pp. 375–390, Jun 1996.

[123] Y. Kanayama, Y. Kimura, F. Miyazaki, and T. Noguchi, "A stable tracking control method for an autonomous mobile robot," in *Robotics and Automation, 1990. Proceedings., 1990 IEEE International Conference on*, pp. 384–389, IEEE, 1990.

[124] C. Samson and K. Ait-Abderrahim, "Feedback control of a nonholonomic wheeled cart in cartesian space," in *Robotics and Automation, 1991. Proceedings., 1991 IEEE International Conference on*, pp. 1136–1141, IEEE, 1991.

[125] R. Fierro and F. Lewis, "Control of a nonholonomic mobile robot: backstepping kinematics into dynamics," in *Decision and Control, 1995., Proceedings of the 34th IEEE Conference on*, vol. 4, pp. 3805–3810 vol.4, Dec 1995.

[126] D.-H. Kim and J.-H. Oh, "Tracking control of a two-wheeled mobile robot using input–output linearization," *Control Engineering Practice*, vol. 7, no. 3, pp. 369–373, 1999.

[127] J.-M. Yang and J.-H. Kim, "Sliding mode control for trajectory tracking of nonholonomic wheeled mobile robots," *Robotics and Automation, IEEE Transactions on*, vol. 15, pp. 578–587, Jun 1999.

[128] T. Fukao, H. Nakagawa, and N. Adachi, "Adaptive tracking control of a nonholonomic mobile robot," *IEEE transactions on Robotics and Automation*, vol. 16, no. 5, pp. 609–615, 2000.

[129] C.-Y. Chen, T.-H. S. Li, Y.-C. Yeh, and C.-C. Chang, "Design and implementation of an adaptive sliding-mode dynamic controller for wheeled mobile robots," *Mechatronics*, vol. 19, no. 2, pp. 156–166, 2009.

[130] G. Oriolo, A. De Luca, and M. Vendittelli, "Wmr control via dynamic feedback linearization: design, implementation, and experimental validation," *Control Systems Technology, IEEE Transactions on*, vol. 10, pp. 835–852, Nov 2002.

[131] J.-X. Xu, Z.-Q. Guo, and T. H. Lee, "Design and implementation of a takagi–sugeno-type fuzzy logic controller on a two-wheeled mobile robot," *IEEE Transactions on industrial electronics*, vol. 60, no. 12, pp. 5717–5728, 2013.

[132] H. Fukushima, K. Muro, and F. Matsuno, "Sliding mode control for transformation to an inverted pendulum mode of a mobile robot with wheel-arms," *Industrial Electronics, IEEE Transactions on*, vol. 62, no. 7, pp. 4257–4266, 2015.

[133] X.-G. Yan, S. K. Spurgeon, and C. Edwards, "Decentralised stabilisation for nonlinear time delay interconnected systems using static output feedback," *Automatica*, vol. 49, no. 2, pp. 633–641, 2013.

[134] X.-G. Yan, S. K. Spurgeon, and C. Edwards, "Memoryless static output feedback sliding mode control for nonlinear systems with delayed disturbances," *Automatic Control, IEEE Transactions on*, vol. 59, pp. 1906–1912, July 2014.

[135] M. Belhocine, M. Hamerlain, and F. Meraoubi, "Variable structure control for a wheeled mobile robot," *Advanced Robotics*, vol. 17, no. 9, pp. 909–924, 2003.

[136] M. Defoort, T. Floquet, A. Kokosy, and W. Perruquetti, "Sliding-mode formation control for cooperative autonomous mobile robots," *Industrial Electronics, IEEE Transactions on*, vol. 55, pp. 3944–3953, Nov 2008.

[137] M. Defoort, T. Floquet, W. Perruquetti, and S. V. Drakunov, "Integral sliding mode control of an extended heisenberg system," *IET control theory & applications*, vol. 3, no. 10, pp. 1409–1424, 2009.

[138] J. H. Lee, C. Lin, H. Lim, and J. M. Lee, "Sliding mode control for trajectory tracking of mobile robot in the rfid sensor space," *International Journal of Control, Automation and Systems*, vol. 7, no. 3, pp. 429–435, 2009.

[139] S. Tokat, I. Eksin, and M. Guzelkaya, "Sliding mode control of high order systems using a constant nonlinear sliding surface on a transformed coordinate axis," *Journal of Vibration and Control*, vol. 14, no. 6, pp. 909–927, 2008.

[140] M. Ertugrul, O. Kaynak, and F. Kerestecioglu, "Gain adaptation in sliding mode control of robotic manipulators," *International Journal of Systems Science*, vol. 31, no. 9, pp. 1099–1106, 2000.

[141] A. Bartoszewicz, "A comment on 'a time-varying sliding surface for fast and robust tracking control of second-order uncertain systems'," *Automatica*, vol. 31, no. 12, pp. 1893–1895, 1995.

[142] Q. P. Ha, D. C. Rye, and H. F. Durrant-Whyte, "Fuzzy moving sliding mode control with application to robotic manipulators," *Automatica*, vol. 35, no. 4, pp. 607–616, 1999.

[143] V. K. Chu and M. Tomizuka, "Sliding mode control with nonlinear sliding surfaces," in *Proceeding 13th IFAC World Congress*, vol. B, (San Francisco, CA), pp. 481–486, 1996.

[144] T. Fukao, H. Nakagawa, and N. Adachi, "Adaptive tracking control of a nonholonomic mobile robot," *Robotics and Automation, IEEE Transactions on*, vol. 16, pp. 609–615, Oct 2000.

[145] R. Silva-Ortigoza, C. Márquez-Sánchez, M. Marcelino-Aranda, M. Marciano-Melchor, G. Silva-Ortigoza, R. Bautista-Quintero, E. Ramos-Silvestre, J. Rivera-Díaz, and D. Muñoz-Carrillo, "Construction of a wmr for trajectory tracking control: experimental results," *The Scientific World Journal*, vol. 2013, 2013.

[146] A. Rojko and K. Jezernik, "Sliding-mode motion controller with adaptive fuzzy disturbance estimation," *IEEE Transactions on Industrial Electronics*, vol. 51, pp. 963–971, Oct 2004.

[147] B. Veselic, B. Perunicic-Drazenovic, and C. Milosavljevic, "High-performance position control of induction motor using discrete-time sliding-mode control," *IEEE Transactions on Industrial Electronics*, vol. 55, pp. 3809–3817, Nov 2008.

[148] J. Liu, S. Vazquez, L. Wu, A. Marquez, H. Gao, and L. G. Franquelo, "Extended state observer-based sliding-mode control for three-phase power converters," *IEEE Transactions on Industrial Electronics*, vol. 64, pp. 22–31, Jan 2017.

[149] J. Liu, W. Luo, X. Yang, and L. Wu, "Robust model-based fault diagnosis for PEM fuel cell air-feed system," *IEEE Transactions on Industrial Electronics*, vol. 63, pp. 3261–3270, May 2016.

[150] D. W. C. Ho and Y. Niu, "Robust fuzzy design for nonlinear uncertain stochastic systems via sliding-mode control," *IEEE Transactions on Fuzzy Systems*, vol. 15, no. 3, pp. 350–358, 2007.

[151] Y. Niu, D. W. C. Ho, and X. Wang, "Robust H_∞ control for nonlinear stochastic systems: A sliding-mode approach," *IEEE Transactions on Automatic Control*, vol. 53, no. 7, pp. 1695–1701, 2008.

[152] G. Klancar and I. Skrjanc, "Tracking-error model-based predictive control for mobile robots in real time," *Robotics and Autonomous Systems*, vol. 55, no. 6, pp. 460 – 469, 2007.

[153] E. Abbena, S. Salamon, and A. Gray, *Modern differential geometry of curves and surfaces with Mathematica*. CRC press, 2017.

[154] I. Boiko and L. Fridman, "Analysis of chattering in continuous sliding-mode controllers," *IEEE Transactions on Automatic Control*, vol. 50, pp. 1442–1446, Sept 2005.

[155] S. O. Madgwick, A. J. Harrison, and R. Vaidyanathan, "Estimation of imu and marg orientation using a gradient descent algorithm," in *Rehabilitation Robotics (ICORR), 2011 IEEE International Conference on*, pp. 1–7, IEEE, 2011.

[156] S. Tong, S. Sui, and Y. Li, "Adaptive fuzzy decentralized output stabilization for stochastic nonlinear large-scale systems with unknown control directions," *Fuzzy Systems, IEEE Transactions on*, vol. 22, pp. 1365–1372, Oct 2014.

[157] A. Ferrara and C. Vecchio, "Second order sliding mode control of vehicles with distributed collision avoidance capabilities," *Mechatronics*, vol. 19, no. 4, pp. 471–477, 2009.

[158] Y.-S. Huang and Z.-Y. Wang, "Decentralized adaptive fuzzy control for a class of large-scale mimo nonlinear systems with strong interconnection and its application to automated highway systems," *Information Sciences*, vol. 274, pp. 210–224, 2014.

[159] X.-G. Yan, C. Edwards, and S. K. Spurgeon, "Output feedback sliding mode control for non-minimum phase systems with non-linear disturbances," *International Journal of Control*, vol. 77, no. 15, pp. 1353–1361, 2004.

[160] B. Labibi and S. M. Alavi, "Inversion-free decentralised quantitative feedback design of large-scale systems," *International Journal of Systems Science*, pp. 1–11, 2014.

[161] "Decentralised stabilisation for nonlinear time delay interconnected systems using static output feedback," *Automatica*, vol. 49, no. 2, pp. 633 – 641, 2013.

[162] G. Walsh, D. Tilbury, S. Sastry, R. Murray, and J.-P. Laumond, "Stabilization of trajectories for systems with nonholonomic constraints," *IEEE Transactions on Automatic Control*, vol. 39, no. 1, pp. 216–222, 1994.

[163] C. L. Hwang, "Comparison of path tracking control of a car-like mobile robot with and without motor dynamics," *IEEE/ASME Transactions on Mechatronics*, vol. 21, pp. 1801–1811, Aug 2016.

[164] J. Mu, X. G. Yan, S. K. Spurgeon, and Z. Mao, "Generalised regular form based smc for nonlinear systems with application to a wmr," *IEEE Transactions on Industrial Electronics*, vol. PP, no. 99, pp. 1–1, 2017.

[165] S. Zhu and Y. He, "A driver-adaptive stability control strategy for sport utility vehicles," *Vehicle System Dynamics*, vol. 55, no. 8, pp. 1206–1240, 2017.

[166] K. Zhang, J. Sprinkle, and R. G. Sanfelice, "Computationally aware control of autonomous vehicles: a hybrid model predictive control approach," *Autonomous Robots*, vol. 39, no. 4, pp. 503–517, 2015.